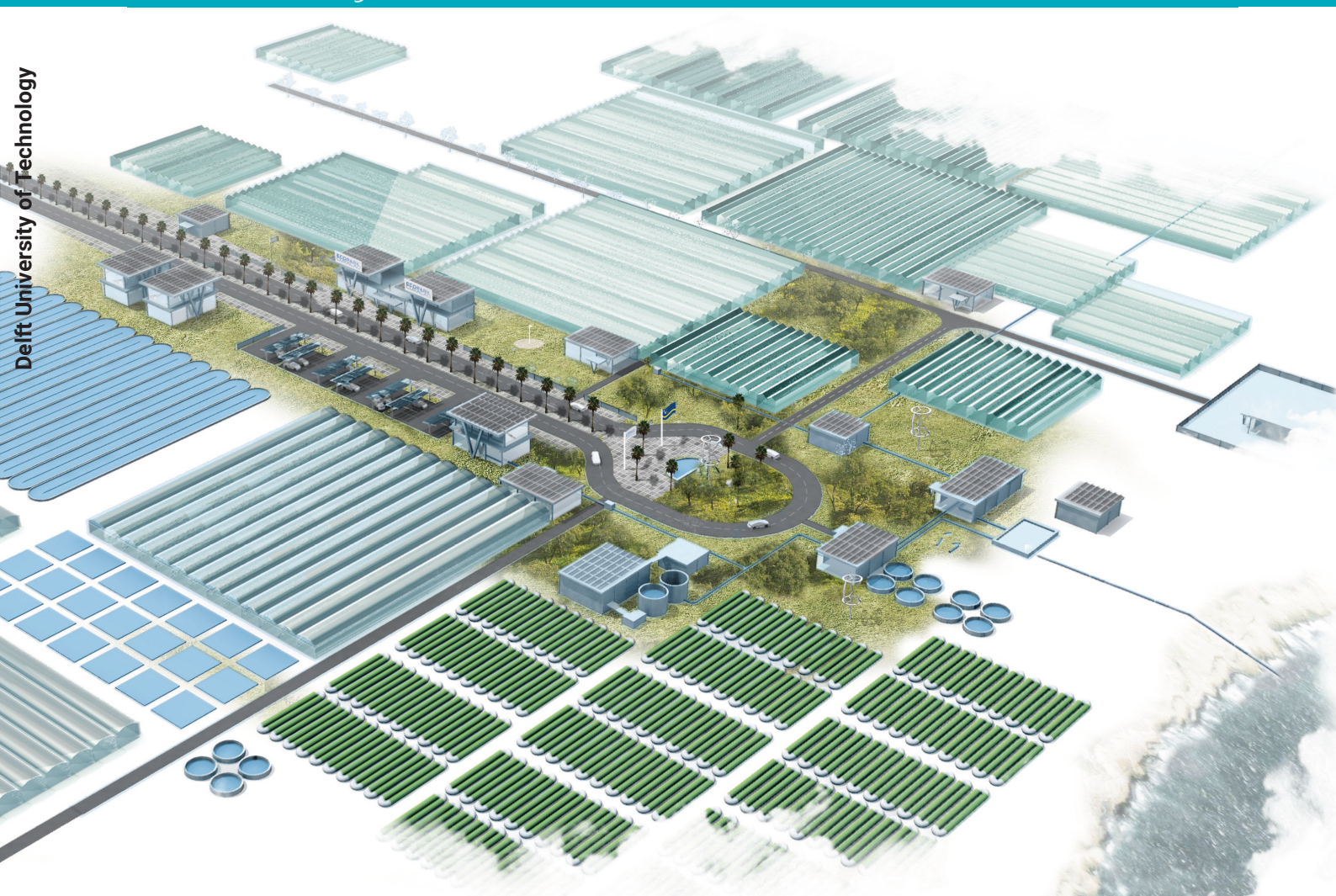


Synergies in an integrated Ocean Thermal Energy system

Integration and optimization of OTEC, SWAC and Ecopark
H.M. Veijer



Synergies in an integrated Ocean Thermal Energy system

Integration and optimization of OTEC, SWAC
and Ecopark

by

H.M. Veijer

to obtain the degree of Master of Science
at the Delft University of Technology,
to be defended publicly on Tuesday October 17, 2017 at 3:00 PM.

Student number:	4098692
Report number:	2855
Project duration:	October 1, 2016 – October 17, 2017
Thesis committee:	Prof. dr. ir. W. de Jong, TU Delft, supervisor
	Dr. C. A. Infante Ferreira, TU Delft
	Ir. T. Woudstra, TU Delft
	Ir. J. A. Kirkenier, Bluerise, supervisor

This thesis is confidential and cannot be made public until October 17, 2022.

An electronic version of this thesis is available at <http://repository.tudelft.nl/>.

"Nothing to worry about, just a little climate change..."

Bill Nye

This study has been conducted using E.U. Copernicus Marine Service Information

Abstract

Small tropical islands are facing major issues. Most of them rely on imported fossil fuels, which makes electricity generation both expensive and unsustainable. Moreover, small tropical islands are more vulnerable to the consequences of climate change than the mainland. Effects of climate change can be: more and more powerful hurricanes, shrinking fresh water resources, crop failures, land loss and coastal ecosystem change. An Ocean Thermal Energy system can be the solution for a tropical island. Cold deep seawater can be pumped up to generate baseload electricity in an onshore Ocean Thermal Energy Conversion power plant. The same deep ocean water can be used to cool houses, hotels, data centers, greenhouses and more. Furthermore, fresh water can be produced in an Ocean Thermal Water Plant and aquaculture and algae farms can use the nutrient-rich, virtually pathogen-free deep ocean water to cultivate fish and algae.

In this work, a comparison has been made for the water usage and cold water pipe diameter between a non-integrated and a time-integrated Ocean Thermal Energy system. The cold deep seawater has to be pumped up by a large and long pipe. To reach the depth of about 1000 m, the cold water pipe can be a few kilometers long, depending on the slope of the seabed. To make an Ocean Thermal Energy system economically more attractive, an optimization study can be made for the maximum water demand and cold water pipe diameter. To do this, a modular model of an Ocean Thermal Energy system is developed in Python 2.7. The model consists of modules for the Ocean Thermal Energy Conversion, Sea Water Air Conditioning, data center cooling, greenhouse cooling and fresh water production.

A case study has been conducted for an Ocean Thermal Energy system in Curaçao. Based on the expected electricity and cooling demands, a comparison has been made between a non-integrated and a time-integrated Ocean Thermal Energy system. The results show that the maximum cold deep seawater mass flow and the required cold water pipe diameter in case of a time-integrated Ocean Thermal Energy system are lower, but the difference with a non-integrated system is not significant.

Peak demands can be compensated with thermal storages. The optimization with thermal storages are applied to Sea Water Air Conditioning, data center cooling, greenhouse cooling and fresh water production. When the daily fluctuations are compensated, the decrease in maximum water demand and cold water pipe diameter is larger compared to the time-integrated Ocean Thermal Energy system. The optimization to compensate seasonal fluctuations result in an even higher decrease in cold water mass flow and pipe diameter. However, very large storage volumes are required and it has to be researched if the reduction in cold water pipe cost outweighs the cost of the thermal storages.

Changing the configuration of the subsystems in the Ocean Thermal energy system also decreases the maximum water demand and cold water pipe diameter. The results show that a significant decrease is possible when only the Ocean Thermal Energy Conversion power plant and the Sea Water Air Conditioning are connected to the cold deep seawater.

The maximum water demands of the subsystem are researched in case that the Ocean Thermal Energy system is expanded or when the Ocean Thermal Energy Conversion power plant is shut down in favor of Sea Water Air Conditioning or data center cooling. Furthermore the sensitivity of key parameters have been investigated to determine the impact of a small change on the maximum water mass flow and the cold water pipe diameter

Acknowledgement

First off all, I would like to thank my supervisor Wiebren de Jong for his guidance and support during my thesis project. Even though you were very busy and my thesis did not completely tie up with your research activities, I was always welcome for advice and a cup of coffee. When I struggled to make progress, your open view gave me often new insight to tackle the problem I faced.

Furthermore I would like to thank Joost Kirkenier, my supervisor at Bluerise. Your critical, but positive and enthusiastic feedback is very contagious. You always made time for me when I knocked on the door to ask a small and easy, or a difficult question.

I would like to thank all the members of the amazing Bluerise team. Everybody was very dedicated to make a better, sustainable future. I am feeling very proud that I could be part of this great team and met so many awesome people. Office life is tough, but you all made it fun! Especially I would like to thank all the fellow graduates and interns for all the great ping pong sessions. You were excellent opponents, I hope we can play another game somewhere in the future.

Lastly, I would like to thank my family and friends. You always supported me, especially in the hard times after I lost my mother back in 2012. Thank you Sander Vieveen, for all the great beer tasting sessions. I really enjoyed our discussions about beer, life and technology. A special thanks to my lovely girlfriend Florieke Rijkeboer. Even though I had less time for you during my thesis, you supported and inspired and above all, loved me. I could not have done this without you and I cannot wait to take the next step in life together with you!

*Henry Veijer,
Delft, October 2017*

Contents

Abstract	iii
Acknowledgement	v
List of Figures	xv
1 Introduction	1
1.1 Problem description	2
1.2 Ocean Thermal Energy system	2
1.3 Relevance	3
1.4 Research objective	3
1.5 Research approach	3
1.6 Outline	4
2 Ocean Thermal Energy system (OTEC, SWAC & Ecopark)	5
2.1 OTEC	5
2.1.1 Advanced OTEC cycle	7
2.2 OTE systems and DOW	8
2.2.1 Research Parks	8
2.2.2 DOW industries	8
2.2.3 Present & Future	9
2.3 OTE subsystems	9
2.3.1 Sea Water Air Conditioning	9
2.3.2 Data center cooling	10
2.3.3 Greenhouse cooling	12
2.3.4 Ocean Thermal Water Production	13
2.3.5 Aquaculture cultivation	15
2.3.6 Algae cultivation	16
2.4 Integration of OTE subsystems	18
2.5 Boundaries	19
3 Modeling	21
3.1 Method	21
3.2 Components	21
3.2.1 OTEC	22
3.2.2 SWAC	24
3.2.3 Data center cooling	26
3.2.4 Greenhouse cooling	28
3.2.5 OTWP	29
3.3 Model integration	32
3.4 Optimization techniques	33
3.4.1 Time-integration	33
3.4.2 Storage	33
3.4.3 Configuration	34
4 Case study: Curaçao	37
4.1 Inputs	37
4.1.1 Seawater temperatures	38
4.1.2 Environmental properties	39
4.1.3 Configuration	41
4.1.4 Demands	41

4.2	Simple demand analysis (non-integrated OTE system)	41
4.3	Time-integrated OTE system	42
4.4	Optimization by storage	45
4.4.1	Optimization by daily storage	45
4.4.2	Optimization by yearly storage	46
4.4.3	Conclusion optimization by storage	47
4.5	Future growth scenario	48
4.5.1	Additional data center in effluent water loop	48
4.5.2	Additional SWAC system in effluent water loop	49
4.5.3	Maximum data center cooling without OTEC	49
4.5.4	Maximum SWAC cooling without OTEC	50
4.5.5	Maximum combined data center cooling	51
4.5.6	Maximum combined SWAC cooling	52
4.5.7	Conclusion future growth scenario	52
5	Results & Discussion	53
5.1	Optimized configuration	53
5.1.1	Optimization by configuration	54
5.1.2	Optimization by both configuration and daily storage	56
5.1.3	Optimization by both configuration and yearly storage	58
5.1.4	Conclusion optimization by configuration	59
5.2	Cases	60
5.2.1	10 MW OTEC power plant	60
5.2.2	20 MW _{th} SWAC	61
5.2.3	Maximum data center cooling demand	62
5.2.4	Maximum greenhouse area	64
5.2.5	Maximum fresh water production	64
5.2.6	Conclusion Cases	65
5.3	Sensitivity analysis	66
5.3.1	Seawater temperature sensitivity	66
5.3.2	Irreversible efficiency sensitivity	67
5.3.3	Heat losses sensitivity	68
5.3.4	Cold water pipe flow velocity sensitivity	69
6	Conclusion and Recommendations	71
6.1	Conclusions	71
6.1.1	Greenhouse storage	72
6.2	Recommendations	72
	Bibliography	75
A	Validation SWAC cooling curve correlation	79
B	Water usages: Optimization methods	83
B.1	Time-integrated OTE system	83
B.2	Optimization by daily thermal storage	84
B.3	Optimization by yearly thermal storage	85
B.4	Optimized configuration	86
B.5	Optimization by both configuration and daily thermal storage	87
B.6	Optimization by both configuration and yearly thermal storage	88
C	Water usages: Future growth scenario	89
C.1	Maximum data center cooling without OTEC	89
C.2	Maximum SWAC cooling without OTEC	90
C.3	Additional data center in the effluent loop	91
C.4	Additional SWAC in the effluent loop	91
C.5	Maximum combined data center cooling	92
C.6	Maximum combined SWAC cooling	93

D	Water usages: Cases	95
D.1	10 MW OTEC power plant	95
D.2	20 MW SWAC	96
D.3	Maximum data center cooling demand without thermal storage	97
D.4	Maximum data center cooling demand with thermal storage	98
D.5	Maximum greenhouse area without thermal storage	99
D.6	Maximum greenhouse area with thermal storage	100
D.7	Maximum fresh water production without thermal storage	101
D.8	Maximum fresh water production with thermal storage	102
E	The flaws of the Meteonorm data	103
E.1	Temperatures	103
E.2	Pressure.	104
E.3	Relative Humidity.	105
E.4	Wind speed	106
E.5	Daily global radiation	107
E.6	Evaluation	108

Nomenclature

Greek Symbols

Δ	Difference	
$\dot{\Phi}_V$	Volume flow	$[m^3/h]$
η	Efficiency	$[-]$
η_{carnot}	Carnot efficiency	$[-]$
Ω	Humidity ratio	$[g/kg]$
Φ	Flow velocity	$[m/s]$
ρ	Density	$[kg/m^3]$

Roman Symbols

\dot{m}	Mass flow	$[kg/s]$
\dot{Q}	Heat	$[W]$
\dot{W}	Work	$[W]$
C_p	Specific heat capacity	$[J/kg/K]$
d_{out}	Outside diameter	$[m]$
f_w	Wind factor	$[-]$
f_{GH}	Greenhouse factor	$[-]$
f_{shade}	Shading factor	$[-]$
G_{global}	Global horizontal radiation	$[W/m^2]$
T	Temperature	$[K]$
v_{wind}	Wind speed	$[m/s]$
A	Area	$[m^2]$
h	enthalpy	$[kJ/kg]$
p	Pressure	$[Pa]$
RH	Relative humidity	$[-]$
V	Volume	$[m^3]$

Abbreviations

AC	Air Conditioning
CAPEX	Capital Expenditures
CMEMS	Copernicus Marine Environment Monitoring Service
CRAC	Computer Room Air Conditioning

CRAH	Computer Room Air Handling
CWP	Cold Water Pipe
DCS	District Cooling System
DOW	Deep Ocean Water
HOST	Hawaii Open Science Park
IT	Information Technology
LCOE	Levelized Cost Of Electricity
NELHA	Natural Energy Laboratory of Hawaii Authority
NEMO	New Energy for Martinique and Overseas
NIOT	National Institute of Ocean Technology
OAPEC	Organization of Arab Petroleum Exporting Countries
OPEX	Operating Expenditures
OTE	Ocean Thermal Energy
OTEC	Ocean Thermal Energy Conversion
OTWP	Ocean Thermal Water Production
PBR	Photobioreactor
PICHTR	Pacific International Center for High Technology Research
RT	Refrigeration Tonnes
SDR	Standard Dimension Ratio
SF	Solar Factor
SIDS	Small Island Developing States
SWAC	Sea Water Air Conditioning
SWGHI	Seawater Greenhouse

Subscripts

<i>air</i>	Air related
<i>avg</i>	Average
<i>C</i>	Cold
<i>conv</i>	Convective
<i>curve</i>	Curve
<i>Data</i>	Associated with Data center cooling
<i>day</i>	Daily
<i>e</i>	Electrical
<i>env</i>	Environmental
<i>fw</i>	Fresh water

gen	Generator
GH	Associated with greenhouse cooling
H	Hot
in	Associated with the inlet stream
irrev	Irreversible
max	Maximum
OTEC	Associated with OTEC
OTWP	Associated with OTWP
out	Associated with the outlet stream
p	Pump
rad	Radiative
stor	Storage related
sw	Seawater
SWAC	Associated with SWAC
t	Turbine
th	Thermal
year	Yearly

List of Figures

1.1	Global ocean temperature difference between surface layer and cold deep sea water (image courtesy of Bluerise)	1
1.2	Thermohaline circulation or the global conveyer belt, figure adapted from the National Oceanic and Atmospheric Administration (NOAA) [38]	2
2.1	Comparison of mixture (solid lines) and pure fluid (dashed lines) idealized cycles, adapted from Iqbal and Starling [20]	7
2.2	The Advanced OTEC cycle, based on the Kalina cycle (image courtesy of Bluerise)	8
2.3	Working principle SWAC with cold deep seawater	10
2.4	Working principle data center cooling with cold deep seawater	11
2.5	Working principle data center cooling combined with the effluent water from the OTEC	12
2.6	Working principle hybrid greenhouse cooling system	13
2.7	Working principle OTWP combined with the effluent water from the OTEC	14
2.8	Schematic overview of a possible configuration of aquaculture with direct cold deep seawater and hot surface water	15
2.9	Schematic overview of a possible configuration of aquaculture with direct cold deep seawater and hot surface water	17
2.10	Schematic overview of a possible configuration of an Ocean Thermal Energy system	18
3.1	Carnot and thermal efficiency versus temperature difference between T_C and T_H	22
3.2	Cold and hot water mass flows versus temperature difference between T_C and T_H for a 10 MW OTEC power plant	24
3.3	The cooling demand curve of the SWAC for Curaçao 2016	25
3.4	Daily internet traffic for North America and Europe [21]	26
3.5	Server power versus CPU processing time [7]	26
3.6	The daily cooling curve for the data center cooling	27
3.7	Mollier diagram for the example with $T_{env} = 28^\circ C$, $P_{env} = 1.01325bar$, $RH = 70\%$, and $T_{air,out} = 15^\circ C$	30
3.8	Schematic overview of the OTE system model	32
3.9	Schematic overview of an OTE system configuration with an optimized design	35
4.1	The location of Hato Curaçao International Airport on the island	37
4.2	Seafloor topography Curaçao - The depth of the deepest data point of Copernicus for Curaçao	38
4.3	Curaçao 2007 - 2016: temperature difference between cold deep seawater and hot surface water for depths 763 meter, 902 meter, 1062 meter and 1245 meter	39
4.4	Curaçao 2007 - 2016: temperature of the cold deep seawater for depths 763 meter, 902 meter, 1062 meter and 1245 meter	39
4.5	The average and standard deviation of critical parameters	40
4.6	Schematic overview of the configuration of the Ocean Thermal Energy system for Curaçao	41
4.7	Curaçao 2007 - 2016: Maximum cold deep seawater usage per year in case of the simple demand analysis	42
4.8	Curaçao 2007 - 2016: Total deep seawater usage in case of the time-integrated OTE system	43
4.9	Curaçao 2007 - 2016: Maximum cold deep seawater usage per year in case of the time-integrated OTE system	43
4.10	Curaçao 2007 - 2016: Ecopark water surplus per year in case of the time-integrated OTE system	44
4.11	Curaçao 2007-2016: Total deep seawater usage in case of optimization by daily storage	45
4.12	Required storage capacity per subsystem in case of optimization by daily storage	46
4.13	Curaçao 2007-2016: Total deep seawater usage in case of optimization by yearly storage	46
4.14	Required storage capacity per subsystem in case of optimization by yearly storage	47

4.15 Curaçao 2007 - 2016: Ecopark water surplus per year in case of the maximum cooling capacity for an additional data center in the effluent water loop	48
4.16 Curaçao 2007 - 2016: Ecopark water surplus per year in case of the maximum cooling capacity for an additional SWAC system in the effluent water loop	49
4.17 Curaçao 2007 - 2016: Total deep seawater usage in case of maximum data center cooling without OTEC	50
4.18 Curaçao 2007 - 2016: Total deep seawater usage in case of maximum SWAC cooling without OTEC	50
4.19 Curaçao 2007 - 2016: Ecopark water surplus in case of maximum combined data center cooling	51
4.20 Curaçao 2007 - 2016: Ecopark water surplus in case of maximum combined SWAC cooling . . .	51
5.1 Schematic overview of the optimized configuration with the data center, greenhouse and OTWP in the Ecopark	53
5.2 Curaçao 2007 - 2016: Total cold deep seawater usage by optimizing the configuration (data center, greenhouse and OTWP in Ecopark)	54
5.3 Curaçao 2007 - 2016: Ecopark water surplus in case of optimization by configuration (data center, greenhouse and OTWP in Ecopark)	55
5.4 Schematic overview of the optimized configuration with SWAC, the data center, the greenhouse and OTWP in the Ecopark	55
5.5 Curaçao 2007 - 2016: Total cold deep seawater usage by optimizing the configuration (SWAC, data center, greenhouse and OTWP in Ecopark)	56
5.6 Curaçao 2007 - 2016: Ecopark water surplus in case of optimization by configuration (SWAC, data center, greenhouse and OTWP in Ecopark)	56
5.7 Curaçao 2007 - 2016: Total cold deep seawater usage in case of optimization by both the configuration and daily storage	57
5.8 Required storage capacity in case of optimization by both configuration and daily storage	57
5.9 Curaçao 2007 - 2016: Ecopark water surplus in case of optimization by both configuration and daily storage	58
5.10 Curaçao 2007 - 2016: Total cold deep seawater usage in case of optimization by both the configuration and yearly storage	58
5.11 Required storage capacity in case of optimization by both configuration and yearly storage	59
5.12 Curaçao 2007 - 2016: Ecopark water surplus in case of optimization by both configuration and yearly storage	60
5.13 Curaçao 2007 - 2016: Total cold deep seawater usage in case of a 10 MW OTEC power plant	61
5.14 Curaçao 2007 - 2016: Ecopark water surplus in case of a 10 MW OTEC power plant	61
5.15 Curaçao 2007 - 2016: Total cold deep seawater usage in case of a 20 MW_{th} SWAC installation . . .	62
5.16 Curaçao 2007 - 2016: Ecopark water surplus in case of a 20 MW_{th} SWAC installation	62
5.17 Curaçao 2007 - 2016: The effluent water mass flow in case of optimization by configuration	63
5.18 Curaçao 2007 - 2016: Maximum DOW water usage in case of maximum data center cooling demand	63
5.19 Curaçao 2007 - 2016: Maximum DOW water usage in case of maximum greenhouse area	64
5.20 Curaçao 2007 - 2016: Maximum DOW water usage in case of maximum fresh water production	65
5.21 Maximum DOW water usage and required cold water pipe outside diameter by changing cold deep seawater temperature	67
5.22 Maximum DOW water usage and required cold water pipe outside diameter by changing the irreversible efficiency	68
5.23 Maximum DOW water usage and required cold water pipe outside diameter by changing the heat loss factor	69
5.24 The required cold water pipe outside diameter by changing the cold water flow velocity	70
A.1 Old terminal cooling load and the measured environmental temperature	79
A.2 Old terminal cooling load and the shifted environmental temperature	80
A.3 The solar factor of Curacao for the months of a year	80
A.4 Old terminal cooling load, the shifted environmental temperature and the calculated cooling load	81
A.5 Old terminal cooling load and the extrapolated calculated cooling load for the year 2014	81

A.6	Old terminal cooling load and the calculated cooling load based on eq. A.1 from 31-02-2014 to 03-02-2014	82
B.1	Water usages of each sub-system in case of the time-integrated OTE system	83
B.2	Water usages of each sub-system in case of optimization by daily thermal storage	84
B.3	Water usages of each sub-system in case of optimization by yearly thermal storage	85
B.4	Water usages of each sub-system in case of optimization by changing the configuration of the OTE system	86
B.5	Water usages of each sub-system in case of both optimization by changing the configuration of the OTE system and daily thermal storage	87
B.6	Water usages of each sub-system in case of optimization by both changing the configuration of the OTE system and yearly thermal storage	88
C.1	Water usages of each sub-system in case of the maximum data center cooling without OTEC	89
C.2	Water usages of each sub-system in case of the maximum SWAC cooling without OTEC	90
C.3	Water usages of the additional data center in the effluent water loop (Ecopark)	91
C.4	Water usages of the additional SWAC system in the effluent water loop (Ecopark)	91
C.5	Water usages of each sub-system in case of the maximum combined data center cooling	92
C.6	Water usages of each sub-system in case of the maximum combined SWAC cooling	93
D.1	Water usages of each sub-system in case of a 10 MW instead of a 500 kW OTEC power plant	95
D.2	Water usages of each sub-system in case of a 20 MW instead of a 7.5 MW SWAC system	96
D.3	Water usages of each sub-system in case of the maximum data center cooling capacity when there are no other sub-systems in the Ecopark	97
D.4	Water usages of each sub-system in case of the maximum data center cooling capacity when there are no other sub-systems in the Ecopark (with daily thermal storage)	98
D.5	Water usages of each sub-system in case of the maximum greenhouse area when there are no other sub-systems in the Ecopark	99
D.6	Water usages of each sub-system in case of the maximum greenhouse area when there are no other sub-systems in the Ecopark (with daily thermal storage)	100
D.7	Water usages of each sub-system in case of the maximum fresh water production when there are no other sub-systems in the Ecopark (With daily thermal storage)	101
D.8	Water usages of each sub-system in case of the maximum fresh water production when there are no other sub-systems in the Ecopark (with daily thermal storage)	102
E.1	Temperatures Hato Curacao International Airport generated with Meteonorm for the years 2007 to 2016	103
E.2	Temperatures Hato Curacao International Airport generated with Meteonorm for the years 2007 to 2016 (zoomed in)	104
E.3	Pressures Hato Curacao International Airport generated with Meteonorm for the years 2007 to 2016	104
E.4	Pressures Hato Curacao International Airport generated with Meteonorm for the years 2007 to 2016 (zoomed in)	105
E.5	Relative Humidity Hato Curacao International Airport generated with Meteonorm for the years 2007 to 2016	105
E.6	Relative Humidity Hato Curacao International Airport generated with Meteonorm for the years 2007 to 2016 (zoomed in)	106
E.7	Wind speed Hato Curacao International Airport generated with Meteonorm for the years 2007 to 2016	106
E.8	Wind speed Hato Curacao International Airport generated with Meteonorm for the years 2007 to 2016 (zoomed in)	107
E.9	Daily global radiation for Hato Curacao International Airport generated with Meteonorm for the years 2007 to 2016	107
E.10	Daily global radiation for Hato Curacao International Airport generated with Meteonorm for the years 2007 to 2016 (zoomed in)	108

Introduction

Solar energy is the biggest energy source that comes to earth. Without the solar energy, the temperature on earth would be much lower [2]. The amount of solar radiation that reaches earth is about $1.73 \cdot 10^5$ TW [58]. Converted to TWh/yr, the solar insolation is $1.52 \cdot 10^9$ TWh/yr and almost 10 000 times higher than the primary energy use of $1.57 \cdot 10^5$ TWh/yr [19]. Most of that solar energy is absorbed by the water in the oceans. Even more, effectively all of the solar energy that reaches earth is captured within a shallow surface layer of 35 to 100 m thick. Wind and waves result in an almost uniform distribution of temperature and salinity in the surface layer. The annual average temperature between approximately 15° north and 15° south of the equator varies from about 27°C and 29°C . Underneath this surface layer the water temperature starts to decrease with depth until a temperature of about 5°C is reached around 1000 meters deep. This cold water comes from the molten ice at the arctic regions. Cold water flows along the bottom of the ocean from the poles to the equator as a result of the higher density and minimal mixing with the warmer water above. The warm surface layer and the cold deep sea water can be seen as large reservoirs, with a temperature difference that varies between the 22°C and 25°C throughout the year. In figure 1.1 the areas with at least 20°C temperature difference between warm surface layer and the cold deep sea water are colored light orange, the area's with at least 22°C temperature difference are colored dark orange.

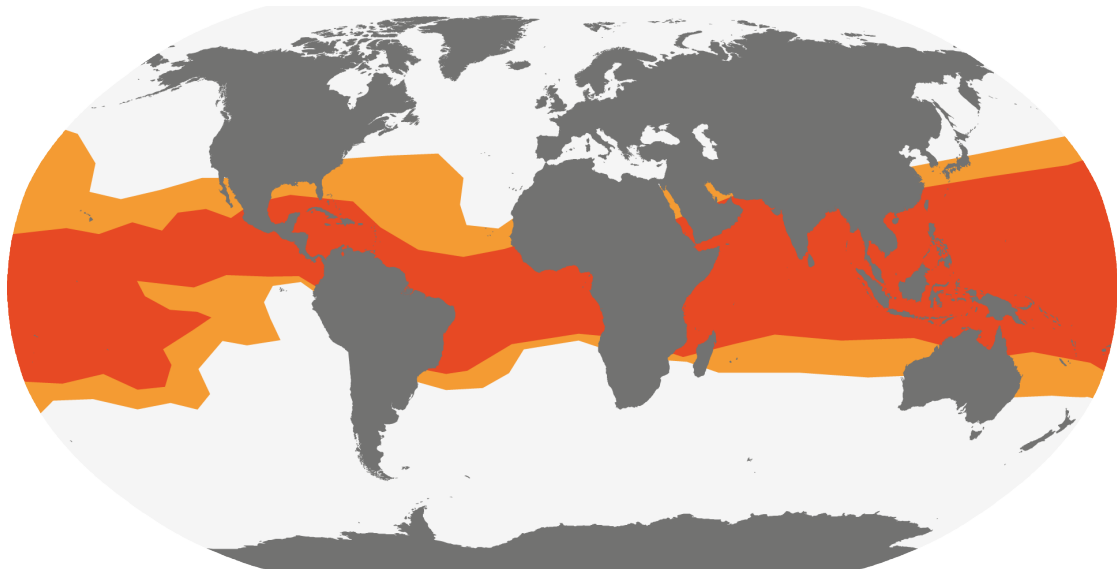


Figure 1.1: Global ocean temperature difference between surface layer and cold deep sea water (image courtesy of Bluerise)

The temperature difference between the cold deep sea water and warm surface water is the moving power of the marine renewable energy source Ocean Thermal Energy Conversion (OTEC). The OTEC process uses this temperature difference to operate a heat engine, which produces electric energy. Because of the relatively constant temperature difference throughout the year, OTEC is very useful for baseload power. This is

a big advantage compared to other renewables that are dependent on (seasonal) weather conditions, such as wind and photovoltaics. A recent study estimates that the maximum world wide potential of OTEC is 30 TW [53], which is about $2.63 \cdot 10^5$ TWh/yr. Compared to the global annual total primary energy supply of $1.57 \cdot 10^5$ TWh/yr (18 TW) in 2013 [19], this potential is almost twice as high as the annual consumption. But a consequence of producing the maximum potential is that it influences the oceanic thermohaline circulation. The thermohaline circulation is the motion of the ocean caused by temperature and salinity driven currents in the deep ocean and wind-driven currents on the surface [39]. The thermohaline circulation can be seen in figure 1.2. The maximum OTEC power production that could be achieved with little effect on the oceanic temperature field is estimated to be of the order of 5-10 TW [53].



Figure 1.2: Thermohaline circulation or the global conveyor belt, figure adapted from the National Oceanic and Atmospheric Administration (NOAA) [38]

1.1. Problem description

Small Island Developing State (SIDS) or tropical islands are facing major issues. Even though the absolute amount of greenhouse gases they emit is low, the emission per capita is high. For example, the number two and three on the list of CO₂ emission per capita are Trinidad and Tobago and Curaçao with about 34 t/person. This is seven times higher than the global average of about 5 t/person [65]. This is because the electricity is mainly produced by fossil fuels. Besides, energy costs are quite high because most islands do not have natural fossil fuel resources and have to import the fuels from some place else.

Furthermore, small island states in general are more vulnerable to climate change than the mainland. This can lead to for example shrinking fresh water resources due to variations in rainfall, crop failures due to too much rain or too little rain, land loss due to sea level rise and coastal ecosystem change due to thermal stress [40].

OTEC can be a solution to the energy problem on tropical islands. OTEC can function as baseload power source in the energy mix. According to Schelleman & Van Weijsten [56] 100% renewable electricity (for tropical islands) can only be realized by using OTEC, since a combination of solar and wind energy would require an immense amount of storage to reach 100% [67]. The downside is that the Levelized Cost Of Electricity (LCOE) is very depending on the scale of the OTEC power plant. A small plant is relatively expensive compared to a large plant, so a large plant is much more favorable. However, the power delivered by a large OTEC power plant with a competitive LCOE might be too much for a small island.

1.2. Ocean Thermal Energy system

A solution to tackle these problems simultaneously is to develop an Ocean Thermal Energy (OTE) system. When the OTEC power plant is placed onshore, the potential of the cold deep sea water can be exploited in more than one way. The cold deep seawater can be used for Sea Water Air Conditioning (SWAC), a dis-

strict cooling system. Furthermore, the effluent water that leaves the OTEC and/or SWAC installations, which will have a temperature of about 11°C, can be used for many other applications like fresh water production, greenhouse cooling, aquaculture and algae cultivation. With these applications, small islands can solve the problems of existing fresh water scarcity and food insecurity or future problems due to climate change. This can make an OTE system to be economically more attractive than just an OTEC power plant.

To make an OTE system even more economically attractive, research can be done towards the synergies between components. A time-dependent integration of the (water) demands of an OTE system components can lead to a lower maximum cold deep seawater mass flow than that all the maximum mass flows are added up. A lower mass flow results in a smaller required cold water pipe (CWP) diameter and the CWP pumps can be smaller. This can lead to a cost reduction, thus making an OTE system more attractive. Currently the time-dependent synergies in an OTE system have not been researched, because the main focus is on OTEC.

1.3. Relevance

Bluerise is a start-up company located in Delft, the Netherlands, that develops solutions to harness the Ocean's power. Bluerise is a technology provider and project developer of Ocean Thermal Energy solutions. The thermal energy stored in the tropical ocean can be used to generate sustainable electricity, cooling, and fresh water. Bluerise is specialized in OTEC, SWAC technologies and related Deep Sea Water applications.

Bluerise provides technology and development plans for implementation of OTEC and SWAC as well as Ocean Ecoparks that utilize the ocean resources by means of innovative technologies for desalination, agriculture and aquaculture among others.

Creative thinking, a sustainable mindset and a fresh 21st century look at all system components drives Bluerise to design economical viable and technically feasible solutions. Bluerise provides consulting and engineering services to governments, project developers, energy companies and utilities.

1.4. Research objective

The main objective of this thesis is to investigate the (water) demands of the subsystems and the time-dependent integration of the (water) demands in an Ocean Thermal Energy (OTE) system. A comparison can be made between a system where all the maximum water demands are added up and a system where synergies are taken into account. This comparison will be done for the maximum cold deep seawater usage or the cold water pipe diameter. Therefore the research question of this thesis is:

'What is the influence of time-dependent integration of the subsystems in an Ocean Thermal Energy system on the cold deep seawater mass flow and cold water pipe diameter?'

The subquestions that will help to answer the research question are:

- *What are possible (downstream) subsystems in an Ocean Thermal Energy system?*
- *What are the expected cold water demands or how can they be estimated for each subsystem?*
- *What are the benefits of having different kinds of energy storage to lower the peak of the cold water demand?*
- *How can the time-dependent synergies in the Ocean Thermal Energy system be optimized?*
- *What are the key parameters in the model and what is their impact on the calculated results?*

1.5. Research approach

The methodology used to answer the research question is as follows:

- A brief literature review on the history of Ocean Thermal Energy systems
- A literature review on the possible components for an OTE system and the associated demand curves.
- Development of submodels to simulate the demands per OTE component.
- Development of a model to combine the submodels to an Ocean Thermal Energy system.
- Select the components that are suitable for integration and optimization.
- Integrate and optimize the model and submodels.
- Researching the sensitivity of a few key parameters on the results.
- Comparing the results of the models with and without synergy and optimization based on the total amount of deep seawater usage and cold water pipe diameter.

1.6. Outline

Chapter 2 starts with the brief literature review on previous research done on Ocean Thermal Energy systems / Ocean Ecoparks. Thereafter the most obvious/common components of an Ocean Thermal Energy system and their working principle will be discussed. Subsequently, in chapter 3 the demands and the modeling of the subsystems, the model integration and possible optimization techniques for an OTE system will be discussed. Hereafter a case study for the island of Curaçao will be made in chapter 4. This chapter also includes the optimization by thermal storage and a some future growth scenarios. In chapter 5 the optimization by changing the OTE configuration and more cases will be investigated and be discussed. Also a sensitivity analysis will be made for some of the key parameters in this chapter. Lastly, the conclusions will be drawn about the results obtained by the base case study and the other results and further recommendations for improving the model will be made in chapter 6.

2

Ocean Thermal Energy system (OTEC, SWAC & Ecopark)

OTEC is the key technology in an Ocean Thermal Energy system. But next to OTEC, there are several other possible subsystems that can contribute from the cold water supply in an OTE system. Also an OTE system without an OTEC power plant is a possibility. The sub-systems that are most likely to be implemented will be discussed in this chapter. In section 2.1 a brief historical background OTEC will be given. Subsequently, in section 2.2 a brief history and future prospects of research and development of Deep Ocean Water (DOW) applications and DOW research parks will be given. Thereafter, in section 2.3 the expected subsystems of an OTE system will be discussed. For each subsystem a problem description concerning the current situation is given and the benefits compared to the existing systems are explained. This is done in subsection 2.3.1 to 2.3.6 for SWAC, data center cooling, greenhouse cooling, fresh water production (OTWP), aquaculture cultivation and algae cultivation, respectively.

2.1. OTEC

Early days of OTEC

The concept of OTEC is not new. In 1881, the French physicist Jacques Arsene D'Arsonval published an article that proposed a heat engine that can derive power from low temperature sources available in nature, with a temperature difference between evaporator and condenser as low as 15°C [2]. D'Arsonval noted that this temperature difference is widely available in nature, especially in the oceans at the equator. In 1928, one of D'Arsonval's students, George Claude, experimented with an open-cycle OTEC with cooling water of a steel power plant in Ougree-Marhaye (Belgium) of 30°C . During the experiment, the turbine generated a power output of 50 kW [2]. The first OTEC power plant was built by Claude in Matanzas, Cuba in 1930. This plant was able to produce 22 kW, but due to power consumed by the water pumps no net power was produced. Even though the technical feasibility of OTEC was proven, the project was terminated after 11 days because of failure of the cold water pipe due to a storm [2]. In 1933 the 10,000-ton cargo vessel '*Tunesie*' was converted by Claude to a floating open-cycle OTEC power plant and moved to Brazil. Unfortunately, the ship sank before it was ready to operate, due to the weather conditions [59]. Despite the misfortune of the '*Tunesie*' project, Claude proposed a 40 MWe OTEC power plant at Abidjan, Ivory Coast to the French government. This site had some favorable conditions for OTEC: the sea was calm, the water of a solar-heated lagoon could be used as warm water source and the coastline is very steep. The government was interested in the Abidjan project and formed a company '*Energie de Mer*' to research the development and implementation. However, in the 1955 the project was abandoned because oil-based electricity generation became cheaper due to large amounts of cheap oil and plans were made to build a large dam with a hydroelectric power plant close to Abidjan [2],[59].

OTEC regained interest in the 1960s by J.H. Anderson and his son James H. Anderson, Jr. They developed a closed-cycle OTEC power plant, designed to be more practical, compact and economical [46]. Although a cost estimate showed that this system was economically competitive with other alternatives like oil, coal or nuclear power, little attention was given to OTEC because the alternatives were seen as the energy of the future [2].

1970s-Now

In the 1970s new interest was shown in OTEC by the US and Japan. One of the reasons was the oil crisis of 1973, an embargo of the Organization of Arab Petroleum Exporting Countries (OAPEC) against countries that supported Israel during the Yom Kippur War [2]. Oil prices were rising worldwide due to this embargo. By 1974, oil prices quadrupled to nearly US\$12 per barrel [5]. But also the awareness for the environment rose in the 1970s, with the report *'The limits to growth'* (1972) of the Club of Rome as best known example. In this report a connection is made between economical growth and the impact of that growth on the environment [34].

An overview of the most important OTEC projects and events since 1970 can be found below.

- 1970-1981, Japan/Nauru. The company Tokyo Electric Power Services starts researching and developing a land-based closed-cycle OTEC power plant on/for the island Nauru in the Pacific Ocean. On 14 October 1981 the power plant became operationable and was able to generate 120 kW electricity [59].
- 1974-1979, Japan. The *'Sunshine project'* was initiated by the Japanese government to develop new energy technologies, which included OTEC. At first, OTEC was considered unlikely, but till 1979 many experts researched the possibilities of OTEC. The conclusion was that OTEC was economically relatively feasible compared to other large scale energy alternatives and could have a substantial contribution to the electrical power generation of the future [59].
- 1974-1979, Hawaii. The Natural Energy Laboratory of Hawaii Authority (NELHA) is established at Kea-hole Point on the Kona coast of Hawaii, dedicated to the support of OTEC and other solar energy programs. A collaboration between the State of Hawaii, Makai Ocean Engineering, Lockheed Martin, Alfa Laval and Dillingham Corporation began to design and develop a small offshore closed-cycle OTEC power plant [2]. The so-called *'Mini-OTEC'* was able to generate about 50 kW and operate for three months in late 1979 and was the first floating OTEC power plant with a net energy output [59].
- 1981-1982, Russia. The Russian engineer Dr. Alexander Kalina developed and patented a thermodynamic cycle which uses a mixture of ammonia and water as working fluid and can be used in OTEC power plants. This mixture has potential to improve the efficiency of OTEC [23].
- 1993, Hawaii. NELHA collaborates with the Pacific International Center for High Technology Research (PICHTR) to develop an open-cycle OTEC power plant of 210 kW. Besides OTEC, the cold water is also used for cooling and fresh water, which can be used for aquaculture or agriculture [2],[41].
- 1994, Japan. Saga University developed a 4.5 kW test setup to research the Uehara cycle. This thermodynamic cycle is designed to have an even higher efficiency than the Kalina cycle [43].
- 2002, India. A 1 MW floating OTEC power plant was tested near the coast of Tamil Nadu by the National Institute of Ocean Technology (NIOT). The project was shut down due to failure of the one kilometer long cold water pipe [47].
- 2013, Japan. The Institute of Ocean Energy of Saga University and Japanese companies completed the installation of a research, development and demonstration 50 kW onshore OTEC power plant on Kumejima. The cold deep seawater is not only used for generating electricity, but also for cooling, aquaculture and agriculture [24].
- 2014, Martinique. The NEMO (New Energy for Martinique and Overseas) project, a collaboration between Akuo Energy and DCNS, got a subsidy up to €72.1 million for the construction of a 16 MW offshore OTEC power plant at Martinique [9].
- 2015, Hawaii. A team up with Makai Ocean Engineering and Lockheed Martin resulted in world's largest grid connected operational OTEC power plant. The 100 kW onshore power plant is able to generate electricity for 120 households [45].

OTEC cycles

Typically, OTEC can be separated in three different types of cycles. Open-cycle systems, closed-cycle systems and hybrid systems. All the three cycles are in essence a (Organic) Rankine cycle.

An open-cycle OTEC system uses seawater as working fluid, where part of the seawater is vaporized in a flash evaporation chamber. The cycle is called 'open' because the working fluid is not recycled to the evaporator after it is condensed. The condensed vapor is free of salt and can be used as fresh water [17].

The closed-cycle OTEC system uses a working fluid with a low boiling point, which is evaporated in a heat exchanger with the hot surface water. In the case of an closed-cycle, the liquid is returned to the evaporator after the condenser. This way the working fluid and the environment can be separated [17].

As the name suggests, the hybrid-cycle is a combination of the open-cycle and closed-cycle OTEC system.

The difference is that first the seawater is evaporated, whereafter the steam is used in a heat exchanger to evaporate the working fluid of a closed-cycle system [17].

Despite the advantage that open-cycle OTEC produces fresh water, larger turbines are needed compared to closed-cycle OTEC to compensate the relatively large volumetric flow rates of low-pressure steam to produce the same amount of power [44].

2.1.1. Advanced OTEC cycle

The Advanced OTEC cycle is a thermodynamic cycle that is inspired by the Kalina cycle. The Kalina cycle is a specific thermodynamic cycle which uses a mixture of two fluids with different boiling points as working fluid, developed and patented by the Russian Dr. Alexander Kalina in 1982 [23]. In this case not all working fluid will evaporate. Therefore the Kalina cycle has an additional separator, absorber and recuperator compared to a standard (Organic) Rankine cycle. This way, only the vaporized working fluid will flow through the turbine. The advantage of a mixture as working fluid is that there is a temperature glide when evaporating or condensing. This results in a evaporating and condensing temperature line that follows the slope of the hot and cold water while heat is exchanged. This results in a higher cycle efficiency than with a pure fluid. A comparison between a mixture and a pure fluid for idealized cycles can be found in figure 2.1.

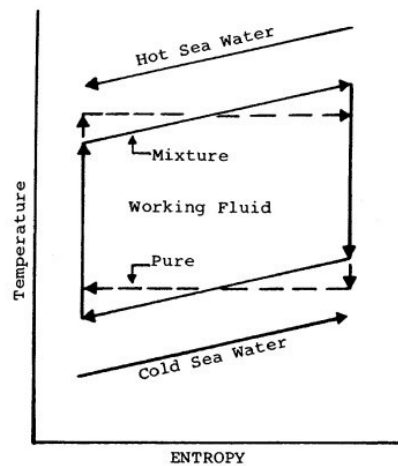


Figure 2.1: Comparison of mixture (solid lines) and pure fluid (dashed lines) idealized cycles, adapted from Iqbal and Starling [20]

The Advanced OTEC cycle which BlueRise is using, uses a mixture of ammonia and water as working fluid. Almost an increase of 80% efficiency has been claimed compared to conventional closed-cycle OTEC systems [16]. Furthermore, only 90% of the heat transfer surface area is needed compared to a pure fluid (for equal properties), which translates directly to a possible reduction of 10% in heat exchanger costs [20]. Since the heat exchangers are expected to be the most expensive parts of the OTEC power plant, every percent reduction in heat exchanger costs is significant for the CAPEX (Capital Expenditures) of the OTEC power plant.

Working principle

In the Advanced OTEC cycle the working fluid is partly vaporized in the evaporator. This is done by the heat transfer from the hot surface water. This results in a pure ammonia vapor and a liquid with a lower ammonia content. In the separator the vapor is separated from the liquid. The vapor is expanded through a turbine, which drives a generator to generate electrical energy. The liquid flows from the separator to the recuperator, where it preheats the working fluid before it enters the evaporator. The streams are mixed before the condenser. The mixture is completely liquefied and cooled in the condenser by the cold deep sea water. After the condenser the working fluid is compressed and pumped to the evaporator. A schematic overview of this process can be seen in figure 2.2

Thanks to its large energy potential and the fact that OTEC is a base-load power source, OTEC has the potential to become a major player in the renewable energy market, especially for SIDS with small, isolated electric grids.

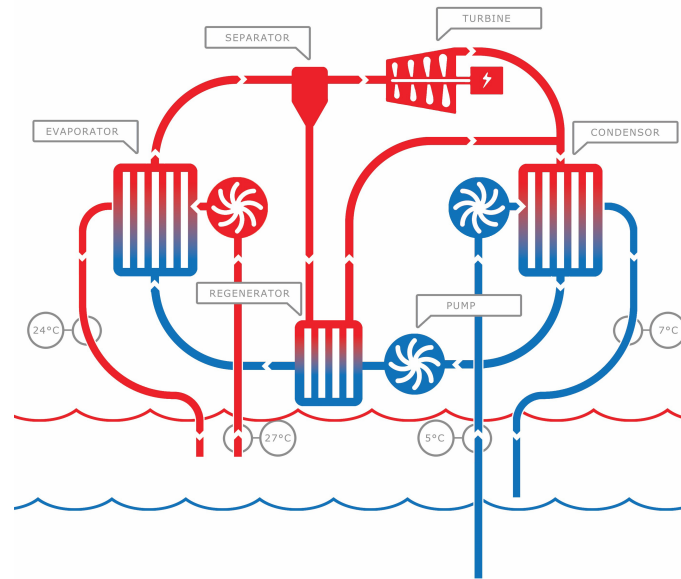


Figure 2.2: The Advanced OTEC cycle, based on the Kalina cycle (image courtesy of Bluerise)

2.2. OTE systems and DOW

In this section a brief history of research and development of OTE systems is given in subsection 2.2.1. A brief history of research and development of DOW industries will be given in subsection 2.2.2. In subsection 2.2.3 the present and future OTEC and OTE projects will be discussed.

2.2.1. Research Parks

In 1976 the Agency of Science and Technology of Japan started researching Deep Ocean Water (DOW). From the start till 1986, an understanding of the characteristics of DOW and the technology for pumping system was developed. Subsequently, a 5-year research program was funded by the agency, which resulted in the establishment of the DOW pumping system in Kochi and Toyama Prefectures [37]. At the time of writing 16 sites in Japan DOW have been researched. The Okinawa Prefecture's Deep Seawater Research Institute on Kumejima is the leader in DOW research and utilization since the opening in the year 2000. On Kumejima the DOW is utilized for different kind of applications such as SWAC, the cooling of greenhouses to grow winter crops during summer, cultivating Kuruma Prawns and sea grapes, producing cosmetics and in a local spa and pool [42].

In 1993 a collaboration between NELHA and PICHTR started developing an open-cycle OTEC in Hawaii to not only produce electricity, but also for cooling and fresh water, which can be used for aquaculture and agriculture [41]. The Hawaii Ocean Science & Technology (HOST) park is the largest DOW related park with an area of 350 ha. The HOST park has proven that DOW can be used for a wide range of applications next to OTEC, such as SWAC, fresh water production, producing pharmaceuticals and mariculture [44].

2.2.2. DOW industries

The concept of using DOW as cold source for a District Cooling System to supply air conditioning was first conceived by NELHA in 1983. The first primitive Sea Water Air Conditioning was used to cool a small research van. The system consisted of a truck radiator, a small box fan and small flow of cold water. The principle of SWAC can also be used with other sources like cold lake water and river water. Examples of existing SWAC installations are in Stockholm, Sweden (since 1995, seawater), Cornell University USA (since 2000, lake water), Toronto, Canada (since 2004, lake water) and Amsterdam, Netherlands (since 2006, lake water). Examples of proposed SWAC installations sites are Honolulu, Hawaii (seawater), Reunion Island (seawater) and Curaçao (seawater). [63].

Since the first design of the open-cycle OTEC in 1928 by Claude, the foundation of OTEC combined with fresh water production was made. This because part of the seawater is vaporized and can be used as fresh

water after it has left the condenser. In 1967 Gerard and Worzel [15] proposed a method to produce fresh water by condensing moisture from humid air whereby DOW can be used as cold source. They proposed to use windmill-driven generators to deliver electricity to pump up the DOW, but an alternative is to combine this method with OTEC. More recently a combination of OTEC and a reverse osmosis process to produce fresh water was proposed by Dyer and Ragan [11].

In 1994 the first Seawater Greenhouse (SWG) was built in Tenerife, Canary Islands, Spain. With the SWG crops could be cultivated and seawater desalinated. Crops such as tomatoes, spinach, dwarf pea, pepper and artichokes were cultivated in a 360 m² greenhouse. Thereafter other seawater greenhouses were built in Al-Aryam Island, Abu Dhabi (2000), Oman (2004), Port Augusta and Australia (2010) [1]. Another SWG is being built in Berbera, Somaliland and should be completed in Spring 2017 [57].

Aquaculture cultivation with nutrient-rich DOW has been developed in several coastal regions since the 1970s [44]. By controlling variables like temperature, salinity and nutrient concentration, DOW can be used for both tropical and cold water marine cultures [37]. The combination with OTEC was first proposed in the beginning of the 1980s by Roels et al. [54] and Daniel [10].

A special kind of aquaculture is the cultivation of algae. Several companies at the HOST park in Hawaii are growing algae with the DOW. Cyanotech Corporation is growing *Spirulina* which for example can be used as food supplements or pigments. Other companies are cultivating microalgae to produce biofuels and edible vegetables [44].

2.2.3. Present & Future

Bluerise is developing an Ocean Ecopark on the island of Curaçao near the Hato International Airport. Ocean Thermal Energy systems can have big advantages for other tropical islands as well. Therefore Bluerise is investigating the possibilities of OTEC combined with other DOW usages for other islands too. But besides the research parks in Japan and Hawaii, Bluerise is the only company known to research and develop Ocean Ecoparks. Most other companies are focusing only on OTEC or SWAC. This is probably because of the limitation of onshore OTEC power plants. Estimates show that the tipping point that offshore OTEC becomes economically more attractive than an onshore OTEC plant is between 5-10 MWe. Thus, when an island has a bigger electricity demand, offshore OTEC will be the obvious choice. Unless the demand of an island is to have an onshore OTEC with an Ocean Thermal Energy system of course.

2.3. OTE subsystems

Small Island Developing States (SIDS) (small tropical islands) are the perfect locations for OTEC and OTE systems. Most of them have diesel generators as base load electricity providers, they need cooling because they are located near the equator and there is a scarcity of fresh water. OTE systems can provide the SIDS with renewable/sustainable alternatives for the conventional technologies. In this section the most obvious technologies that can be linked with OTEC/DOW are explained. The problem with the conventional technology is described for each component, followed by the solution that can tackle the problem with help of DOW. This will be done for SWAC, data center cooling, greenhouse cooling, fresh water production, aquaculture cultivation and algae cultivation, respectively.

2.3.1. Sea Water Air Conditioning

The environmental temperature is most of the time high in regions where OTEC is feasible. The high air temperature is the cause of the hot surface water that drives the OTEC cycle. High air temperatures are not comfortable for humans beings. Therefore a lot of cooling capacity is needed to cool houses, school, office buildings, hotels etcetera. Normally this is done by Air Conditioning (AC). Conventional AC is expensive to operate due to large electrical power requirements, because this process uses evaporative cooling of a gas to transfer heat from the heat source (the environment) to the working fluid.

A renewable alternative for conventional AC is Sea Water Air Conditioning (SWAC). SWAC uses the cold water from the bottom of the ocean or from the bottom of a lake to cool fresh water in a heat exchanger. Thereafter the chilled fresh water can be used in a District Cooling System (DCS) for supplying cold water to buildings for air conditioning.

The biggest advantage of SWAC is that it can save up to 85% of energy consumed compared to conventional AC systems. This reduction is a result of to the fact that no fossil fuels are used and individual AC systems are less efficient and more expensive than a DCS [32].

Working principle

The working principle of SWAC relies on that of a District Cooling System. But instead of a chiller, the cold deep seawater of the effluent water coming from the OTEC is used to cool the water in a DCS. When the seawater replaces an existing DCS with a chiller that is designed for cooling water to a temperature of about 6°C , the cold deep seawater should be used as cold source. First the cold deep seawater of about 5°C is pumped to a cooling station. In that cooling station the DOW flows through a heat exchanger. On the other side of the heat exchanger fresh water cools down to about 6°C due to the heat transfer to the cold seawater. The chilled fresh water then flows through the DCS to the users. There the cold water is used in an air conditioner to cool air. The heated up fresh water flows back to the cooling station where it is cooled and the cycle can be repeated. The less cold effluent seawater can flow to the Ecopark where it can be used for other purposes.

In the case that a completely new DCS has to be built, it might be considered to connect the DCS, and therefore the SWAC, to the effluent water of the OTEC. The effluent water of about 11°C is cold enough to be used as a cold source for the DCS. Though, it has to be checked if the effluent water mass flow is high enough to satisfy the SWAC demand. A schematic overview of a SWAC system connected to the cold deep seawater via a DCS can be found in figure 2.3.

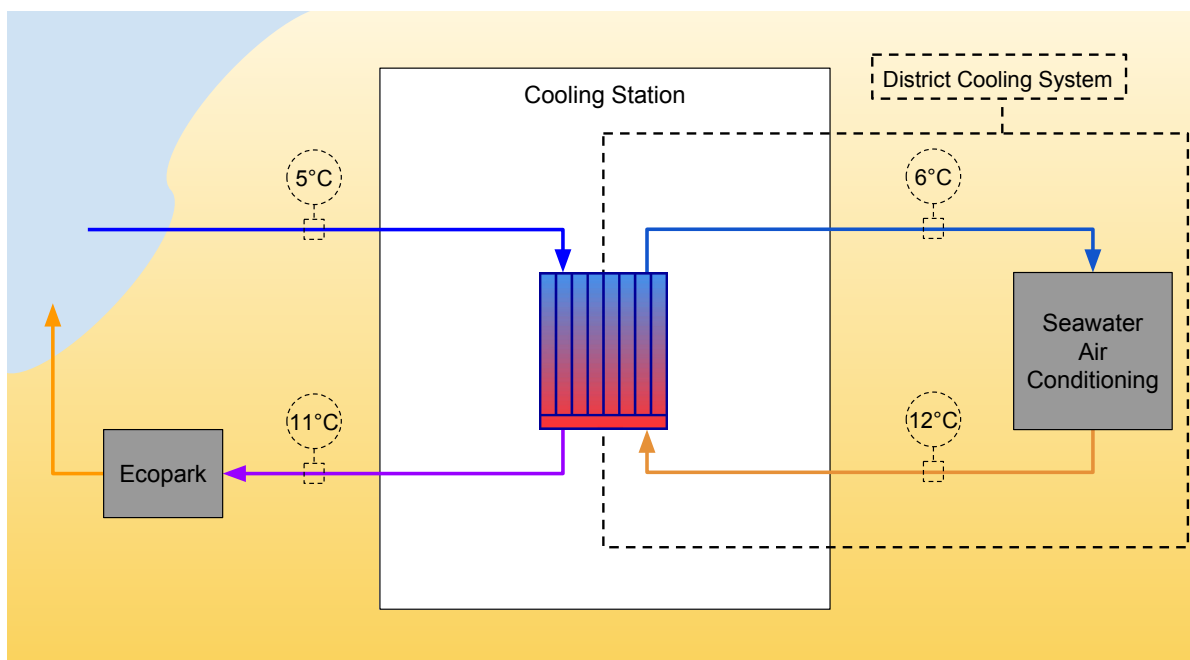


Figure 2.3: Working principle SWAC with cold deep seawater

The cold water usage of the SWAC installation is directly coupled to the cooling demand of the DCS. When the temperature difference between inlet and outlet of the DOW side is kept constant, this results in a higher mass flow rate of the water with a higher cooling demand. It is important to have a good approximation of the cooling demand, because it can be expected that the cooling demand fluctuates a lot over a year.

2.3.2. Data center cooling

A data center is a place that accommodates many computing resources that collect, store, share, manage, and distribute a large volume of data. It consists of all necessary data center facility elements (space, power, and cooling) and IT infrastructure elements (server, storage, and network) based on business requirements, according to Wu and Buyya [66]. Cooling is one of the three main concerns for a data center. Without a cooling system, a data center could not operate. The CAPEX of cooling equipment can be up to 50% for some high density data centers. Conventionally, a chiller is used in combination with a Computer Room Air Conditioning (CRAC) or a Computer Room Air Handling (CRAH) unit to deliver cold air to the racks with IT equipment [66]. The cooling of water is an energy intensive process, since a chiller makes use of evaporative cooling to reject heat to the environment, just like an AC.

Another way to cool a data center is to use liquid cooling instead of an air-cooled system. In general liquids have a higher heat capacity than air, so a smaller liquid mass flow rate is needed compared to air

cooling [66]. Liquid cooling can even become necessary when cooling demands of high-density racks incline to a level that it is almost impossible to cool with air.

Both types of data center cooling can be combined with an OTE system. The data center can be cooled with either the cold deep seawater or the effluent water coming from the OTEC. The main advantage of using this cold water is that there is no need for a chiller. This way a lot electrical energy can be saved, which has a positive effect on the OPEX of the data center.

Working principle

In the case of a data center different cooling strategies are possible, depending on the current equipment. When there is an existing data center that is designed with a chiller that cools water to a certain temperature it will be difficult to operate with a different temperature. Therefore it might be needed that the data center has to use water with a temperature of 8°C or lower like in the case of a chiller [66]. When this is the case, the data center needs to be included into the DCS that is connected to the cold deep seawater. The chilled water in the DCS can be used directly to cool the air or a liquid in with a CRAH unit.

On the other hand, when a data center needs to be built or when it is no problem to change cooling equipment, the cooling can be designed in such a way that it can make use of the effluent water of about 11°C that comes from the OTEC power plant. This way it is possible to reduce the mass flow of the cold deep seawater and still deliver the required cooling demand. With the same supply temperature of the air (or liquid in case of liquid cooling), the effluent water mass flow needs to be higher to reach the same cooling demand compared to the previous case. But this does not have to be a problem when there is sufficient effluent water from the OTEC.

The effluent water of the OTEC can be used in a heat exchanger to cool fresh water in a DCS. The chilled water in the DCS of about 12°C can be used to cool air in a CRAH unit or to cool another liquid when liquid cooling is used. A schematic overview of data center cooling with the use of cold deep seawater and cooling with the effluent water coming from the OTEC in combination with air cooling can be found in figures 2.4 and 2.5, respectively. The temperatures in these figures are estimates or based on maximum allowable temperatures minus a safety factor and desired air/liquid supply temperatures by Wu and Buyya [66].

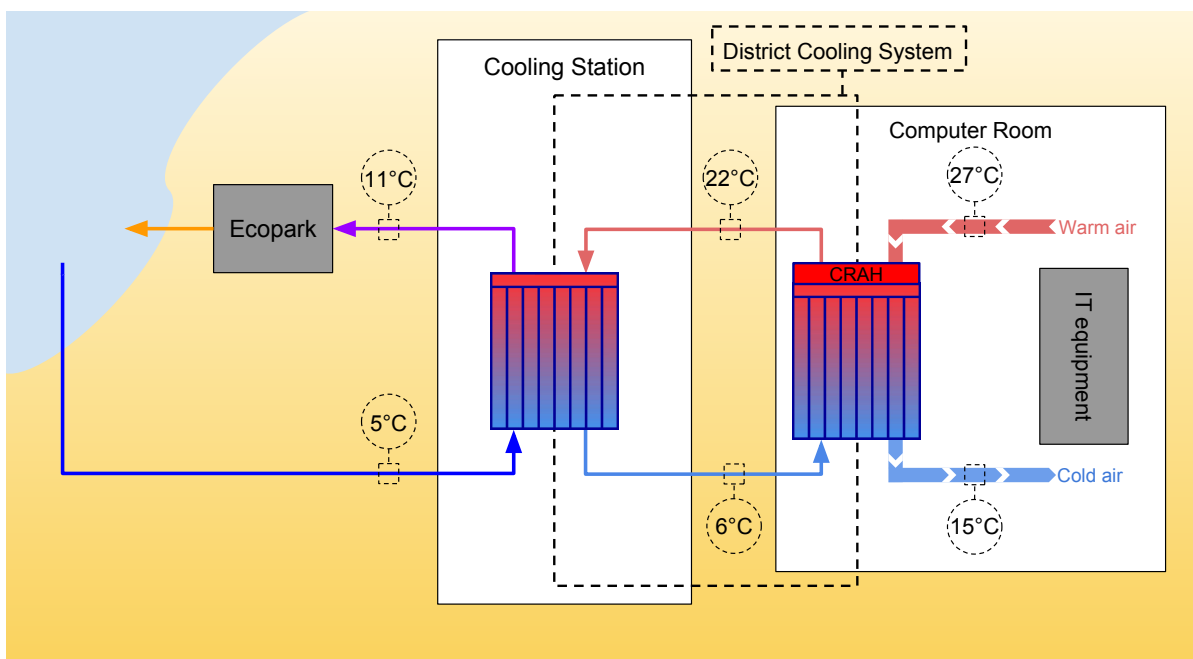


Figure 2.4: Working principle data center cooling with cold deep seawater

The water usage of the data center can be coupled to the cooling demand of the data center. The cooling load of the data center only depends on the operation rate of the IT equipment. Therefore the cooling load is constant throughout the year regardless of temperature or season [7]. The operation rate of the IT equipment can change day by and a weekly pattern can probably be made to estimate the operation rate.

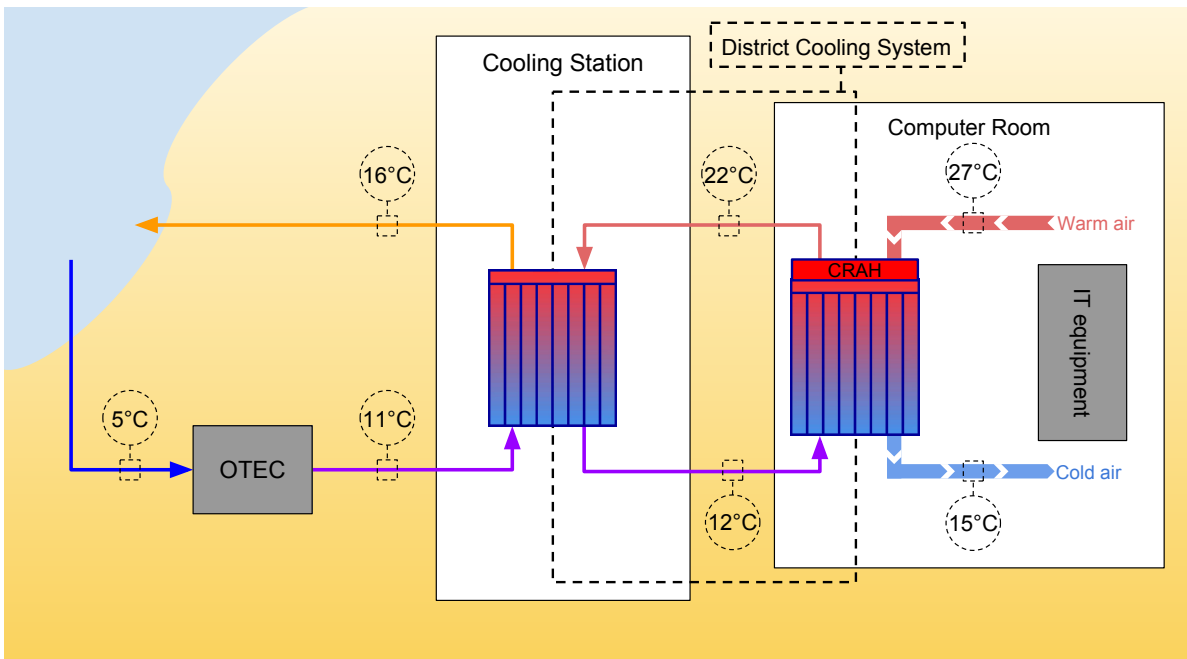


Figure 2.5: Working principle data center cooling combined with the effluent water from the OTEC

2.3.3. Greenhouse cooling

Greenhouse cultivation is a way to grow crops on locations where the climate is normally not suitable for that crop. This way crops can be cultivated even in the desert. With greenhouses, crops can be protected from bad weather, high temperatures and humidity levels. For tropical and subtropical regions cooling is considered to be the most important aspect for successful crop cultivation [31]. But the existing cooling techniques are not good enough. Refrigeration techniques to cool the air inside greenhouses are expensive and evaporative cooling is not very effective because of the high relative humidity levels in these regions [31].

Cold deep seawater can be a solution for cheaper and sustainable greenhouse cooling. Both the cold deep seawater and the effluent cold water from the OTEC power plant, can be used as cold source, depending on the type of crops or time of the day.

One way to use the cold water is to cool the air in an AC unit. Compared to regular AC systems much less electrical power is needed, because the part with evaporative cooling of a working fluid to transfer heat is replaced by the cold water.

Another way to use the cold water is a so called *Seawater Greenhouse* (SWG). This type of installation is developed for arid conditions: climates with high temperatures and little rain. The biggest difference with the method above is that the cold water is also used to produce fresh water, which can be used as irrigation water [1].

A third option is *cold agriculture*. With this method the cold water flows through a PVC pipe system in the soil of the crops. This way many plants can grow in a tropical climate. Three possible processes can be pointed out to explain the working principle of cold agriculture. By cooling the roots, a large temperature difference exist between the roots and the leaves. This enhances the transport of nutrients and fluids to the leaves which results in enhanced growth. The second process is the condensation of water around the pipes when the temperature is below the dew-point. The condensate is fresh water which operates as irrigation water. The fresh water supplied by this process is at least 33% of the water demand by the crops. The last possible process to explain this method is that nutrient flow towards the roots is enhanced by the condensed water flow [60].

Working principle

Three possibilities to cool greenhouses have been discussed. Since the SWGH is developed for arid conditions and the *cold agriculture* is only applied in experimental research, the scope of this research is limited to the option of using cold water to cool an air conditioning unit.

Three main configurations can be distinguished for the cooling of greenhouses. The first one is to connect the greenhouse directly to the cold deep seawater via a DCS. This way the supply temperature of the cold

water will be around 6°C . In a heat exchanger the hot air from inside the greenhouse is cooled with the cold water.

The second configuration is to connect the greenhouse to the effluent water coming from the OTEC. The supply temperature of the cold water than will be around 11°C . The biggest advantage compared to the first configuration is that less water has to be pumped up from the bottom from the ocean. A disadvantage is that more water is needed because of the smaller temperature difference between the cold and warm side of the heat exchanger. Furthermore, this also means that the coldest supply temperature will be higher, because it can not go colder than the 11°C .

A third option is a hybrid system of the two configurations above. This means both a connection with cold deep seawater / district cooling system and the effluent water of the OTEC. A reason to implement this system can be that the desired indoor temperatures of the greenhouse can be different between daytime and nighttime. For example, when the desired temperature during the day is about 28°C , the greenhouse can be cooled with the effluent water of the OTEC. If then the desired indoor temperature during the night is about 16°C , the greenhouse can be cooled with the cold deep seawater / DCS water. This can probably be accomplished without an increase in maximum cold water mass flow, because it is expected that the cold water mass flow at nighttime is significantly lower. So in the end, the cold water that is not used by the SWAC during night is used to cool the greenhouse. A schematic overview of the hybrid configuration can be found in figure 2.6. The temperatures are based on the information of Priva or estimated.

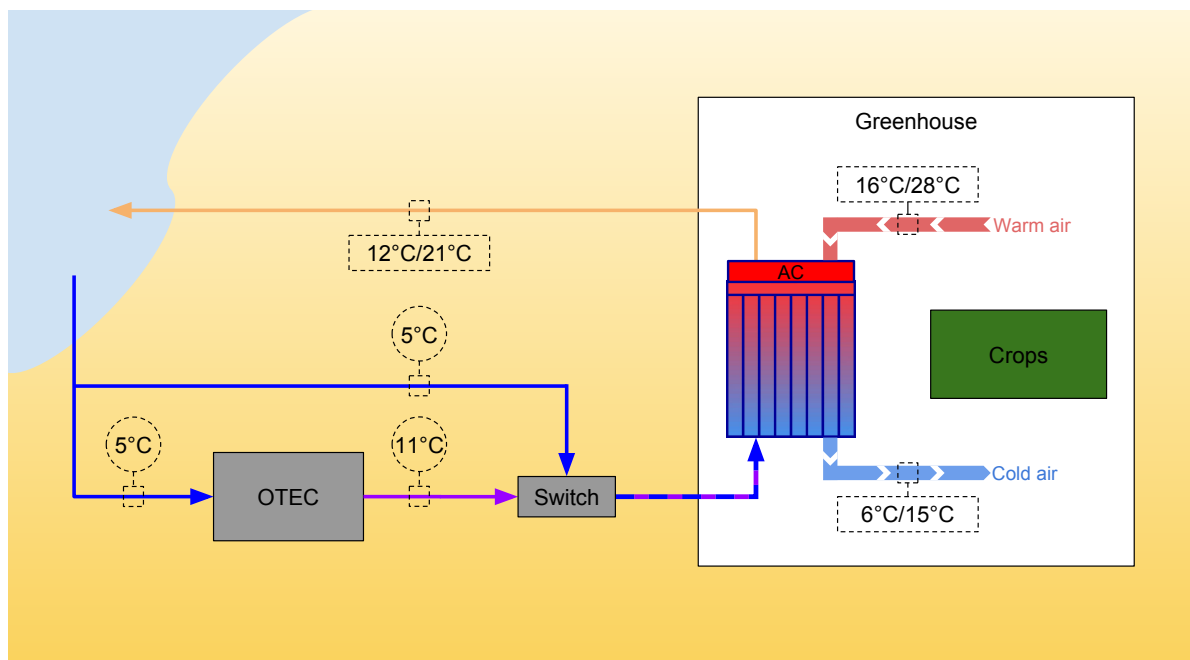


Figure 2.6: Working principle hybrid greenhouse cooling system

The cooling load determines the water usage of a greenhouse. The cooling load depends on various variables, such as: the outdoor temperature, desired indoor temperature, solar radiation, wind speed and the area of the greenhouse. To calculate the cooling load, an energy balance can be made for a greenhouse. All the heat gains added should equal the cooling load. In this calculation the heat accumulation can be neglected, because the assumption is made that the windows of the greenhouse are very thin and does not accumulate heat.

2.3.4. Ocean Thermal Water Production

Less than 3% of the water on planet earth is fresh water. The other 97% is undrinkable (sea)water. More than 2.5% of the 3% is frozen water stored in the Arctic, Antarctica, glaciers and snow. So that leaves only 0.5% of the total amount of water that is available for human beings. The fresh water is not equally divided over the planet. Some places have abundant of fresh water, other places have almost no fresh water [14].

For most tropical islands it is 'feast or famine' when it comes to rainfall. In the wet seasons there is too much rain, while in the dry season there is too little rain. Many tropical islands already facing water scarcity during a period of the year. With the expected climate change, the weather extremes will become bigger.

Global warming can cause extreme droughts, unusually heavy rainfall and floods, especially on small tropical islands [40]. This will lead to larger periods of water shortage for these islands.

Due to the fact that tropical islands are surrounded by seawater, desalination plants are often the obvious solution for the lack of sufficient natural fresh water resources. 90% of these desalination plants use a thermal process or reverse osmosis [8]. These processes are very energy intensive, using thermal heat or electrical energy. These conventional processes rely on fossil fuels as energy source, which makes these processes strongly dependent on the fossil fuel prices. Furthermore, the waste product of these processes is brine water: water with a higher salinity than the normal seawater. This brine water is dumped into the ocean.

A sustainable way to produce fresh water is to couple desalination techniques to renewable energy sources. Most renewable energy sources are not suitable, because of the inconsistent nature of these sources. This means that either the energy or fresh water should be stored, or that the desalination process should be designed in such a way that it is able to operate perform well in transient state. Furthermore, most of the renewable energy sources cannot compete with the costs of fossil fuel energy sources [8].

This is not a problem for Ocean Thermal Water Production (OTWP). This thermal desalination process makes use of the effluent water coming from the outlet of the OTEC to cool humid air and condense part of the water into liquid. This system benefits from low-cost power, which can be derived from the OTEC power plant.

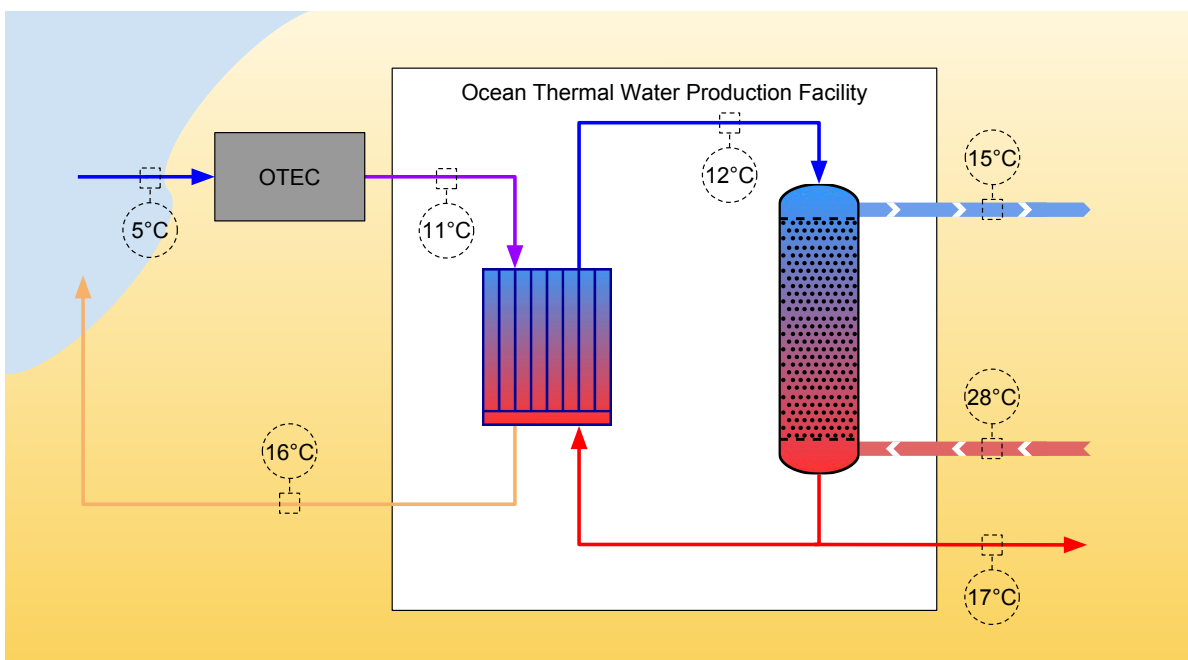


Figure 2.7: Working principle OTWP combined with the effluent water from the OTEC

Working principle

The production of fresh water with the effluent water from the OTEC is more complex than SWAC. The production of fresh water is accomplished by condensing part of the water present in the humid air. First the effluent water of the OTEC or SWAC plant of about 11°C is used as heat sink for the OTWP system. Warm fresh water is cooled to a temperature of about 12°C by the cold water in the heat exchanger. The temperature of 12°C has been chosen because the colder the fresh water, the more new fresh water could be produced per kg cold water.

Cooled fresh water flows to the top of a direct contact condenser, while warm humid air is introduced at the bottom. Packing material inside the column is used to increase the contact area between the water and the humid air, which improves both the heat and mass transfer. The humid air cools down to below the wet-bulb temperature. At this point the air is saturated (100% relative humidity). When the humid air is cooled down even further, water vapor starts to condensate because the maximum amount of water that can be contained by the air is exceeded. The result is that at the fresh water outlet the mass flow is higher than at the inlet, because water vapor is converted into liquid water. Even so, the mass flow of the humid air will be lower at the outlet of the humid air, because it contains less water. After the condenser the fresh water will be

split in two streams. One stream, with the same mass flow as at the inlet of the condenser, flows back to the heat exchanger to close the cycle. The remainder, the amount of water that is produced during this process, can be used for other purposes.

The produced fresh water is almost pure water that does contain hardly any minerals and therefore is not suitable as drink water because consumption can lead to health risks [29]. The solution is to remineralise the water so that the health risks will disappear and the produced water can be used as drinking water. A schematic overview of the OTWP process can be found in figure 2.7. The temperatures in this figure are based on the results of a case study for an OTWP on Curaçao by Lopez [33].

2.3.5. Aquaculture cultivation

In the report 'Fish to 2030: Prospects for Fisheries and Aquaculture', Msangi et al. [36] estimate that by 2030, 62% of all consumed seafood will need to be farmed, including fish for foods and fishmeal, in order to meet demand. Demand is greatest in certain regions, particularly Asia, where approximately 70% of fish will be consumed. The report states that aquaculture will help satisfy the world's growing appetite for fish as human populations continue to grow. Therefore an urgent need for sustainable aquaculture is needed.

The deep seawater that is pumped up for OTEC can be used for sustainable aquaculture. The first of three reasons why the DOW can be used for aquaculture cultivation is that the deep seawater is nutrient-rich. This is beneficial for the growth rate of fish or other sea animals. The second advantage of DOW is that it is virtually pathogen-free. This means that there are almost no bacteria, no viruses and has very few viable plant cells. The result is the possibility of cultivating very sensitive larval stages. The last advantage of the deep seawater is the temperature. Animals that cannot tolerate tropical temperatures can be cultivated. Furthermore, temperatures can be easily be maintained by controlling the cold water flow rate or by combining DOW with surface seawater. This way every possible temperature between the cold water and the surface water can be obtained throughout the year [10].

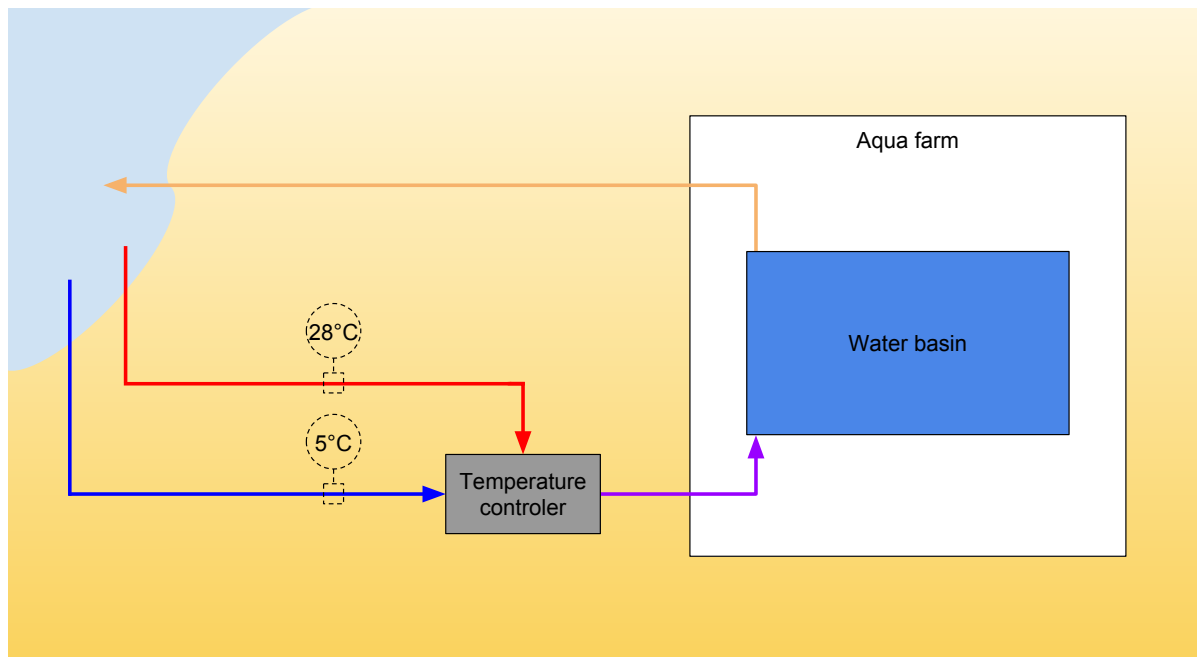


Figure 2.8: Schematic overview of a possible configuration of aquaculture with direct cold deep seawater and hot surface water

Working principle

The nutrient-rich, virtually pathogen-free and cold deep seawater can be used for aquaculture cultivation. The (cold) seawater can be used in basin to grow the fish, shrimps and other sea animals. The required water temperatures can vary between different species. Therefore the aqua farm should probably be connected to both the cold deep seawater as the hot surface water. The deep seawater can be mixed with the hot surface water to reach the desired temperature. Depending on which species are cultivated, it can be possible to use the effluent water of the OTEC as cold water source. Furthermore, it also might be possible to connect it to the effluent water of the Ecopark. A schematic overview of aquaculture with direct cold deep seawater and

hot surface water can be seen in figure 2.8.

2.3.6. Algae cultivation

A special kind of aquaculture cultivation is algae production. Algae can be separated in two main categories: macroalgae and microalgae. Macroalgae are better known as seaweed and is plant like, while microalgae are unicellular species.

Macroalgae

Seaweeds have been used for food and nonfood purposes for thousands of years. In Southeast Asia most countries have a long history of using edible seaweeds. For example, in Japan seaweed is used to make *nori*, the dried seaweed sheets used for sushi and in Indonesia and Malaysia seaweeds are used in salads. In Europe seaweeds were not directly used for food. Seaweeds were used to feed animals since approximately 100 BC (Greece), for agricultural applications (Ireland and Scotland) or for medicinal purposes (Mediterranean countries). Where seaweeds are taken from natural resources in Europe, seaweeds are mostly cultivated in Asia for multiple purposes [61].

Almost 21 million tons of seaweeds are utilized worldwide (2012). More than 94% of the seaweeds are produced by aquaculture, leaving less than 6% of the total amount of seaweeds being harvested from nature [64]. One of the things that make seaweed farming sustainable is that no pesticides or other chemicals are used. Compared to regular agriculture or fish farming, the production costs can be lower and the production is more sustainable when no chemicals or pesticides are used [52].

Microalgae

Microalgae are very small plants that can live in aquatic habitats like lakes, rivers or seas/oceans. It is estimated that more than one hundred thousand species of algae exist, whereof only about ten thousand have been classified and only about 20 species are used for economic purposes [48].

Microalgae can be used in many different ways. For a long time they have been used as food supplements like antioxidant pigments, fatty acids and proteins. Furthermore microalgae can be used as animal feed. Normally fish are fed with fish meal: *a product obtained by drying and grinding or otherwise treating fish or fish waste to which no other matter has been added* (FAO, 1986). Instead of using fish meal, algae can be used as supplement or might completely replace fish meal [48]. Another possible application for microalgae is to use it for bioplastics and other chemicals. For example, in Germany more than 5% of the imported crude oil is used for the production of plastics. By using microalgae instead of crude oil for the production of these products the plastic industry can be made (more) sustainable [48]. Likewise, microalgae can be used to produce biofuels. The first generation of biofuels were made out of crops like sugarcane and corn. Disadvantages of the first generation are that they rely on food crops and have low yields. The second generation biofuels are made of nonfood crops as biomass. The net energy of the ethanol obtained by these biomass sources is higher than the first generation, but complex fuel processing increased the cost and lowered the yield. Eventually the third generation biofuels were developed to cope with the food versus fuel problem. This problem is solved with algae cultivation because it is independent of agricultural production [4]. Even more, microalgae can produce up to five times more biomass per unit area than conventional sources of biomass [48].

For the production of macro- and microalgae the DOW pumped up for OTEC can be used as water source. Many algae species can grow in salt water [48]. Furthermore are all the advantages mentioned for aquaculture in subsection 2.3.5 applicable for algae cultivation. The nutrient-rich, virtually pathogen free and easily adaptable water temperature combine the ideal growth conditions for algae. The last factor needed to grow algae is sunlight, but that would not be a problem for tropical islands.

Cultivation techniques macroalgae

In nature, seaweeds grow typically in relatively shallow coastal waters. This is due to the fact that seaweeds need sufficient sunlight to grow and they need to have a foundation on which they are attached to grow, normally the sea floor. The roots of seaweeds are only used for the attachment to the substrate, like an anchor. Contrary to land-based plants, the supply of nutrients, water and dissolved gases goes through their entire body instead of through the roots.

Main seaweed cultivation techniques are: line cultivation, net cultivation, floating raft cultivation and tank or pond cultivation. The first three techniques are sea-based and do not need OTEC water to grow. Tank or pond cultivation can make use of OTEC water. The advantage of tank or pond cultivation compared to

the other techniques is that the habitat can be controlled for optimal growth and is suitable for intensive production. Furthermore, seaweed species that normally grow in other climate conditions can be cultivated. Tank or pond cultivation is often considered for intensive, small scale applications but are also suitable for large scale applications, like the Green Desert Project destined for coastal areas in the Sahara [62].

Cultivation techniques microalgae

The first way to cultivate microalgae is the *Raceway Pond*. A raceway pond is a closed-loop flow channel. The algal broth is continuously mixed by a paddle wheel in a channel with a depth of approximately 25-30 cm. A raceway pond can come in different sizes, but typically they will not exceed a surface area of 0.5 ha, although they can be larger. The advantages of a raceway pond are that they are inexpensive and effective. However, they suffer from a relatively low productivity and they are sensitive for weather influences and contaminations, because they are not separated from the environment [6].

The other way to cultivate microalgae is to make use of a *Photobioreactor* (PBR). There is a diversity in PBR configurations, such as flat panel, cylindrical or tubular systems. This variety in technologies is a consequence of research in optimizing light capture, system integration, scale of production, algae species, temperature, etcetera. The benefit compared to a raceway pond is that a PBRs can cultivate algae with higher biomass yields and have significant smaller footprints. The disadvantages are that PBRs are more complex and are more expensive than raceway ponds [50].

The working principles for both macroalgae and microalgae combined with OTEC are quite the same. The effluent water coming from the OTEC is transported to the production facility. At the production facility the cold water can be mixed with hot surface water to control the temperature of the water. Furthermore fresh water can be mixed to control the salinity or the nutrient level. Then the mixture can flow into the tank, pond or photobioreactor where the algae can grow. It might be needed to cool the mixture of water and algae for optimal growth rates. In that case cold water can be used to cool the mixture. A schematic view of algae cultivation combined with OTEC can be seen in figure 2.9.

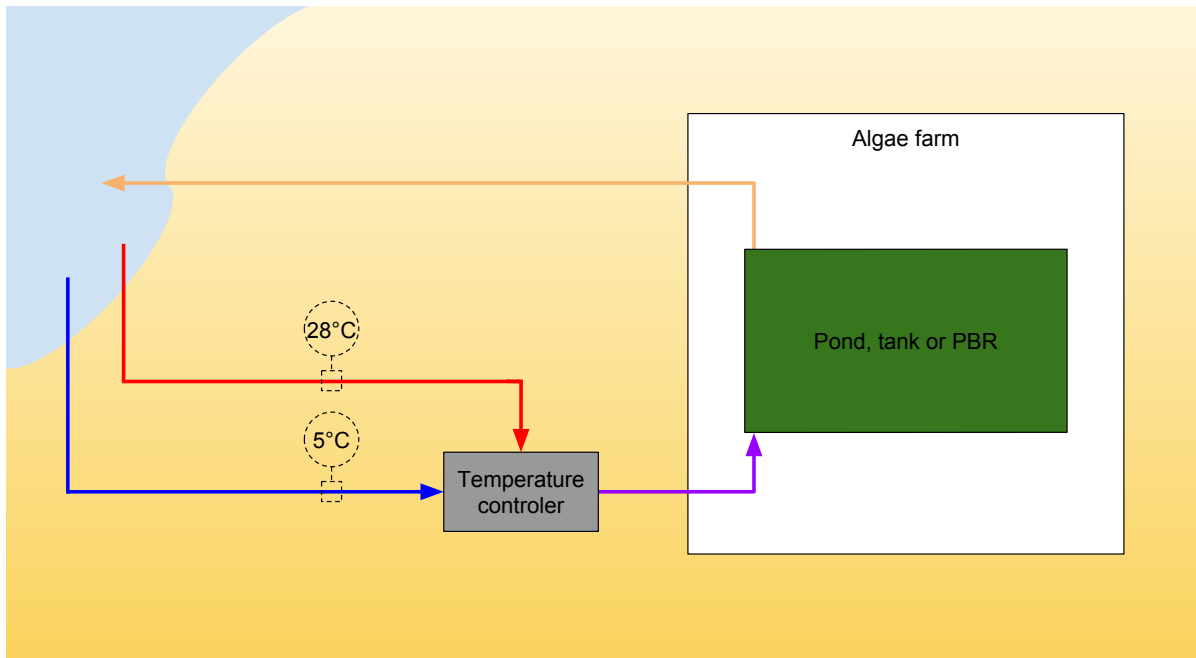


Figure 2.9: Schematic overview of a possible configuration of aquaculture with direct cold deep seawater and hot surface water

Because of the scope of this research, the biorefinery and product development part of algae will not be investigated. Only the water usage for the cultivation of algae will be taken into account.

The water usage of algae cultivation depends on a lot of variables. The annual water input ($m^3/m^2/yr$) needed for cultivating is the sum of all the water losses as shown in eq. 2.1 [13]:

$$V_{input} = V_{fill} \cdot F_{freq} + V_{evap} + V_{leakage} + V_{blowdown} + V_{photo} + V_{harvest} + V_{drying} + V_{biomass} + V_{graywater} \quad (2.1)$$

In this equation V_{input} is the total volume to be added to the system in ($m^3/m^2/yr$). V_{fill} is the water required to fill up the system and F_{freq} is the frequency of fillings per year. $V_{leakage}$ is the water leakage rate per year, $V_{blowdown}$ the water removed to control the system and V_{photo} the water loss due to photosynthesis (negligible). Furthermore, $V_{harvest}$ is the water loss due to the water that is carried out of the pond as a result of harvesting. V_{drying} and $V_{biomass}$ are part of the biorefinery process and will not be taken into account in this research. When the nutrients are perfectly recycled, the gray water footprint $V_{graywater}$ can also be. However, the biggest water loss for open systems comes from evaporation. The evaporation rate is related to the solar radiation, wind velocity, temperature and relative humidity. Since a PBR is a closed system, evaporation is not a problem [13].

From all these water losses, only V_{fill} , $V_{harvest}$ and $V_{blowdown}$ ($V_{leakage}$ can be neglected) have to be compensated with seawater. The other water losses, like due to evaporation, have to be compensated with fresh water. This would imply that the water demand will not be constant, but more in batches. Only the water usage due to blowdown, to control salinity, nutrient level and temperature, is probably quite stable but can fluctuate by weather influences.

2.4. Integration of OTE subsystems

An OTE system is a system where all the DOW subsystems are integrated. But the integration can be done in various ways and therefore several configurations are possible. An OTE system can be separated into two or three layers. The primary layer contains the subsystems that are connected to the cold deep seawater. The secondary layer contains all the subsystems that are connected to the effluent water coming from the primary layer. In between a hybrid layer is possible for subsystems that can use both the cold deep seawater and the effluent water from the primary layer.

A possible configuration for an OTE system can be seen in figure 2.10. This configuration has OTEC, SWAC and data center cooling connected to the cold deep seawater and OTWP, greenhouse cooling, aquaculture and algae cultivation connected to the effluent from OTEC, SWAC and data center cooling. Furthermore aquaculture and algae cultivation are also connected to the warm effluent water from the OTEC. With all the methods described in subsection 2.3.1 to 2.3.6 a lot more configurations can be made, but figure 2.10 is only used as example of a possible configuration.

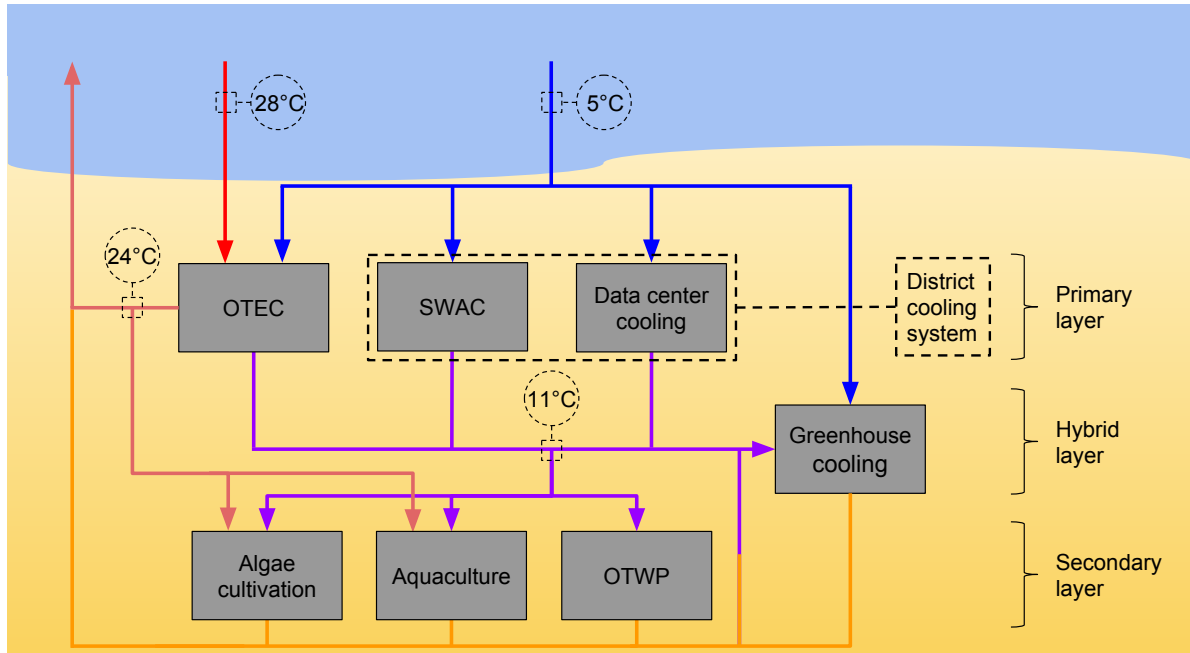


Figure 2.10: Schematic overview of a possible configuration of an Ocean Thermal Energy system

2.5. Boundaries

Before the model can be developed it has to be considered for each subsystem if it is relevant to model it. It is estimated that OTEC and SWAC will use the largest amounts of cold water. Thereby it is expected that the demand of SWAC can vary a lot per day, because the cooling demand depends on the temperature and solar radiation. The variation of DOW usage by OTEC will not vary much per day, but seasonal changes can have effect on the water usage. Furthermore the cooling demand of a data center can be high, so it will be modeled too. Greenhouse cooling will also be taken into account, because it is expected that the water usage can vary a lot per day. The fresh water production in the OTWP installation will also be modeled because the fresh water produced can be a very valuable product for the local market.

Aquaculture and algae cultivation will be left out in the model of a OTE system. Firstly, many species can be farmed or cultivated, all with different environmental conditions. It is not clear in advance which species will be cultivated, so it will be difficult to make assumptions for environmental conditions. Furthermore, for aquaculture it can probably be assumed that the water usage will be constant over day and may vary a bit over a year. Also For algae cultivation the seawater usage can be assumed to be like a batch process. This water usage also depends on species and intensity of cultivation and is hard to predict for a general model.

At last, the flow rates for these two subsystems is estimated to be low. For example, for a raceway pond the evaporation rate in tropical region is estimated to be $4.59 \text{ m}^3 / \text{m}^2 / \text{yr}$. This is the same as $1.46 \cdot 10^{-7} \text{ kg} / \text{s} / \text{m}^2$. Compared with the largest *Spirulina* farm of the world (2015, California, USA)[30] with a surface area of about $185,000 \text{ m}^2$ (37 ponds of 5000 m^2), the evaporation rate would be $27 \text{ kg} / \text{s}$. Assuming that the water loss due to evaporation is larger than water loss that has to be compensated with seawater, that on tropical islands the algae farm will be smaller and that algae cultivation does not uses cold deep seawater and therefore does not has an impact on the CWP diameter, it seems reasonable to not take aquaculture and algae cultivation into account.

3

Modeling

In this chapter it will be explained how all the subsystems and OTE system are modeled. In section 3.1 the method to approach all the subsystems and the integration into an OTE system will be discussed. After that the modeling of each component will be discussed in section 3.2. The model integration into an OTE system will be discussed in section 3.3. Lastly, three optimization methods will be discussed in section 3.4.

3.1. Method

Before the model can be developed, it has to be considered what the goal of the model is and how this goal can be reached. The main goal of the model is to integrate all the subsystems of an OTE system, to investigate the synergies and research if time-dependent integration of the subsystems yield significant advantages in cold deep seawater usage compared to a non-integrated system. Therefore it is necessary to make clear what time-integrated and non-integrated OTE system means in this context.

- Non-integrated: An OTE system where all the components are connected, but synergies are not taken into account. The water demand is delivered at the moment that it is needed. The maximum water usage is calculated as the sum of the maximum values of the subsystems.
- Integrated: An OTE system where all the components are connected and time-integrated. The water demands of the subsystems are added before the maximum of the total water usage is calculated, so synergies are taken into account. When peak demands are all at the same time, the maximum water usage is the same as with the non-integrated OTE system. However, when the peak demands of the subsystems are not at the same time, the maximum total water usage will be lower than in case of the non-integrated OTE system.

The comparison between the non-integrated and the integrated OTE system will be done in a quasi-static model. This means that for each component the water demand will be calculated with a step size of an hour for the timespan of a year. Seasonal variations will be visible and the water demands can be added together. The dynamic behavior is not taken into account in this way, but it is assumed that this will not have a significant impact on the order of magnitude and the fluctuations in water demands.

The model will be written in Python version 2.7 [51]. Python is a widely used high-level programming language for general-purpose programming. The main reason to use Python is that BlueRise makes use of Python as programming language.

The Python model will be made in a modular way. The water usages of the subsystems will be calculated in a module and the modules are connected in a main-file to simulate the complete OTE system. All the subsystems will have the same output, namely the water usage of the component for the timespan of a year. This way it will be easy to interchange a module for an optimized module of the same component.

3.2. Components

The modeling of the components is an essential part of this master thesis. Because of the complexity and the many components, it has been chosen to simplify the components when necessary. This way the simulation

time is reduced. The way each component is modeled will be discussed in this section. This will be done for OTEC, SWAC, data center cooling, greenhouse cooling and OTWP in subsections 3.2.1 to 3.2.5, respectively.

3.2.1. OTEC

There are two ways to calculate the water usage of the OTEC cycle. The first one is to look at it as a wind turbine. It has a rated capacity, but the capacity factor is well below 1. This way the OTEC power plant will produce the rated capacity for a certain time period per year, while for the other period it will be less.

The other way to look at an OTEC cycle is to produce the rated capacity no matter what the external conditions are. This way the capacity factor is 1, but this results in larger fluctuations in water usage. Since the purpose of OTEC is to supply base-load electricity, the OTEC module is modeled in this way.

The modeling of the thermodynamics of the OTEC can be very hard and complicated. To make this more simple a power curve can be made. This power curve is based on the Carnot efficiency. The Carnot efficiency can be calculated with eq. 3.1, where T_C and T_H are the temperature of the cold deep seawater and the temperature of the hot surface water (in K), respectively.

$$\eta_{carnot} = 1 - \frac{T_{sw,C}}{T_{sw,H}} \quad (3.1)$$

But since the Carnot efficiency is the maximum theoretical efficiency, this efficiency has to be corrected with another factor. A rule of thumb for OTEC is that the efficiency due to all the irreversibilities is about 50% of the Carnot efficiency. With a factor of $\eta_{irrev} = 0.47$ and an expected thermal efficiency of 3-4% [26] for an OTEC power plant, this model is quite close with a thermal efficiency of 3.2% and 4.0% for a temperature difference of 20°C and 26°C, respectively. Therefore the thermal efficiency can be calculated with eq. 3.2, and the results for the Carnot efficiency and the thermal efficiency versus the temperature difference between the cold deep seawater and the hot surface water can be seen in figure 3.1.

$$\eta_{th} = \eta_{irrev} \cdot \left(1 - \frac{T_C}{T_H}\right) \quad (3.2)$$

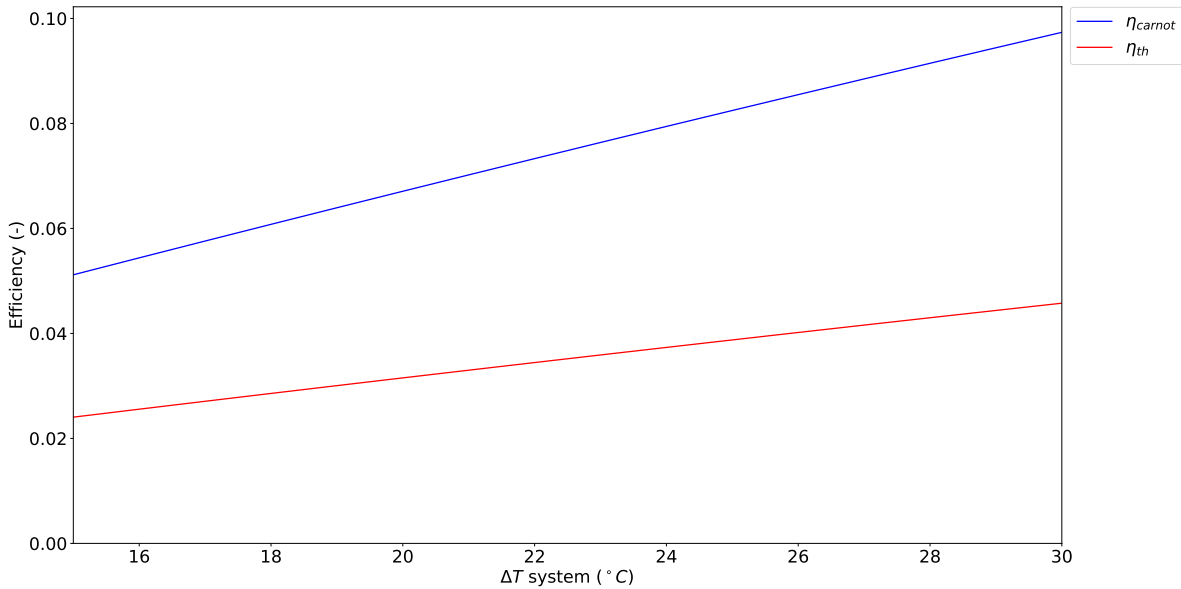


Figure 3.1: Carnot and thermal efficiency versus temperature difference between T_C and T_H

Furthermore, the thermal efficiency can also be calculated as the work done by the system divided by the heat into the system as can be seen in eq. 3.3:

$$\eta_{th} = \frac{\dot{W}_t - \dot{W}_p}{\dot{Q}_H} \quad (3.3)$$

The formula to calculate the electrical power demand (P_e) can be found in eq. 3.4. Since the P_e and η_{gen} are known inputs, eq. 3.4 can be rearranged to calculate the turbine work, see eq. 3.5.

$$\dot{P}_e = \eta_{gen} \cdot (\dot{W}_t - \dot{W}_p) \quad (3.4)$$

$$\dot{W}_t = \frac{P_e}{\eta_{gen}} + \dot{W}_p \quad (3.5)$$

There are still two unknowns in eq. 3.5, namely the turbine work and the pumping power. The pumping power is the power required to pump up the cold deep seawater from the bottom of the ocean and the power required to circulate the working fluid. For OTEC the power required to pump up the DOW is quite large and the energy losses due to pumping are estimated to be about 20-30% [24]. When it is assumed that the pumping power is 25% of the turbine work [24], eq. 3.5 can be rewritten to eq. 3.6.

$$\dot{W}_t = \frac{4}{3} \frac{P_e}{\eta_{gen}} \quad (3.6)$$

However, to calculate the mass flow of the cold water, the heat rejection in the condenser should be calculated. The heat rejection of the system (the cooling) can be calculated with the energy balance, see eq. 3.7.

$$\dot{Q}_C = \dot{Q}_H - \dot{W}_t \quad (3.7)$$

By combining and rearranging eq. 3.2, 3.3, 3.6 and 3.7, the heat rejection in the condenser can be calculated with eq. 3.8.

$$\dot{Q}_C = \frac{4}{3} \frac{P_e}{\eta_{gen}} \cdot \left(\frac{1 - \eta_{th}}{\eta_{th}} \right) \quad (3.8)$$

Now the mass flows of the cold and hot water side can be calculated. In eq. 3.9 the formula to calculate the cold deep seawater mass flow is shown and the formula to calculate the hot surface water mass flow can be seen in 3.10

$$\dot{m}_{C,OTEC} = \frac{\dot{Q}_C}{C_{p,sw} \cdot \Delta T_{sw,C}} \quad (3.9)$$

$$\dot{m}_{H,OTEC} = \frac{\dot{Q}_H}{C_{p,sw} \cdot \Delta T_{sw,H}} \quad (3.10)$$

Because the temperature changes relative to the absolute temperatures are quite small, it is assumed that the $C_{p,sw}$ is a constant of 4.18 kJ/kgK. The ΔT is the difference between the inlet temperature of the condenser/evaporator and the outlet of the condenser/evaporator. This temperature difference has to be taken as input of the model. Since the inlet temperature of the condenser and evaporator are specified due to the cold deep sea water and the hot surface water, only the outlet temperatures have to be chosen. The outlet temperature of the OTEC is important for all the other applications that can make use of the 'waste' water. For this model the temperature of the waste water is set to 11°C. This is because of the restriction for SWAC, and this will be explained in detail in subsection 3.2.2. The temperature difference of the hot water is set to be 4°C at all time.

As an example, the calculated cold and hot water mass flows with this model for a 10 MW OTEC power plant versus the temperature difference between the cold and hot water can be seen in figure 3.2. The temperature inputs for this example are:

- $T_{C,in}$ = 5°C
- $T_{C,out}$ = 11°C
- $T_{H,in}$ = 15°C to 30°C
- $T_{H,out}$ = $T_{H,in} - 4^\circ C$

In this figure it can be seen that the required hot water mass flow varies from about 25 000 kg/s to 15 000 kg/s for a temperature difference of 15°C to 30°C, respectively. The cold deep seawater mass flow varies from about 16 000 kg/s to about 10 000 kg/s. It could be expected that the mass flow of the hot water side would be

higher, because $\dot{Q}_H > \dot{Q}_C$ (eq. 3.7) and $\Delta T_H < \Delta T_C$.

Furthermore it can be seen that the lines of both mass flows are not linear. This means that slope increases with a lower ΔT and decreases with a higher ΔT between the cold and hot water side. This is an effect of the fraction in eq. 3.2.

The inputs needed for the OTEC module are:

- Electricity demand (P_e)
- Temperature cold deep seawater ($T_{C,in}$)
- Temperature hot surface water ($T_{H,in}$)
- Specific heat capacity of seawater ($C_{p,sw}$)
- Temperature of the cold effluent water ($T_{C,out}$)
- Temperature of the hot effluent water ($T_{H,out}$)

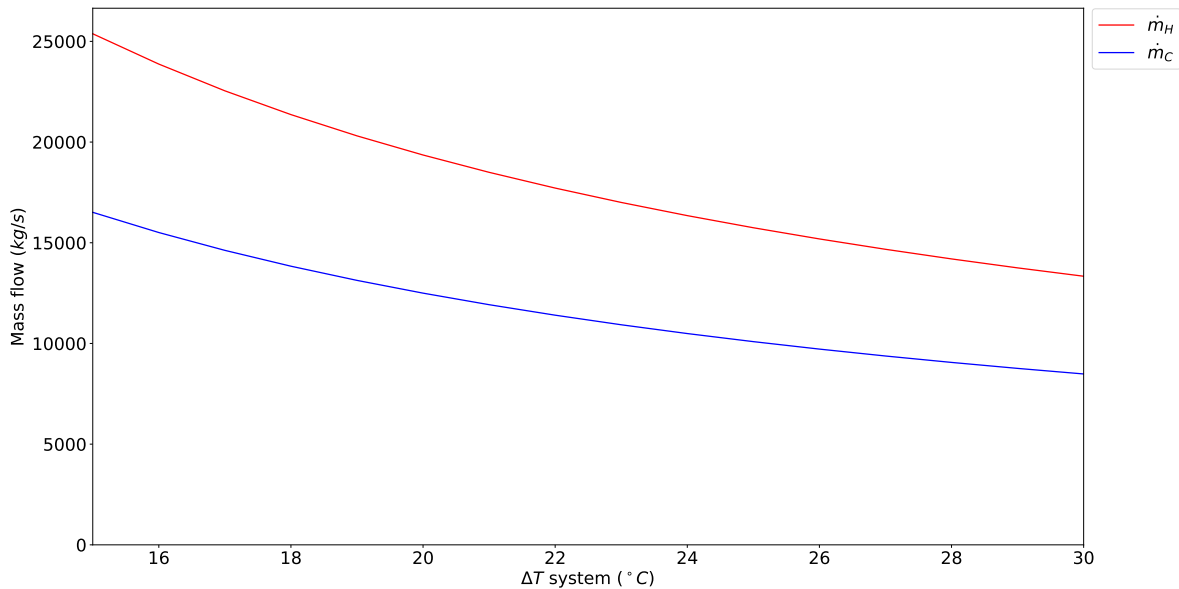


Figure 3.2: Cold and hot water mass flows versus temperature difference between T_C and T_H for a 10 MW OTEC power plant

3.2.2. SWAC

The difficult part of the SWAC module is to model the demand curve. For some locations with existing buildings the cooling demand curve can be constructed with the help of measurements. But for other locations the cooling demand curve of the DCS might not be present. The only way to get detailed information is to monitor the cooling demand of every single building that would be connected to the cooling network. This would cost a lot of time to investigate, and might be impossible when the buildings are not built yet. Since the purpose of this model is not to be very detailed but give a good overview of the interaction between the applications, a simple method has to be developed to estimate the cooling demand curve of the SWAC.

The easiest way to develop a cooling demand curve is to use a sinusoidal function. Every day a top peak demand can be expected somewhere around 6PM, depending on the location and end user. The bottom peak demand should then be equal to the lowest point of the sinusoidal wave. But just like the weather, the cooling demand is not the same every day. Therefore the seasonal changes have to be implemented in the demand curve.

These seasonal changes can be taken into account when the cooling demand is calculated per hour with a simple energy balance. With an desired indoor temperature, the cooling demand can be calculated as a function of the outdoor temperature, solar radiation and total surface/volume that needs to be cooled. Since not all buildings have the same shape, it should be investigated if different calculations have to be done for different types of buildings or that one calculation for an average building is enough. The disadvantages of setting up such an energy balance are that it can be very time consuming to calculate the cooling demand for each building and that heat accumulation is not taken into account with this calculation, while this might have a huge impact on the cooling demand.

Therefore a model is made to predict the cooling demand as function of the temperature and the solar radiation which takes heat accumulation into account. This is done with the help of measured data of the cooling of Hato Curaçao International airport by Greenvis [27]. The validation of this correlation to estimate the cooling demand can be found in appendix A.

The correlation can be seen in eq. 3.11. The output of this correlation is the cooling demand in percentage of the maximum cooling demand in a year. In this correlation SF is the Solar Factor. The SF is a factor consists of the monthly average solar radiation divided by the monthly average of the month with the highest average solar radiation. The environmental temperatures are in °C. The heat accumulation is modeled by taking the temperature measured four hours before the peak demand. This way the peak in cooling demand happens four hours after the maximum temperature is reached. The cooling curve for Curaçao 2016 can be seen in figure 3.3.

$$\dot{Q}_{curve,SWAC}(h) = SF \cdot \frac{T_{env}(h-4)}{T_{env,max}} \quad (3.11)$$

To calculate the actual cooling, the cooling demand curve can be multiplied by the maximum expected cooling demand of the DCS, as can be seen in eq. 3.12

$$\dot{Q}_{C,SWAC} = \dot{Q}_{SWAC,max} \cdot \dot{Q}_{curve,SWAC} \quad (3.12)$$

Now that the demand curve can be calculated as a function of the environmental temperature and solar factor, the calculation for the cold deep seawater mass flow is straightforward. The fresh water in the district cooling system is cooled with the cold deep sea water in a heat exchanger. The energy balance of a the heat exchanger can be found in eq. 3.13.

$$\dot{m}_{fw,SWAC} \cdot C_{p,fw} \cdot (T_{fw,in} - T_{fw,out}) = \dot{m}_{C,SWAC} \cdot C_{p,sw} \cdot (T_{C,out} - T_{C,in}) \quad (3.13)$$

Eventually by rewriting eq. 3.13, the deep seawater mass flow for SWAC can be calculated with eq. 3.14.

$$\dot{m}_{C,SWAC} = \frac{\dot{m}_{fw,SWAC} \cdot C_{p,fw} \cdot (T_{fw,in} - T_{fw,out})}{C_{p,sw} \cdot (T_{C,out} - T_{C,in})} \quad (3.14)$$

It can be assumed that $C_{p,fw}$ and $C_{p,sw}$ are constant because of the small temperature differences.

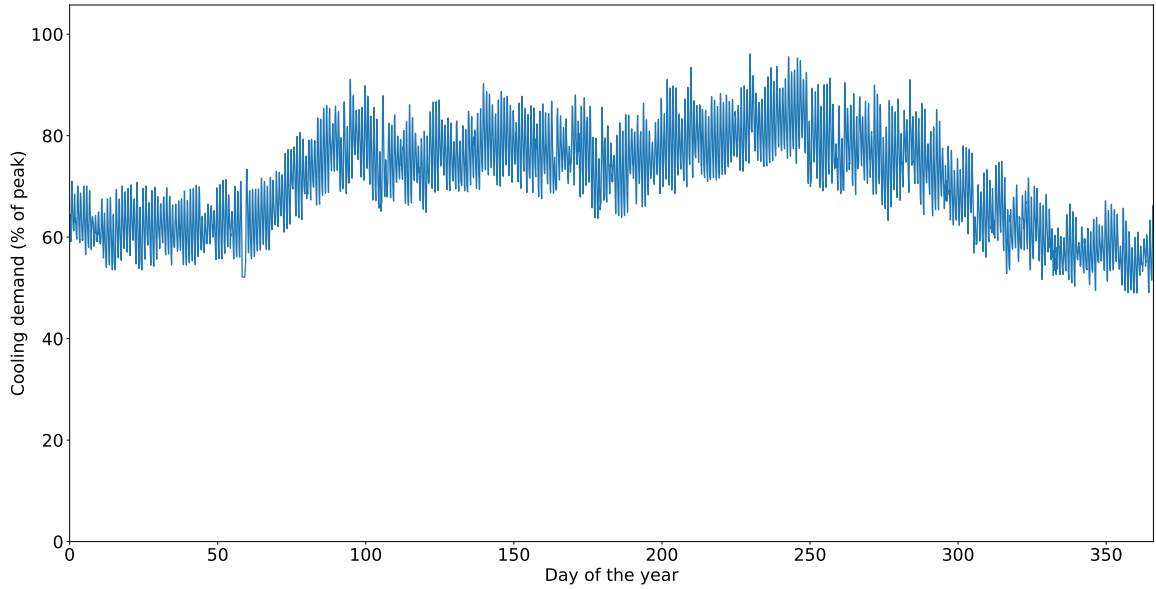


Figure 3.3: The cooling demand curve of the SWAC for Curaçao 2016

The inputs for the SWAC module are:

- Maximum cooling demand ($\dot{Q}_{SWAC,max}$)
- Temperature of the cold water at inlet ($T_{C,in}$)
- Temperature of the cold effluent water ($T_{C,out}$)
- Specific heat capacity of fresh water ($C_{p,fw}$)
- Specific heat capacity of seawater ($C_{p,sw}$)
- Environmental temperature (T_{env})
- Solar Factor (SF)

3.2.3. Data center cooling

To model the data center cooling load, a few assumptions are made. First of all the assumption is made that the data center cooling is independent on the outside environment. In other words, it is assumed that the cooling load induced by the temperature difference between inside and outside the data center is very small compared to the heat generated by the IT equipment [7].

Furthermore there is a daily fluctuation in energy consumed by the IT equipment. When more people are using the internet, more IT equipment is used in a data center and the cooling load will be higher. The peak demand of the internet usage can be expected at 8PM, while the bottom low point is between 4 AM and 6 AM in the morning, as can be seen in figure 3.4.

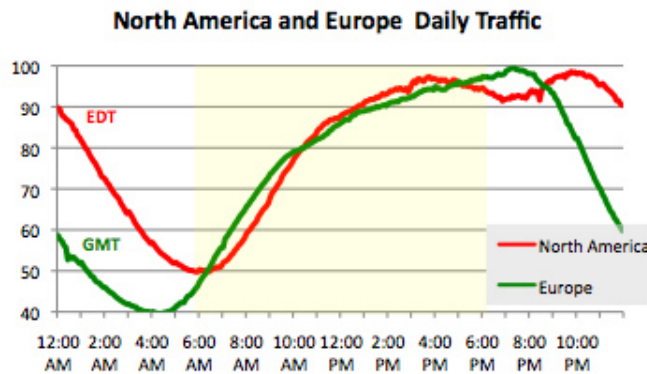


Figure 3.4: Daily internet traffic for North America and Europe [21]

Although the internet usage bottom point is about 50% of the peak usage, this is not the case for the cooling demand of the data center. Low processor activity does not translate directly into low power consumption of the server. Even in idle mode most of the server processors consume 70-85% of the peak power [7], as can be seen in figure 3.5.

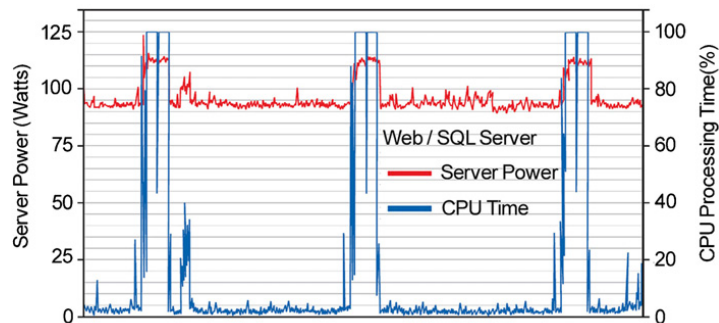


Figure 3.5: Server power versus CPU processing time [7]

The assumed capacity factor of the bottom low peak for this model is 90%. The value of 90% is assumed because with 40-50% bottom low internet usage, 40-50% of the servers are consuming 100% of the peak power

and 50-60% of the servers are consuming 70-85% of the peak power. There also might be a difference between the internet usage during the week and in the weekend, but this is not taken into account in this research.

A data center cooling curve can be constructed based on figures 3.4 and 3.5 and the assumed capacity factor of 90% for the bottom peak demand. The cooling curve is constructed out of four parts. The first part is from 0h to 5h, the second part is from 5h to 10h, the third part is from 10h to 21h and the last part is from 21h to 24h. All four parts can be described as a part of a sinusoid. The functions for the four parts can be found in eq. 3.15 and the simulated daily cooling curve generated with this equation can be seen in figure 3.6.

$$\dot{Q}_{curve,Data}(h) = \begin{cases} 0.95 + 0.05 \cdot \cos\left(\frac{h+3}{16} \cdot 2\pi\right) & \text{if } h < 5 \\ 0.96 - 0.06 \cdot \cos\left(\frac{h-5}{20} \cdot 2\pi\right) & \text{if } 5 < h < 10 \\ 0.96 + 0.04 \cdot \sin\left(\frac{h-10}{44} \cdot 2\pi\right) & \text{if } 10 < h < 21 \\ 0.95 + 0.05 \cdot \cos\left(\frac{h-21}{16} \cdot 2\pi\right) & \text{if } h > 21 \end{cases} \quad (3.15)$$

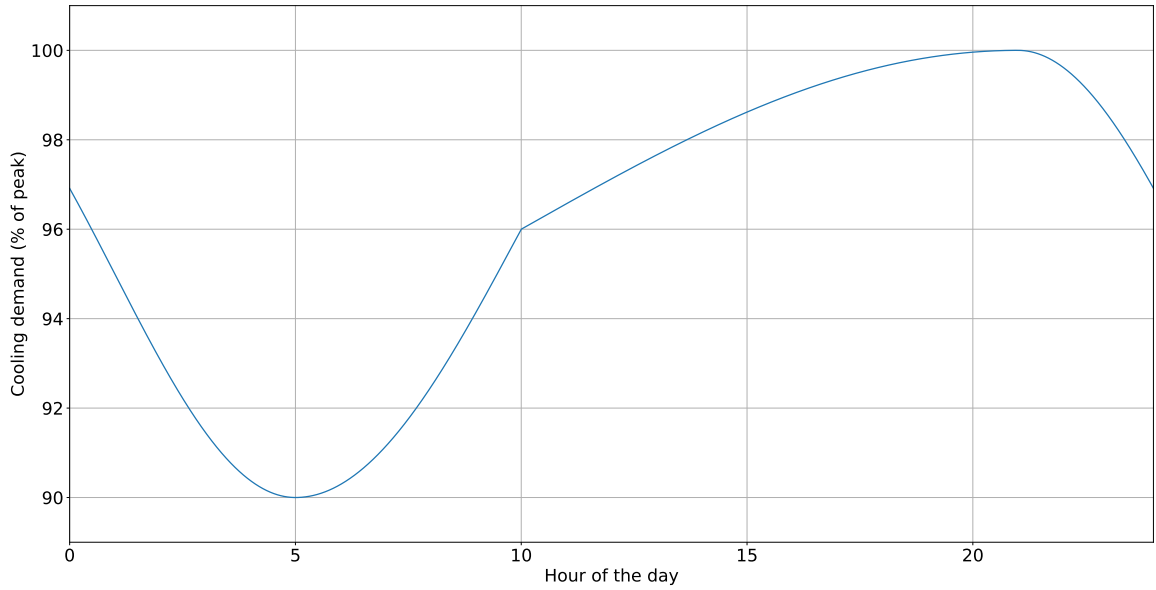


Figure 3.6: The daily cooling curve for the data center cooling

The cooling curve in figure 3.6 can be repeated day after day to eventually generate an hourly cooling curve for the timespan of a year. At the point of $h = 10$ there is a small hitch in the function. This point is continuous but not differentiable, because the slope of the function is not the same for the limits on both sides.

The cooling demand can be calculated by multiplying the maximum cooling demand $\dot{Q}_{C,max}$ with the cooling curve $\dot{Q}_{curve,Data}$, see eq. 3.16:

$$\dot{Q}_{C,Data} = \dot{Q}_{C,max} \cdot \dot{Q}_{curve,Data} \quad (3.16)$$

In this equation $\dot{Q}_{C,max}$ is an input. The maximum cooling demand can be calculated in a few ways, but for this model it is assumed that the maximum value is known. The model is made in such a way that $\dot{Q}_{C,max}$ can be entered in both kilowatts (kW) and Refrigeration Tonnes (RT) as unit.

The cooling demand calculated in eq. 3.16 should be the load that normally is cooled by a chiller. This means that it includes the losses due to the heat transfer of the chilled water to the cooling fluid. Furthermore it is assumed that the heat transfer losses from the cold source (cold deep seawater or effluent water) to the fresh water are negligible compared to the total heat transfer, which means that the heat exchanger efficiency is assumed to be 100%. The mass flow of the cold water demand for the data center can be calculated with eq. 3.17.

$$\dot{m}_{C,Data} = \frac{\dot{Q}_{C,Data}}{C_p \cdot (T_{C,out} - T_{C,in})} \quad (3.17)$$

In this formula, both $T_{C,in}$ and $T_{C,out}$ depend on the configuration of the data center in the OTE system. When the data center is connected to the DCS that uses the cold deep seawater as cold source, $T_{C,in} = 6^\circ\text{C}$ and $T_{C,out} = 11^\circ\text{C}$. When the data center is connected to the DCS that makes use of the effluent water coming from the OTEC as cold source, $T_{C,in} = 11^\circ\text{C}$ and $T_{C,out}$ depends on the return temperature for the cooled air or liquid. Furthermore the specific heat capacity, C_p , of the water is assumed to be constant, since the temperature difference between inlet and outlet is small.

The inputs needed for this module are:

- Maximum cooling demand ($\dot{Q}_{C,max}$)
- Unit of maximum cooling demand (kW or RT)
- Water temperature at inlet ($T_{C,in}$)
- Water temperature at outlet ($T_{C,out}$)
- Specific heat capacity of water (C_p)

3.2.4. Greenhouse cooling

To calculate the cooling demand of a greenhouse, an energy balance over the greenhouse needs to be made. This is done for a greenhouse with an area of 1 ha. It is assumed that a greenhouse with an area of x ha will have an x times higher cooling demand than a greenhouse of 1 ha.

For the calculation of the cooling demand, only the convective and the radiative heat transfer are taken into account. This is based on the calculations done by Priva, a company that is specialized in (sustainable) climate control for buildings and greenhouses [49].

The convective cooling load of a greenhouse can be calculated with eq. 3.18, better known as Newton's law of cooling.

$$\dot{Q}_{C,conv} = h \cdot A_{GH} \cdot (T_{env} - T_{GH,desired}) \quad (3.18)$$

A disadvantage of this calculation is that the convective heat transfer coefficient has to be calculated. This can be very difficult, because heat transfer correlations that depend on various dimensionless numbers should be used to calculate the heat transfer coefficient.

Another way to calculate the convective heat transfer is to make use of an simplified correlation. The correlation used by Priva to calculate the convective heat transfer can be found in eq. 3.19 [49]. Compared to eq. 3.21, the heat transfer coefficient is replaced by a two factors and the wind speed. The greenhouse factor f_{GH} and the wind factor f_w are constant, while the wind speed can be taken from environmental data. The values of the greenhouse and wind factor are taken from the data of Priva (Bron).

$$\dot{Q}_{C,conv} = f_{GH} \cdot \frac{100 + f_w \cdot v_{wind}}{100} \cdot A_{GH} \cdot (T_{env} - T_{GH,desired}) \quad (3.19)$$

The formula for the radiative cooling demand can be found in eq. 3.20. The global horizontal radiation G_{Global} is the power in W/m^2 received from the sun. The shading factor f_{shade} is the fraction of radiation that is blocked by shades and does not enter the greenhouse. The value of the shading factor is also based on the model of Priva (bron).

$$\dot{Q}_{C,rad} = A_{GH} \cdot \frac{G_{global}}{1000} \cdot (1 - f_{shade}) \quad (3.20)$$

The total cooling demand does not equal the sum of the conductive and the radiative cooling demand. The convective cooling will only be taken into account when $T_{env} > T_{GH,desired}$, because otherwise the convective cooling will be negative. The calculation of the total cooling demand $\dot{Q}_{C,GH}$ can be found in 3.21.

$$\dot{Q}_{C,GH} = \begin{cases} \dot{Q}_{C,rad} & \text{if } T_{env} < T_{GH,desired} \\ \dot{Q}_{C,conv} + \dot{Q}_{C,rad} & \text{if } T_{env} \geq T_{GH,desired} \end{cases} \quad (3.21)$$

A drawback of modeling the greenhouse cooling demand this way is that thermal accumulation is not taken into account. Since greenhouses are made from glass, this is not a problem for the building. But the heat accumulation in the soil might be present in reality. Furthermore with this calculations the inside temperature is kept constant by cooling at the same rate as heat is coming into the greenhouse. In reality there might be a dynamic system to control the temperature between certain limits. However, this calculation can give a good

insight in the maximum amounts of cooling needed.

When it is assumed that the heat exchanger has an efficiency of 100%, the formula to calculate the greenhouse water usage can be found in eq. 3.22.

$$\dot{m}_{C,GH} = \frac{\dot{Q}_{C,GH}}{C_p \cdot (T_{C,out} - T_{C,in})} \quad (3.22)$$

Just like the data center cooling, the greenhouse cold water demand depends on the configuration in the OTE system. In the first configuration the greenhouse is connected to the DCS with the cold deep seawater as cold source. In that case $T_{C,in} = 6^\circ C$ and $T_{C,out} = 11^\circ C$. The second configuration is to connect the greenhouse to effluent water cooled DCS in the Ecopark. Then the $T_{C,in} = 11^\circ C$ and $T_{C,out}$ will depend on $T_{GH,desired}$. A third configuration is a hybrid system, with both connections to the deep seawater and the waste water. This might be beneficial for some crops that only have to be cooled to a low temperature during a part of the day or night. In this case $T_{GH,desired}$ becomes a variable. During daytime the greenhouse can be cooled with waste water, when $T_{GH,desired}$ is high (for example around $28^\circ C$). During the night the greenhouse can be cooled with the deep seawater to a lower temperature (for example around $16^\circ C$).

The inputs needed for this module are:

- Total greenhouse area (A_{GH})
- Environmental temperature (T_{env})
- Water temperature at inlet ($T_{C,in}$)
- Water temperature at outlet ($T_{C,out}$)
- Global horizontal solar radiation (G_{global})
- Desired greenhouse indoor temperature ($T_{GH,desired}$)
- Wind speed (v_{wind})
- Greenhouse factor (f_{GH})
- Wind factor (f_w)
- Shading factor (f_{shade})

3.2.5. OTWP

For the calculation of the amount of fresh water that can be produced per kg of air, a h-s diagram for air (better known as Mollier diagram or psychrometric chart) can be used. The Mollier diagram is a thermodynamic chart for properties of humid air at constant pressure, usually the pressure at sea level. The parameters used in this chart are the dry-bulb temperature, wet-bulb temperature, dew point temperature, relative humidity, humidity ratio, specific enthalpy and specific volume. When two of these parameters are known, the other parameters are fixed.

Since this chart can not be used for calculations with Python, the Humid Air Properties function of CoolProp is used [3]. The equations for the Humid Air Properties implemented in CoolProp are based on a publication by Hermann et al. [18], which describes the outcome of the ASHRAE research project ASHREA-RP1485. The same source has been used in the ASHRAE Handbook 2009 to generate reference saturation property tables. Three inputs are needed for the Humid Air Properties, compared to two for the Mollier diagram. This is because the pressure is fixed for the Mollier diagram, while the pressure is variable for the Humid Air Properties module of CoolProp.

To make it clear how the produced amount of water is calculated with the Humid Air Properties in Coolprop, an example is made based on the Mollier diagrams that can be found in figure 3.7. First the humidity ratio (Ω_{in}) of the air at the inlet is calculated. The humidity ratio is the amount of water vapor per kg dry air. The humidity ratio at the inlet can be calculated with the environmental temperature, the relative humidity and the environmental pressure. The values of these parameters are:

- $T_{air,in}$ = $28^\circ C$
- $p_{ai,in}$ = 1.01325 bar
- $RH_{air,in}$ = 70%
- Ω_{in} = 17 g/kg

This can also be seen at point 1 in figure 3.7. The cooling of air can be best simulated as an adiabatic process. This means that the cooling till the saturation/dew point is isenthalpic. The wet-bulb temperature corresponding to the air at the inlet can be calculated with Coolprop. In the example the wet-bulb temperature at the dew-point is 24°C, see point 2 in figure 3.7.

At the dew-point the relative humidity is 100%, which means that the air cannot absorb more water at that point. Together with the wet-bulb temperature and the pressure, the humidity ratio at the wet-bulb point can be determined. This is the maximum humidity ratio, and in this example $\Omega_{max} = 18.6 \text{ g/kg}$.

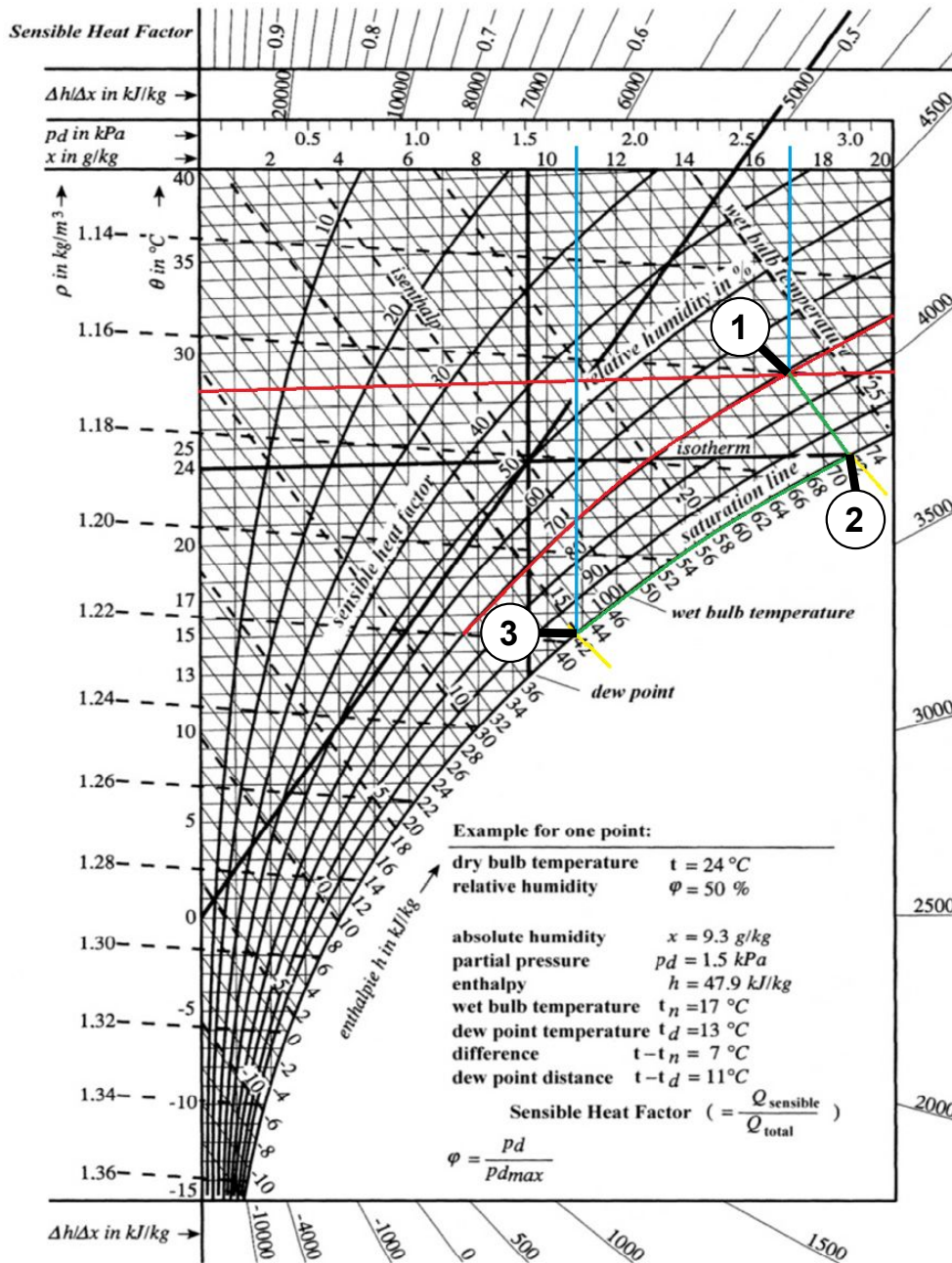


Figure 3.7: Mollier diagram for the example with $T_{env} = 28^\circ\text{C}$, $P_{env} = 1.01325 \text{ bar}$, $RH = 70\%$, and $T_{air,out} = 15^\circ\text{C}$

The next thing to determine is the humidity ratio at the outlet. This depends on the outlet air temperature. The outlet air temperature $T_{air,out}$ can be chosen, but depends on the pinch temperature in the heat exchanger. In this example the air is cooled till 15°C . With this temperature, the relative humidity of 100% and

the environmental pressure, the humidity ratio at the outlet can be determined. The humidity ratio at the outlet in this example is $\Omega_{out} = 11 \text{ g/kg}$, see point 3 in figure 3.7.

Now the difference in humidity ratio can be calculated with eq. 3.23.

$$\Delta\Omega = \Omega_{max} - \Omega_{out} \quad (3.23)$$

In case of the example, $\Delta\Omega = 7.6 \text{ g/kg}$. The required air flow at the inlet that is needed to produce the demanded fresh water output then can be calculated with eq. 3.24 and the air mass flow at the outlet can be calculated with 3.25 (with $\Delta\Omega$ in kg/kg).

$$\dot{m}_{air,in} = \frac{\dot{m}_{fw,demand}}{\Delta\Omega} \quad (3.24)$$

$$\dot{m}_{air,out} = \dot{m}_{air,in} \cdot (1 - \Delta\Omega) \quad (3.25)$$

Eventually the required cooling demand that is needed to cool the air from point 1 to point 3 can be calculated. Therefore the enthalpies should be known for point 1 and point 3. The enthalpy at the inlet $h_{air,in}$ can be calculated with $T_{air,in}$, $p_{air,in}$ and $RH_{air,in}$. The enthalpy at point 3, $h_{air,out}$, can be calculated with $T_{air,out}$, $p_{air,out}$ and $RH_{air,out} = 1$. For the example in figure 3.7, the enthalpies are:

- $h_{air,in} = 72 \text{ kJ/kg}$
- $h_{air,out} = 42 \text{ kJ/kg}$

Next the cooling demand is calculated in eq. 3.26.

$$\dot{Q}_{C,air} = \dot{m}_{air,in} \cdot h_{air,in} - \dot{m}_{air,out} \cdot h_{air,out} \quad (3.26)$$

The hot air is cooled in a direct contact condenser with cold fresh water, see figure 2.7. This condensation process is difficult to model exactly, because it depends on many variables and heat/mass transfer correlations. Therefore it is much easier to model the condenser in an ideal situation with 100% efficiency. It is assumed that this does not affect the cold water demand significantly, because an exact model is used to optimize the cost and size of an OTWP, not the cold water usage. So in this case it can be assumed that the heat rejected by the hot air equals the heat absorbed by the fresh water, which means that $\dot{Q}_{C,air} = \dot{Q}_{C,fw}$.

The last part to calculate is the cold water demand of the OTWP installation. It can be assumed that the heat rejected by the fresh water in the heat exchanger equals the heat absorbed by the effluent water in the Ecopark (the cooling demand of the OTWP), which means that $\dot{Q}_{C,fw} = \dot{Q}_{C,OTWP}$. With that assumption the effluent water demand can be calculated with eq. 3.27.

$$\dot{m}_{C,OTWP} = \frac{\dot{Q}_{C,OTWP}}{C_p \cdot (T_{C,out} - T_{C,in})} \quad (3.27)$$

In this formula, $T_{C,in}$ depends on the output temperature of the OTEC/SWAC water. $T_{C,out}$ is a variable and should be estimated properly. The limiting factor here is that $T_{C,out}$ cannot be higher than $T_{fw,out}$, which will be around 17°C .

The demand curve of the OTWP can be managed in two ways. The first is to adjust the cycle to have a steady output of the demand in kg/s fresh water. This means that the cold water coming from OTEC/SWAC should be variable. The second is to predict the temperature and relative humidity of the coming day to calculate the average water flow coming from the OTEC/SWAC to fulfill the demand over a day. Furthermore the operational hours of the OTWP can be 24/7 or just a part of the day/night. Even though at night may sound strange, this is possible because of the relative high temperatures at night and stable relative humidity for tropical regions. In this model the demand of the OTWP is modeled to have a fixed water production.

The inputs of the OTWP module are:

- Fresh water demand $\dot{m}_{fw,demand}$ (in $\frac{m^3}{day}$)
- Environmental temperature ($T_{air,in}$)
- Environmental pressure ($p_{air,in}$)
- Relative Humidity ($RH_{air,in}$)
- Temperature air out ($T_{air,out}$)
- Water temperature at inlet ($T_{C,in}$)
- Water temperature at outlet ($T_{C,out}$)
- Fresh water temperature at condenser inlet ($T_{fw,in}$)
- Fresh water temperature at condenser outlet ($T_{fw,out}$)

3.3. Model integration

Now that all the subsystems are modeled, all these modules can be combine to model the OTE system. The subsystems are modeled in such a way that they can be imported as functions in a master file. A block-chain overview of the model can be seen in figure 3.8. First the Inputs will be loaded in the Master file. In the Input file the demands are given for each component. But also parameters like the location, the year for which the calculations should be made, the depth of the CWP, the maximum flow speed of the deep seawater in the CWP, the desired indoor temperature for the greenhouse and some temperatures for the OTWP cycle. The model is made in such a way that only inputs in the Inputs file have to be changed, to keep the model clear.

Secondly, the Seawater Temperatures and the Environmental Data modules will be loaded into the Master file. The outputs of the Seawater Temperatures module, $T_{sw,C}$ and $T_{sw,H}$, depends on location, year and depth of the CWP. The outputs of the Environmental Data module are the air temperature, environmental pressure, relative humidity, solar radiation, solar factor and wind speed and are depending on the location and year.

After that the modules of the subsystems will be imported in the Master file. Each subsystem is modeled as a function with the water usage as output. This way the function is imported in the Master file and can be used with the inputs mentioned in section 3.2. In the Master file the total cold deep seawater usage and Ecopark water usage is calculated. With the water usage and the maximum flow speed of the deep seawater the CWP outer diameter can be calculated.

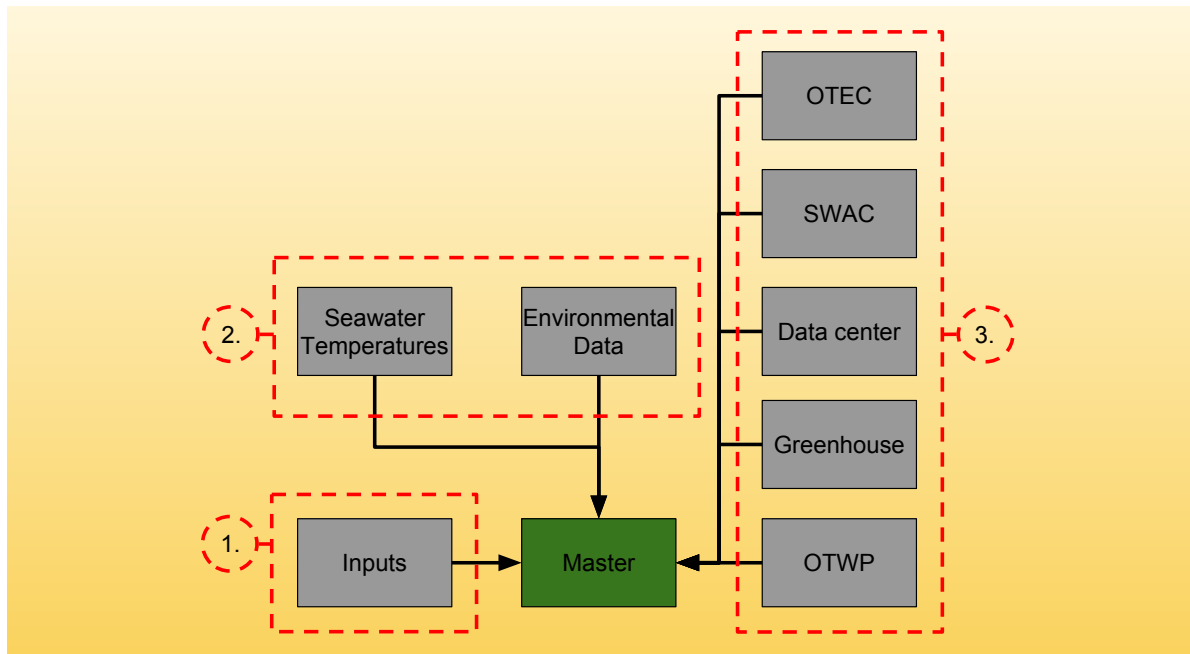


Figure 3.8: Schematic overview of the OTE system model

3.4. Optimization techniques

Since the goal of this research is to make clear if it is beneficial to optimize CWP diameter with regard to time-dependent integration of the subsystems in an OTE system, three possible ways to optimize the water usage will be given in this section. First the possible optimization by spreading the demands over the day will be discussed in subsection 3.4.1. Secondly, in subsection 3.4.2 the possibility to optimize the cold water usage by implementing (thermal) storages in the OTE system to lower the cold water peak demands of the subsystems will be discussed. The last optimization method to discuss is to change the OTE system configuration. This will be done in subsection 3.4.3.

3.4.1. Time-integration

One way to optimize the water usage is by time-dependent integration. This way the water usage per subsystem can be shifted or spread over a period of time, to avoid that all the peak demands are at the same time. For each component it can be checked if it is possible to shift the demand or not.

The cold water demand of the OTEC power plant cannot be shifted, because otherwise it is not generating the demanded electricity output. Even so the cold water demand of the DCS cannot be shifted, because otherwise the SWAC and data center receive too little cold water. This can lead to houses that cannot be cooled or data center component failure because of too high temperatures. Furthermore also the demand of the greenhouses cannot be shifted, because this might lead to crop failure.

For the OTWP installation it can be expected that it is possible to shift the cold water demand. Tropical islands are known for the high temperatures, also during night. Furthermore, the fluctuations in relative humidity between day and night are not very high, so that the fresh water production can be done at night. The disadvantages are that the size of the installation should be larger, because the same amount of water should be produced in a smaller time period, and that the efficiency might be lower because of the less ideal circumstances.

Since demand shifting is only possible for OTWP, and OTWP does not impact the cold deep seawater usage, time-dependent integration is not built in the model. However, when other subsystems than described above are implemented, it should be checked if time-dependent integration is possible or not.

3.4.2. Storage

Another way to optimize the cold water usage discussed is optimization through storage. By using a storage, the peak demands can be flattened. When this is done for a few components, this might result in a decrease of maximum cold water usage and thus in a smaller CWP diameter.

It is assumed that the thermal storage has an efficiency of 100%. Although this might not represent the real case, this will give a good approximation of the required size of the thermal storage. This can be seen as a best-case scenario for thermal storage. When the result is that a 100% efficient thermal storage is not feasible, then it will not be feasible at all. When the result is that a 100% efficient thermal storage is feasible, it should be further investigated if a non-ideal thermal storage is feasible too.

Two kinds of storages methods will be researched in this subsection. The first storage method is daily storage, the second one is the yearly storage method.

Daily storage

The daily storage method is to compensate for the peak demand per day. To do this, first the average water usage is calculated. After that it can be calculated how much more cooling has to come from the storage. This water mass flow that is needed from the storage can be calculated with eq. 3.28. In this equation \dot{Q}_C is the cooling demand of the subsystem, ΔT is the temperature difference between the cold water input and output and ΔT_{stor} is the temperature difference between the storage and the water output of the subsystem.

$$\dot{m}_{C,stor} = \frac{\dot{m}_{avg,day} \cdot C_p \cdot \Delta T - \dot{Q}_C}{C_p \cdot \Delta T_{stor}} \quad (3.28)$$

When $\dot{m}_{avg,day} \cdot C_p \cdot \Delta T$ is lower than \dot{Q}_C , water will be taken out of the storage and $\dot{m}_{C,stor}$ is negative. Other way around when \dot{Q}_C is lower than $\dot{m}_{avg,day} \cdot C_p \cdot \Delta T$, water will be put into the storage and $\dot{m}_{C,stor}$ is positive. To give a better idea of how big the storage capacity should be, the hourly volume flow in or out of the storage can be calculated with eq. 3.29.

$$\dot{\phi}_{V,stor} = \frac{\dot{m}_{C,stor} \cdot 3600}{\rho} \quad (3.29)$$

The water volume in the storage can be calculated by integrating the volume flow rate. Since the volume flow rate is calculated in $\frac{m^3}{h}$ this is simply done by adding the all the flow rates as can be seen in eq. 3.30.

$$V_{stor}(h) = \sum_{i=0}^h \dot{\phi}_{V,stor}(i) \quad (3.30)$$

However, the values of V_{stor} can be negative. Therefore the minimum value of the storage capacity should be added. Then the required size of the storage can be calculated as the maximum value of V_{stor} .

It is assumed that the storage is partly filled at the beginning of every year. The fraction depends on the subsystem and other conditions. It might happen that the water level in the storage is lower at the end of the year than at the beginning. A solver is used to ensure that the water level will be the same at the beginning and the end of the year, so that the net water usage is zero. This is done by varying $\dot{m}_{avg,day}$.

Yearly storage

Instead of just compensating the daily fluctuations in water usage, it can be researched what the benefits could be of compensating seasonal fluctuations by a thermal storage. This will be modeled in the same way as the daily storage with one difference. In eq. 3.28 $\dot{m}_{avg,day}$ is replaced with a yearly average mass flow, as can be seen in eq. 3.31.

$$\dot{m}_{C,stor} = \frac{\dot{m}_{avg,year} \cdot C_p \cdot \Delta T - \dot{Q}_C}{C_p \cdot \Delta T_{stor}} \quad (3.31)$$

The yearly average mass flow is calculated as the mass flow that is needed in a year so that the combined mass flow into the subsystem and the storage is constant.

The volume flow and the required storage capacity can be calculated with eq. 3.29 and eq. 3.30, just like in the case of the daily storage. It is very likely that the required storage capacity for yearly storage will be higher than for daily storage. Therefore it should be checked in every case what the required capacity is and if such capacity is feasible, both technical and economical.

Assumptions

A few assumptions are made to make the modeling of the storage easier, without losing the relevance. First of all it is assumed that the storage is perfectly isolated and therefore adiabatic. Consequently the temperatures inside the storage are constant.

The storages are divided in two categories: storage of cold deep seawater and storage of effluent water. Even though the maximum temperature of the deep seawater will be around $5.5^\circ C$, it is assumed that the temperature of the cold water storage is $6^\circ C$. Furthermore the temperature of the storage of the effluent water is assumed to be $11^\circ C$ year round. This is the same temperature as the effluent water.

3.4.3. Configuration

The optimization of the water usage can be done by adapting the configuration of the OTE system. With adapting the configuration is meant that some of the subsystems can be connected to the effluent stream instead of a connection to the cold deep seawater. The subsystems that might be suitable to make use of the effluent water are data center cooling, greenhouse cooling and OTWP. When the current air conditioning is based on a chiller with supply temperature of $6^\circ C$ to $8^\circ C$, SWAC cannot be used in the effluent stream because of the requirement that the cold water should be about $5^\circ C$. Otherwise it might be possible to design a SWAC systems that uses the effluent water as cold source. As an example, the schematic overview of the configuration in figure 3.9 can have more optimized water usage than the configuration show in figure 2.10 because more subsystems are connected to the effluent water. The model is made in such a way that it is easy to adapt the configuration, so that it is easy to investigate the ideal configuration.

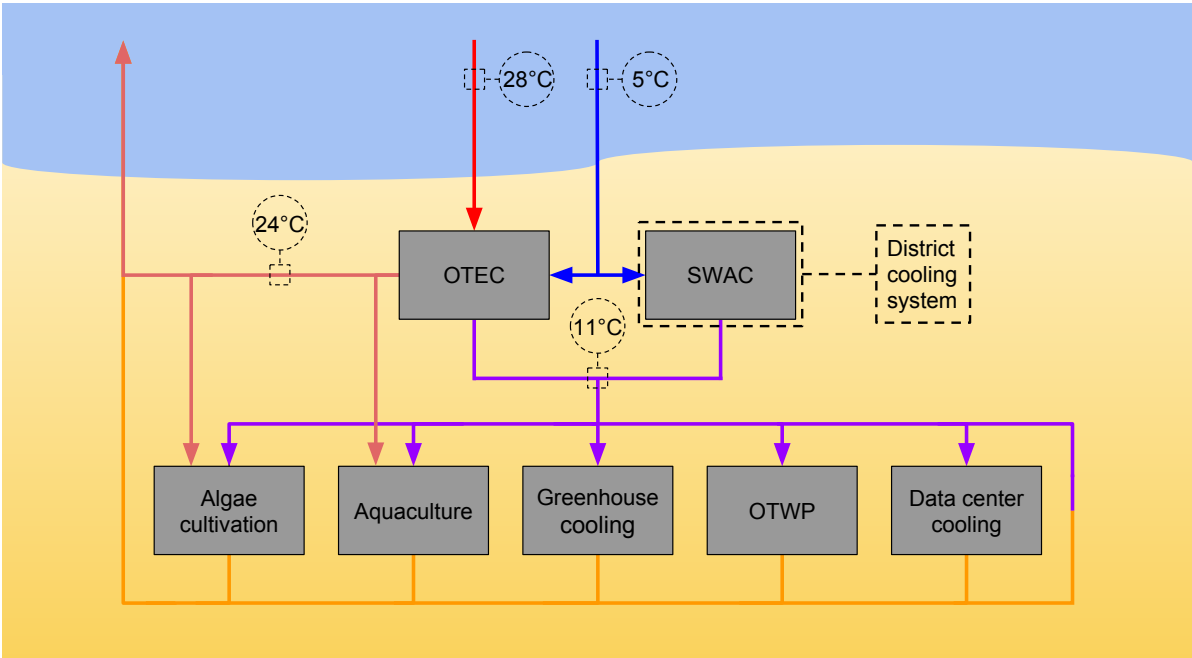


Figure 3.9: Schematic overview of an OTE system configuration with an optimized design

4

Case study: Curaçao

To compare the effects of the integration and optimization of the OTE system, a case study will be made. So for the same input parameters the differences in outputs will be discussed. The base case will be a case study for the island of Curaçao. It is assumed that an Ocean Thermal Energy system with OTEC, SWAC, OTWP, data center cooling and greenhouse cooling will be build next to the airport of Curaçao. In section 4.1 the input parameters will be discussed. Thereafter the results will be shown for the normal Ocean Thermal Energy system in section 4.2. The integrated OTE system and the different optimizations will be discussed in section 4.3.

4.1. Inputs

Before a comparison can be made, all the input parameters have to be known for the location. The location for the OTE system is near Hato Curaçao International Airport, see figure 4.1.

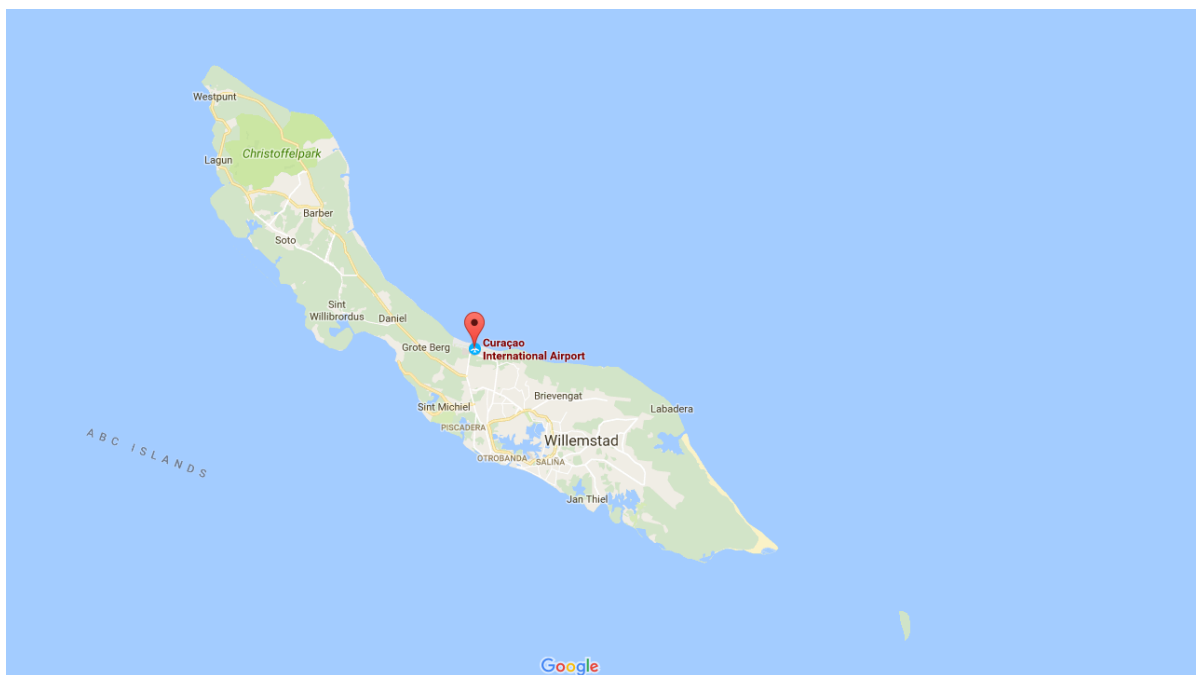


Figure 4.1: The location of Hato Curaçao International Airport on the island

The airport is located in the middle of the north-east side of the island. This means that the cold water pipe has to be deployed on that side of the island.

There are a lot of inputs that influence the water demands of the OTE subsystems. The inputs can be separated in four main categories, namely:

- Seawater temperatures.
- Environmental properties.
- Configuration.
- Demands.

The seawater temperatures will be discussed in subsection 4.1.1. After that the environmental properties will be discussed in subsection 4.1.2. Lastly, the demands of the subsystems will be discussed in subsection 4.1.4.

4.1.1. Seawater temperatures

The most important input parameters to know are the cold deep sea and the hot surface water temperature. This is because these two inputs are the key parameters of OTEC and SWAC. OTEC and SWAC have both different requirements when it comes to water temperatures. For OTEC the *temperature difference* between the cold deep seawater and the hot surface water should be more than 20°C . For SWAC the *cold deep seawater temperature* should be lower than 5.5°C .

The seawater temperatures can be found with the Copernicus Marine Environment Monitoring Service (CMEMS). In this case the GLOBAL_ANALYSIS_FORECAST_PHY_001_024 data is used. The outputs are delivered as daily means. The horizontal resolution of the map is $1/12^{\circ}$ and 50 vertical levels ranging from 0 to 5728 meters are present in this dataset.

The first thing to do is to determine the depth of the sea around Curaçao. This can give a good approximation for the location of the CWP intake. In figure 4.2 the depth of the deepest data point of Copernicus can be seen. So this is not the actual depth at that location, but the actual depth is between this depth and the depth of the next data point of the CMEMS data.

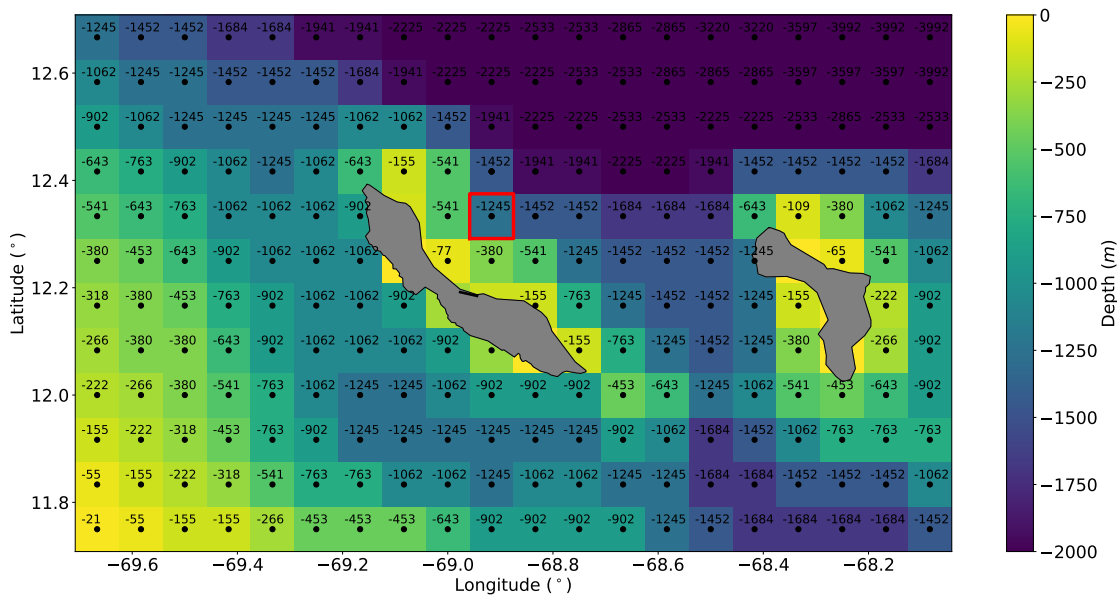


Figure 4.2: Seafloor topography Curaçao - The depth of the deepest data point of Copernicus for Curaçao

From figure 4.2 it can be seen that slope of the shore is not ideal on the north-east side of the island. The rule of thumb for OTEC is that the intake of the CWP should be at a depth of 1000 m. The data point closest to the airport with a depth of 1000 m or more is the one in the red box in figure 4.2. The location of this data point is about 15 km offshore.

The seawater temperatures of different depths and different years can be compared with each other to determine the depth of the CWP. In figure 4.3 the temperature difference between can be seen for the depth of 763 meter, 902 meter, 1062 meter and 1245 meter, respectively.

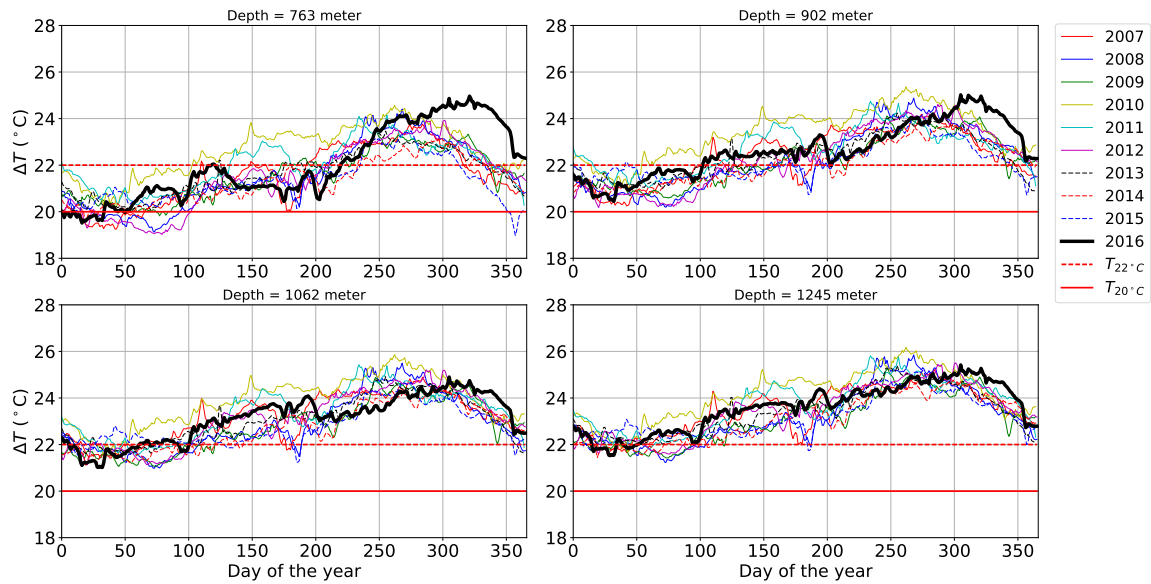


Figure 4.3: Curaçao 2007 - 2016: temperature difference between cold deep seawater and hot surface water for depths 763 meter, 902 meter, 1062 meter and 1245 meter

From figure 4.3 it can be seen that a depth of 902 meter is sufficient to fulfill the requirement of at least 20°C temperature difference for OTEC. However, when looking at cold deep seawater temperature in figure 4.4, it can be seen that a depth of 902 meter is not sufficient to fulfill the requirement of SWAC. Even at a depth of 1062 meter the temperature of the deep seawater was above 5.5°C for a short period of time between 2007 to 2016. But since it was only a short period and the ten year average temperature is well below 5.5°C , the cold seawater temperatures of 1062 meter depth are taken as input for this case study.

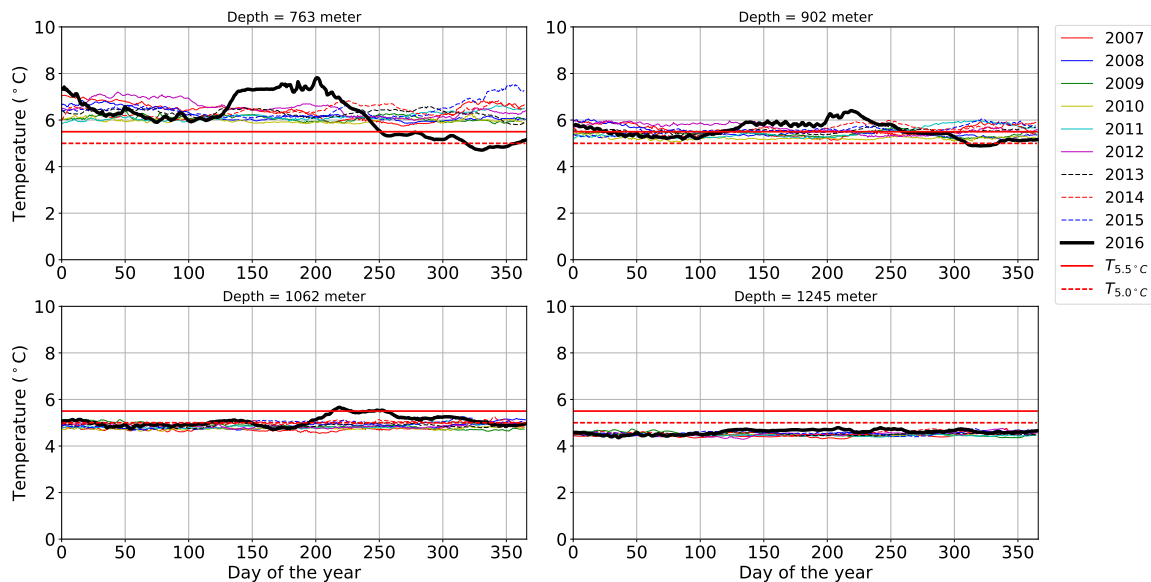


Figure 4.4: Curaçao 2007 - 2016: temperature of the cold deep seawater for depths 763 meter, 902 meter, 1062 meter and 1245 meter

4.1.2. Environmental properties

A weather station is present near the airport, but at the moment only data from the year 2015 is available. Therefore the data source for air temperatures, environmental pressure, relative humidity, wind velocity and solar radiation come from the software package Meteonorm [35]. Meteonorm has more than 2000 active

users and is included in almost every PV, solar thermal or building simulation software on the market.

The disadvantage of Meteonorm is that the environmental data are not the measured values, but calculated data. This is stochastically generated interpolated data is only based on measurements. The data represents a *typical year*, not a historical year. So basically, the *typical year* represents a hypothetical year based on historical (interpolated) climate data for the selected location.

Despite that this might not represent the real historical values for the environmental data, it can give a good approximation of the reality. The shortcomings of the Meteonorm data are further discussed in appendix E

For the year 2016 the values of the temperature, pressure, relative humidity, wind speed, hourly global horizontal radiation and daily global horizontal radiation can be found in figure 4.5a to figure 4.5f, respectively.

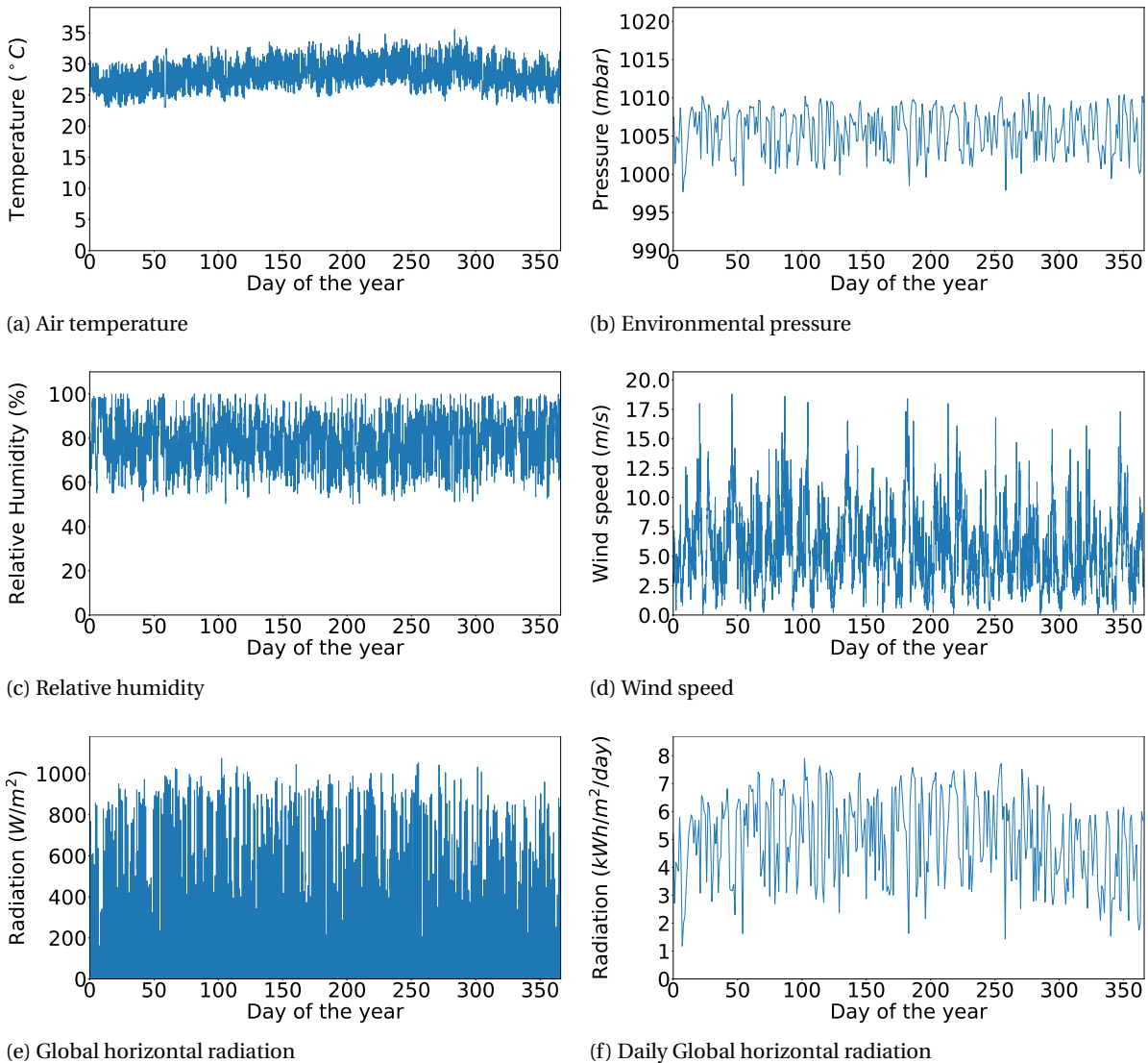


Figure 4.5: The environmental data for Curaçao from Meteonorm for the year 2016

4.1.3. Configuration

The configuration of all the subsystems in the Ocean Thermal Energy system is the next input of the model. For each subsystem, except OTEC, it can be chosen whether it has to use the cold deep seawater or the effluent water. The configuration of the Curaçao base case is as follows: The OTEC, SWAC and data center cooling are connected to the cold deep seawater, the greenhouse cooling is connected to both the cold deep seawater and the effluent water and the OTWP plant is connected to the effluent water. The schematic overview of this configuration can be seen in figure 4.6.

In this figure it can be seen that the greenhouse has a dual connection. During the day the greenhouse is cooled with the effluent water to a temperature of 28°C, while at night the cold deep seawater is used to cool the greenhouse to a temperature of 16°C. Furthermore, the subsystems aqua farms and algae cultivation are not taken into account in this model, for the reasons that are given in 2.5.

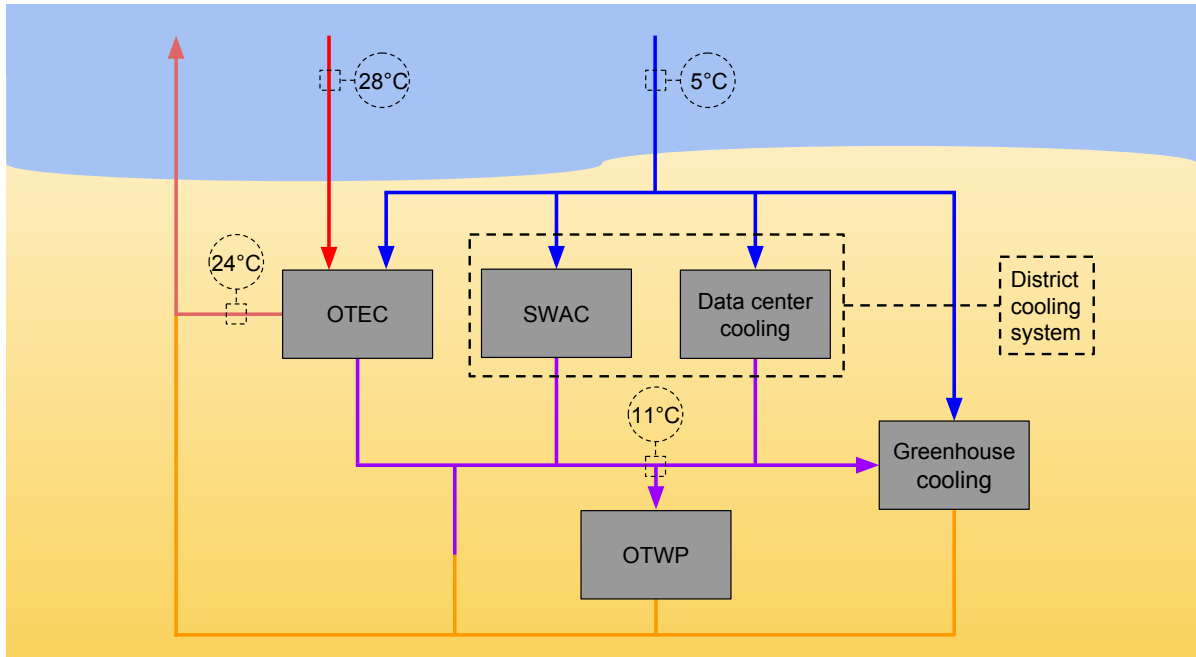


Figure 4.6: Schematic overview of the configuration of the Ocean Thermal Energy system for Curaçao

4.1.4. Demands

The last parameters that need to be known are the power demand of the OTEC, the maximum cooling demands of the SWAC installation and the data center, the total area of greenhouses and the demanded fresh water production rate for the OTWP. The demands are based on the expected demands for the first stage of development of the OTE system in Curaçao.

- OTEC: 500 kW
- SWAC: 7.5 MW_{th}
- OTWP: 25 m^3/day
- Data center: 720 RT (Refrigeration Tonnes)
- Agriculture: 3 ha

These values are used as input in the model, together with the seawater temperatures and environmental properties.

4.2. Simple demand analysis (non-integrated OTE system)

The easiest way to estimate the total cold deep seawater usage of the OTE system is to calculate the water usage for each application and add the maximum values to calculate the maximum of the total deep seawater usage and the pipe diameter. The disadvantage of this method is that peaks of the water usage per subsystem are not at the same time, the estimated total water usage is too high and that a bigger cold water pipe will be installed than needed.

The results for the simple demand analysis for the years 2007 to 2016 can be found in figure 4.7. In this figure the total cold deep seawater usage can be seen.

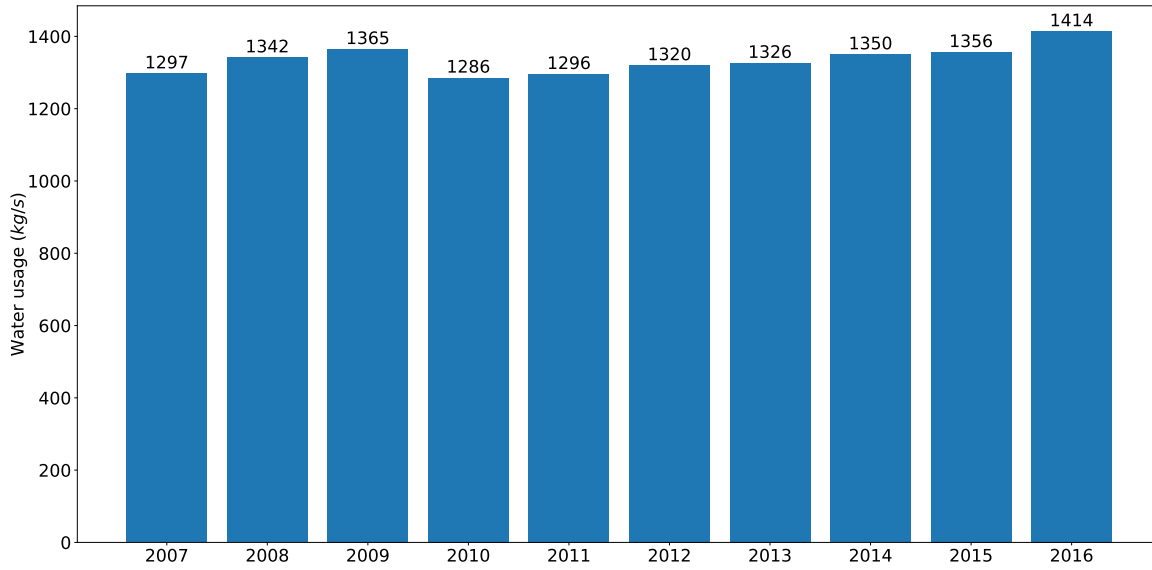


Figure 4.7: Curaçao 2007 - 2016: Maximum cold deep seawater usage per year in case of the simple demand analysis

The diameter of the CWP can be directly coupled to the water usage of the OTE system. The required outside diameter of the CWP can be calculated with eq. 4.1:

$$d_{out} = \frac{SDR}{SDR - 2} \cdot \sqrt{\frac{\dot{m}_{C,max}}{\frac{1}{4} \cdot \pi \cdot \rho \cdot \phi_{C,max}}} \quad (4.1)$$

with:

- $\dot{m}_{C,max}$, the maximum cold water mass flow in kg/s
- $\phi_{C,max}$, the maximum cold water velocity in the CWP in m/s
- ρ , the density of the water in kg/m^3
- SDR (Standard Dimension Ratio), the ratio of pipe diameter to wall thickness

In the case of the simple demand analysis the maximum cold deep seawater mass flow of the years 2007 to 2016 is 1414 kg/s , the maximum flow velocity in the cold water pipe is 1.5 m/s , the density of the cold water of about $5^\circ C$ is approximately 1000 kg/s and the ratio of the pipe diameter to wall thickness is 17. By filling out these values, the formula to calculate the outside diameter of the cold water pipe can be found in equation 4.2.

$$d_{out} = \frac{17}{17 - 2} \cdot \sqrt{\frac{1414}{\frac{1}{4} \cdot \pi \cdot 1000 \cdot 1.5}} = 1.242 \quad m \quad (4.2)$$

4.3. Time-integrated OTE system

Instead of just looking at the maximum water usage per subsystem and adding the maxima, a time-integrated approach can be used to calculate the maximum mass flow of the total cold deep seawater usage. By using this method the disadvantage of overestimating the water demand and pipe diameter is solved.

First the cold water demands per subsystem are calculated for every hour of the day for the timespan of a year. Then the demands can be divided in two categories, namely the category that uses the cold deep seawater and the category that uses the effluent water. Next the total cold deep seawater usage can be calculated for every hour by adding the demands of the subsystems in each category. This is done for the years 2007 to 2016 and the results of the total cold deep seawater usage can be found in figure 4.8. The water usage per subsystem for the time-integrated system can be found in appendix B.

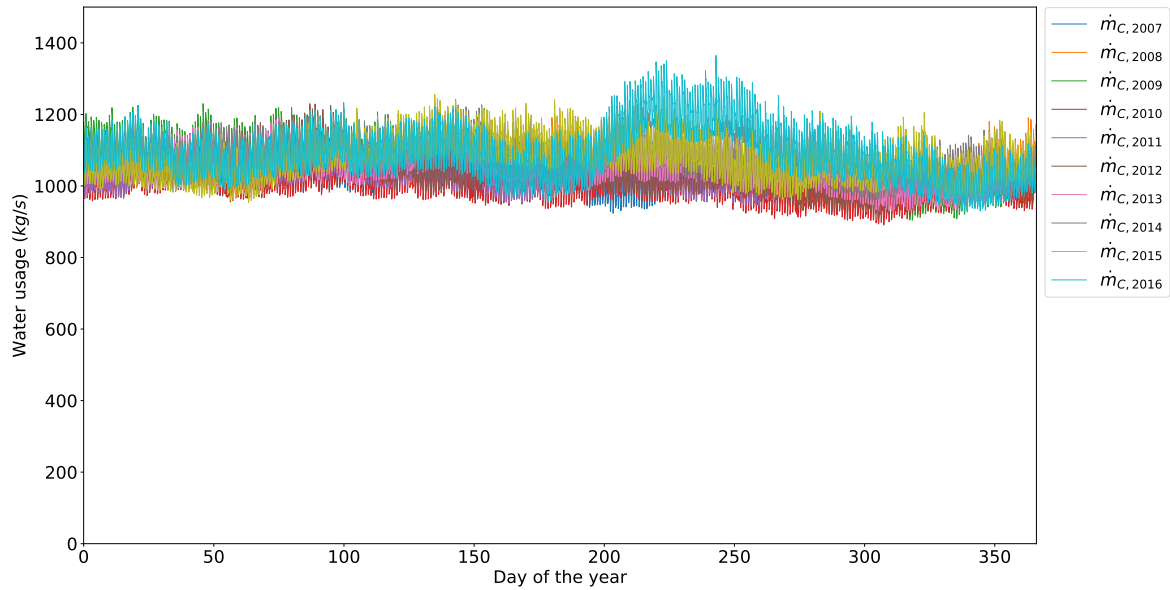


Figure 4.8: Curaçao 2007 - 2016: Total deep seawater usage in case of the time-integrated OTE system

It can be seen that there is a clear peak in water usage in 2016 (from about day 200 to 275) with a cold deep seawater demand of 1365 kg/s, while the maximum total water usage is quite stable in all the other years and fluctuates between 1171 and 1265 kg/s (see figure 4.9). The reason for this peak is the peak in cold deep seawater temperature and the lowest temperature difference in the same period (see figure 4.4 and figure 4.3). This leads to a lower thermal efficiency of the OTEC and thus in a higher cold water mass flow. Nevertheless the difference between the daily minimum and maximum are typically around between 100 and 200 kg/s.

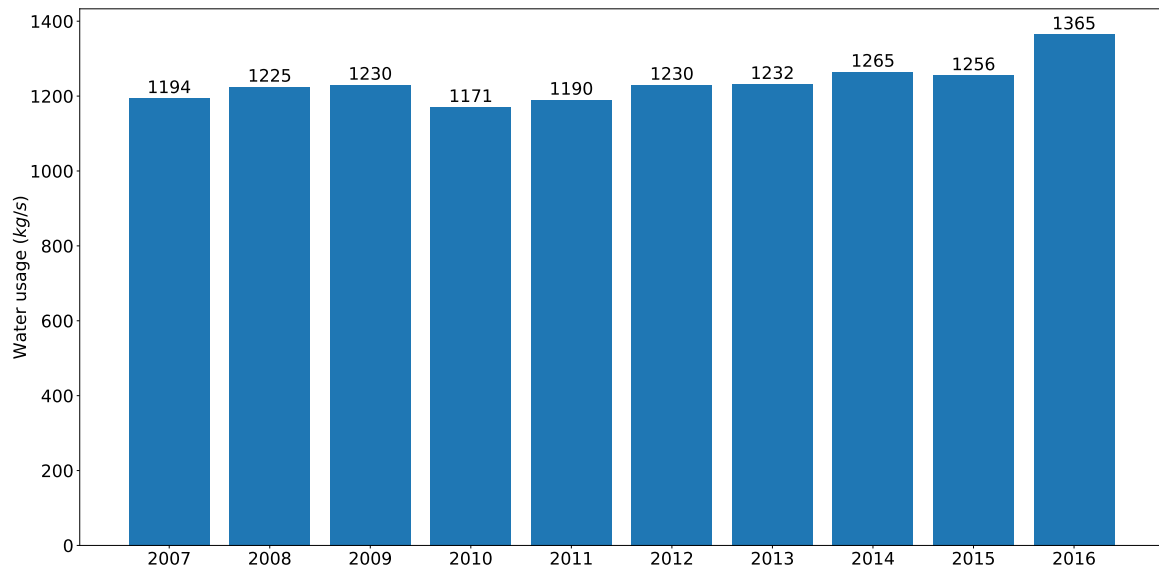


Figure 4.9: Curaçao 2007 - 2016: Maximum cold deep seawater usage per year in case of the time-integrated OTE system

The required cold water pipe diameter for this time-integrated OTE system can be calculated with eq. 4.1. The filled in equation for this case can be seen in eq. 4.3

$$d_{out} = \frac{17}{17-2} \cdot \sqrt{\frac{1365}{\frac{1}{4} \cdot \pi \cdot 1000 \cdot 1.5}} = 1.22 \text{ m} \quad (4.3)$$

When the simple demand analysis and the time-integrated analysis are compared, it can be seen that for each year the water usage is lower in case of the time-integrated analysis. The average decrease in mass flow is 99.4

kg/s for these 10 years. However, when looking at the two highest water usages of both cases the difference is only 49 kg/s. This is a decrease of 3.5% compared to the simple demand analysis. The required cold water pipe outside diameter decreased 1.61% from 1.242 to 1.22 m.

It is interesting to see what the results would be when 2016 was not taken into account, so when this research was done one year before. In that case the maximum water flow for the simple demand analysis would be 1365 kg/s and for the time-integrated analysis 1265 kg/s. The decrease in maximum cold water mass flow then would be 100 kg/s, a reduction of 7.3% compared to the simple demand analysis. The cold water pipe diameter would be reduced from 1.22 to 1.17 m, a reduction of 4.0%. This is quite a difference compared to the calculations which include 2016. It is the result of unusual seawater temperatures in 2016 (see figure 4.4). With recent trends in climate change, it can be expected that more years with unusual seawater temperatures will appear in the future. Therefore it is a good thing that the year 2016 is taken into account, so that maximum water usage is not underestimated.

The last thing to look into is the water usage of the Ecopark, in this case the effluent water usage of the greenhouse cooling and of the OTWP installation. The needed effluent water mass flow cannot be higher than the cold deep seawater mass flow. Therefore the Ecopark water surplus can be seen in figure 4.10. The Ecopark water surplus is the cold deep seawater mass flow minus the needed effluent water mass flow for the greenhouse cooling and the OTWP installation.

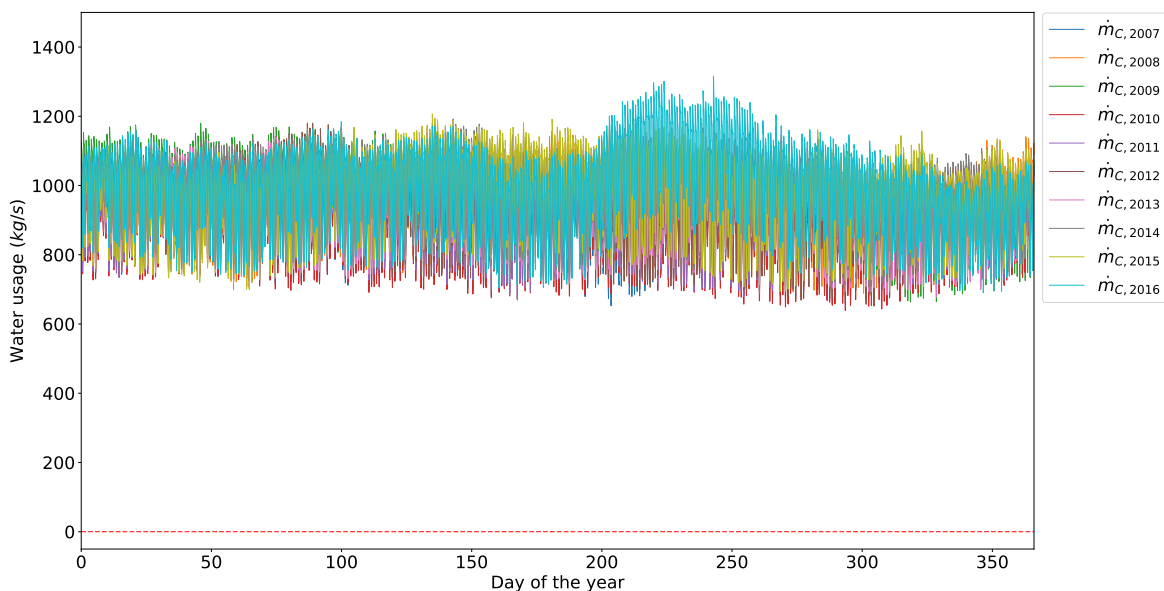


Figure 4.10: Curaçao 2007 - 2016: Ecopark water surplus per year in case of the time-integrated OTE system

The Ecopark water surplus is always positive, so there is sufficient effluent water to supply the demands of the greenhouses and the OTWP installation. Even more, there is plenty effluent water that is not used in this case. This gives possibilities for future growth of the Ecopark. Either the greenhouse cooling demand or the fresh water production can be increased or other subsystems can make use of the effluent water.

4.4. Optimization by storage

To optimize and reduce the maximum water demands and cold water pipe diameter, thermal storage tanks could be added to the OTE system. This way peak demands in water usage can be lowered so that the pipe diameter can be reduced. Two storage techniques will be discussed, namely the daily storage and the yearly storage. The optimization by daily and yearly thermal storage will be discussed in subsection 4.4.1 and subsection 4.4.2, respectively.

4.4.1. Optimization by daily storage

The optimization by daily storage is done as described in section 3.4.2. The same configuration is used as for the base case, see figure 4.6. The results for the water usage by daily storage can be seen in figure 4.11. The daily storage is applied to each subsystem except for OTEC. The water usages per subsystem can be found in appendix B.

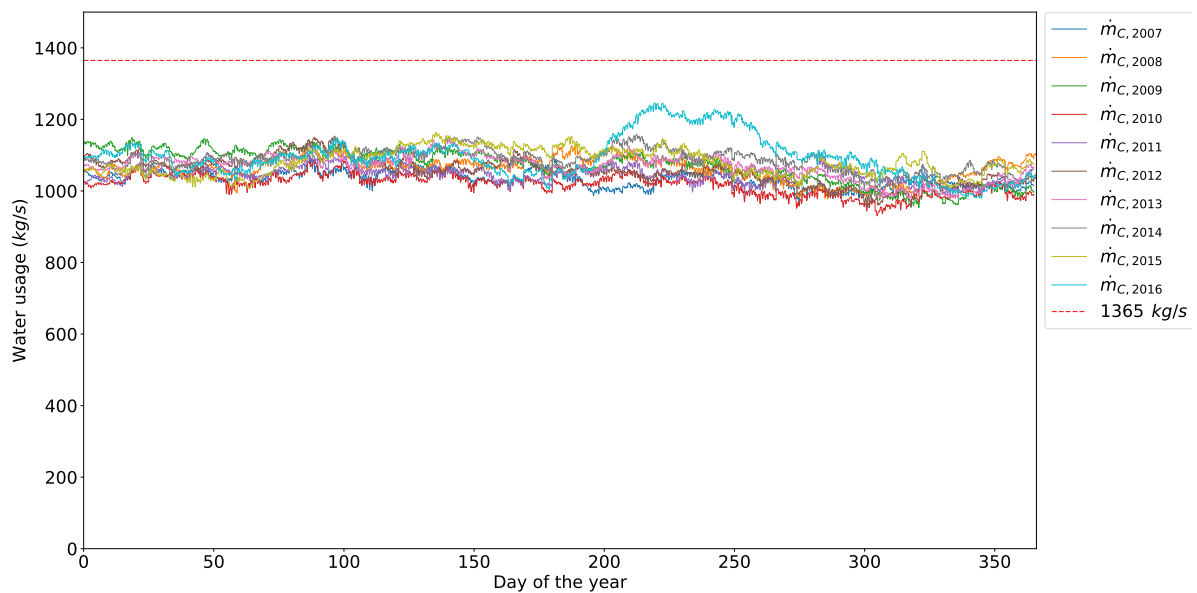


Figure 4.11: Curaçao 2007-2016: Total deep seawater usage in case of optimization by daily storage

In this case the maximum water usage in the period is 1246 kg/s in the year 2016. The required CWP diameter is 1.166 m . This is a reduction of 8.7% in maximum cold water mass flow and 4.4% in pipe diameter compared to the base case. In figure 4.12 the required storage capacity for SWAC, data center cooling, greenhouse cooling and OTWP can be found for every year.

The required storage capacities are:

- SWAC: 3927 m^3
- Data center: 943 m^3
- Greenhouse DOW: $14\,541 \text{ m}^3$
- Greenhouse Ecopark: 3754 m^3
- OTWP: 44 m^3

The storage capacity needed for the greenhouse cooling that is connected to the DOW is the highest with about $14,500 \text{ m}^3$. This is quite large, but not impossible. The largest thermal energy storages tanks is around 6.1 MG (mega gallon) by DN Tanks. Converted to cubic meters, this is about $23,000 \text{ m}^3$. Furthermore there are also options to combine multiple smaller storage tanks to satisfy the required storage capacity.

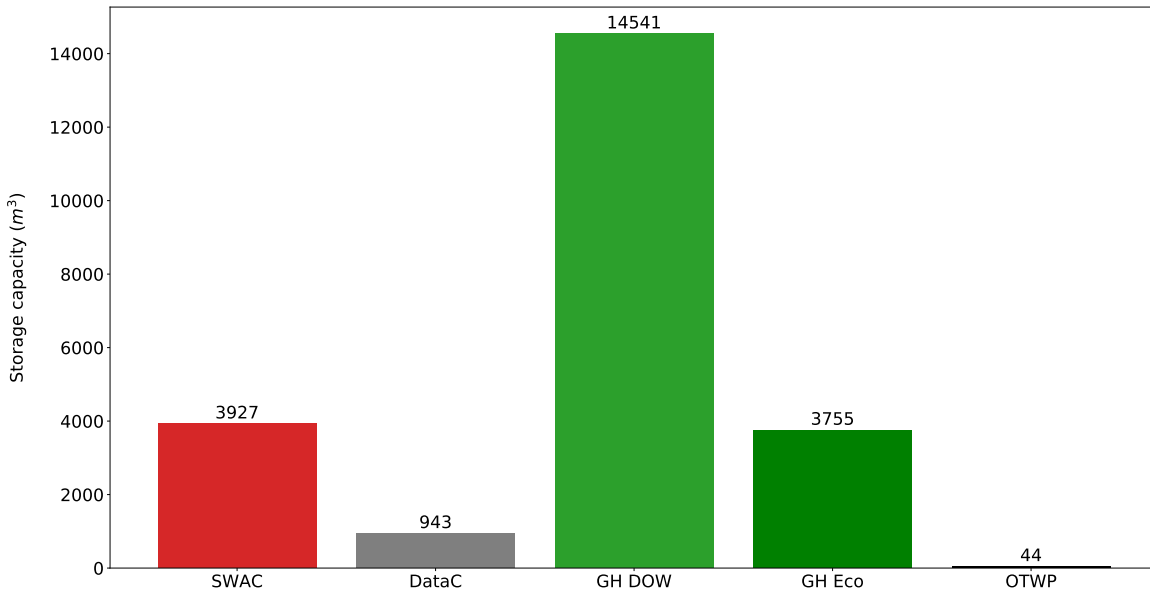


Figure 4.12: Required storage capacity per subsystem in case of optimization by daily storage

4.4.2. Optimization by yearly storage

The yearly storage optimization is done as described in 3.4.2. The same configuration is used as for the base case, see figure 4.6. The results for the water usage by yearly storage can be seen in figure 4.13. The yearly storage is applied to each subsystem except for OTEC. The water usages per subsystem can be found in appendix B.

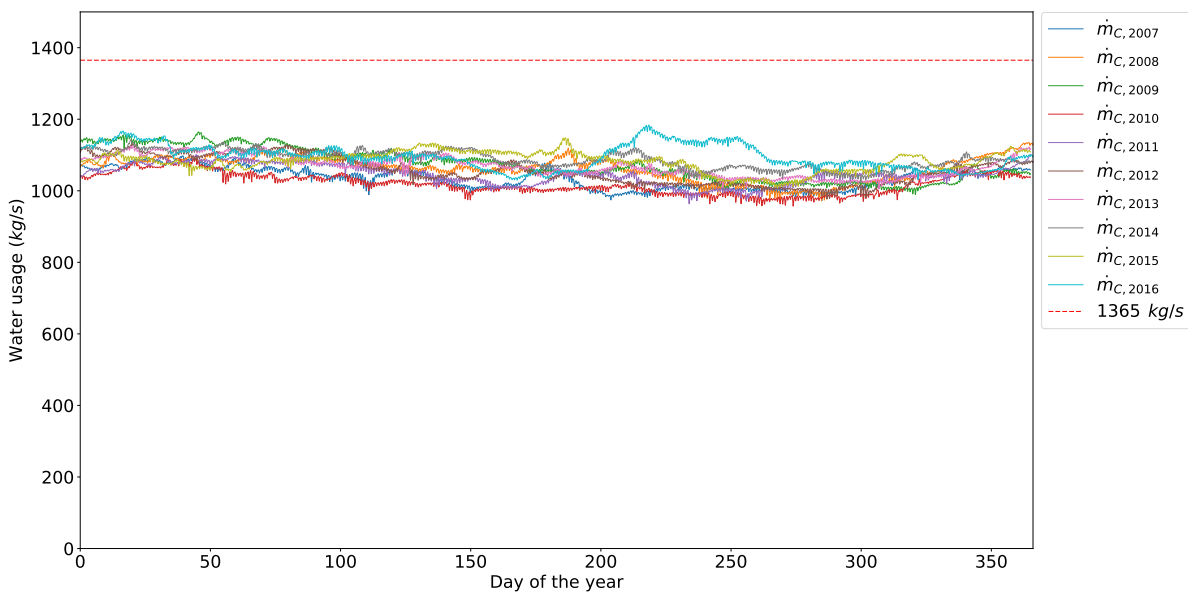


Figure 4.13: Curaçao 2007-2016: Total deep seawater usage in case of optimization by yearly storage

Compared to figure 4.11 it can be seen that the water usage curves have been flattened throughout the year. The maximum water usage is in the year 2016 and is 1184 kg/s. The required CWP diameter, which can be calculated with eq. 4.3, is 1.136 m. This is a reduction of 6.9% compared to the base case.

It is very interesting to see how big the storage capacity should be in this case. Since the seasonal peaks need to be compensated instead of the daily peaks, it can be expected that the SWAC storage capacity will be very high. This is because the SWAC water usage fluctuates the most over a year compared to the data center cooling, greenhouse cooling and OTWP, as can be seen in appendix B.

The required storage capacity needed per subsystem in case of yearly storage can be found in figure 4.14. The maximum storage capacities are:

- SWAC: 422 027 m^3
- Data center: 50 773 m^3
- Greenhouse DOW: 63 544 m^3
- Greenhouse Ecopark: 86 098 m^3
- OTWP: 1437 m^3

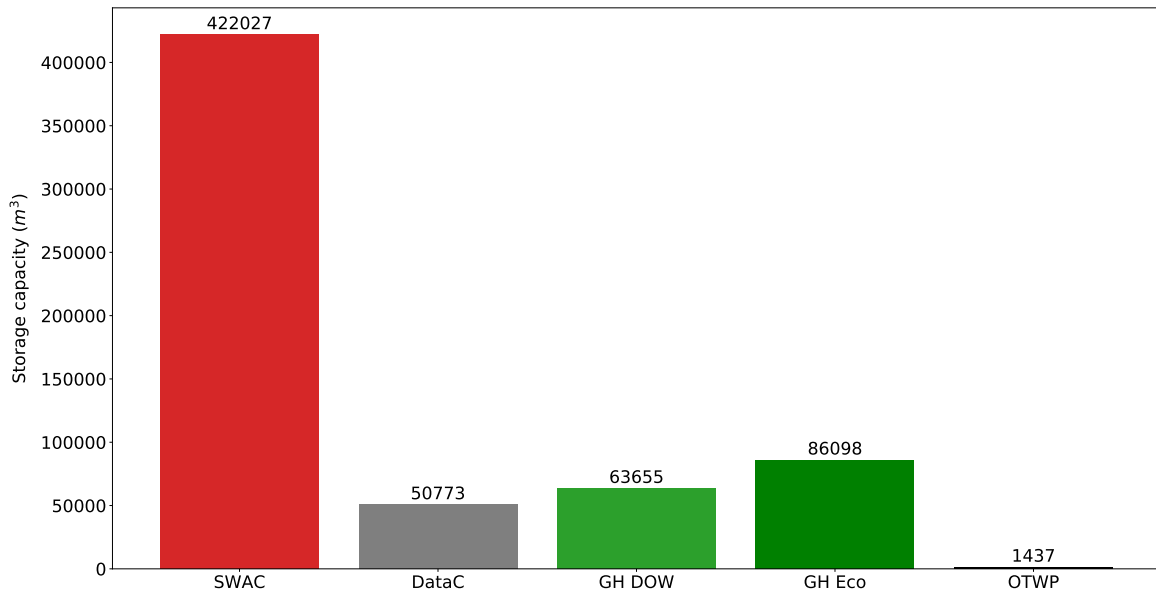


Figure 4.14: Required storage capacity per subsystem in case of optimization by yearly storage

The storage capacities are way higher than for the daily storage. The required storage capacity for SWAC is a whopping 107 times higher than the required space needed for daily storage. If the combined storage capacity is expressed in storage tanks of 6.1 MG, at least 27 of these big tanks are needed. The costs of these 27 tanks are unknown, but it can be questioned if this is a cheaper option than a 6.9% bigger CWP.

4.4.3. Conclusion optimization by storage

In this section two scenarios have been discussed, namely the optimization of the time-integrated OTE system with daily storage and with yearly storage. Both scenarios show that reduction of peak water mass flows can be accomplished and therefore the pipe diameter can be decreased. With the daily storage the peak demand decreases from 1365 to 1245 kg/s and the pipe diameter can be reduced from 1.22 to 1.165 m. The maximum cold deep seawater mass flow with yearly storage decreases from 1365 to 1183 kg/s so that the required cold water pipe diameter reduces from 1.22 to 1.136 m.

However, the implementation of optimization by storage means that thermal storage has to be built to store cold water. For the daily storage the total required storage capacity based on the years 2007 to 2016 is 23,204 m^3 and for the yearly storage the required volume is 621,159 m^3 . For both cases it should be investigated if the cost savings in pipe diameter are higher than the costs of the storage capacity. The daily storage might be feasible, but it is very likely that yearly storage is more expensive than the reduction in costs by a smaller cold water pipe.

4.5. Future growth scenario

The assumed demands of the base case are based on the expected demands of the first phase of the Ocean Thermal Energy system on Curaçao. But after the first phase it is planned to expand the OTE system. The district cooling system, the data center and the OTWP can be expanded and more greenhouses might be built. Therefore it is interesting to investigate some future growth scenarios and to see for example what the maximum demand could be for a subsystem.

In subsection 4.5.1 it will be investigated what the maximum cooling demand would be when a second district cooling system is placed in the effluent water loop for data center cooling. After that the same will be investigated for a second district cooling system in the effluent loop for SWAC in subsection 4.5.2. Subsequently it will be researched what the maximum district cooling capacity could be with the 1.22 m pipe when the OTEC is shut down in subsection 4.5.3. In subsection 4.5.4 the same calculations will be made to determine the maximum cooling capacity of the SWAC when the OTEC is shut down. A combination of the data center cases mentioned above will be researched in subsection 4.5.5 to determine the maximum possible data center cooling capacity with the 1.22 m cold water pipe. The same will be investigated for a combination of the SWAC cases in subsection 4.5.6

4.5.1. Additional data center in effluent water loop

As can be seen in figure 4.10 a lot of effluent water is unused in the base case. Furthermore the district cooling system is connected to the cold deep seawater because the existing buildings that need to be cooled are designed to work with a cooling water temperature of 6°C . But when buildings need to be built, they can be designed to work with a higher cooling water temperature. This means that the effluent water can be used as cooling source for a second district cooling system. In this subsection it will be researched what the maximum cooling capacity of the second district cooling system would be.

To calculate the maximum cooling capacity of the second district cooling system the model is adapted so that a second data center module is added. The `fzero` function of Python can be used to find the maximum cooling demand with the restriction that the Ecopark water surplus should always be greater or equal to zero. The `fzero` function is a root finding algorithm of the SciPy ecosystem within Python [22]. It is assumed that the output temperature of the effluent water is 16°C , so that the temperature difference is 5°C between input and output of the district cooling network.

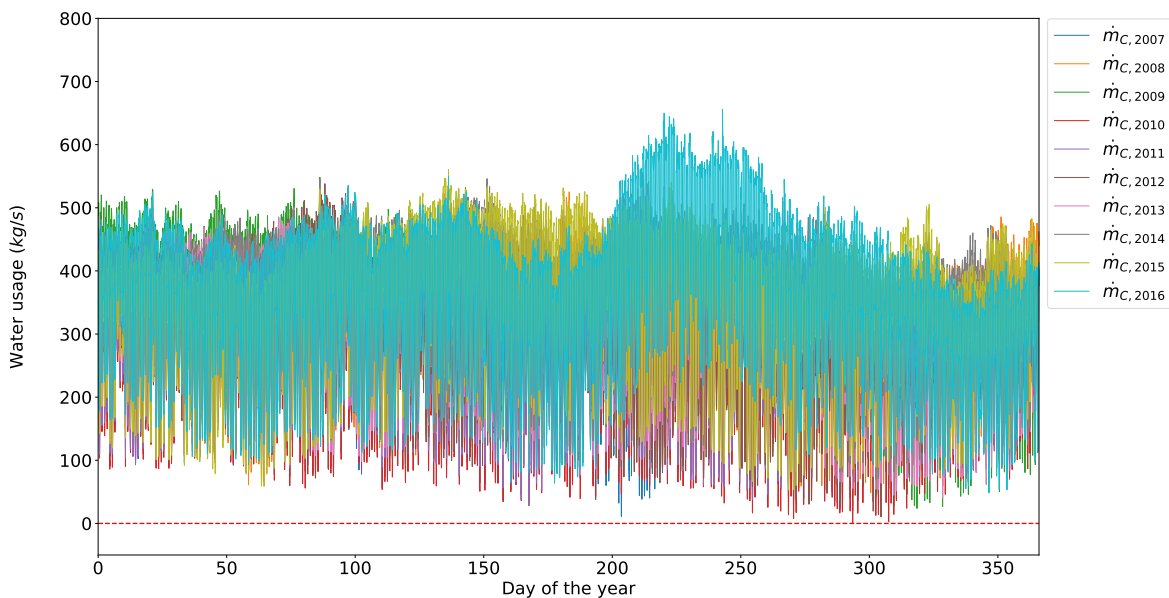


Figure 4.15: Curaçao 2007 - 2016: Ecopark water surplus per year in case of the maximum cooling capacity for an additional data center in the effluent water loop

The maximum cooling capacity for the additional data center is 3398 RT. This capacity is 4.7 times higher than the data center in the base case. It can be checked if the Ecopark surplus is always greater than zero with this cooling capacity. Therefore this value can be used as input in the model. The results can be seen in figure

4.15. It can be seen that the Ecopark water surplus is always positive and that the minimum value is about zero, which indicates that the cooling capacity of 3923 RT is indeed the maximum value for the additional data center cooling in the effluent water loop. The water usages per subsystem can be found in appendix C.

4.5.2. Additional SWAC system in effluent water loop

The unused water in the effluent loop can also be used for an additional SWAC system. New buildings can be designed to make use of the 11°C effluent water instead of the 5°C cold deep seawater. The same method is used to calculate the maximum cooling capacity as in subsection 4.5.1. This means that the f_{zero} function in python is used to find the maximum SWAC cooling capacity with the restriction that the Ecopark water surplus should be positive, because otherwise more water is used than that is delivered to the Ecopark.

The maximum SWAC cooling capacity in this case is 16.81 MW_{th} . This capacity is 1.96 times higher than the SWAC in the base case. To check if the Ecopark water surplus is always above zero, this maximum capacity is used as input in the model. The results can be seen in figure 4.16. This figure shows clearly that the Ecopark water surplus is greater or equal to zero for every moment. Furthermore, the minimum value is about 0 kg/s , which means that this cooling capacity is indeed the maximum. The water usages per subsystem can be found in appendix C.

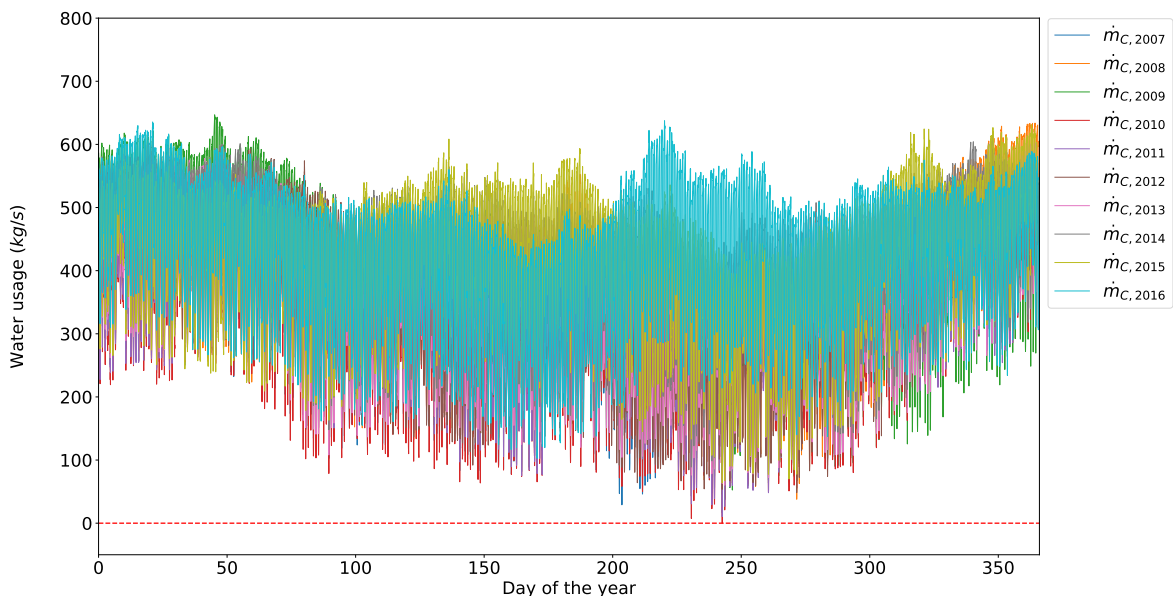


Figure 4.16: Curaçao 2007 - 2016: Ecopark water surplus per year in case of the maximum cooling capacity for an additional SWAC system in the effluent water loop

4.5.3. Maximum data center cooling without OTEC

OTEC uses quite a lot of cold deep seawater in proportion to the district cooling system. Running the small OTEC power plant in Curaçao might become economically less attractive than using the cold deep seawater for the cooling network. Therefore the scenario might occur that the OTEC power plant is shut down and all the cold deep seawater will be used for district cooling.

Therefore it is investigated what the maximum cooling capacity could be in the case that all the cold deep seawater is used for the district cooling system. This is done for the cold water pipe diameter calculated in section 4.3. The f_{zero} function of Python is used to find the maximum value of the data center cooling capacity. In the model the OTEC demand is set to zero, the data center demand as a variable and the f_{zero} function returns the maximum mass flow minus 1365, which is the maximum mass flow in the 1.22 m cold water pipe.

The results can be seen in figure 4.17. It can be seen that the cold deep seawater mass flow is below or equal the maximum of 1365 kg/s . Therefore it can be concluded that the maximum cooling capacity for the data center without OTEC is 5817 RT, which is 8.1 times higher than the demand in the base case. The water usages per subsystem can be found in appendix C.

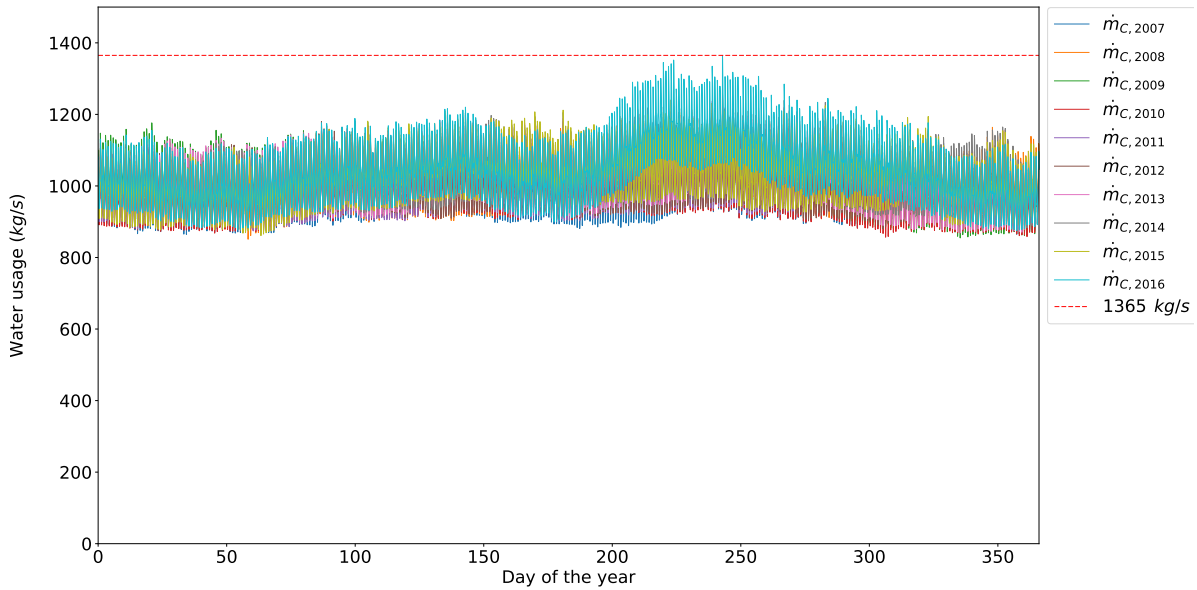


Figure 4.17: Curaçao 2007 - 2016: Total deep seawater usage in case of maximum data center cooling without OTEC

4.5.4. Maximum SWAC cooling without OTEC

The same calculations as for the data center in subsection 4.5.3 can be done for the maximum cooling capacity of the SWAC installation. The f_{zero} function is used again, but this time with the SWAC demand as variable instead of the data center demand.

The minimum value for the cooling capacity for the years 2007 to 2016 is about $26.36 MW_{th}$. This is a gain of $18.86 MW_{th}$ and 3.5 times the demand of the base case. The demand of $26.36 MW_{th}$ can be used as input in the model to check if the maximum water usage in this case is about 1365 kg/s . The results are shown in figure 4.18. This figure shows that the maximum value of the cold deep seawater usage is never above 1365 kg/s and that this is also the maximum mass flow. This means that the cooling capacity of $26.36 MW_{th}$ is indeed the maximum cooling capacity in this case. The water usages per subsystem can be found in appendix C.

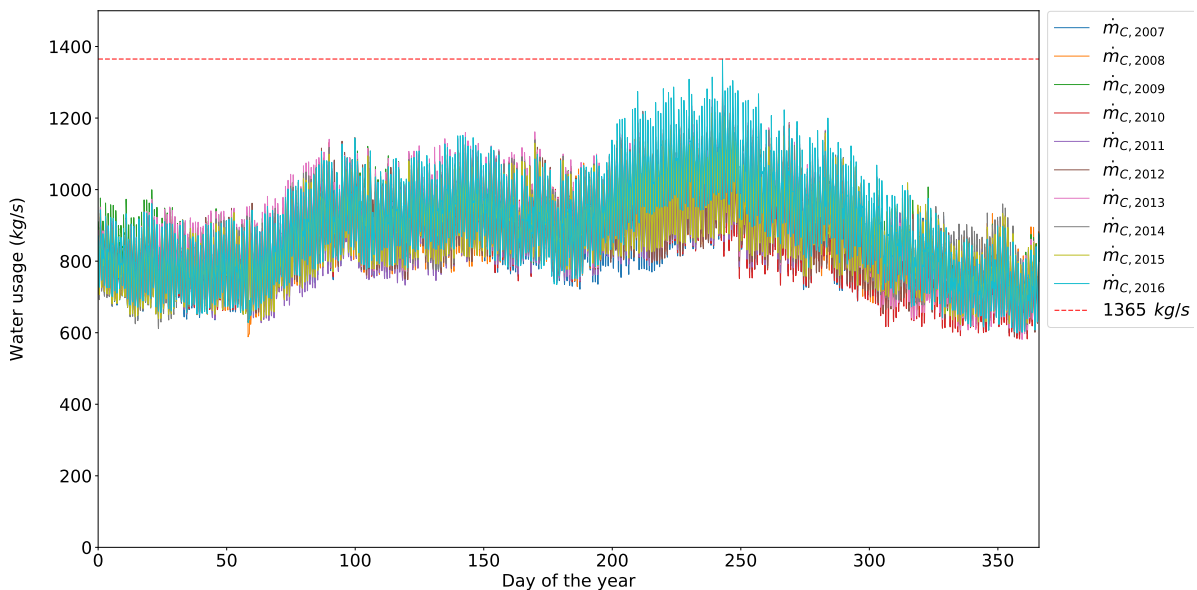


Figure 4.18: Curaçao 2007 - 2016: Total deep seawater usage in case of maximum SWAC cooling without OTEC

4.5.5. Maximum combined data center cooling

In this subsection the maximum combined data center cooling capacity is calculated, so when the OTEC is not in operation and the Ecopark water surplus is used for an additional data center. This is not the same as just adding the capacities calculated in subsection 4.5.1 and subsection 4.5.3. The capacity of the data center that uses the cold deep seawater is the same, but the capacity of the data center that uses the effluent water will be different. Again the `fzero` function of Python is used to calculate maximum cooling capacity, with the data center demand as variable and the restriction that the Ecopark water surplus should always be positive.

The maximum data center cooling capacity in the Ecopark is 3810 RT. In figure 4.19 it can be seen that the minimum value of the Ecopark water surplus is zero, which means that the cooling capacity of 3810 RT is indeed the maximum value. So the total data center cooling capacity is 9627 RT, which is more than 13 times the demand of the base case. The water usages per subsystem can be found in appendix C.

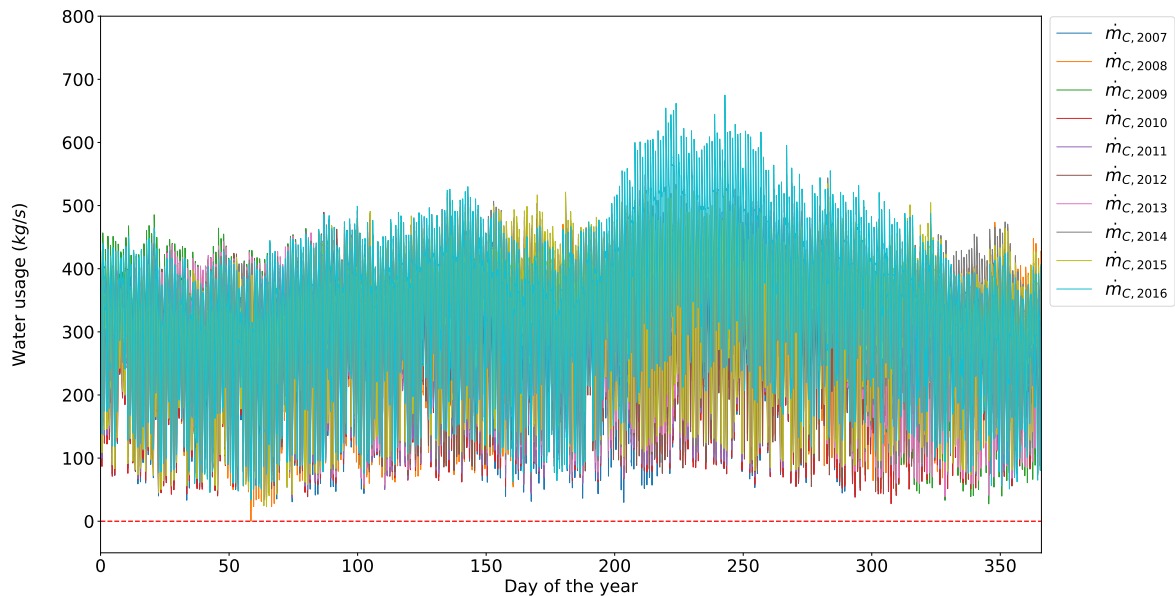


Figure 4.19: Curaçao 2007 - 2016: Ecopark water surplus in case of maximum combined data center cooling

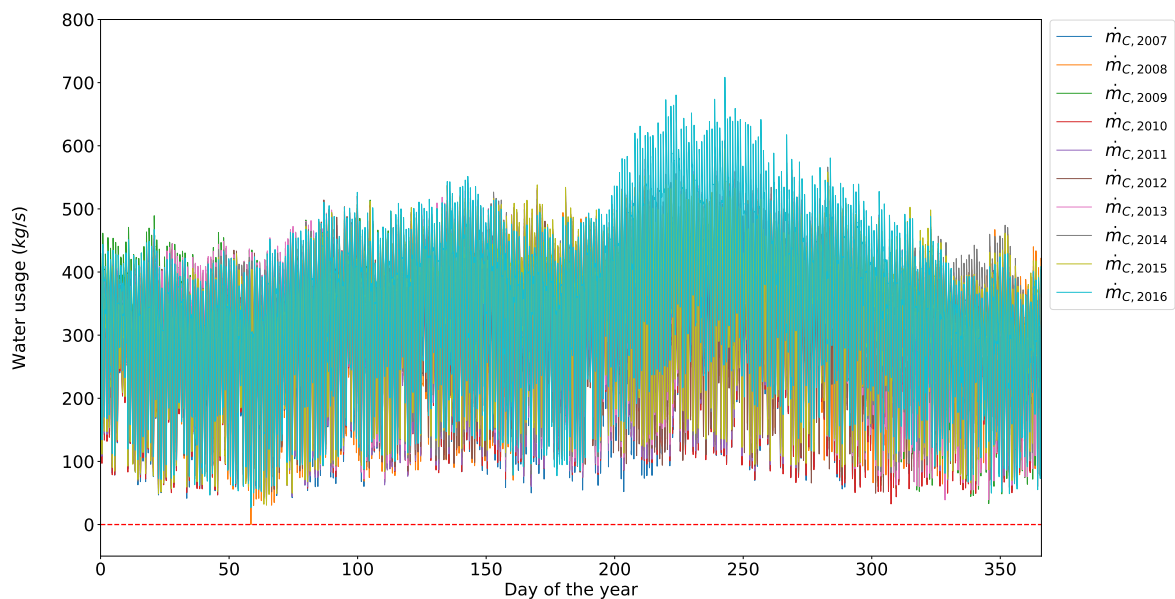


Figure 4.20: Curaçao 2007 - 2016: Ecopark water surplus in case of maximum combined SWAC cooling

4.5.6. Maximum combined SWAC cooling

In this subsection the maximum combined SWAC cooling capacity is calculated, so when the OTEC is not in operation and the Ecopark water surplus is used for an additional SWAC system. Just like for the data center, the capacities calculated in subsection 4.5.2 and subsection 4.5.4 cannot be added to get the maximum total capacity. The capacity of the SWAC that uses the cold deep seawater is the same, but the capacity of the SWAC system that uses the effluent water will be different.

The `fzero` function of Python is used to calculate the maximum cooling capacity, with the SWAC demand as variable and the restriction that the Ecopark water surplus should always be positive.

The maximum data center cooling capacity in the Ecopark is 13.37 MW_{th} . It can be seen that the Ecopark water surplus is always above zero and that the minimum value is zero, which means that the cooling capacity of 13.37 MW_{th} is indeed the maximum SWAC cooling capacity.

Now the maximum values from the primary layer and secondary layer SWAC cooling can be summed to calculate the total maximum. The total SWAC cooling capacity is 32.23 MW_{th} , which is an increase of almost 430% compared to the base case SWAC demand. The water usages per subsystem can be found in appendix C.

4.5.7. Conclusion future growth scenario

The future growth scenarios show that the OTE system has a lot of potential to grow. When all the Ecopark water surplus is used for an additional data center in the effluent water loop, the maximum cooling capacity of the additional data center is 3398 RT. Even so, the maximum cooling capacity of an additional SWAC system in the effluent water loop is 16.81 MW_{th} .

In the case that the OTEC power plant is shut down in favor of expanding the data center cooling, the maximum data center cooling capacity becomes 5817 RT. When the cold deep seawater is used for expanding the SWAC system, the maximum SWAC cooling capacity becomes 26.36 MW_{th} .

When both the OTEC power plant is shut down and the Ecopark water surplus is used for an additional data center, the maximum combined data center cooling capacity becomes 9627 RT. Even so, when both the OTEC power plant is shut down and the Ecopark water surplus is used for an additional SWAC system, the maximum combined SWAC cooling capacity becomes 32.23 MW_{th} .

5

Results & Discussion

In chapter 4 the maximum water usage and the outside pipe diameter are calculated for the Curaçao base case. The optimization by daily or and yearly storage showed that they have the potential to reduce the maximum mass flow and pipe diameter, but it is unclear if the cost reduction is larger than the cost of building the storage. Another optimization method is to change the configuration of the OTE system. The options that will be given in section 5.1 are only theoretical, since some subsystems cannot be placed in the Ecopark due to restrictions of the current setup.

It will be interesting to see what the maximum cold water mass flow and the pipe diameter would be if the a bigger OTEC plant or SWAC installation are deployed instead of the current sizes. Furthermore it would be interesting to know what the maximum demand could be for each subsystem in the Ecopark when the other subsystem are turned off. These cases will be discussed for the optimized configuration case in section 5.2.

Lastly a sensitivity analysis will be made in section 5.3. The sensitivity of the seawater temperature, the Carnot efficiency and cooling demand will be investigated in this section.

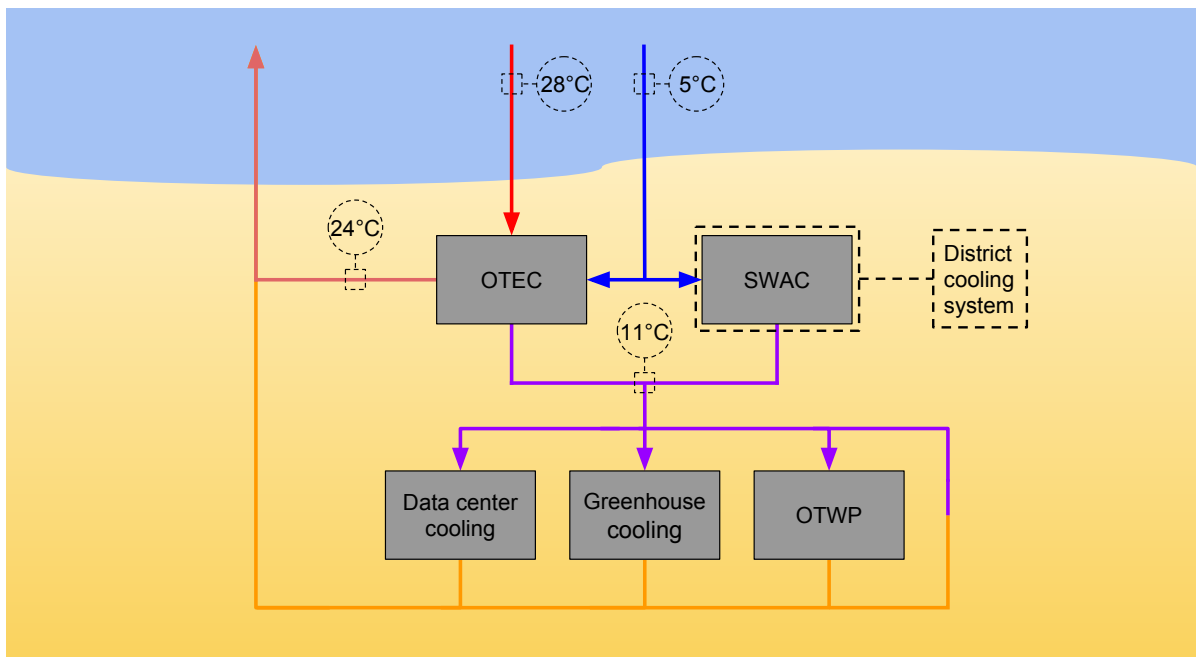


Figure 5.1: Schematic overview of the optimized configuration with the data center, greenhouse and OTWP in the Ecopark

5.1. Optimized configuration

In this section a few optimizations by configuration will be discussed and compared. The optimization by configuration will be separated into four case. The optimization by changing the configuration will be dis-

cussed in subsection 5.1.1. The combined optimization by configuration and daily or yearly storage discussed in resp. subsection 5.1.2 and subsection 5.1.3.

5.1.1. Optimization by configuration

To optimize the water usage by the configuration of an OTE system, it is necessary to put as much subsystems in the Ecopark as possible. Because of the requirements of OTEC, this subsystems should always be connected to the cold deep seawater. This leaves SWAC, data center cooling, greenhouse cooling and OTWP (and aquaculture and algae cultivation) as subsystems to be connected to the effluent water in the Ecopark. The first configuration to discuss is the one where OTEC and SWAC are connected to the cold deep seawater and the other three subsystems to the effluent water in the Ecopark. The second configuration is the case that only OTEC is connected to the cold deep seawater and all the other components to the effluent water in the Ecopark.

Optimized configuration: data center, greenhouse and OTWP in Ecopark

The optimized configuration for this case can be seen in figure 5.1. In this case the OTEC plant and the SWAC installation are connected to the cold deep seawater and the data center, greenhouses and OTWP are connected to the effluent water in the Ecopark.

The results of the water usage for the optimization by configuration can be found in figure 5.2. The maximum cold deep seawater usage of the years 2007 to 2016 is 1101 kg/s . This is a decrease of 19.3% compared to the base case. The required CWP outside diameter corresponding to this water usage can be calculated with eq. 4.1 and is 1.096 m. So by changing the configuration the CWP diameter can be reduced with 10.2%.

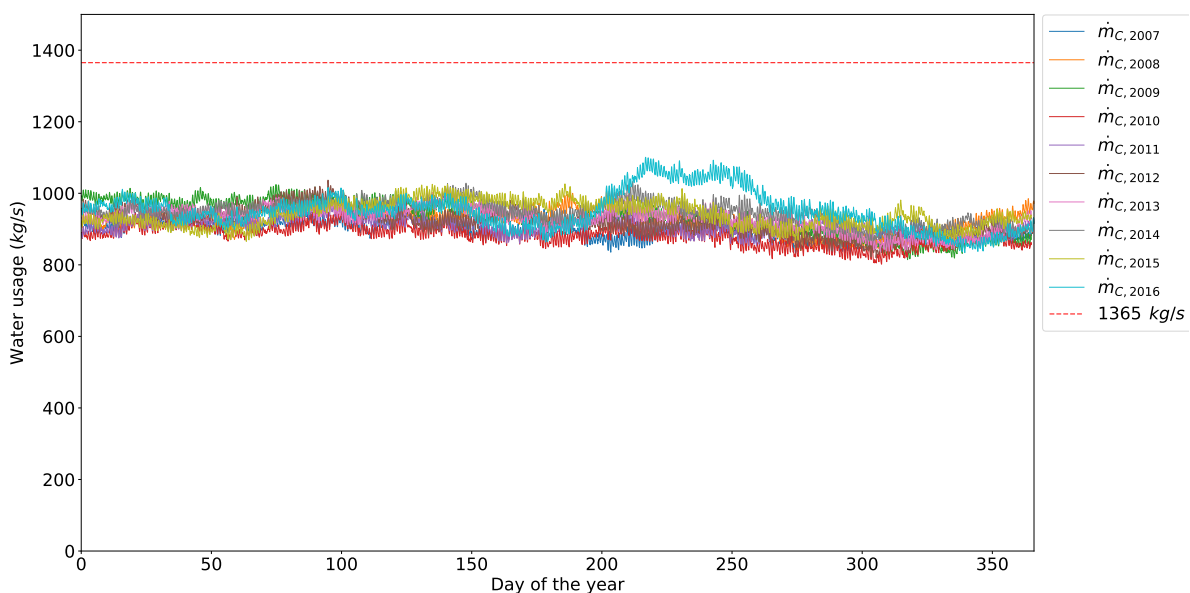


Figure 5.2: Curaçao 2007 - 2016: Total cold deep seawater usage by optimizing the configuration (data center, greenhouse and OTWP in Ecopark)

Now it has to be checked if the Ecopark water surplus is always positive. The results are shown in figure 5.3. It can be seen that Ecopark water surplus is always positive and for that reason there is never an effluent water shortage in the Ecopark. The water usages per subsystem can be found in appendix B.

Optimized configuration: SWAC, data center, greenhouse and OTWP in Ecopark

The SWAC in Curaçao is designed to deliver cooling water with a temperature of $6^{\circ}C$. However it would be interesting to see if it is possible to connect the SWAC to the effluent water of the OTEC. This way the maximum cold water mass flow would be reduced even further than in the previous case. The schematic overview of this configuration can be seen in figure 5.4. In this figure it can be seen that only the OTEC is connected to the cold deep seawater and that the SWAC, data center, greenhouse and OTWP are connected to the effluent water of the OTEC in the Ecopark.

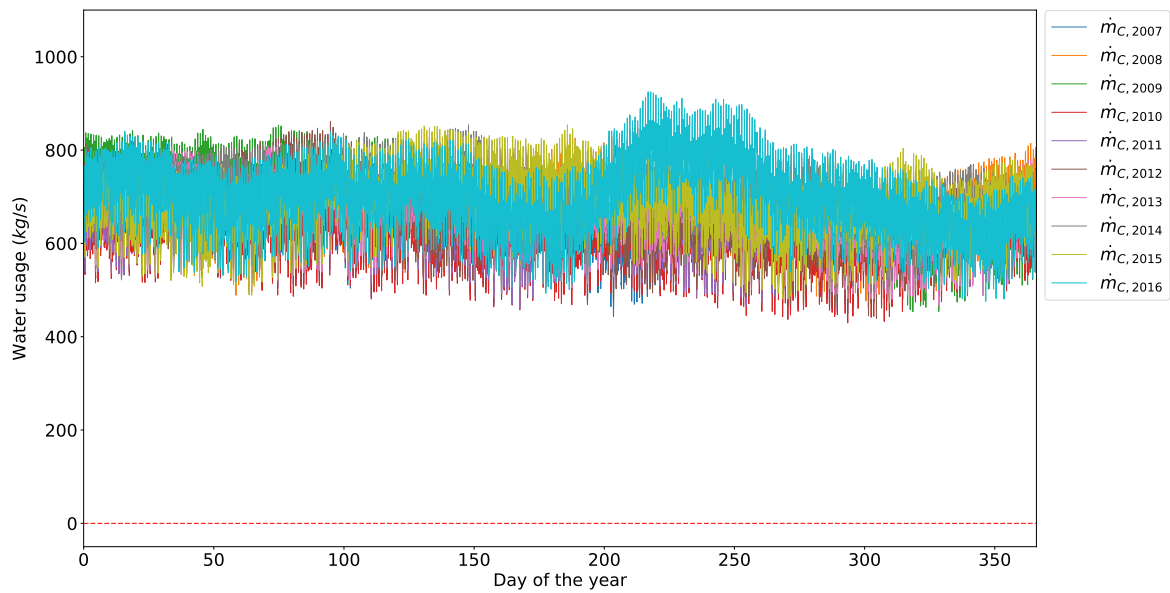


Figure 5.3: Curaçao 2007 - 2016: Ecopark water surplus in case of optimization by configuration (data center, greenhouse and OTWP in Ecopark)

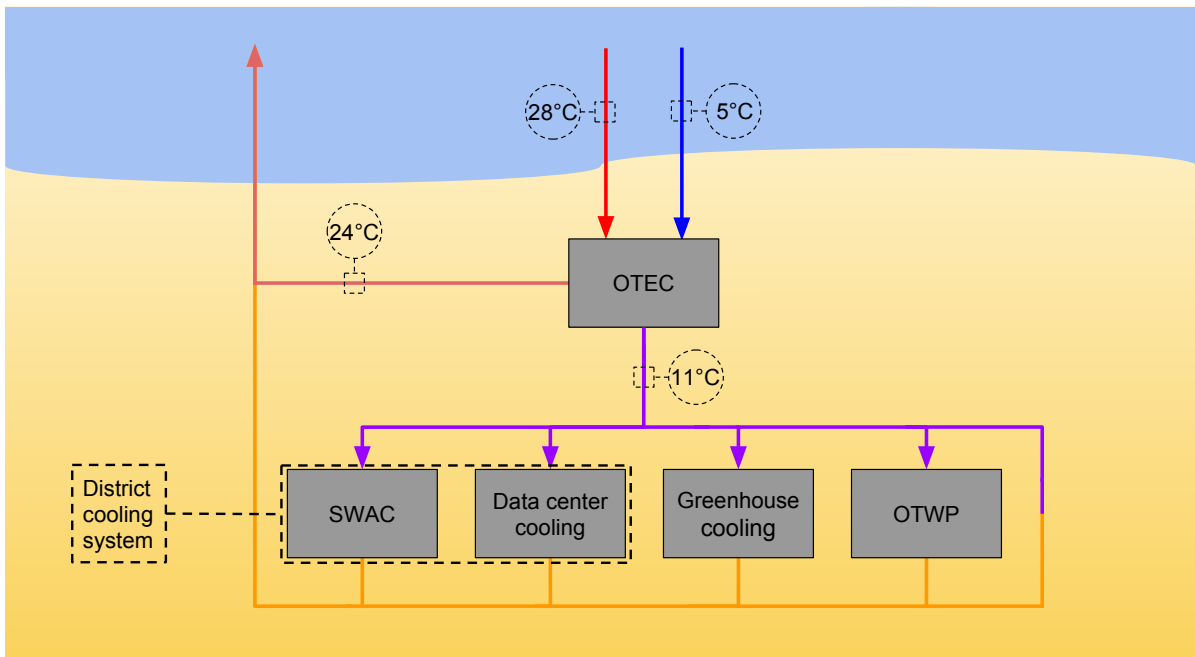


Figure 5.4: Schematic overview of the optimized configuration with SWAC, the data center, the greenhouse and OTWP in the Ecopark

The results of the calculation of the cold deep seawater mass flow in this case can be seen in figure 5.5. Compared to the base case, the maximum water usage decreased with 39.6 % from 1365 to 824 kg/s. The corresponding cold water pipe outside diameter is 0.948 m, which is 0.272 m smaller compared to the base case. The water usages per subsystem can be found in appendix B.

The next thing to do is to check the Ecopark water surplus. The water surplus is shown in figure 5.6. The figure shows that the Ecopark water surplus is below zero for some times in some years. This means that there would be a water shortage in the Ecopark and that not all subsystems can get enough effluent water. This might lead to big problems for some subsystems. For example, when the greenhouse cannot be cooled this might lead to crop failure and when the data center is not cooled enough this might lead to internet malfunction and broken components.

The conclusion of this case is that it would not be possible to deploy an OTE system with this configura-

tion and demands. This configuration is only possible when a larger OTEC power plant is built that uses a higher cold deep seawater mass flow or when the subsystems in the Ecopark would use less effluent water.

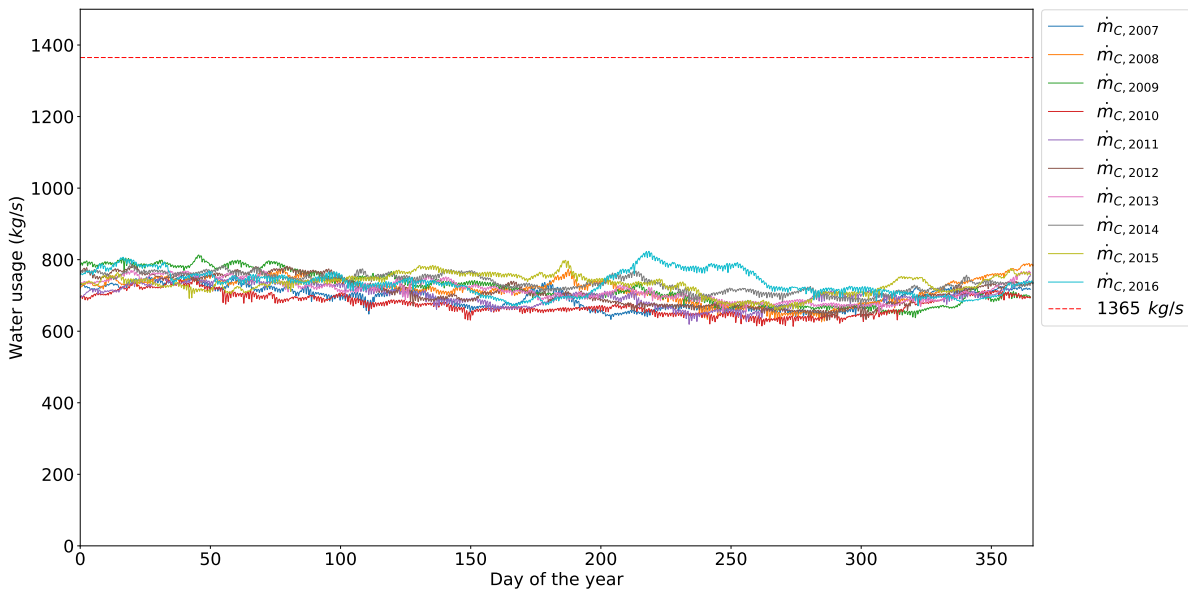


Figure 5.5: Curaçao 2007 - 2016: Total cold deep seawater usage by optimizing the configuration (SWAC, data center, greenhouse and OTWP in Ecopark)

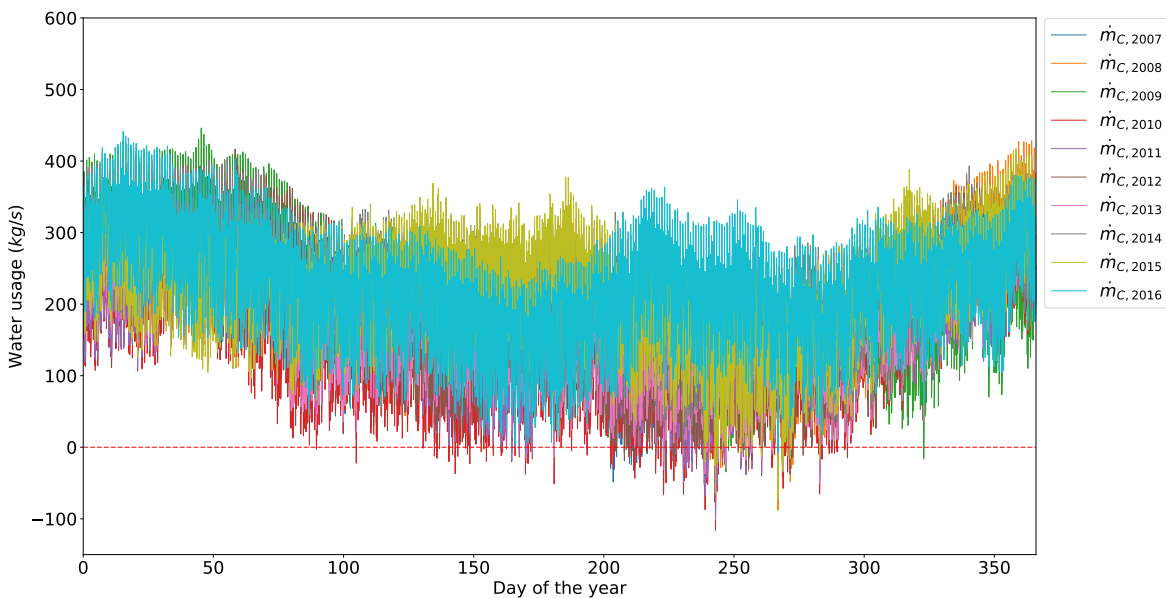


Figure 5.6: Curaçao 2007 - 2016: Ecopark water surplus in case of optimization by configuration (SWAC, data center, greenhouse and OTWP in Ecopark)

5.1.2. Optimization by both configuration and daily storage

In this case the water usage and therefore the CWP diameter is optimized by both changing the configuration of the OTE system and by daily storage. The configuration is the same as the case in subsection 5.1.1.

Since with this configuration only the OTEC and SWAC subsystems are directly connected to the cold deep seawater, the impact of the daily storage on the cold deep seawater usage is only related to SWAC. Therefore it can be expected that the influence of the daily storage on the water usage is smaller than in the case described in subsection 4.4.1.

The results of the optimization by both changing the configuration and the daily storage can be seen in figure 5.7. The maximum DOW water usage in this case is 1089 kg/s. This is a reduction of 20.2% compared

to the base case. The CWP diameter with this maximum mass flow is 1.090 m. Compared to the base case, this is a reduction of 10.7%. But when these numbers are compared to the case where only the configuration is changed, the reduction is only 1.1% for the mass flow and 0.5% for the diameter.

The storage capacity needed for this can be seen in figure 5.8. Compared to figure 4.12, it can be seen that the storage capacity for the data center is reduced and the storage capacity for greenhouse connected to DOW is zero (because the greenhouse is only connected to the effluent water). The storage capacity for SWAC is exactly the same, which could be expected since nothing changed for this subsystem. The storage capacity needed for the greenhouse increased a bit compared to the case in subsection 4.4.1. This is not a big increase, but since now the greenhouse is only connected to the effluent water, the water usage is more constant throughout the day and therefore the required storage capacity is not as big the sum of the two greenhouse thermal storages calculated in subsection 4.4.1. First the effluent water was only used during daytime, while in this case also during the night the effluent water is used. The average water usage of the greenhouse is higher because of this, but less storage is needed.

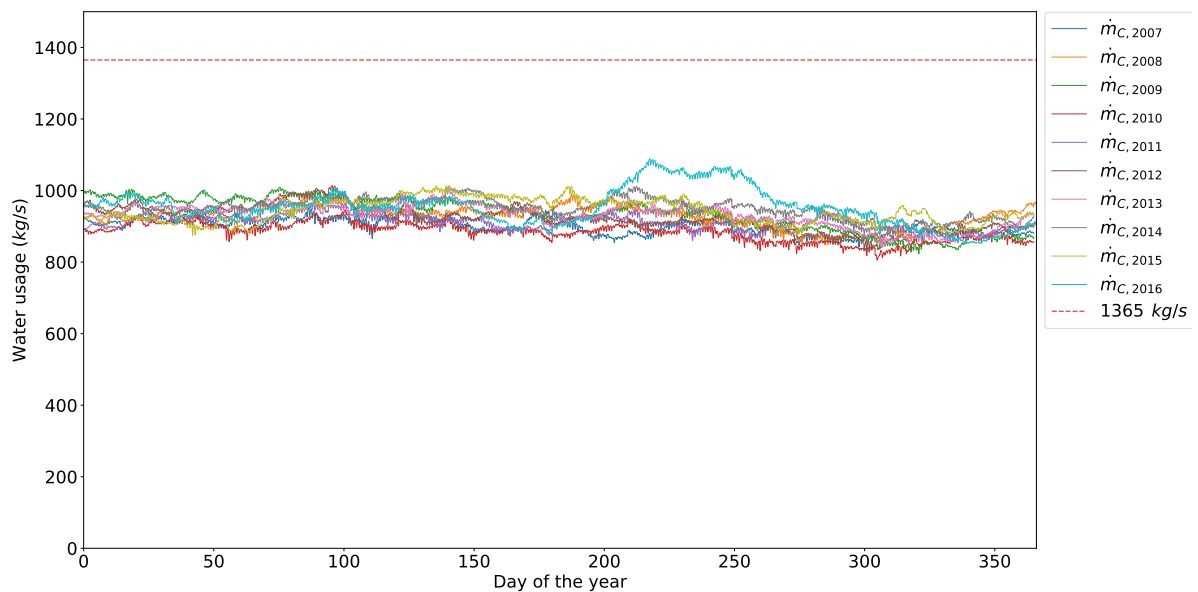


Figure 5.7: Curaçao 2007 - 2016: Total cold deep seawater usage in case of optimization by both the configuration and daily storage

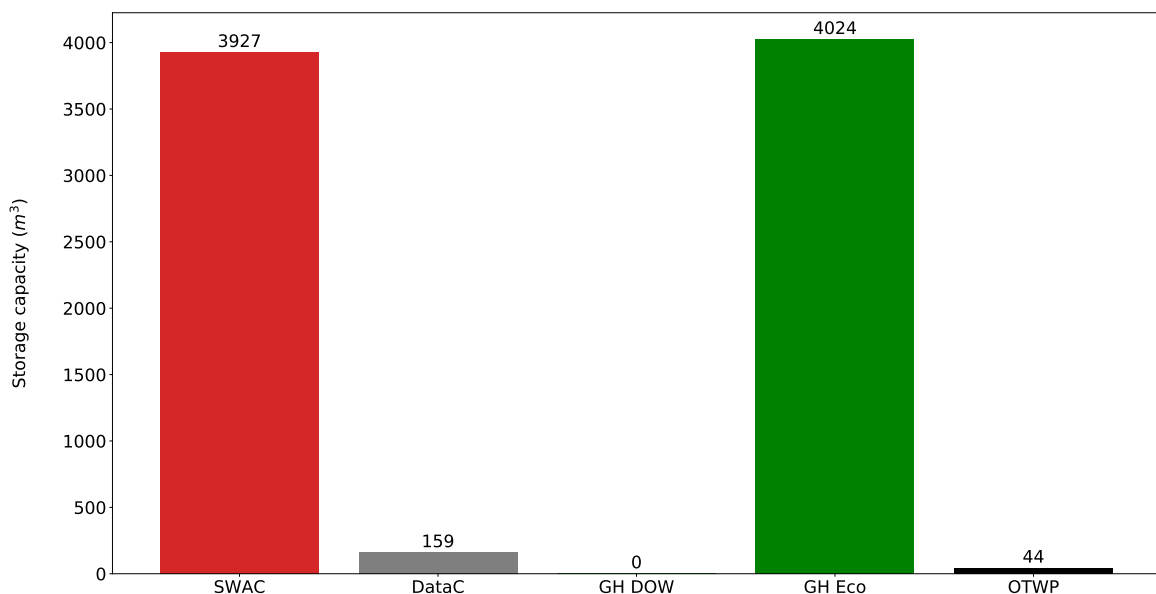


Figure 5.8: Required storage capacity in case of optimization by both configuration and daily storage

Although the maximum cold water mass flow is lower than compared to the optimization by only changing the configuration, the difference is very small and therefore it might be economically less attractive to add storage to the optimized configuration than installing a pipe that is a fraction bigger.

The last thing to check is the Ecopark water surplus. The results of the calculation of the Ecopark water surplus can be found in figure 5.9. Compared to figure 5.3 it can be seen that there is a lot less fluctuation in Ecopark water surplus mass flow. Also the minimum value of the Ecopark water surplus has gone up from 430 to 540 kg/s. This means that by the daily storage the Ecopark potential has grown, because more effluent water is available. The water usages per subsystem can be found in appendix B.

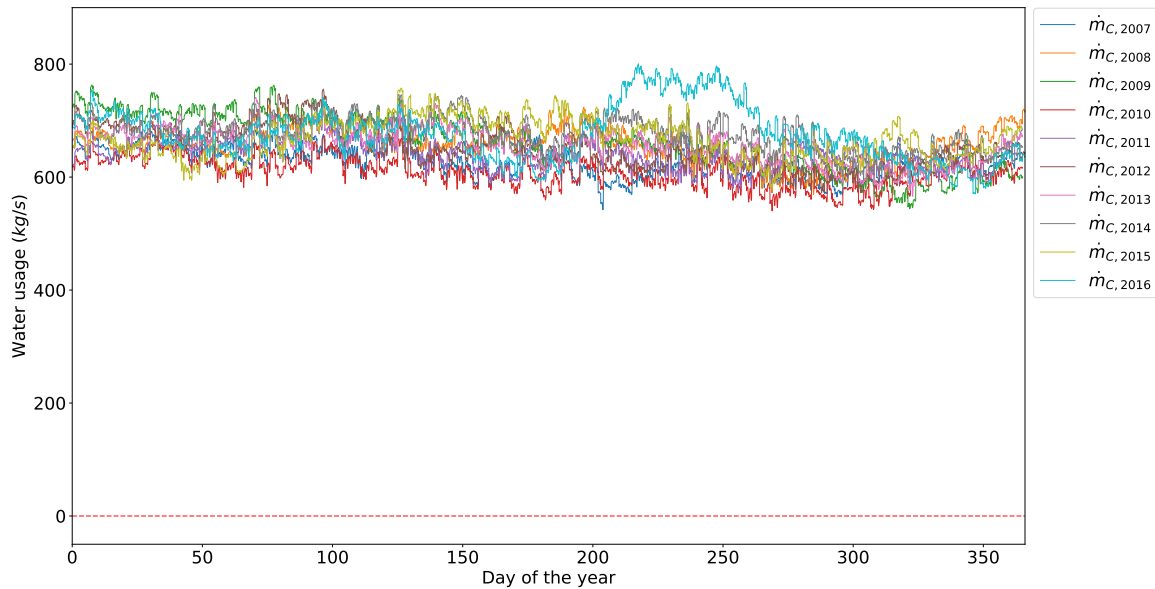


Figure 5.9: Curaçao 2007 - 2016: Ecopark water surplus in case of optimization by both configuration and daily storage

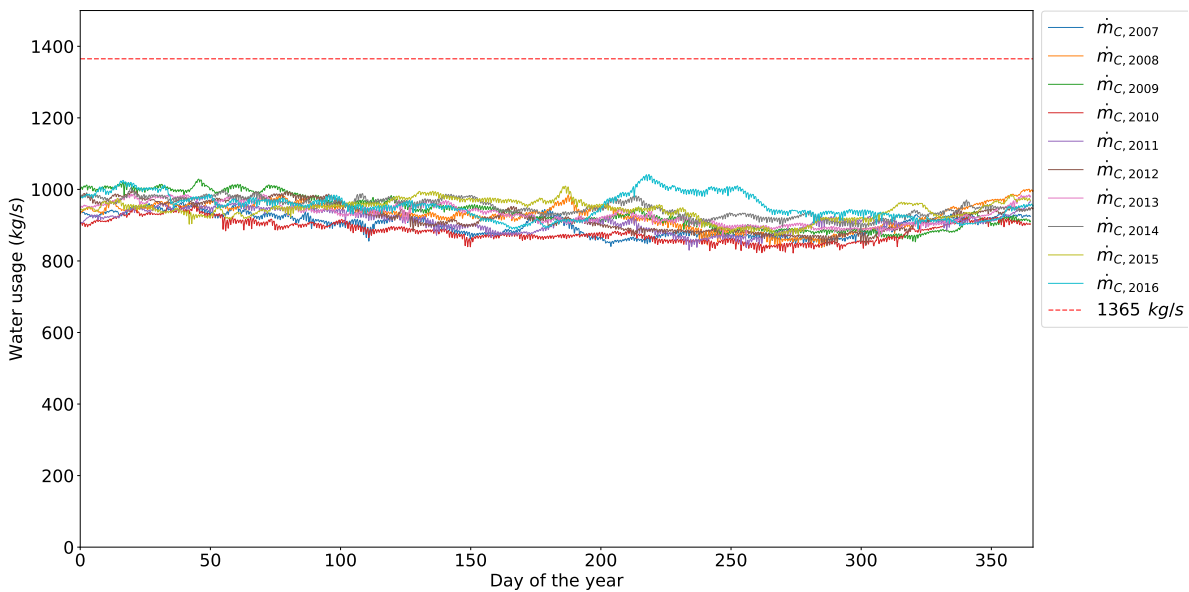


Figure 5.10: Curaçao 2007 - 2016: Total cold deep seawater usage in case of optimization by both the configuration and yearly storage

5.1.3. Optimization by both configuration and yearly storage

The last case to investigate is the optimization by both changing the configuration and the yearly storage. From what has been seen in the case discussed in subsection 4.4.2 subsection 5.1.2, it can be expected that

this optimization technique might not reduced the required CWP diameter a lot compared to only changing the configuration and that the storage capacity needed for this reduction is very high.

The results of this optimization method are shown in figure 5.10. The maximum water usage occurs in 2016 and is 1042 kg/s. This is an decrease of 23.7% compared to the base case. The CWP diameter corresponding to the maximum water usage is 1.066 m. Compared to the base case this is a reduction of approximately 12.6%. But compared to the optimization by only changing the configuration this reduction is only 5.4% in mass flow and 2.7% in pipe diameter.

The reduction in diameter comes from the added storage of the SWAC. The required storage capacity for SWAC (and other subsystems) to obtain this reduction can be seen in figure 5.11.

It can be seen that the required storage capacity for SWAC is about 422,000 m³ and is the same as the required capacity for only yearly storage. More than 18 storage tanks of 6.1 MG are needed to fulfill this storage demand. It is very likely that the costs for 18 storage tanks are higher than installing a CWP that has a 2.7% bigger diameter.

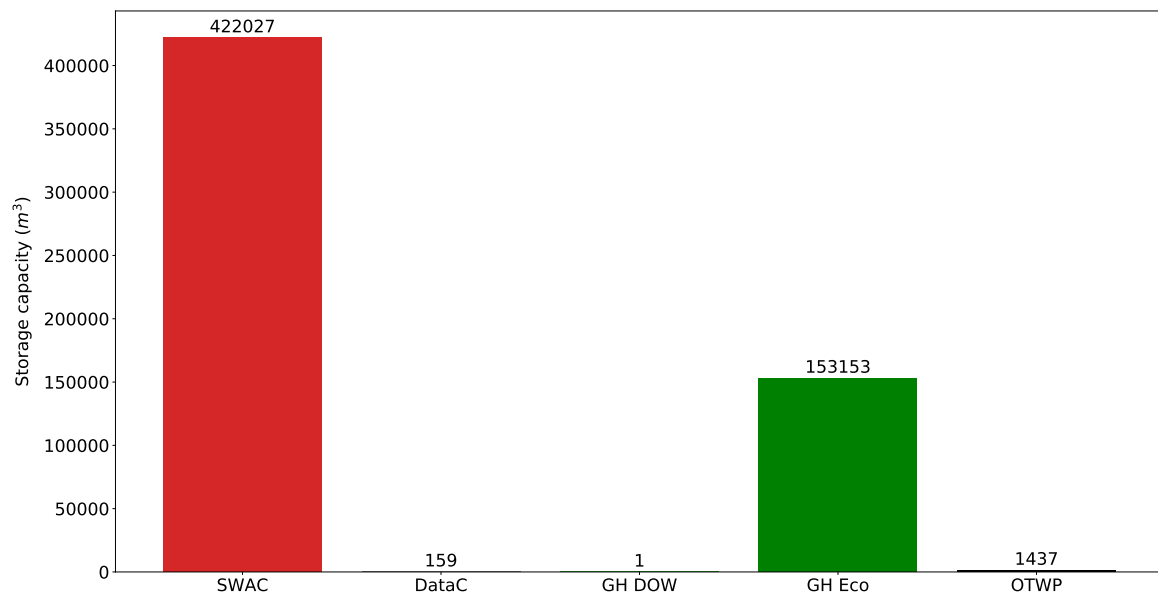


Figure 5.11: Required storage capacity in case of optimization by both configuration and yearly storage

The last thing to do is to check if the Ecopark water surplus is positive for every hour in the period from 2007 to 2016. The results of this calculation can be found in figure 5.12. As can be seen, the Ecopark water surplus is never negative in this case. The minimum value is 548 kg/s, which is higher than the minimum in case of optimization by both configuration and daily storage, but the difference is only 8 kg/s. So the potential of the Ecopark does not go up significantly compared to the case discussed in subsection 5.1.2. The water usages per subsystem can be found in appendix B.

5.1.4. Conclusion optimization by configuration

It can be seen that optimization by configuration shows significant reduction in maximum cold water mass flow and cold water pipe diameter. Theoretically the cold water mass flow could be reduced with 19.3% and the cold water pipe with 10.2%. The optimized configuration with also the SWAC system in the Ecopark is not possible with the Curaçao specific demands, because then there will be a effluent water shortage.

The daily and yearly thermal storage combined with the optimized configuration show that further optimization is possible, but the benefits in maximum cold deep seawater usage compared to the case with only optimized configuration are small. On the other side, the benefits in effluent water mass flow in the Ecopark are significant whereby the potential of the Ecopark is larger in case of daily and yearly thermal storage.

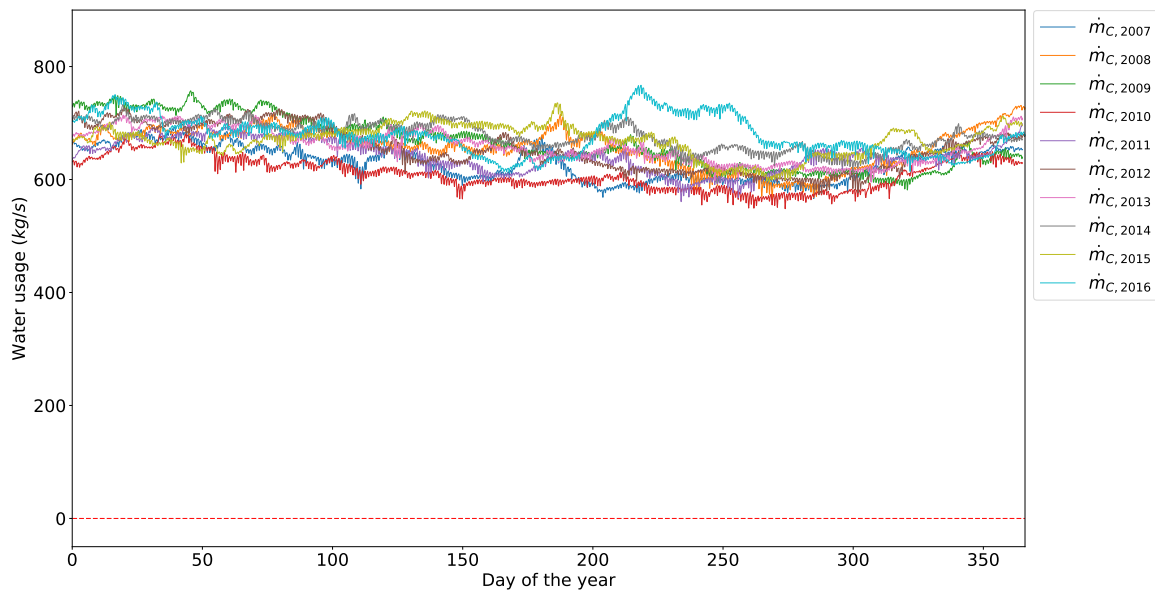


Figure 5.12: Curaçao 2007 - 2016: Ecopark water surplus in case of optimization by both configuration and yearly storage

5.2. Cases

It is interesting to research the behavior of the water usage when some of the demands are changed or what the maximum demand could be for each subsystem in the Ecopark. In subsection 5.2.1 the water usage of the OTE system with a 10 MW OTEC power plant will be researched. After that the water usage with a SWAC demand of $20 MW_{th}$ will be investigated in subsection 5.2.2. Subsequently the maximum possible demand of the data center cooling (with and without storage) will be researched when there are no other subsystems in the Ecopark (no greenhouse cooling and no OTWP) in subsection 5.2.3. The same will be done for greenhouse cooling in subsection 5.2.4 and for OTWP in subsection 5.2.5. The calculations for the 10 MW OTEC and $20 MW_{th}$ SWAC will be done for the base case configuration as shown in figure 4.6. The other three calculations will be done for the optimized configuration as shown in figure 5.1.

5.2.1. 10 MW OTEC power plant

A 500 kW OTEC power plant is planned for Curaçao. However, this will be pilot OTEC power plant. It is estimated that on shore OTEC power plants of about 5 to 15 MW will be economically feasible. Therefore it is interesting to know what the water usage of a bigger OTEC is, to compare the water usage with the other subsystems and what the diameter of the cold water pipe would be in that case. For that reason the Ocean Thermal Energy system with a 10 MW instead of a 500 kW OTEC power plant is researched. The results for the DOW water usage can be found in figure 5.13.

As can be expected, the deep seawater usage has increased. The maximum daily water usage is 16860 kg/s, which is 12.4 times greater than the OTE system with a 500 kW OTEC power plant. The required outside pipe diameter should be 4.29 m, which is a 3.5 times bigger than the pipe needed for an OTE system with a 500 kW OTEC plant. A cold water pipe with a outside diameter of 4.29 m seems very big, but the answer found with this model corresponds to the outcomes of previous research done for 10 MW OTEC [55],[28].

With such high cold deep seawater mass flow, the effluent water mass flow coming from the OTEC cold water output will also be very high. The Ecopark water surplus, so the effluent water from OTEC and SWAC, data center minus the water used in the Ecopark, can be found in figure 5.14. This gives much possibilities for the Ecopark subsystems. For example, when all the effluent water is used for fresh water production, the OTWP plant could theoretically produce $6345 m^3/day$ (without storage). This is more than 250 times the production with the normal configuration. This is enough to replace 25% of the reverse osmosis drink water supply of the island and to supply 16% of the daily average drinking water consumption [25]. The water usages per subsystem can be found in appendix D.

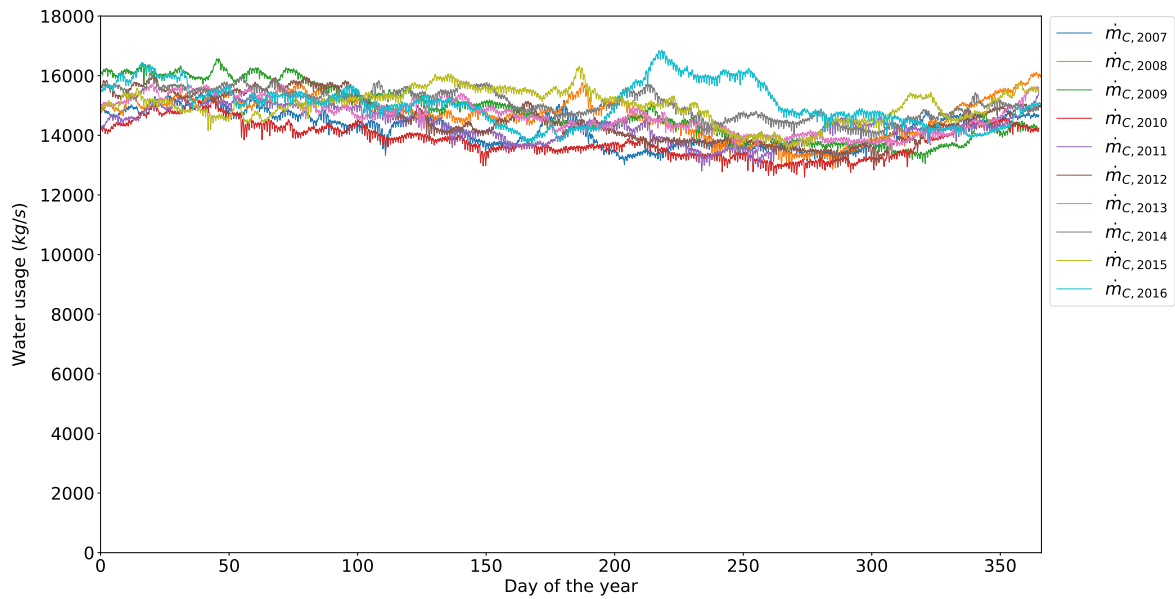


Figure 5.13: Curaçao 2007 - 2016: Total cold deep seawater usage in case of a 10 MW OTEC power plant

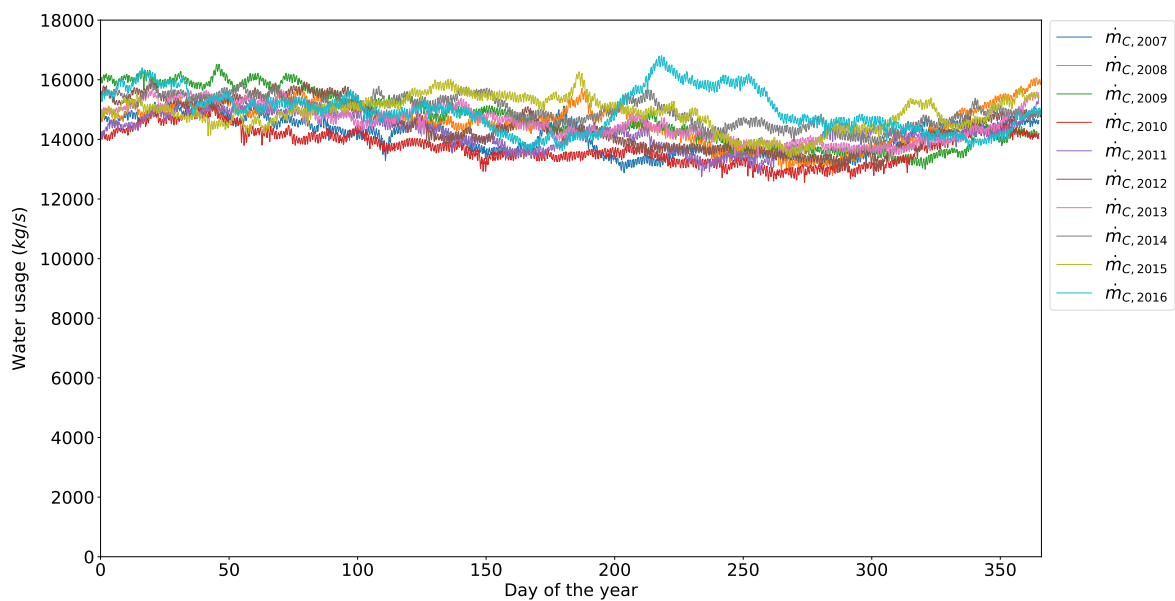


Figure 5.14: Curaçao 2007 - 2016: Ecopark water surplus in case of a 10 MW OTEC power plant

5.2.2. 20 MW_{th} SWAC

The cooling capacity of 7.5 MW_{th} is based on the cooling needed for Hato Curaçao Airport. When other big (new) buildings are connected to the district cooling system, the water usage of the SWAC installation will increase. To see what the impact is on the total water usage of the OTE system, it is researched what the effects are when a 20 MW_{th} instead of a 7.5 MW_{th} SWAC system is installed. The results for the cold deep seawater usage can be found in figure 5.15.

The maximum water usage of the OTE system increases from 1365 kg/s to 1882 kg/s. The outside diameter of the required cold water pipe should be 1.432 m, compared to 1.22 m in the case of a 7.5 MW_{th} SWAC system. Furthermore it can be seen when figure 5.15 is compared to figure 4.11, that the daily fluctuations have become bigger with the 20 MW_{th} SWAC. This is a behavior that could be expected since the daily fluctuation in water usage of the SWAC is bigger than the daily fluctuation of OTEC.

The Ecopark water surplus, so the effluent water that is not used when the area of greenhouse is 3 ha and

the fresh water production is $25 \text{ m}^3/\text{day}$, can be found in figure 5.16. The minimum water surplus is 905 kg/s . This surplus can be used for additional SWAC, data center or greenhouse cooling, OTWP or another additional subsystem in the Ecopark. The water usages per subsystem can be found in appendix D.

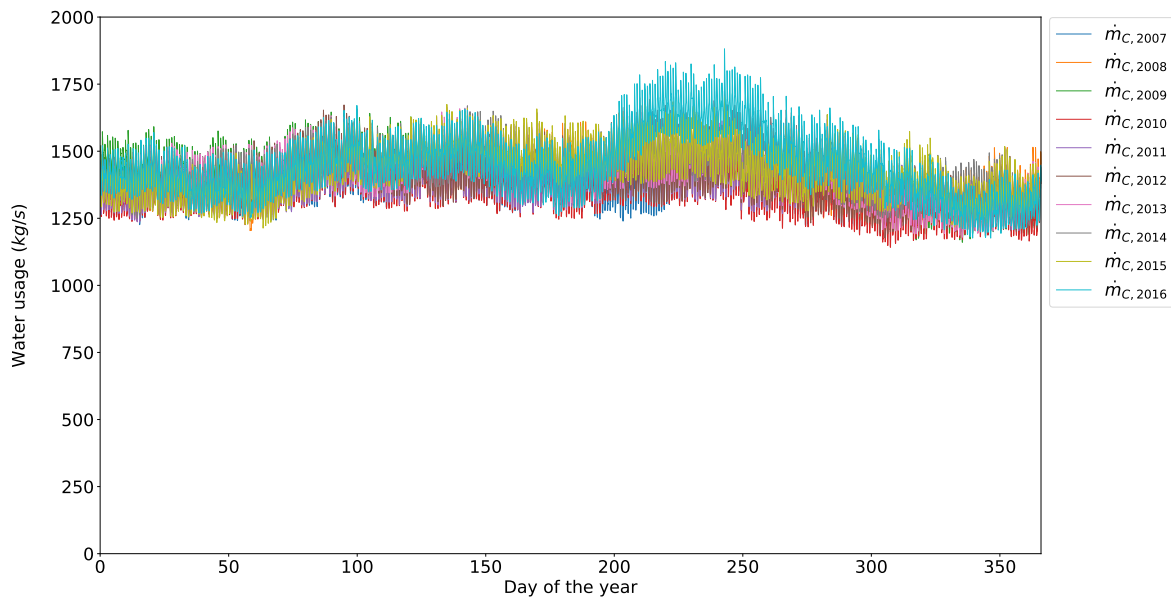


Figure 5.15: Curaçao 2007 - 2016: Total cold deep seawater usage in case of a 20 MW_{th} SWAC installation

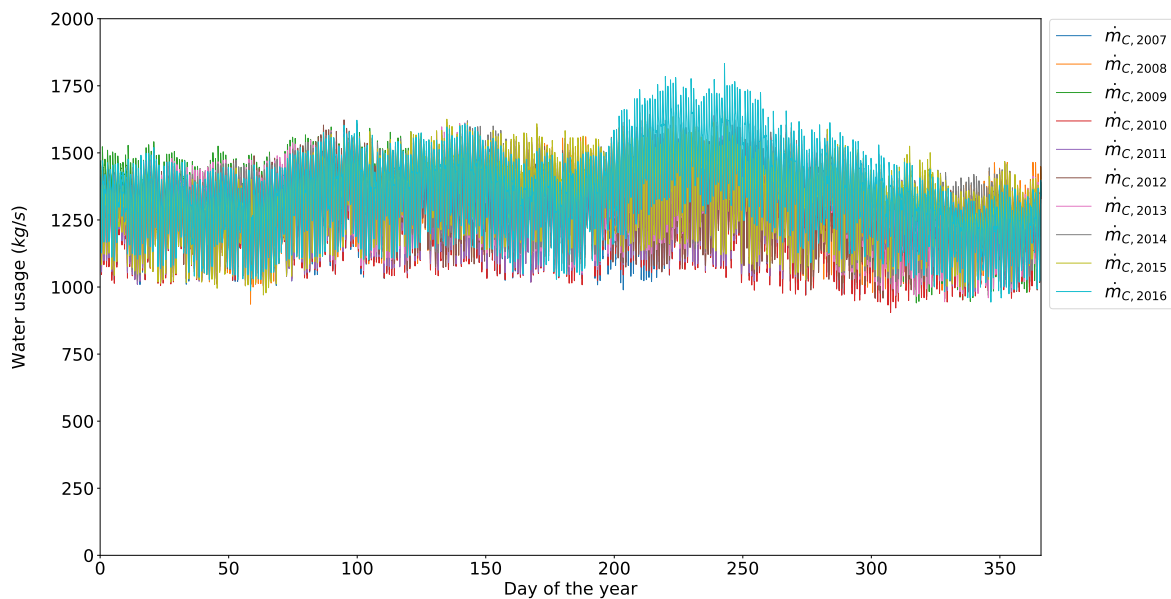


Figure 5.16: Curaçao 2007 - 2016: Ecopark water surplus in case of a 20 MW_{th} SWAC installation

5.2.3. Maximum data center cooling demand

Until now the optimization was mainly focused on the reduction of the cold deep seawater usage. But it is also interesting to see what the maximum possible demands are for each subsystem in the Ecopark when there are no other other subsystem present. Furthermore it is also interesting to see if optimization by daily storage has impact on the maximum demands. In this subsection this will be done for the data center cooling, while in subsection 5.2.4 and subsection 5.2.5 this will be done for the greenhouse cooling and the fresh water production, respectively. The calculations are done for the optimized configuration as shown in figure 5.1.

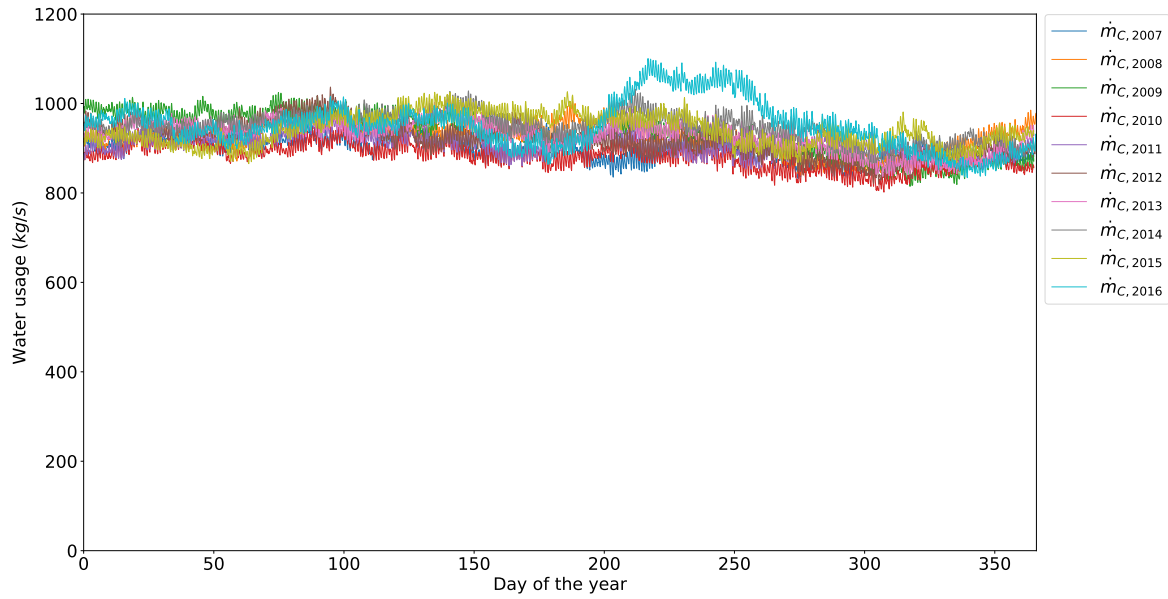


Figure 5.17: Curaçao 2007 - 2016: The effluent water mass flow in case of optimization by configuration

Without storage

First of all the effluent water flow of the system has to be looked into. The water flow of the effluent water can be seen in figure 5.17. For every year it can be calculated what the maximum data center cooling demand is so that the Ecopark water surplus is never below zero. The lowest maximum cooling capacity is 4832 RT from the year 2010. The Ecopark water surplus for all years with the data center cooling demand of 4832 RT can be found in figure 5.18. It can be seen that the Ecopark water surplus is always above zero between 2007 and 2016. So the maximum data center cooling demand will be 4832 RT, which is six times higher than the current demand. The water usages per subsystem can be found in appendix D.

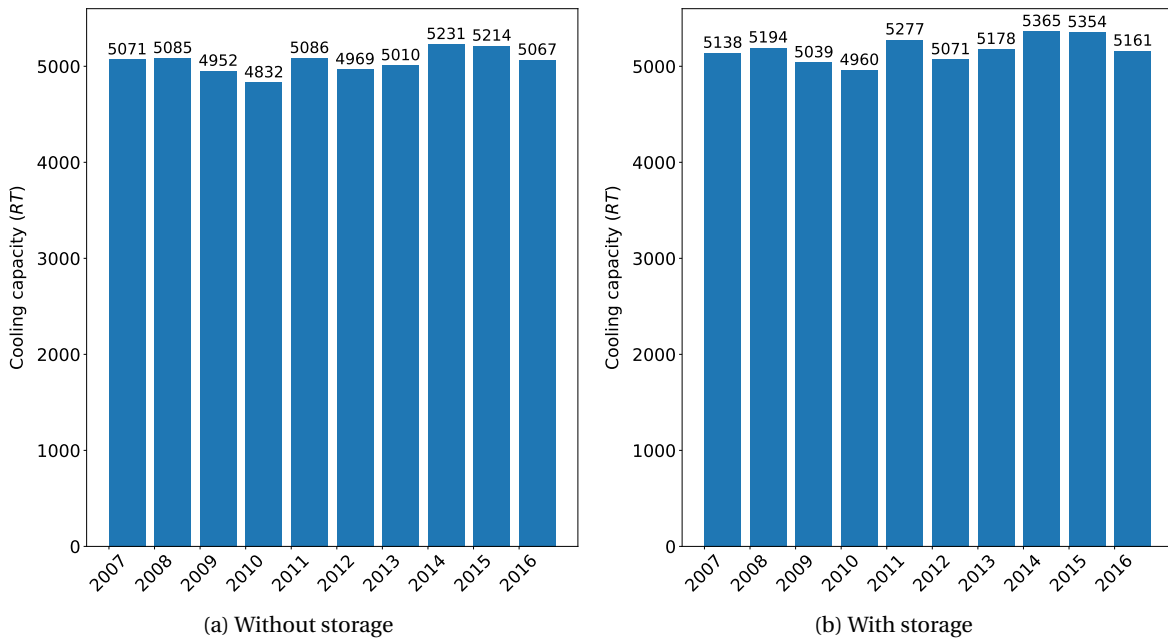


Figure 5.18: Curaçao 2007 - 2016: Maximum DOW water usage in case of maximum data center cooling demand

With storage

The same calculations can be made for the case when daily storage is applied to the data center. The maximum data center cooling demand with storage so that the Ecopark water storage is never negative is 4960 RT.

The Ecopark water surplus for all years with storage with a maximum cooling capacity of 4960 RT can be seen in figure 5.18b.

When the maximum cooling capacity of the case with and without storage are compared, it can be concluded that daily storage has hardly any effect. Thereby, the storage capacity needed in this case would be 1116 m^3 . It might not be worth the effort to apply storage to the data center to improve the Ecopark water usage. The water usages per subsystem can be found in appendix D.

5.2.4. Maximum greenhouse area

In this subsection the maximum greenhouse area will be determined for the OTE system with the optimized configuration. Furthermore it will be researched if a daily storage capacity has an impact on the maximum greenhouse area.

Without storage

Just like in subsection 5.2.3 the maximum greenhouse area can be calculated for each year with taken in mind that the Ecopark water surplus should be always positive. The maximum greenhouse area can be calculated with the fzero function in python, with the greenhouse area as variable input to find the root of the minimal Ecopark water surplus. The lowest maximum greenhouse area of all the years is 10.4 ha. The maximum greenhouse area for all the years can be found in figure 5.19a. Compared to the original greenhouse area, this is 3.5 times more. This is not a high increase and can be explained by the highly fluctuating water usage of the greenhouse cooling. The water usages per subsystem can be found in appendix D.

With storage

The same calculations can be made for this case with a storage capacity for the greenhouse cooling. For every year the maximum greenhouse area is calculated, the results can be found in figure 5.19b.

The lowest maximum greenhouse area is 17.1 ha for the year 2010. Compared to the case without storage, this is an increase of almost 65%. The required storage capacity would be 23885 m^3 , which is about 1400 m^3 per hectare. Therefore daily storage might a good option to increase the possible greenhouse area in this Ecopark, but a feasibility study has to be made to determine if the cost for the daily thermal storage are lower than the gained benefits from a larger greenhouse area. The water usages per subsystem can be found in appendix D.

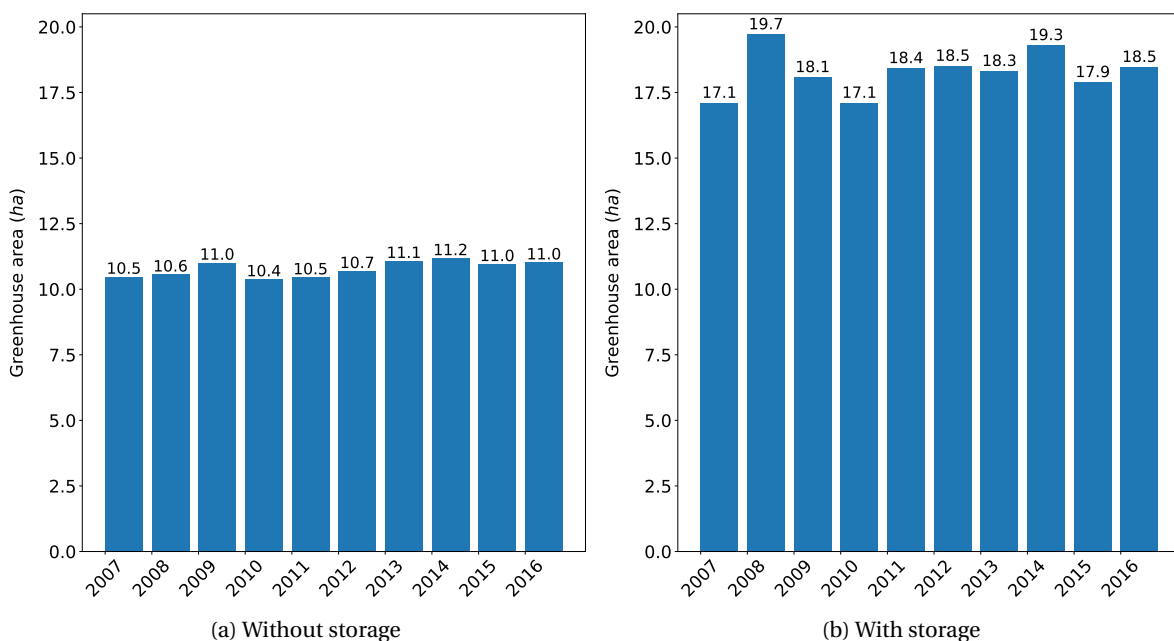


Figure 5.19: Curaçao 2007 - 2016: Maximum DOW water usage in case of maximum greenhouse area

5.2.5. Maximum fresh water production

The last case to research is the maximum possible fresh water production when there are no other subsystems. Furthermore it will be investigated if a daily storage capacity has a significant influence on the maxi-

mum possible water production or not.

Without storage

For each year it is calculated what the maximum fresh water production is per year so that the effluent water flow will not be exceeded. Again this is done with the `fzero` function in Python, with the water production rate as variable input to find the root of the minimal Ecopark water surplus. The results can be found in figure 5.20a. It can be seen that the lowest maximum fresh water production is approximately $393 \text{ m}^3/\text{day}$. So the maximum OTWP potential in case of the optimized configuration is almost 16 times higher than the base case production. The water usages per subsystem can be found in appendix D.

With storage

For each year calculations are made to determine the maximum fresh water production rate with storage applied. The results can be found in figure 5.20b. From this figure it can be seen that the lowest maximum fresh water production rate is almost $398 \text{ m}^3/\text{day}$. Compared to the case without storage, this is only an increase of 1.3% in fresh water production. The storage capacity needed for this increase is 690 m^3 . This is not much, but probably not worth the small increase in fresh water production. The water usages per subsystem can be found in appendix D.

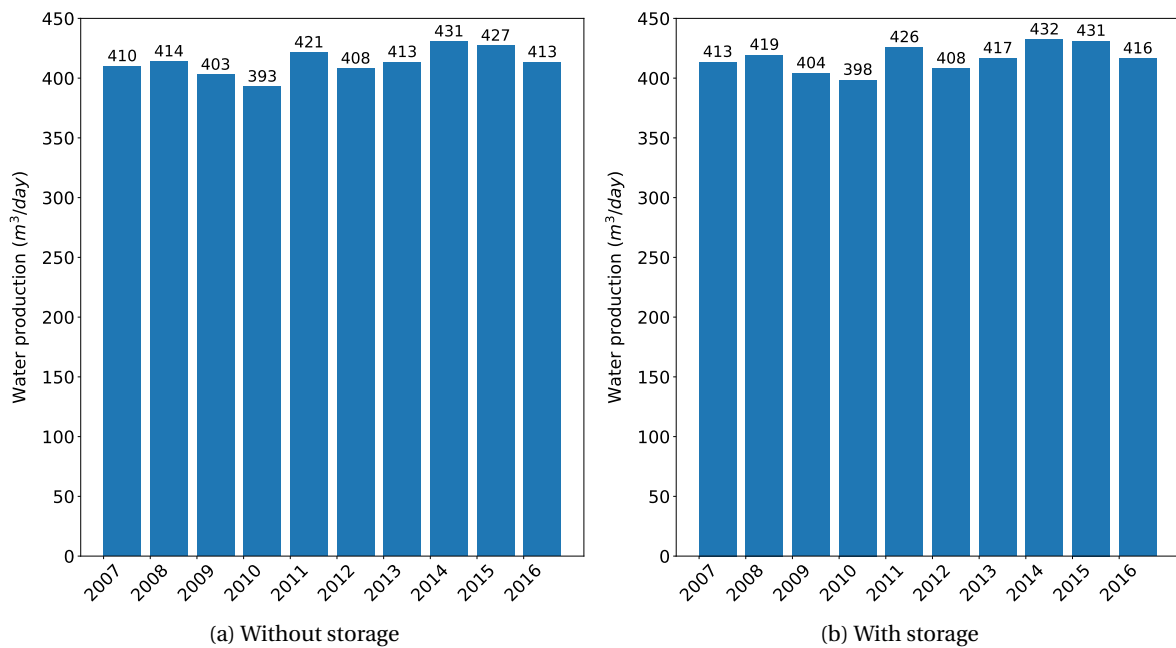


Figure 5.20: Curaçao 2007 - 2016: Maximum DOW water usage in case of maximum fresh water production

5.2.6. Conclusion Cases

From the first two cases it can be concluded that the model works fine for other inputs of the OTEC and SWAC demand than only for the base case. The case of an 10 MW OTEC power plant showed that the calculated required pipe diameter is almost the same as the pipe diameter calculated by others. The case of a 20 MW_{th} SWAC showed that required pipe diameter only increases about 20 cm when the SWAC demand increases from 7.5 MW_{th} to 20 MW_{th} .

The last three cases showed the potential of the data center cooling demand, greenhouse area and fresh water production when all the effluent water in the Ecopark is used by each system, with and without daily storage. The maximum data center cooling capacity can increase from 720 to 4832 RT when all the effluent water is used for data center cooling. Adding daily storage can increase the maximum capacity to 4960 RT, but this difference is so small that it is estimated that it is not feasible to implement the storage.

The total greenhouse area can be expanded from 3 to 10.4 ha when the entire effluent water mass flow is used for greenhouse cooling. In contrary to data center cooling, adding the daily thermal storage option has a significant effect on the maximum greenhouse area. In this case the total greenhouse area can increase to 17.1 ha. However, it should be investigated if this is economically feasible.

When all the effluent water is used to produce fresh water, the water production rate can be increased 15.7

times, namely from $25 \text{ m}^3/\text{day}$ to $393 \text{ m}^3/\text{day}$. Just like in the case of the data center cooling, the increase in fresh water production with thermal storage is not significant.

5.3. Sensitivity analysis

A lot of assumptions are made by developing this model. Some assumptions might be a little of, and therefore the results of the model can deviate from the reality. A sensitivity analysis can be made for a few variables to investigate the uncertainty in output. In subsection 5.3.1 the uncertainty of the cold deep seawater temperature on the outputs is investigated. Subsequently the sensitivity of the OTEC efficiency will be researched in subsection 5.3.2. In subsection 5.3.3 it will be investigated what the impact is on the cold water usage and the pipe diameter when the heat exchanger efficiency is not 100% but less.

5.3.1. Seawater temperature sensitivity

The subsystems that make use of the cold deep seawater are very dependable on the temperature of the water. A change in cold water temperature leads to a higher or lower required mass flow. Therefore it is interesting to investigate what the maximum mass flow and the cold water pipe outside diameter would be when the cold water temperature is changed.

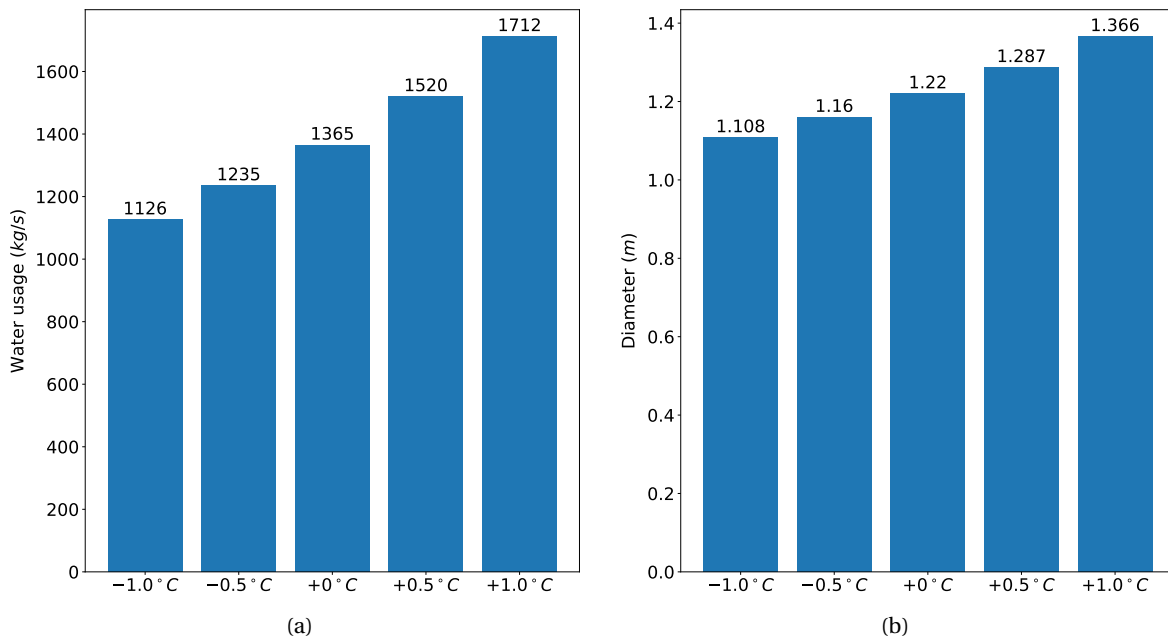
In this subsection it is investigate what the effect is on the maximum mass flow rate and the pipe diameter when the seawater temperature is changed. This is done for an annual seawater temperature change of -1.0°C , -0.5°C , $+0.5^\circ\text{C}$ and $+1.0^\circ\text{C}$ compared to the base case.

The results of this investigation can be found in figure 5.21. In subfigure 5.21a the maximum water usage of the years 2007 to 2016 are shown. As can be expected the maximum water mass flow decreases when the cold deep seawater is colder and the maximum water usage increases when the cold deep seawater temperature goes up.

The same trend can be seen in subfigure 5.21b for the required cold water pipe outside diameter. When the seawater temperature goes down, the pipe diameter decreases and when the seawater temperature goes up, the required pipe diameter increases.

Furthermore it can be seen in subfigure 5.22c that the minimum Ecopark water surplus is positive for every temperature change. The potential of the Ecopark will decrease with lower deep seawater temperatures, but an effluent water shortage is not an issue.

From the results it can be concluded that the maximum cold water mass flow and the required pipe diameter are quite sensitive for temperature changes of the cold deep seawater. This is something that could have been expected, because all the temperature differences in subsystems are small so a temperature change of 0.5°C or 1.0°C is a relative big change.



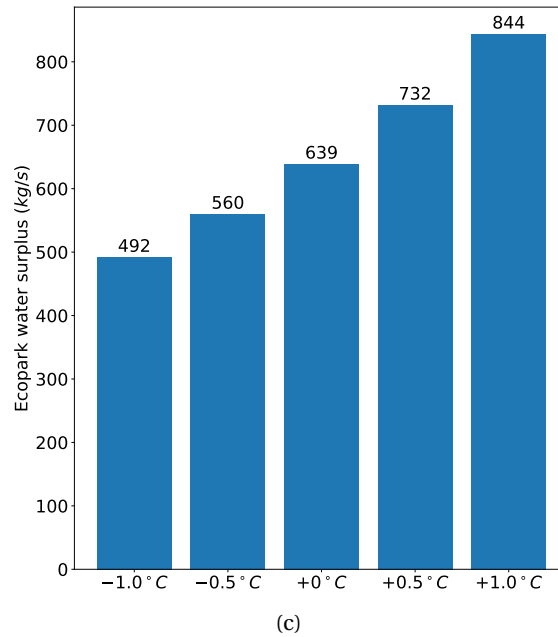


Figure 5.21: Maximum DOW water usage and required cold water pipe outside diameter by changing cold deep seawater temperature

5.3.2. Irreversible efficiency sensitivity

In subsection 3.2.1 in eq. 3.2 it is assumed that the thermal efficiency of the OTEC cycle can be calculated with the Carnot efficiency times an efficiency factor for the irreversible losses. It is assumed that the irreversible efficiency is 0.47, because with this value the efficiency of the OTEC cycle varies between 3.2% and 4.0% for a temperature difference of 20°C and 26°C, respectively.

However, the efficiency of the OTEC cycle might be different than assumed. Therefore it is interesting to research what the impact is on the maximum water usage and pipe diameter when the value of the irreversible efficiency is less or more than the assumed value of 0.47. The maximum water usage and pipe diameter is calculated for the values ± 0.05 and ± 0.1 with respect to the original value of 0.47. The results of these calculations can be seen in figure 5.22.

In subfigure 5.22a the maximum water usage of the years 2007 to 2016 are shown. As can be expected the maximum water mass flow increases when the thermal efficiency decreases and the maximum water usage decreases when the thermal efficiency increases. The same trend can be seen in subfigure 5.22b for the required cold water pipe outside diameter. When the thermal efficiency goes down, the required pipe diameter increases and when the thermal efficiency increases, the required pipe diameter decreases.

Subfigure 5.22c shows the Ecopark water surplus. The water surplus decreases when the irreversible losses are lower, but stays well above zero. This means that even when the assumed value for η_{irrev} is not completely correct, the Ecopark will not face an effluent water shortage.

From the results it can be concluded that the maximum cold water mass flow and the required pipe diameter are quite sensitive for efficiency change of the OTEC cycle. When the efficiency decreases 10% point, the maximum mass flow increases 12.7% and the pipe diameter increases 6.1%. Even so when the efficiency decreases 5% point, the maximum mass flow increases 5.6% and the pipe diameter increases 2.8%.

On the other hand, when the efficiency increases 5% point, the maximum mass flow decreases 4.8% and the pipe diameter decreases 2.4%. Lastly when the efficiency increases 10% point, the maximum mass flow decreases 8.8% and the pipe diameter decreases 4.5%.

From this sensitivity analysis it can be concluded that the efficiency of the OTEC cycle has a significant impact on the maximum water usage and pipe diameter. Therefore the efficiency should be estimated with great care, because otherwise the cold water pipe diameter can be over- or underestimated.

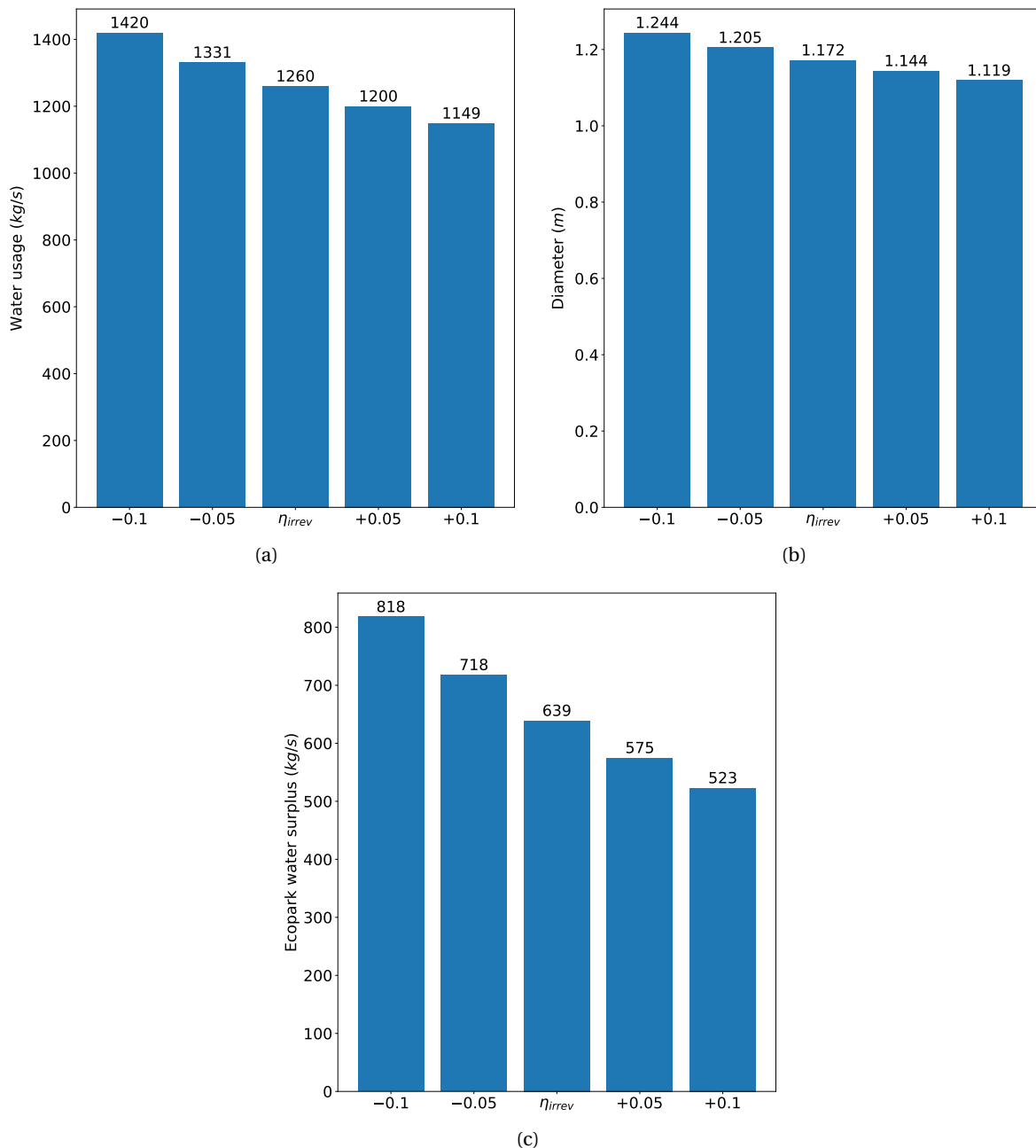


Figure 5.22: Maximum DOW water usage and required cold water pipe outside diameter by changing the irreversible efficiency

5.3.3. Heat losses sensitivity

In the model the assumption is made that there are no heat losses in the OTE system. However, this will not be the case in reality. Therefore a sensitivity analysis is made for the heat losses. The cases with an efficiency of 99%, 98%, 97%, 96% and 95% are compared to the case with 100%. The heat losses are implemented in the model as efficiency factor (heat loss factor) in the heat exchangers. The results from this sensitivity analysis can be seen in figure 5.23.

In subfigure 5.23a the cold deep seawater usage for the efficiency from 100% to 95%. It can be seen that per percentage point decrease of the efficiency the maximum cold water mass flow increases approximately 13 kg/s. Even so it can be seen in subfigure 5.23b that the required pipe diameter increases by approximately 0.008 m for every percent point efficiency decrease.

Furthermore it can be seen in subfigure 5.23c that an increase in heat losses (lower efficiency) even leads to a higher Ecopark water surplus. This can be explained by the fact that the combined heat losses in the primary layer of the OTE system are bigger than the combined heat losses in the Ecopark.

From the heat losses sensitivity analysis it can be concluded that heat losses have a small, but not to be neglected effect on the cold deep seawater mass flow and the cold water pipe diameter. A decrease from 100% to 95% efficiency leads to an increase of 6.5% and 3.3% in maximum cold water usage and pipe diameter, respectively.

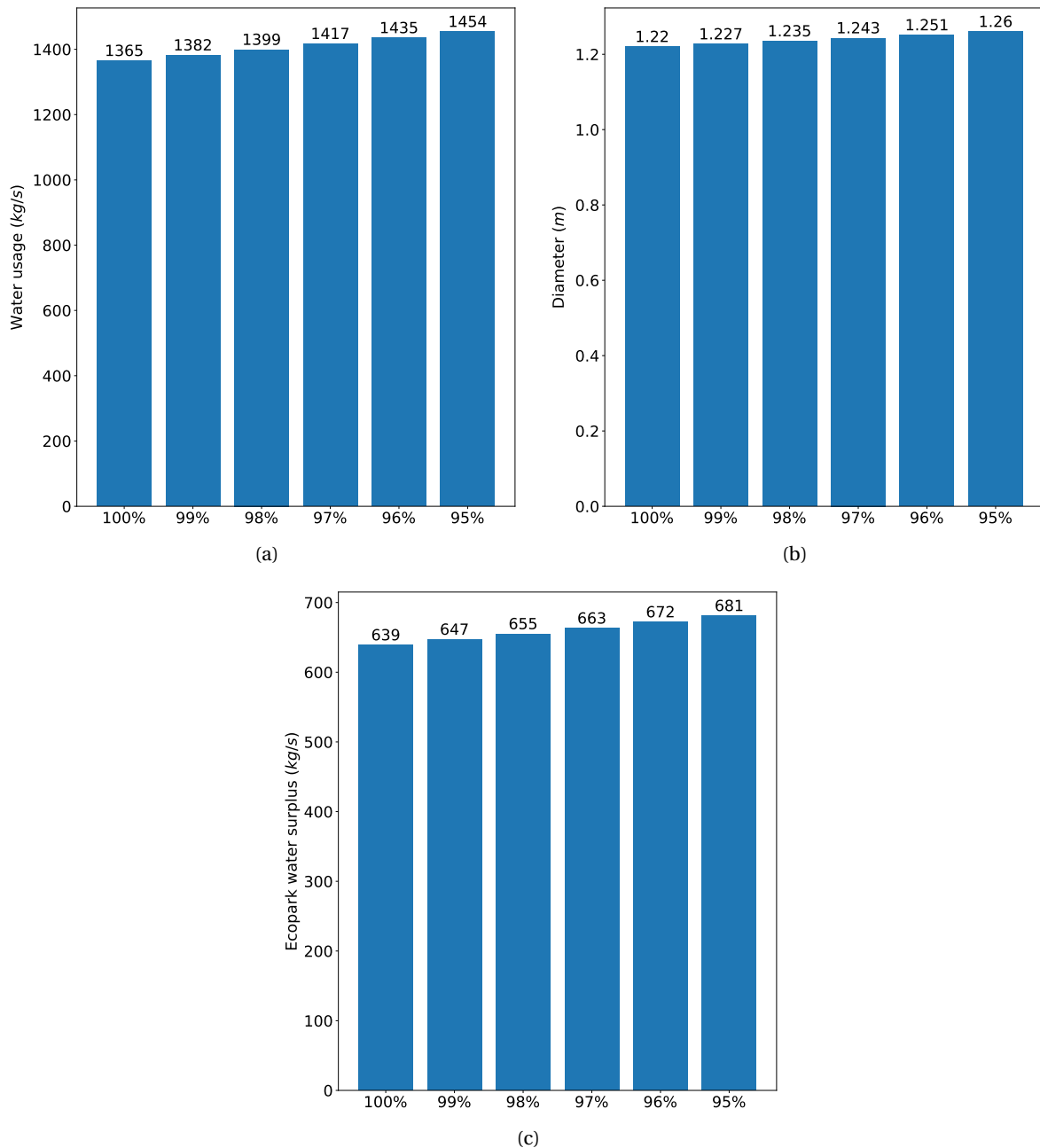


Figure 5.23: Maximum DOW water usage and required cold water pipe outside diameter by changing the heat loss factor

5.3.4. Cold water pipe flow velocity sensitivity

In the model the cold water pipe diameter is calculated with an assumed flow velocity of 1.5 m/s. However, the cold water flow velocity might differentiate from the assumed value. Therefore the sensitivity of the flow velocity will be investigated in this subsection.

In figure 5.24 the required pipe diameter for the velocities of 1.3, 1.4, 1.5, 1.6 and 1.7 m/s can be found. The required pipe diameter change per step of 0.1 m/s is about 0.04 m, which is an increase or decrease of 3.3% per step of 0.1 m/s compared to the assumed diameter.

On the other hand, the flow velocity does not influence the cold deep seawater mass flow and the effluent water mass flow. They are the same as in the case study for Curaçao.

It can be concluded that the model is quite sensitive on the cold deep seawater flow velocity. The flow velocity should be estimated with great care, because the impact on the calculation of the required pipe diameter is significant. However, the flow velocity has no influence on the cold deep seawater and effluent mass flow.

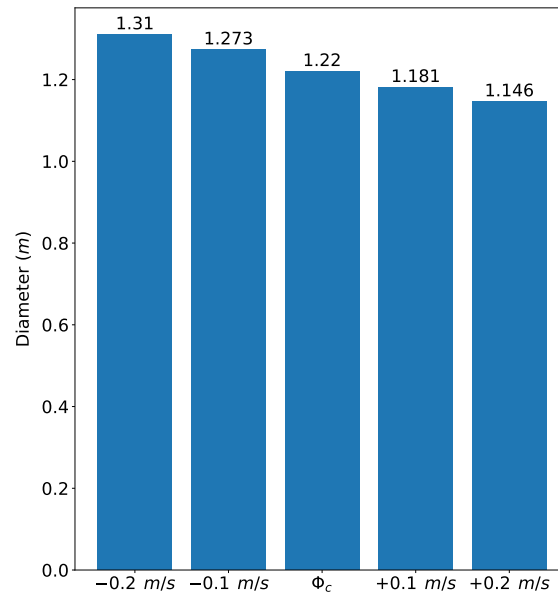


Figure 5.24: The required cold water pipe outside diameter by changing the cold water flow velocity

6

Conclusion and Recommendations

The objective of this thesis was to research the water demands of the subsystems and the time-dependent integration of the water demands in an Ocean Thermal Energy system. The corresponding research objective of this thesis was: *'What is the influence of time-dependent integration of the subsystems in an Ocean Thermal Energy system on the cold deep seawater mass flow and cold water pipe diameter?'*

To answer the research question, a modular model of an OTE system has been developed in Python. The modules that have been developed as subsystems are: OTEC, SWAC, data center cooling, greenhouse cooling and OTWP. The output of each module is the cold water demand, so that outputs can be combined in the main-file to calculate the total cold deep seawater usage and the required cold water pipe diameter. The model calculates the cold deep seawater mass flow for the length of one year on an hourly basis.

6.1. Conclusions

Seawater temperature fluctuation

The most important input parameters are the cold deep seawater temperature and the hot surface water temperature. For the base case study for Curaçao the seawater temperatures have been investigated for the years 2007 to 2016. The seawater temperature analysis gave a great insight in the fluctuation of the seawater temperatures over the years. The differences in seawater temperatures between years are larger than expected. Especially the year 2016 shows a different behavior than the years before. Therefore it can be concluded for the seawater temperatures that it is very important to have seawater temperature data of many years. This way peak and bottom seawater temperatures, which in the end determine the size of the cold water pipe, can be taken into account. Otherwise it can happen that the cold water pipe diameter is too small and that the subsystems in an OTE cannot operate.

Time-integrated OTE system

The cold deep seawater usage and the required pipe diameter of the simple demand analysis and the time-integrated OTE system are calculated and compared. In case of the simple demand analysis the maximum cold deep seawater mass flow was 1414 kg/s and the corresponding required pipe outside diameter is 1.242 m. In case of the time-integrated system the maximum water usage is 1365 kg/s and the required CWP diameter is 1.22 m. So the cold water mass flow decreased 49 kg/s (3.6%) and the required pipe outside diameter decreased 0.022 m (1.80%). It can be concluded that the difference between the simple demand analysis and the time-integrated OTE system is not significant and that therefore the optimization of an OTE system by time-dependent integration is not significant.

However, when the year 2016 is excluded, the difference is more significant. In case of the simple demand analysis the maximum mass flow would be 1365 kg/s and the required pipe diameter 1.22 m. In case of the time-integrated system the maximum mass flow would be 1265 kg/s and the required pipe diameter 1.174 m. This is a reduction of 7.3% and 3.8% in cold water mass flow and CWP outside diameter, respectively.

Daily and yearly thermals storage

The OTE system's maximum cold water usage and required cold water pipe outside diameter can be optimized by adding daily or yearly thermal storages. The maximum cold deep seawater mass flow is 1246 kg/s

and the corresponding required pipe diameter is 1.166 m in case of the daily thermal storage. This is a decrease of 8.7% and 4.4%, respectively and the total required storage volume is 23 000 m^3 . In case of the yearly thermal storage, the maximum cold water mass flow is 1184 kg/s and the CWP outside diameter is 1.136 m. This is a decrease of 13.3% and 6.9%, respectively and the total required storage volume is about 624 000 m^3 .

Even though the results look promising for the maximum cold deep seawater mass flow and the pipe diameter, the large required storage volume is expected to cost a lot. Therefore it should be researched if the daily or yearly thermal storage are cheaper than a larger CWP diameter.

6.1.1. Greenhouse storage

The only subsystem where daily storage makes a significant difference is greenhouse cooling, because the cooling demand of the greenhouse fluctuates a lot over a day. When the greenhouses are connected to the effluent water, the maximum greenhouse area can be increased from 10.4 ha to 17.1 ha by adding a daily thermal storage of 23 885 m^3 .

Move subsystems downstream

The best way to optimize an OTE system is to add as many subsystems downstream in the Ecopark, so that they use the effluent water coming from the OTEC and SWAC. Compared to the Curaçao case study, the maximum cold water mass flow could be reduced from 1365 to 1101 kg/s and the required CWP diameter could be reduced from 1.22 to 1.096 m when the data center, greenhouses and OTWP are placed in the Ecopark. This is a decrease of 19.3% and 10.2%, respectively. Adding daily or yearly thermal storages can decrease the maximum mass flow and the pipe diameter even further, but the decrease is not significant compared to the case of an optimized configuration.

Large-scale OTEC power plant

The calculation of the OTE system with a 10 MW instead of a 500 kW OTEC power plant showed that the water usage of the other subsystems are almost neglectable compared to the water usage of the OTEC. Since it is expected that other OTE systems will be combined include an 5 to 15 MW OTEC, the optimization of the OTEC power plant is expected to be more significant than optimization by configuration of an OTE system.

Summary

It can be conclude that the optimization by time-dependent integration is not significant and that it is beneficial to add as many subsystems downstream in the Ecopark that are using the effluent water to optimize the cold deep seawater mass flow and the required cold water pipe diameter.

6.2. Recommendations

Even though the model showed great results in predicting the mass flows in the OTE system and the cold water pipe diameter, there are plenty of opportunities to improve the model.

Less simplified subsystem modules

For future research, it is recommended to change the modules of the subsystems with less simplified ones. This might be crucial to determine peak demands and to get an even better approximation of the maximum water usage and CWP diameter.

Environmental data

Furthermore, it is recommended to use measured or better environmental data instead of the data of Meteoronorm. The disadvantage of Meteoronorm is that the data is generated by a model. Even though this gives a good approximation, it can be seen that it is not measured data. It will be interesting to compare the results of this model for the data of Meteoronorm and measured data.

Economical optimization

In this research the optimization is made only in terms of cold deep seawater mass flow and cold water pipe diameter. Therefore it will also be interesting to see an economical optimization for the Curaçao base case study. Especially in case of the daily and yearly thermal storages it would be interesting to see some real number to compare the cost of building the storage and the savings on having a smaller CWP.

Heat losses

In almost every case heat losses are not taken into account, but they can really make a significant difference in water usage since the temperature differences in the subsystems are very small. Examples of heat losses that could be taken into account are heat exchanger losses and heat losses due to transportation of the water.

Other OTE system sites

This model has only been tested for an OTE system located on Curaçao. It will be interesting to see how the model behaves for different locations and what the results will be for those locations. Furthermore, the model could not be validated because there is no data available. When the OTE system on Curaçao is built and measured data is available, it will be interesting to see the differences between this model and the measured data.

Graphical User Interface

The final recommendation is to develop a GUI for this model to make it more user friendly. The model is developed in such a way that the case specific inputs are in one file and the outputs are in another file. Therefore it should not be too hard to make a GUI for this model.

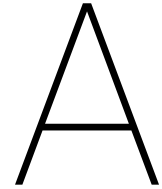
Bibliography

- [1] Al-Ismaïli, A.M. and Jayasuriya, H. **Seawater greenhouse in Oman: A sustainable technique for fresh-water conservation and production.** *Renewable and Sustainable Energy Reviews*, 54:653 – 664, 2016.
- [2] Avery, W.H. and Wu, C. **Renewable energy from the ocean - A guide to OTEC.** New York, NY (United States); Oxford Univ. Press, 1994.
- [3] Bell, I.H., Wronski, J., Quoilin, S., and Lemort, V. **Pure and Pseudo-pure Fluid Thermophysical Property Evaluation and the Open-Source Thermophysical Property Library CoolProp.** *Industrial & Engineering Chemistry Research*, 53(6):2498–2508, 2014.
- [4] Bharathiraja, B., Jayamuthunagai, J., Chakravarthy, M., Kumar, R.R., Yogendran, D., and Praveenkumar, R. **Algae: Promising Future Feedstock for Biofuels.** In Singh, B., Kuldeep, B., and Faizal, B., editors, *Algae and Environmental Sustainability*, pages 1–8. Springer, 2015.
- [5] CBC News Online. **The price of oil - in context**, 2006. URL <https://web.archive.org/web/20070609145246/http://www.cbc.ca/news/background/oil/>. (Accessed: 2017-03-23).
- [6] Chisti, Y. **Large-Scale Production of Algal Biomass: Raceway Ponds**, pages 21 – 40. Springer International Publishing, 2016.
- [7] Cho, J., Lim, T., and Kim, B.S. **Viability of datacenter cooling systems for energy efficiency in temperate or subtropical regions: Case study.** *Energy and Buildings*, 55:189 – 197, 2012.
- [8] Cipollina, A. Micale, G. and Rizzuti, L. **Seawater Desalination - Conventional and Renewable Energy Processes.** Springer Berlin - Heidelberg, 2009.
- [9] Courtland, R. **Ocean Thermal Energy: Back from the deep.** *IEEE Spectrum*, 51(9):18, 2014.
- [10] Daniel, T. **Aquaculture using cold OTEC water.** In *OCEANS'85 - Ocean Engineering and the Environment*, pages 1284 – 1289. IEEE, 1985.
- [11] Dyer, D.F. and Ragan, J.S. **Novel reverse osmosis desalination of sea water.** *WIT Transactions on Ecology and the Environment*, 168:127 – 137, 2012.
- [12] FAO Fisheries Department and others. **The production of fish meal and oil.** Food and Agriculture Organization (FAO) of the United Nations, 1986.
- [13] Farooq, W., Suh, W.I., Park, M.S., and Yang, W.-J. **Water use and its recycling in microalgae cultivation for biofuel application.** *Bioresource Technology*, 184:73 – 81, 2015. Advances in biofuels and chemicals from algae.
- [14] Fry, A. and Haden, E. **Facts and trends: Water**, 2007. URL http://www.unwater.org/downloads/Water_facts_and_trends.pdf.
- [15] Gerard, R.D. and Worzel, J.L. **Condensation of Atmospheric Moisture from Tropical Maritime Air Masses as a Freshwater Resource.** *Science*, 157(3794):1300–1302, 1967. doi: 10.1126/science.157.3794.1300.
- [16] Ghosh, T. and Prelas, M. **Energy Resources and Systems - volume 1: Fundamentals and Non-Renewable Resources**, volume 1. Springer Science & Business Media, 2009.
- [17] Ghosh, T. and Prelas, M. **Energy Resources and Systems - volume 2: Renewable Resources**, volume 2. Springer Science & Business Media, 2011.
- [18] Herrmann, S., Kretschmar, H.-J., and Gatley, D.P. **Thermodynamic Properties of Real Moist Air, Dry Air, Steam, Water, and Ice (RP-1485).** *HVAC&R Research*, 15(5):961–986, 2009.

- [19] IEA. **Key World Energy Statistics 2015**. http://www.iea.org/publications/freepublications/publication/KeyWorld_Statistics_2015.pdf, 2015.
- [20] Iqbal, K. and Starling, K. **Use of Mixtures as Working Fluids in Ocean Thermal Energy Conversion Cycles**. In *Proceedings of the Oklahoma Academy of Science*, volume 56, pages 114–120, 1976.
- [21] Jackson, M. **European v USA Broadband Internet Usage and Surfing Trends**. 2009. URL <http://www.ispreview.co.uk/story/2009/08/19/european-v-usa-broadband-internet-usage-and-surfing-trends.html>. (Accessed: 2017-06-22).
- [22] Jones, E., Oliphant, T., Peterson, P., et al. **SciPy: Open source scientific tools for Python**, 2001–. URL <http://www.scipy.org/>. (Accessed: 2017-09-13).
- [23] Kalina, A.I. **Generation of energy by means of a working fluid, and regeneration of a working fluid**, August 31 1982. US Patent 4,346,561.
- [24] Kempener, R. and Neumann, F. **Ocean Thermal Energy Conversion Technology Brief**, 2014. URL http://www.irena.org/DocumentDownloads/Publications/Ocean_Thermal_Energy_V4_web.pdf.
- [25] Kim-Hak, D., Dixon, M.B., Galan, M.A., Boisseau, F., Gallastegui, J., and Martina, R. **Santa Barbara, Curacao desalination plant expansion using NanoH₂O thin film nanocomposite (TFN) SWRO membrane**. *Desalination and Water Treatment*, 55(9):2446–2452, 2015.
- [26] Kirkenier, J.A. **Techno-economic optimization of Organic Rankine Cycles using working fluid mixtures for 10 to 25 MW OTEC power plants**. Master's thesis, Delft University of Technology, 2014.
- [27] Klaver, H. and Braam, P. **Cooling demant determination and grid route exploration cooling project Curacao airport**. Technical report, Bluerise internal document, 2014.
- [28] Kleute, B.J. and Vroom, M. **Offshore Ocean Thermal Energy Conversion - Feasibility study of a 10 MW installation**. Technical report, Bluerise internal document, 2014.
- [29] Kozisek, F. **Health risks from drinking demineralised water**. *Nutrients in Drinking Water*, pages 148–163, 2005.
- [30] Kumar, K., Mishra, S.K., Shrivastav, A., Park, M.S., and Yang, J.-W. **Recent trends in the mass cultivation of algae in raceway ponds**. *Renewable and Sustainable Energy Reviews*, 51:875 – 885, 2015.
- [31] Kumar, K.S. Tiwari, K.N. and Jha, M.K. **Design and technology for greenhouse cooling in tropical and subtropical regions: A review**. *Energy and Buildings*, 41(12):1269 – 1275, 2009.
- [32] Looney, C.M. and Oney, S.H. (Ph.D.). **Seawater District Cooling and Lake Source District Cooling**. *Energy Engineering*, 104(5):34–45, 2007.
- [33] Lopez, M.C.M. **Ocean Thermal Water Production - Atmospheric water extraction**. Master's thesis, Delft University of Technology, 2016.
- [34] Meadows, D.H. and Club of Rome. **The Limits to growth: A report for the Club of Rome's project on predicament of mankind**. Universe Books, New York, 1972.
- [35] Meteororm, a product by Meteotest. **Meteororm**, 2015. URL <http://www.meteororm.com/>.
- [36] Msangi, S., Kobayashi, M., Batka, M., Vannuccini, S., Dey, M.M., and Anderson, J.L. **Fish to 2030: Prospects for Fisheries and Aquaculture**. *World Bank Report*, (83177-GLB), 2013.
- [37] Nakasone, T. and Akeda, S. **The application of deep sea water in Japan**. *UJNR Aquaculture Panel Proceedings, UJNR Technical Report*, (28):69 – 75, 1999. URL <http://www.lib.noaa.gov/retiredsites/japan/aquaculture/proceedings/report28/Nakasone.pdf>.
- [38] National Oceanic and Atmospheric Administration. **Currents - The Global Conveyor Belt**, 2017. URL https://oceanservice.noaa.gov/education/tutorial_currents/05conveyor2.html. (Accessed: 2017-09-13).

- [39] National Oceanic and Atmospheric Administration. **What is the global ocean conveyor belt?**, 2017. URL <https://oceanservice.noaa.gov/facts/conveyor.html>. (Accessed: 2017-09-13).
- [40] Nurse, L. A., McLean, R. F., Agard, J., Briguglio, L. P., Duvat-Magnan, V., Pelesikoti, N., Tompkins, E., and Webb, A. **Small islands**. In *Climate Change 2014: Impacts, Adaptation, and Vulnerability. Part B: Regional Aspects. Contribution of Working Group II to the Fifth Assessment Report of the Intergovernmental Panel on Climate Change*.
- [41] Ocean Thermal Energy Corporation. **Ocean Thermal Energy Conversion: A Brief History**. URL <http://otecorporation.com/technology/a-brief-history/>. (Accessed: 2017-03-23).
- [42] Okinawa Prefecture's Deep Seawater Research Institute. **Seawater Uses**. URL <http://otecokinawa.com/en/OTEC/WaterUse.html>. (Accessed: 2017-04-24).
- [43] Organization for Promotion of Ocean Thermal Energy Conversion (OPOTEC). **Uehara Cycle**. URL http://www.opotec.jp/english/uehara_cycle.html. (Accessed: 2017-03-23).
- [44] Osorio, A.F., Arias-Gaviria, J., Devis-Morales, A., Acevedo, D., Velasquez, H.I., and Arango-Aramburo, S. **Beyond electricity: The potential of ocean thermal energy and ocean technology ecoparks in small tropical islands**. *Energy Policy*, 98:713 – 724, 2016. ISSN 0301-4215.
- [45] OTEC Foundation. **World's largest OTEC plant connected to grid**, 2015. URL <http://www.otecnews.org/2015/08/worlds-largest-otec-plant-connected-to-grid/>. (Accessed: 2017-03-23).
- [46] OTEC International, LLC. **OTEC History**. URL <http://www.oteci.com/otec-at-work/test-page/>. (Accessed: 2017-03-23).
- [47] Pillai, I.R. and Banerjee, R. **Renewable energy in India: Status and potential**. *Energy*, 34(8):970–980, 2009. Energy and its sustainable development for India Energy and its sustainable development for India.
- [48] Posten, C. and Chen, S.F. **Microalgae Biotechnology**. In *Advances in Biochemical Engineering/Biotechnology*, volume 153. Springer, 2016.
- [49] Priva. **Project cooling Curacao kas Priva**. Technical report, Bluerise internal document, 2014.
- [50] Pruvost, J., Cornet, J.-F., and Pilon, L. **Large-Scale Production of Algal Biomass: Photobioreactors**, pages 41 – 66. Springer International Publishing, 2016.
- [51] Python Software Foundation. **Python Language Reference**. URL <http://www.python.org>.
- [52] Radulovich, R., Neori, A., Valderrama, D., Reddy, C.R.K., Cronin, H., and Forster, J. **Chapter 3 - Farming of seaweeds**. In Tiwari, B.K. and Troy, D.J., editors, *Seaweed Sustainability*, pages 27 – 59. Academic Press, San Diego, 2015.
- [53] Rajagopalan, K. and Nihous, G.C. **Estimates of global Ocean Thermal Energy Conversion (OTEC) resources using an ocean general circulation model**. *Renewable Energy*, 50:532–540, 2013.
- [54] Roels, O.A., Laurence, S., and Hemelryck, L. van . **The utilization of cold, nutrient-rich deep ocean water for energy and mariculture**. *Ocean Management*, 5(3):199 – 210, 1979.
- [55] Sario, A. de. **Cold-Water Pipeline Deployment for Offshore OTEC Power Plants**. Master's thesis, Delft University of Technology, 2017.
- [56] Schelleman, F. and Weijsten, B. van . **Renewable Energy Future for the Dutch Caribbean Islands Bonaire, St. Eustatius and Saba**, 2016. URL <https://zoek.officielebekendmakingen.nl/blg-776649.pdf>.
- [57] Seawater Greenhouse. **Low-cost, rugged and modular**. URL <https://seawatergreenhouse.com/somaliland>. (Accessed: 2017-04-24).
- [58] (Stathis) Michaelides, Efstathios E. **Solar Energy**, pages 195–230. Springer Berlin Heidelberg, Berlin, Heidelberg, 2012.

- [59] Takahashi, M.M. ***DOW: Deep Ocean Water as Our Next Natural Resource***. Terra Scientific Publishing Company, Tokyo, 1991.
- [60] Takahashi, M.M. and Huang, P.-Y. **Novel Renewable Natural Resource of Deep Ocean Water (DOW) and their Current and Future Practical Applications**. *Kurosio Science*, 6:101 – 113, 2012. URL <https://ir.kochi-u.ac.jp/dspace/bitstream/10126/5075/1/6.1.11.pdf>.
- [61] Tiwari, B.K. and Troy, D.J. **Chapter 1 - Seaweed sustainability – food and nonfood applications**. In Tiwari, B.K. and Troy, D.J., editors, *Seaweed Sustainability*, pages 1–6. Academic Press, San Diego, 2015.
- [62] Iersel, S. van and Flammini, A. **Algae-based biofuels: applications and co-products**. 2010.
- [63] War, J.C. **Seawater Air Conditioning (SWAC) - A renewable energy alternative**. In *OCEANS'11 MTS/IEEE KONA*, pages 1–9, Sept 2011.
- [64] White, W.L. and Wilson, P. **Chapter 2 - World seaweed utilization**. In Tiwari, B.K. and Troy, D.J., editors, *Seaweed Sustainability*, pages 7 – 25. Academic Press, San Diego, 2015.
- [65] World Bank. **CO2 emissions (metric tons per capita)**, 2015. URL <http://data.worldbank.org/indicator/EN.ATM.CO2E.PC>. (Accessed: 2017-05-09).
- [66] Wu, C and Buyya, R. **Cloud Data Centers and Cost Modeling - A Complete Guide to Planning, Designing and Building a Cloud Data Center**. Morgan Kaufmann, 2015.
- [67] Zwerver, A. M. J. **OTEC in the energy mix – island case study**. In *4th International OTEC Symposium*, 2016.



Validation SWAC cooling curve correlation

The correlation that is used to predict the cooling demand as function of the temperature and solar radiation which takes heat accumulation into account is based on measured data of Greenvis [27]. Greenvis performed measurements on the chiller in the old terminal of Hato Curacao International Airport from 31-01-2014 to 03-02-2014. The calculated cooling load and the measured environmental temperature can be found in figure A.1.

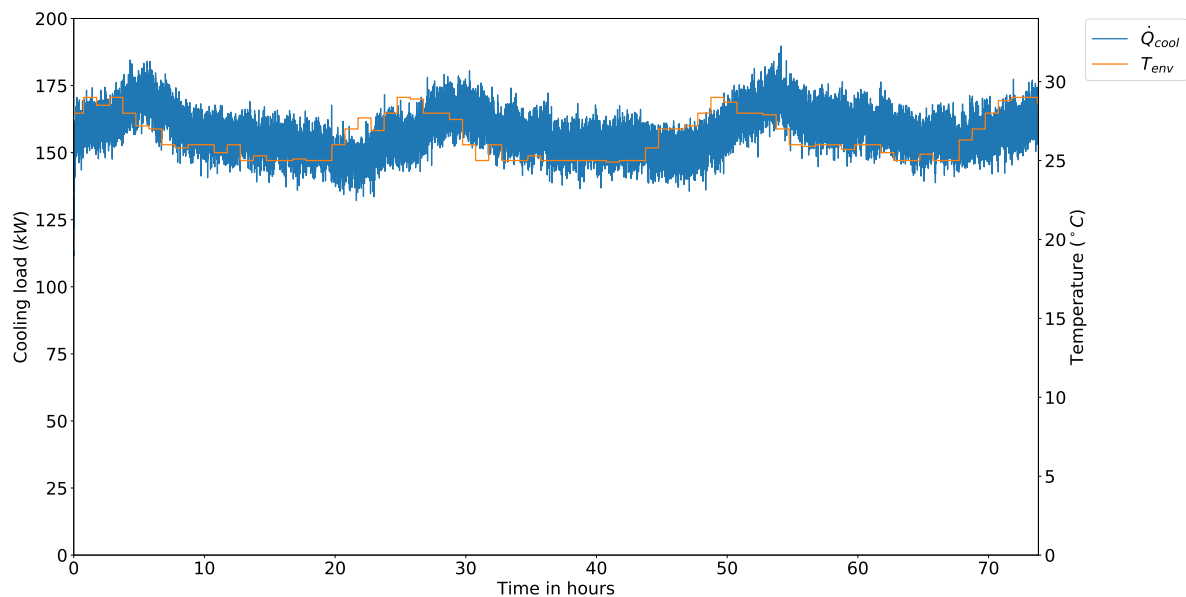


Figure A.1: Old terminal cooling load and the measured environmental temperature

It can be seen that there is a correlation between the temperature and the cooling load. The peaks of the cooling load maximum and minimum are shifted about four hours maximum environmental temperature. This behavior can be explained by heat accumulation inside the building. In figure A.2 the result can be seen when the temperature curve is shifted four hours to the right. It can be seen that now the maximum cooling load almost perfectly concur with the maximum environmental temperature.

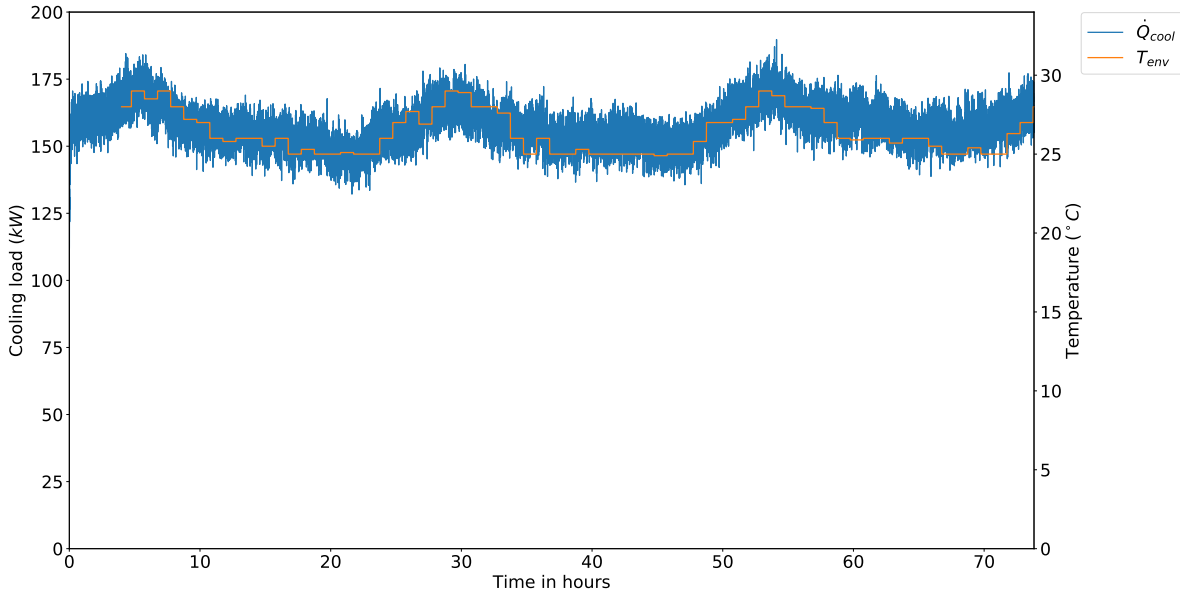


Figure A.2: Old terminal cooling load and the shifted environmental temperature

Since this has to be a generic model, it is preferred to have a function that is dependable on the maximum cooling load. Furthermore, it is obvious to include the environmental temperature as input. The last obvious variable to include is the solar radiation. This can be done by the solar factor. The solar factor SF is the ratio between the average monthly solar radiation and the maximum average solar radiation over a year. The solar factor for Curacao based on the data of Meteonorm can be seen in figure A.3.

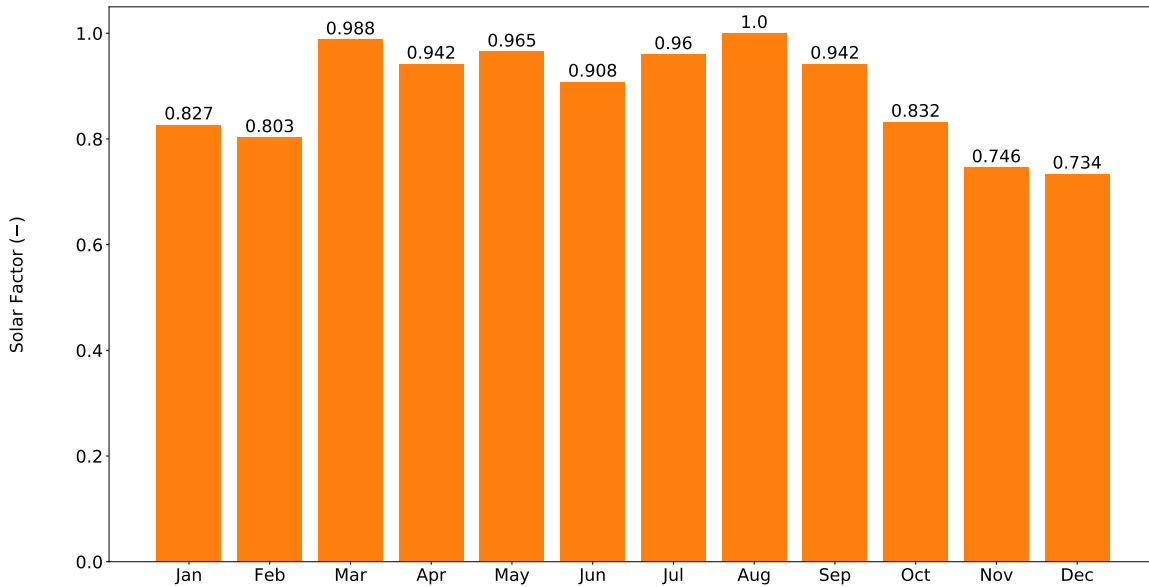


Figure A.3: The solar factor of Curacao for the months of a year

The correlation found can be seen in eq. A.1. The cooling load depends on the solar factor SF, the shifted temperature $T_{env}(h-4)$, the maximum environmental temperature of the year $T_{env,max}$ and the maximum cooling demand of the year \dot{Q}_{max} .

$$\dot{Q}_{cool}(h) = \dot{Q}_{max} \cdot SF \cdot \frac{T_{env}(h-4)}{T_{env,max}} \quad (A.1)$$

It can be checked if this leads to the right cooling curve. The solar factor in the month february is 0.803 and the maximum temperature of the year 2014 is 35°C . The maximum cooling capacity of the chiller is not know, but it is expected that it is about 250 kW. The result of the calculation of the cooling load with this correlation can be found in figure A.4. It can be seen that the green line of the calculated cooling demand is almost following the orange line of the temperature and the blue line of the measured cooling demand.

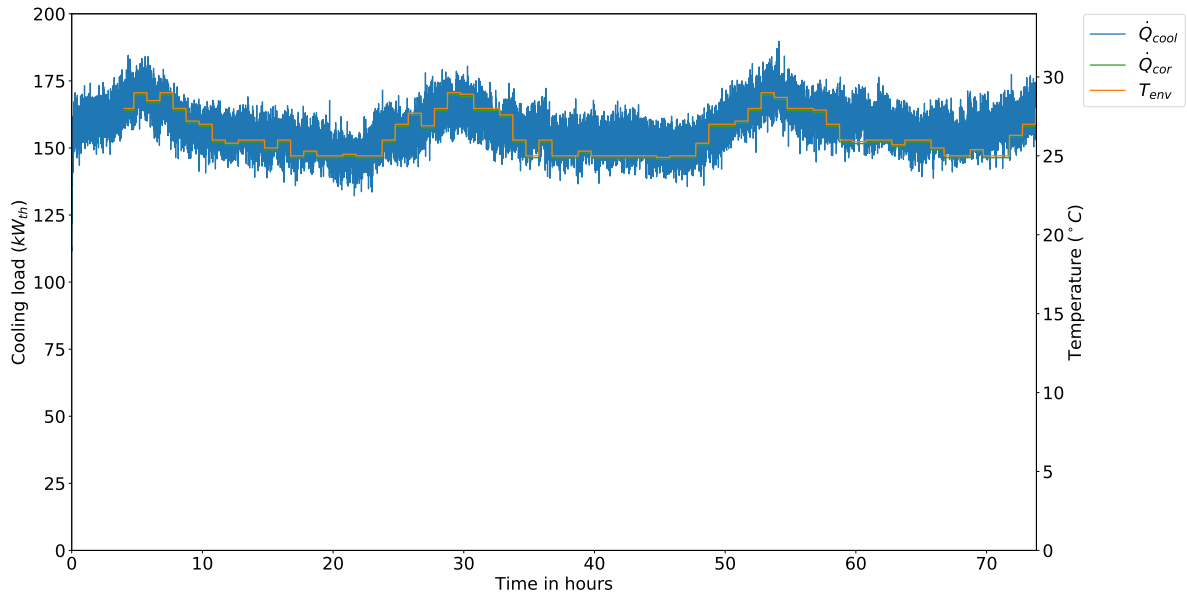


Figure A.4: Old terminal cooling load, the shifted environmental temperature and the calculated cooling load

Now the SWAC cooling correlation can be extrapolated for the year 2014. The temperature data of the entire year is taken from Meteonorm. In figure A.5 both the measured cooling demand and the extrapolated cooling demand for the year 2014 based on the correlation can be seen.

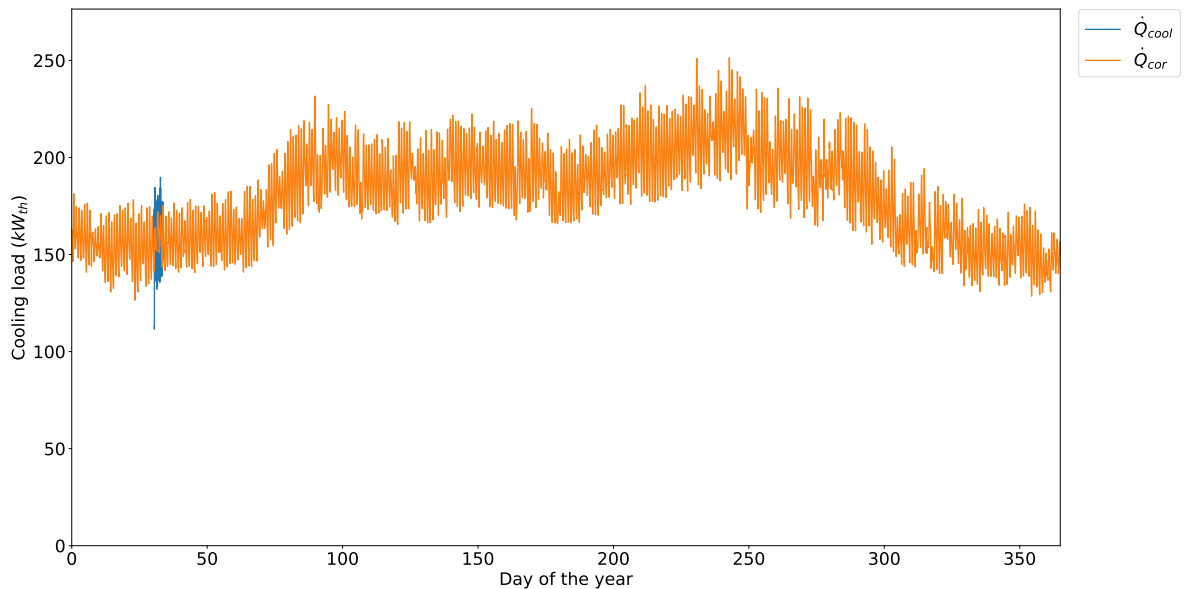


Figure A.5: Old terminal cooling load and the extrapolated calculated cooling load for the year 2014

In figure A.6 the same can be seen, but then zoomed into the period from 31-02-2014 to 03-02-2014. The calculated cooling demand deviates a bit more compared to figure A.4, but the maximum of the measured

and the calculated cooling demand occur on the same time. The deviation can probably be explained by the temperature data of Meteonorm. The temperatures are not measured, but calculated based on an hourly based climate model. Therefore the minimum and maximum temperatures might be different than the values of the measured temperature.

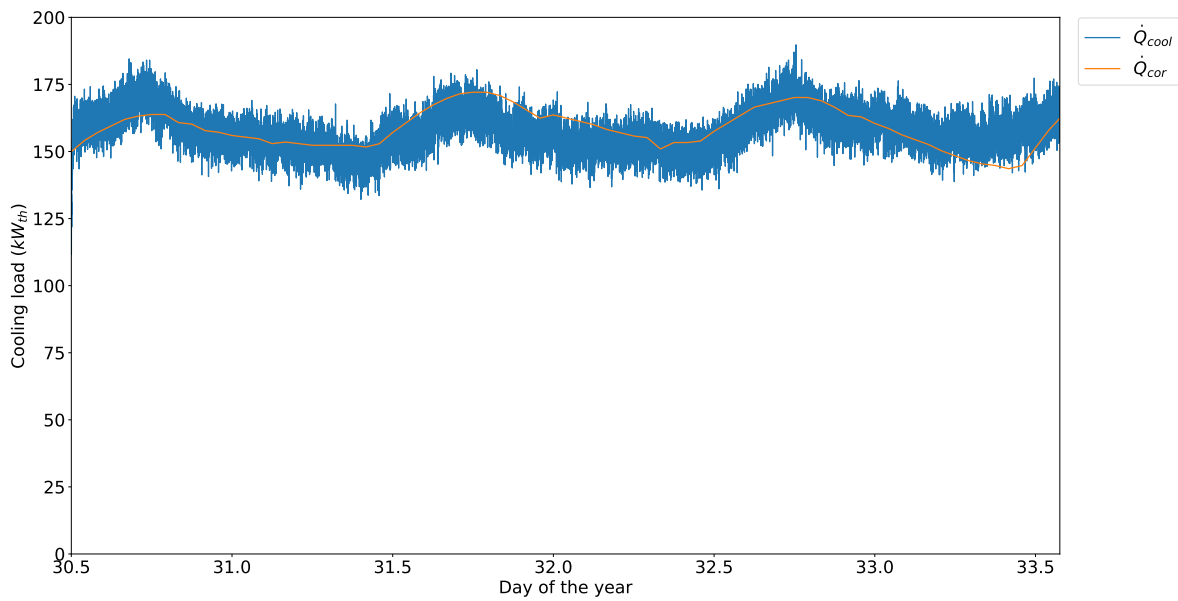


Figure A.6: Old terminal cooling load and the calculated cooling load based on eq. A.1 from 31-02-2014 to 03-02-2014

B

Water usages: Optimization methods

B.1. Time-integrated OTE system

In this section the water usages per sub-system can be found in case of the time-integrated OTE system. In the top-left corner of figure B.1 the water usage of the OTEC power plant can be seen. In the top-right corner the water usage of the SWAC connected to the DOW can be seen. Then in the left center the water usage of the data center connected to the DOW can be found. The water usage of the DOW-connected greenhouse can be found in right center. In the bottom-left corner the effluent water usage of the greenhouse in the Ecopark can be found. Lastly, the effluent water usage of the OTWP in the Ecopark can be seen in the bottom-right corner.

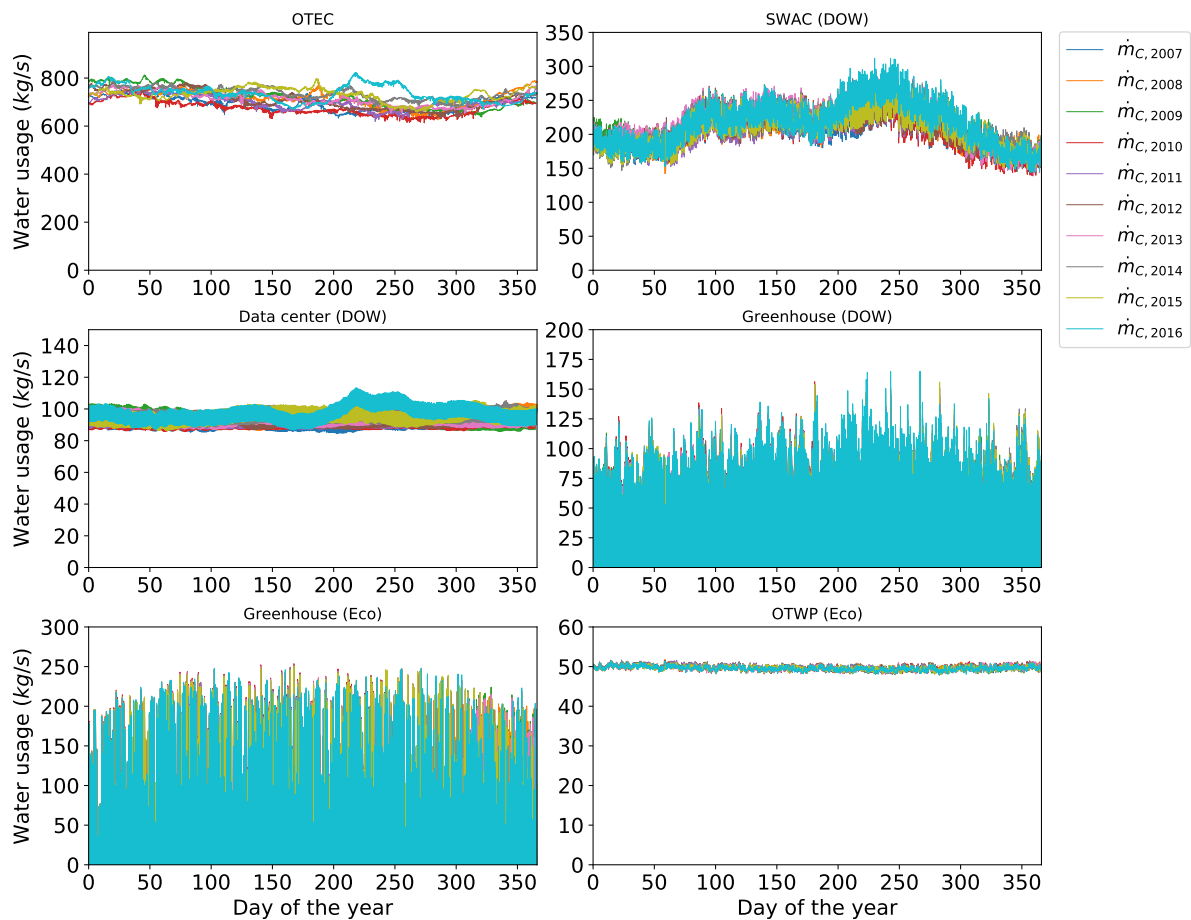


Figure B.1: Water usages of each sub-system in case of the time-integrated OTE system

B.2. Optimization by daily thermal storage

In this section the water usages per sub-system can be found in case of the optimization by daily thermal storage. In the top-left corner of figure B.2 the water usage of the OTEC power plant can be seen. In the top-right corner the water usage of the SWAC connected to the DOW can be seen. Then in the left center the water usage of the data center connected to the DOW can be found. The water usage of the DOW-connected greenhouse can be found in right center. In the bottom-left corner the effluent water usage of the greenhouse in the Ecopark can be found. Lastly, the effluent water usage of the OTWP in the Ecopark can be seen in the bottom-right corner.

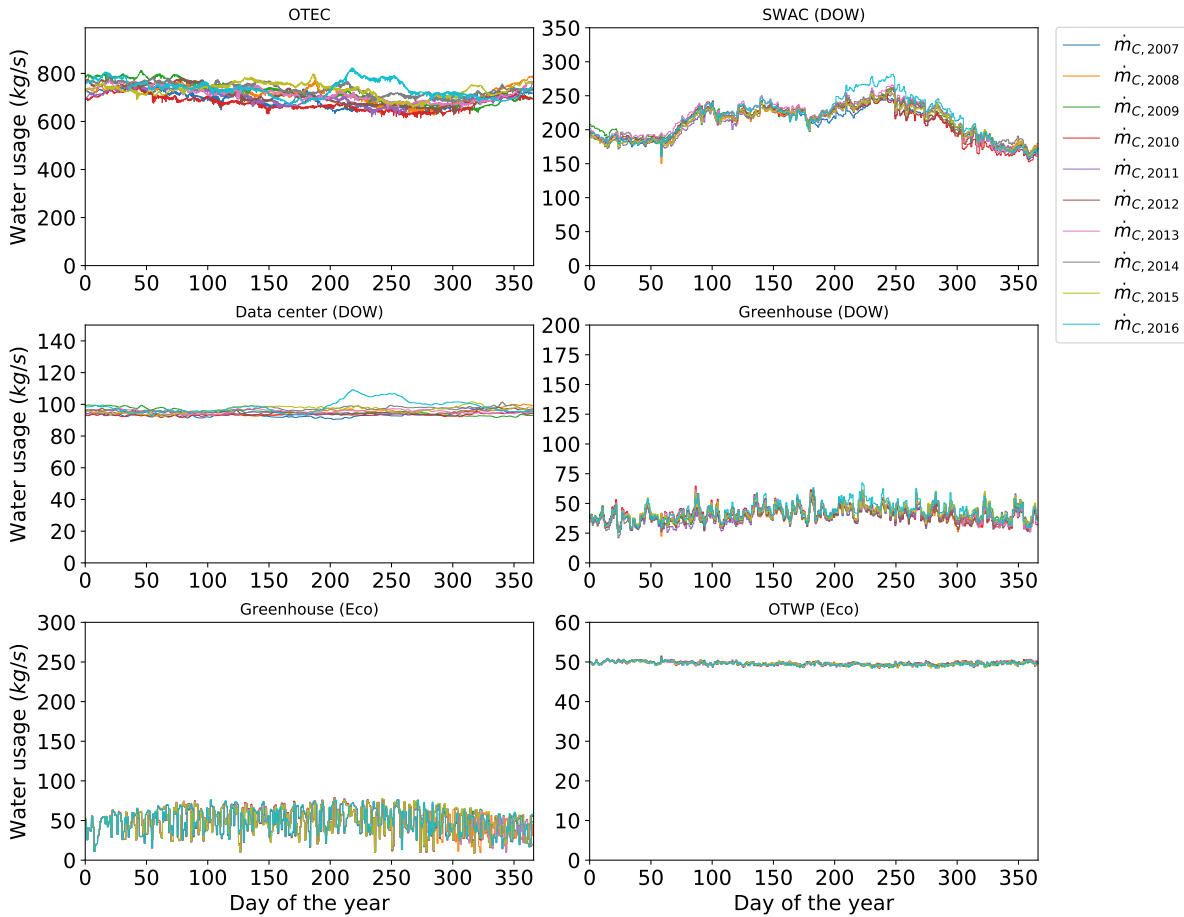


Figure B.2: Water usages of each sub-system in case of optimization by daily thermal storage

B.3. Optimization by yearly thermal storage

In this section the water usages per sub-system can be found in case of the optimization by yearly thermal storage. In the top-left corner of figure B.2 the water usage of the OTEC power plant can be seen. In the top-right corner the water usage of the SWAC connected to the DOW can be seen. Then in the left center the water usage of the data center connected to the DOW can be found. The water usage of the DOW-connected greenhouse can be found in right center. In the bottom-left corner the effluent water usage of the greenhouse in the Ecopark can be found. Lastly, the effluent water usage of the OTWP in the Ecopark can be seen in the bottom-right corner.

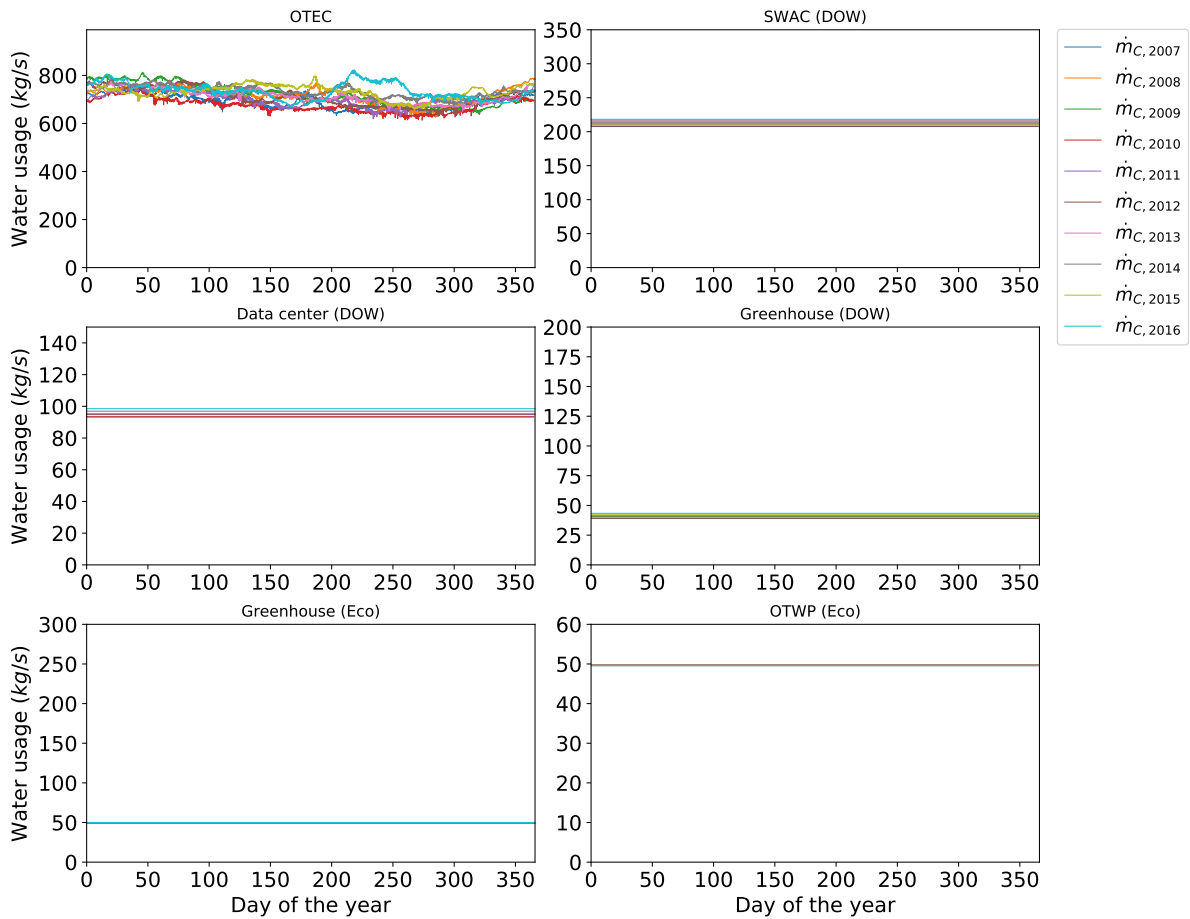


Figure B.3: Water usages of each sub-system in case of optimization by yearly thermal storage

B.4. Optimized configuration

In this section the water usages per sub-system can be found in case of the optimization by changing the configuration of the OTE system. In the top-left corner of figure B.4 the water usage of the OTEC power plant can be seen. In the top-right corner the water usage of the SWAC connected to the DOW can be seen. Then in the left center the effluent water usage of the data center connected to the Ecopark can be found. The water usage of the DOW-connected greenhouse can be found in right center. In the bottom-left corner the effluent water usage of the greenhouse in the Ecopark can be found. Lastly, the effluent water usage of the OTWP in the Ecopark can be seen in the bottom-right corner.

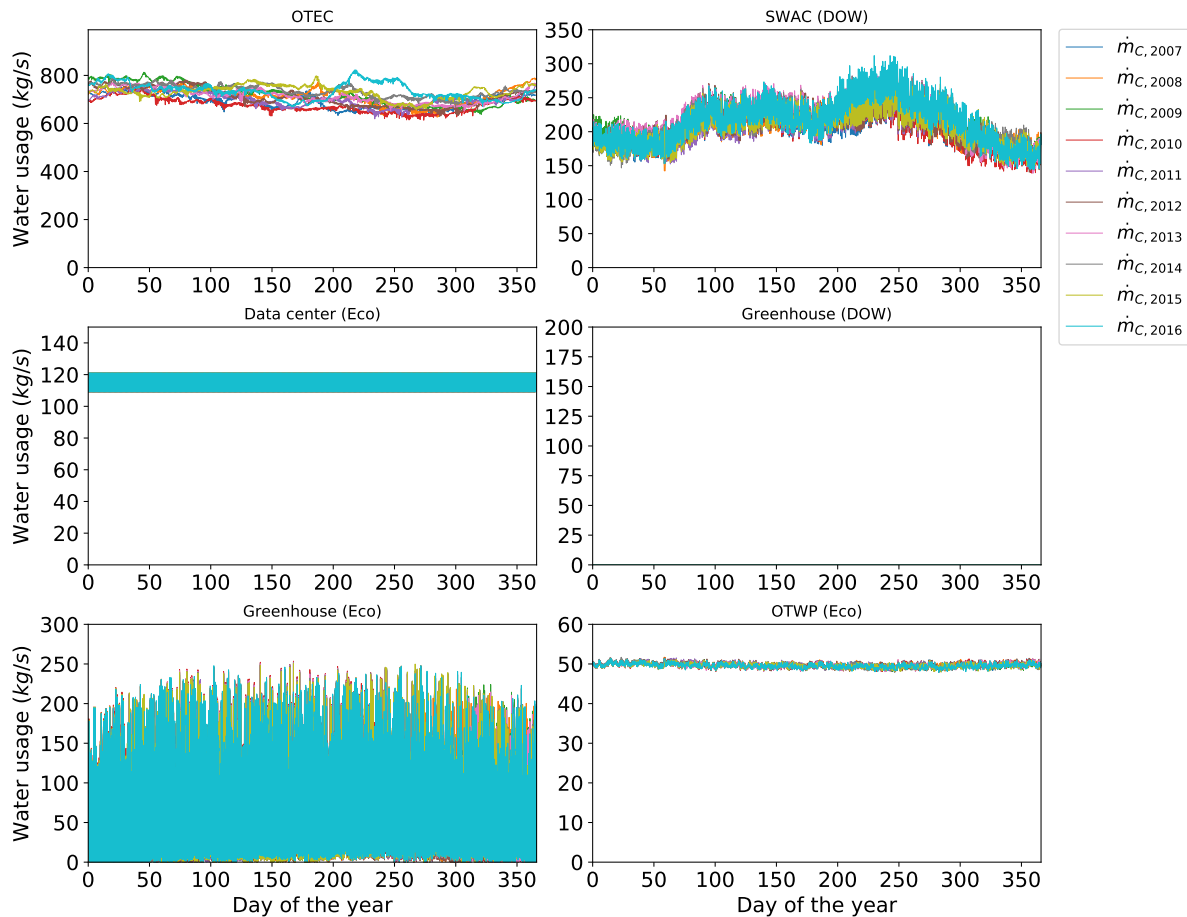


Figure B.4: Water usages of each sub-system in case of optimization by changing the configuration of the OTE system

B.5. Optimization by both configuration and daily thermal storage

In this section the water usages per sub-system can be found in case of the optimization by both changing the configuration of the OTE system and daily thermal storage. In the top-left corner of figure B.5 the water usage of the OTEC power plant can be seen. In the top-right corner the water usage of the SWAC connected to the DOW can be seen. Then in the left center the effluent water usage of the data center connected to the Ecopark can be found. The water usage of the DOW-connected greenhouse can be found in right center. In the bottom-left corner the effluent water usage of the greenhouse in the Ecopark can be found. Lastly, the effluent water usage of the OTWP in the Ecopark can be seen in the bottom-right corner.

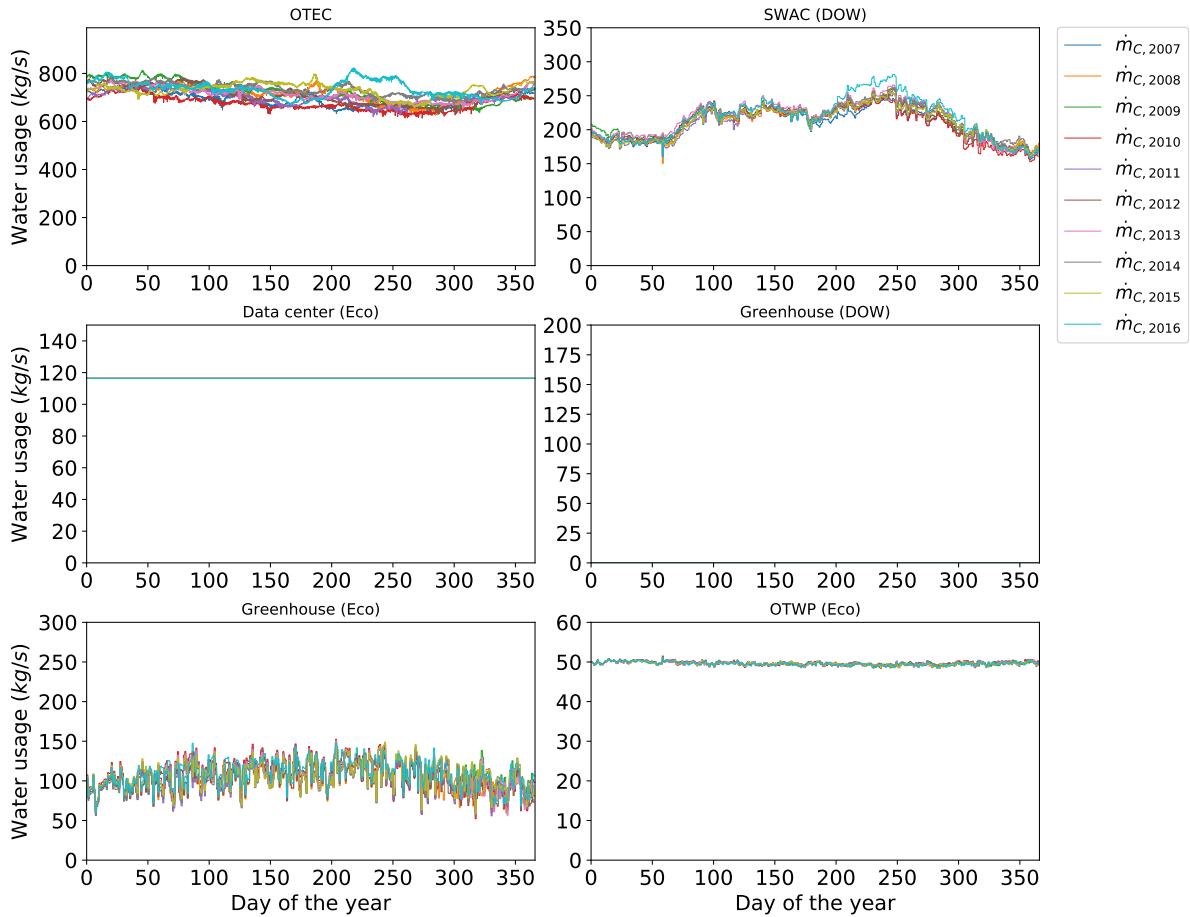


Figure B.5: Water usages of each sub-system in case of both optimization by changing the configuration of the OTE system and daily thermal storage

B.6. Optimization by both configuration and yearly thermal storage

In this section the water usages per sub-system can be found in case of the optimization by both changing the configuration of the OTE system and yearly thermal storage. In the top-left corner of figure B.6 the water usage of the OTEC power plant can be seen. In the top-right corner the water usage of the SWAC connected to the DOW can be seen. Then in the left center the effluent water usage of the data center connected to the Ecopark can be found. The water usage of the DOW-connected greenhouse can be found in right center. In the bottom-left corner the effluent water usage of the greenhouse in the Ecopark can be found. Lastly, the effluent water usage of the OTWP in the Ecopark can be seen in the bottom-right corner.

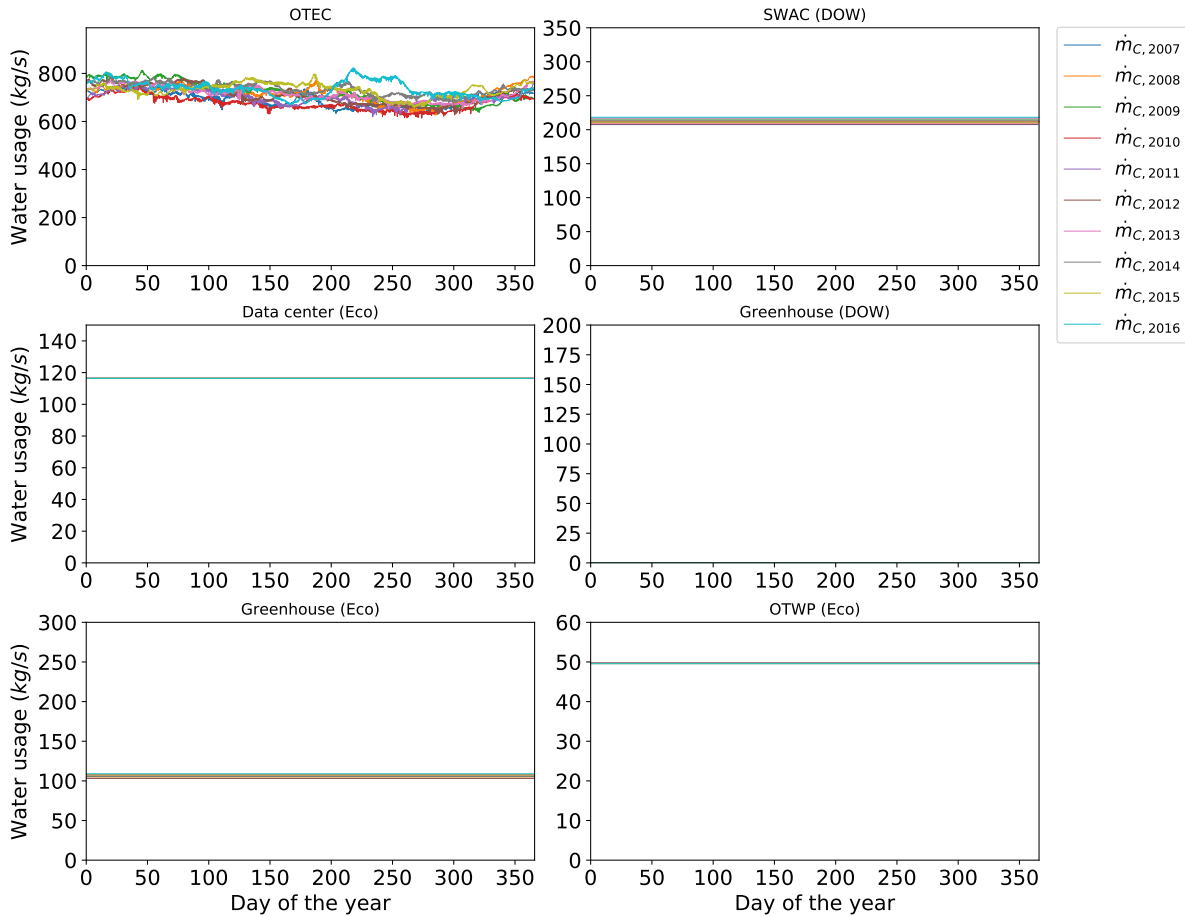


Figure B.6: Water usages of each sub-system in case of optimization by both changing the configuration of the OTE system and yearly thermal storage

C

Water usages: Future growth scenario

C.1. Maximum data center cooling without OTEC

In this section the water usages per sub-system can be found in case of the maximum data center cooling without OTEC. In the top-left corner of figure C.1 the water usage of the OTEC power plant can be seen. In the top-right corner the water usage of the SWAC connected to the DOW can be seen. Then in the left center the water usage of the data center connected to the DOW can be found. The water usage of the DOW-connected greenhouse can be found in right center. In the bottom-left corner the effluent water usage of the greenhouse in the Ecopark can be found. Lastly, the effluent water usage of the OTWP in the Ecopark can be seen in the bottom-right corner.

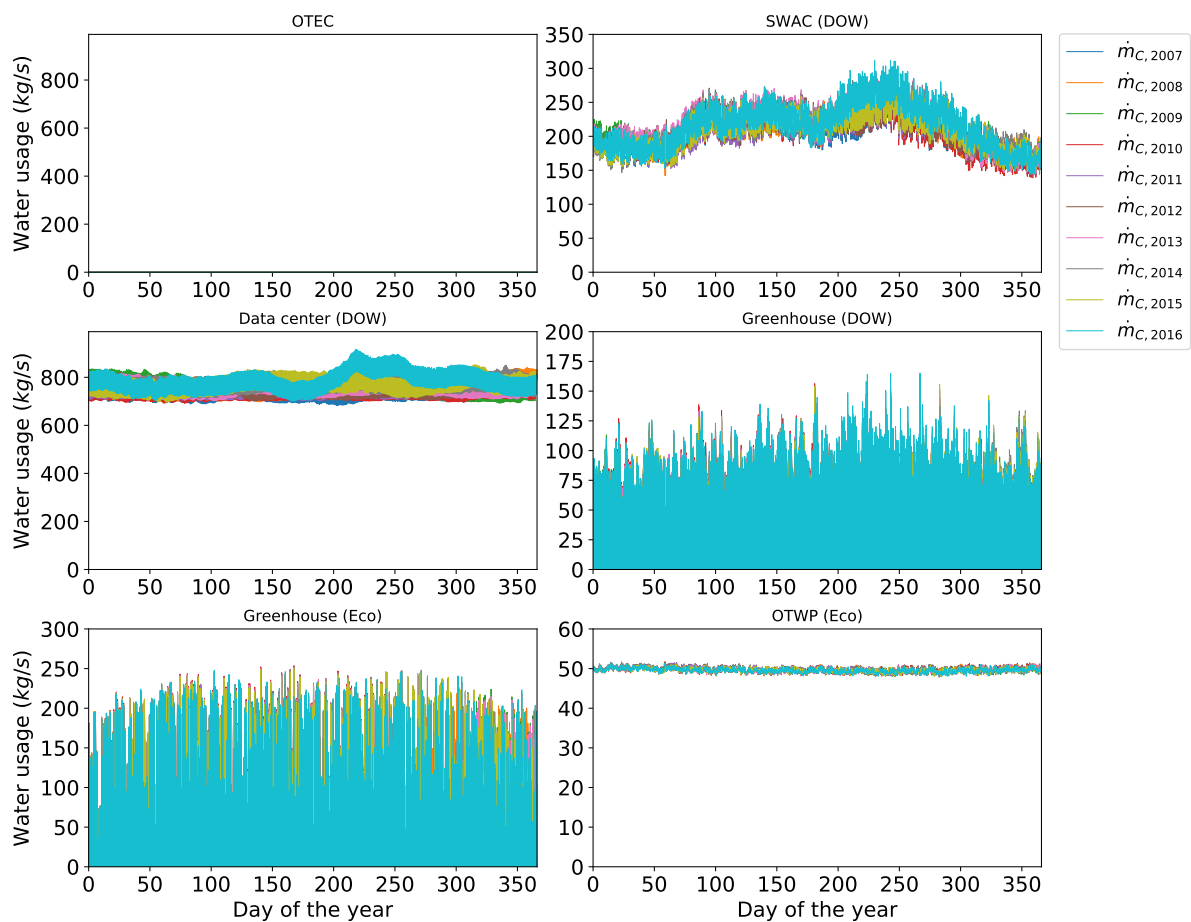


Figure C.1: Water usages of each sub-system in case of the maximum data center cooling without OTEC

C.2. Maximum SWAC cooling without OTEC

In this section the water usages per sub-system can be found in case of the maximum SWAC cooling without OTEC. In the top-left corner of figure C.2 the water usage of the OTEC power plant can be seen. In the top-right corner the water usage of the SWAC connected to the DOW can be seen. Then in the left center the water usage of the data center connected to the DOW can be found. The water usage of the DOW-connected greenhouse can be found in right center. In the bottom-left corner the effluent water usage of the greenhouse in the Ecopark can be found. Lastly, the effluent water usage of the OTWP in the Ecopark can be seen in the bottom-right corner.

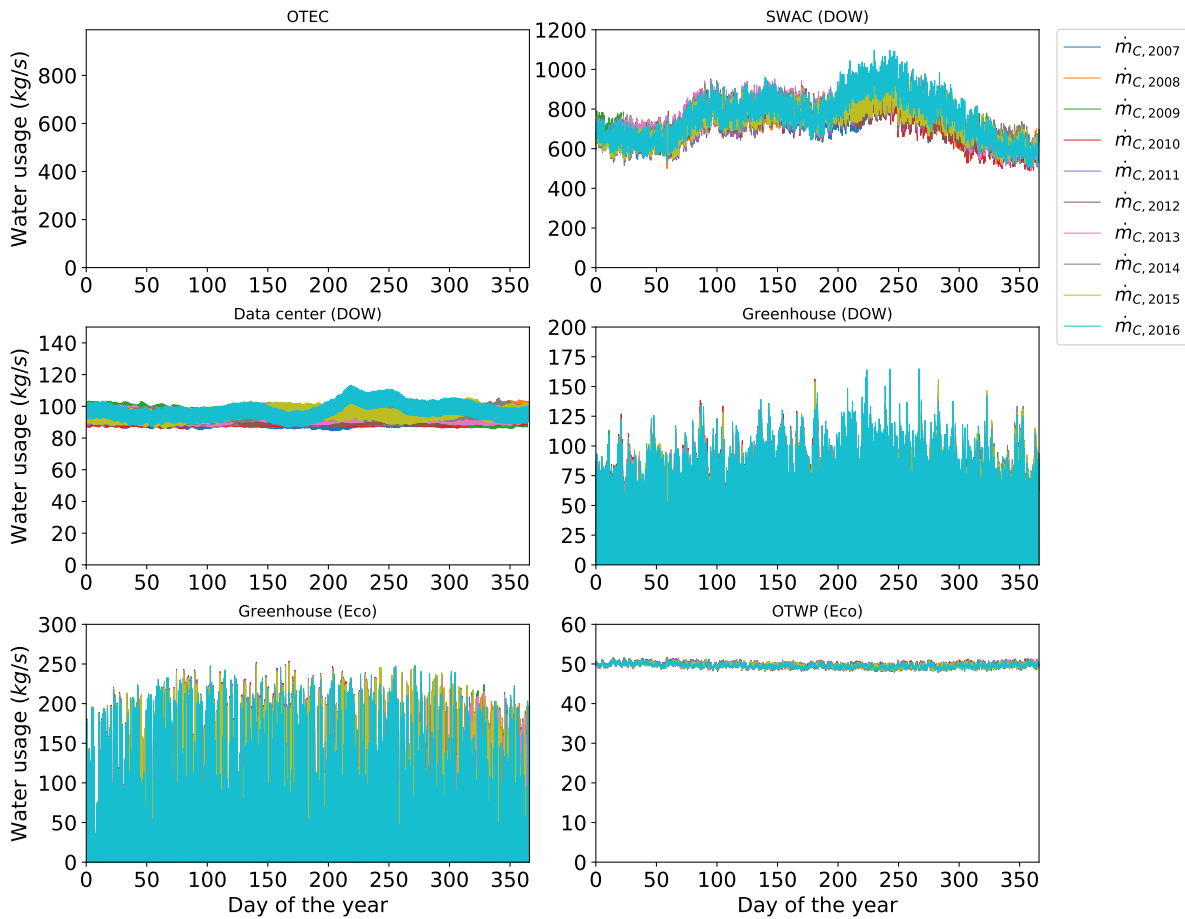


Figure C.2: Water usages of each sub-system in case of the maximum SWAC cooling without OTEC

C.3. Additional data center in the effluent loop

The water usage per sub-system in case of the additional data center in the effluent loop is the same as in case of time-integrated OTE system, see figure B.1. The only difference is the additional data center water usage in the Ecopark. The water usage of the additional data center in the Ecopark can be seen in figure C.3.

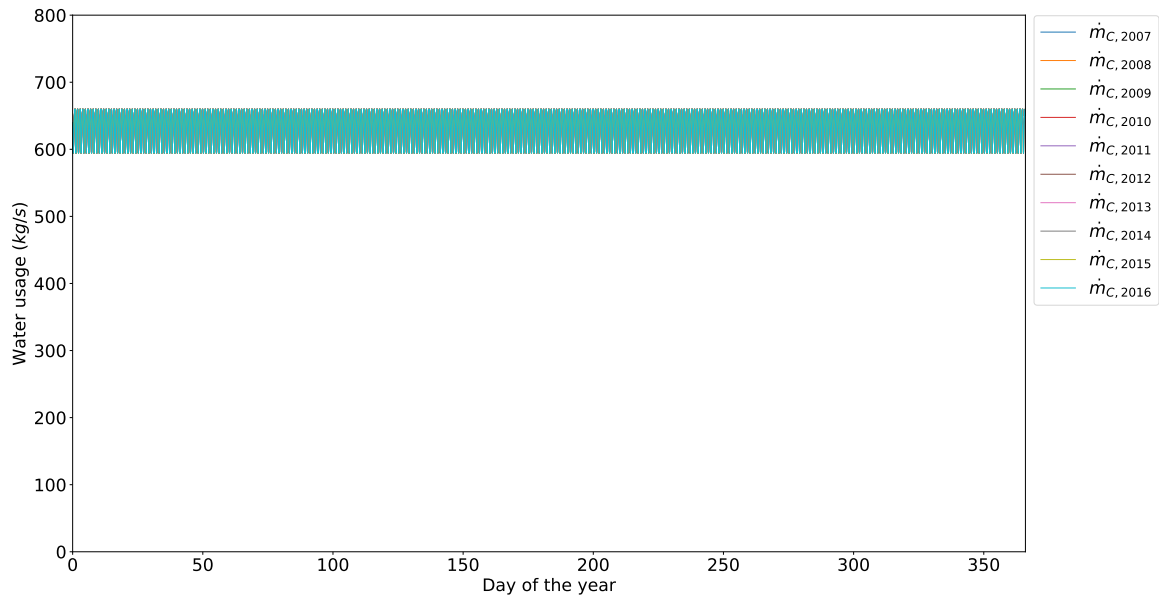


Figure C.3: Water usages of the additional data center in the effluent water loop (Ecopark)

C.4. Additional SWAC in the effluent loop

The water usage per sub-system in case of the additional SWAC in the effluent loop is the same as in case of time-integrated OTE system, see figure B.1. The only difference is the additional SWAC water usage in the Ecopark. The water usage of the additional SWAC system in the Ecopark can be seen in figure C.4.

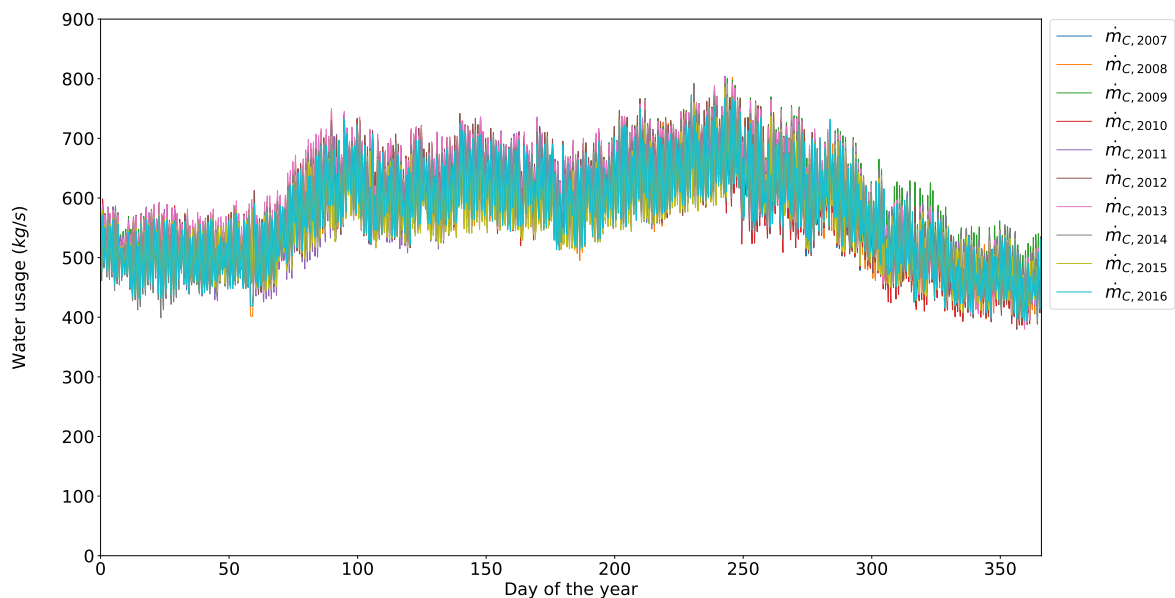


Figure C.4: Water usages of the additional SWAC system in the effluent water loop (Ecopark)

C.5. Maximum combined data center cooling

In this section the water usages per sub-system can be found in case of the maximum combined data center cooling. In the top-left corner of figure C.5 the water usage of the SWAC connected to the DOW can be seen. In the top-right corner the water usage of the data center connected to the DOW can be seen. Then in the left center the water usage of the data center connected to the Ecopark can be found. The water usage of the DOW-connected greenhouse can be found in right center. In the bottom-left corner the effluent water usage of the greenhouse in the Ecopark can be found. Lastly, the effluent water usage of the OTWP in the Ecopark can be seen in the bottom-right corner.

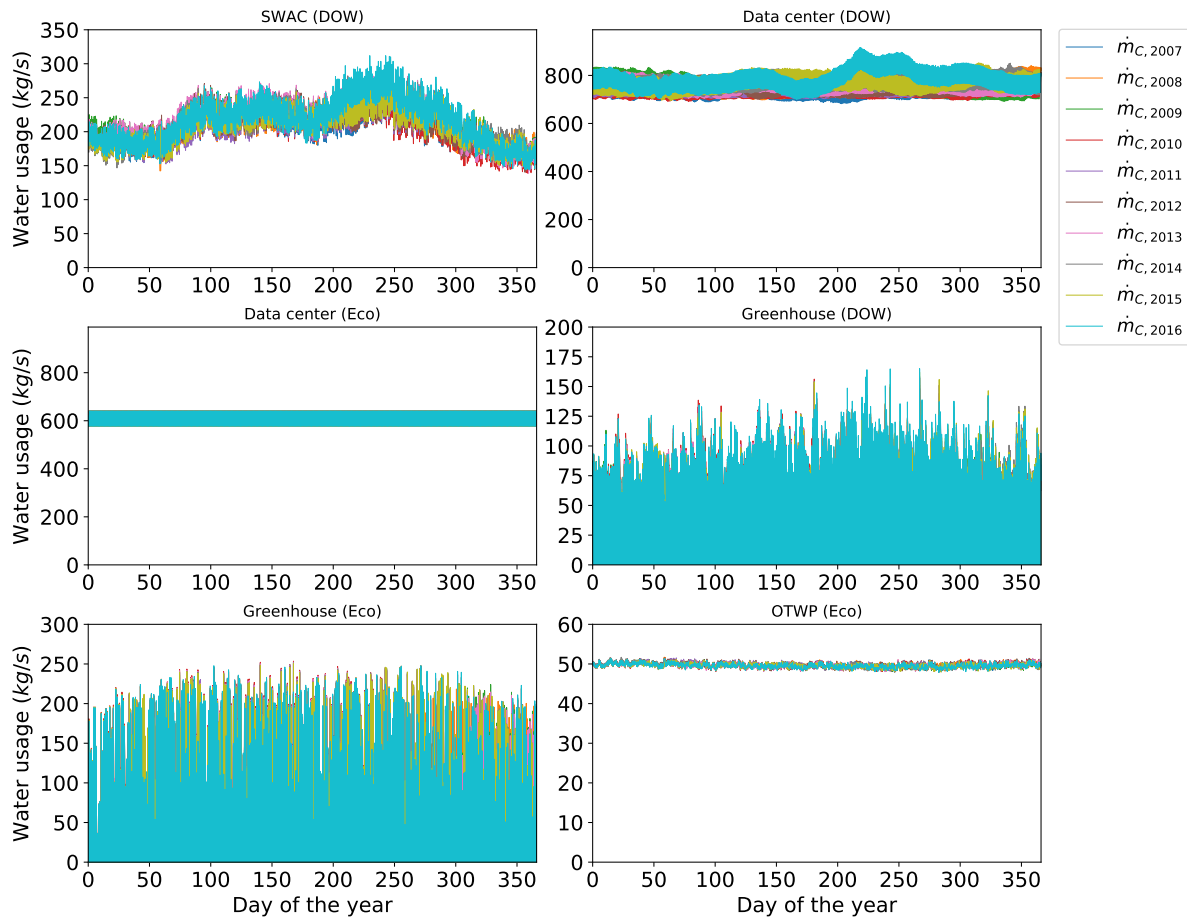


Figure C.5: Water usages of each sub-system in case of the maximum combined data center cooling

C.6. Maximum combined SWAC cooling

In this section the water usages per sub-system can be found in case of the maximum combined SWAC cooling. In the top-left corner of figure C.6 the water usage of the SWAC connected to the DOW can be seen. In the top-right corner the water usage of the SWAC connected to the effluent water of the Ecopark can be seen. Then in the left center the water usage of the data center connected to the Ecopark can be found. The water usage of the DOW-connected greenhouse can be found in right center. In the bottom-left corner the effluent water usage of the greenhouse in the Ecopark can be found. Lastly, the effluent water usage of the OTWP in the Ecopark can be seen in the bottom-right corner.

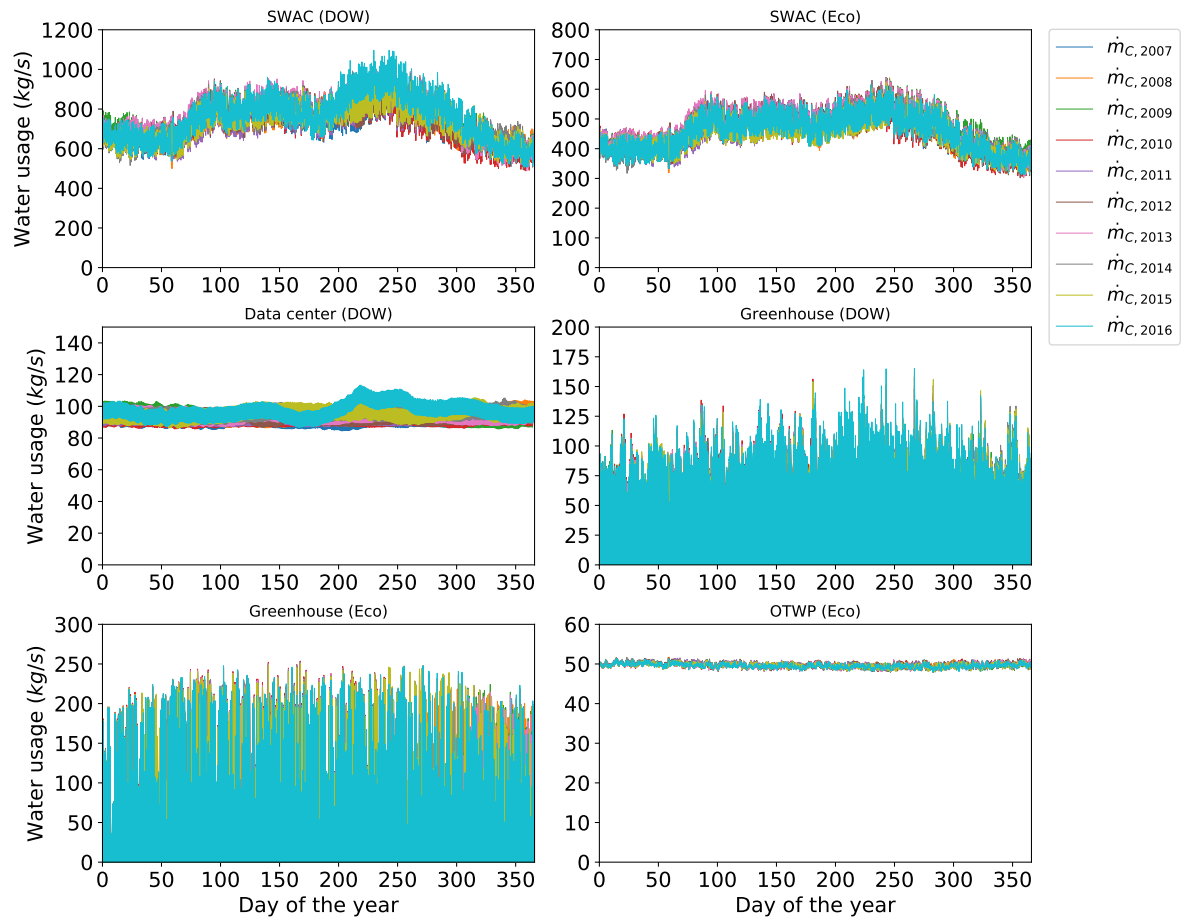
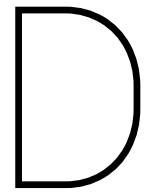


Figure C.6: Water usages of each sub-system in case of the maximum combined SWAC cooling



Water usages: Cases

D.1. 10 MW OTEC power plant

In this section the water usages per sub-system can be found in case of a 10 MW instead of a 500 kW OTEC power plant. In the top-left corner of figure D.1 the water usage of the 10 MW OTEC can be seen. In the top-right corner the water usage of the SWAC system connected to the DOW can be seen. Then in the left center the water usage of the data center connected to the cold deep seawater can be found. The water usage of the DOW-connected greenhouse can be found in right center. In the bottom-left corner the effluent water usage of the greenhouse in the Ecopark can be found. Lastly, the effluent water usage of the OTWP in the Ecopark can be seen in the bottom-right corner.

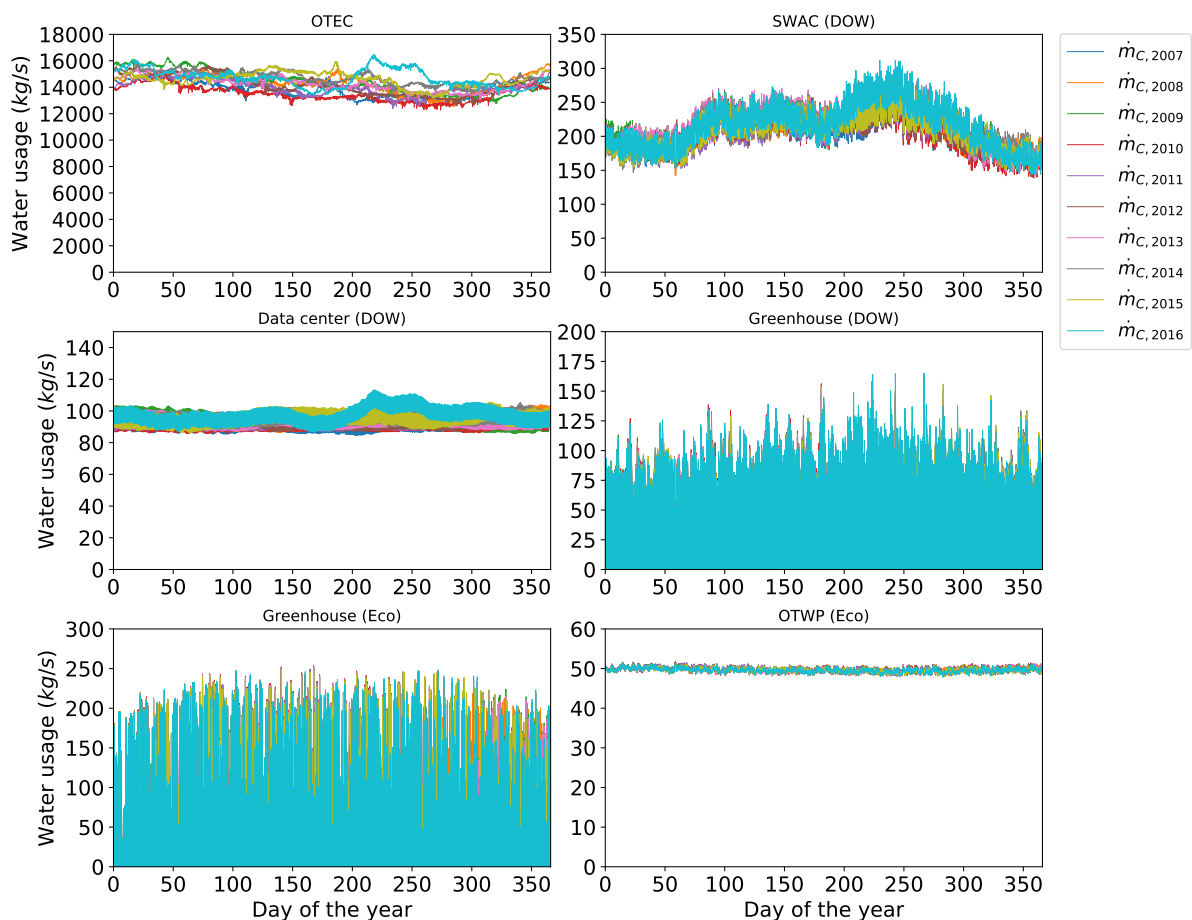


Figure D.1: Water usages of each sub-system in case of a 10 MW instead of a 500 kW OTEC power plant

D.2. 20 MW SWAC

In this section the water usages per sub-system can be found in case of a 20 MW instead of a 7.5 MW SWAC system. In the top-left corner of figure D.2 the water usage of the OTEC can be seen. In the top-right corner the water usage of the 20 MW SWAC system connected to the DOW can be seen. Then in the left center the water usage of the data center connected to the cold deep seawater can be found. The water usage of the DOW-connected greenhouse can be found in right center. In the bottom-left corner the effluent water usage of the greenhouse in the Ecopark can be found. Lastly, the effluent water usage of the OTWP in the Ecopark can be seen in the bottom-right corner.

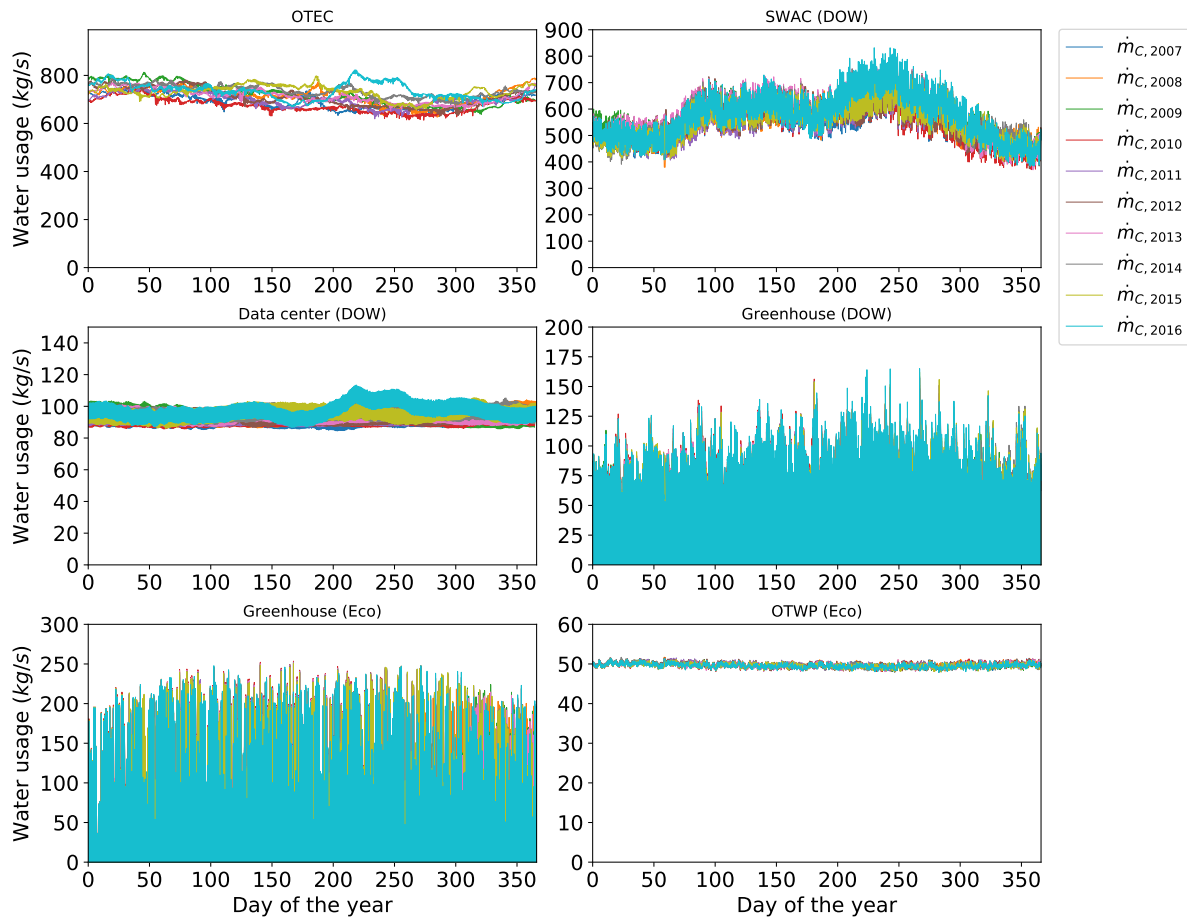


Figure D.2: Water usages of each sub-system in case of a 20 MW instead of a 7.5 MW SWAC system

D.3. Maximum data center cooling demand without thermal storage

In this section the water usages per sub-system can be found in case of the maximum data center cooling capacity when only the data center uses the effluent water in the Ecopark. In the top-left corner of figure D.3 the water usage of the OTEC can be seen. In the top-right corner the water usage of the SWAC system connected to the DOW can be seen. Then in the left center the water usage of the data center connected to the effluent water can be found. The water usage of the DOW-connected greenhouse, the Ecopark-connected greenhouse and the OTWP are zero, and can be found in the left center, bottom-left corner and the bottom-right corner, respectively.

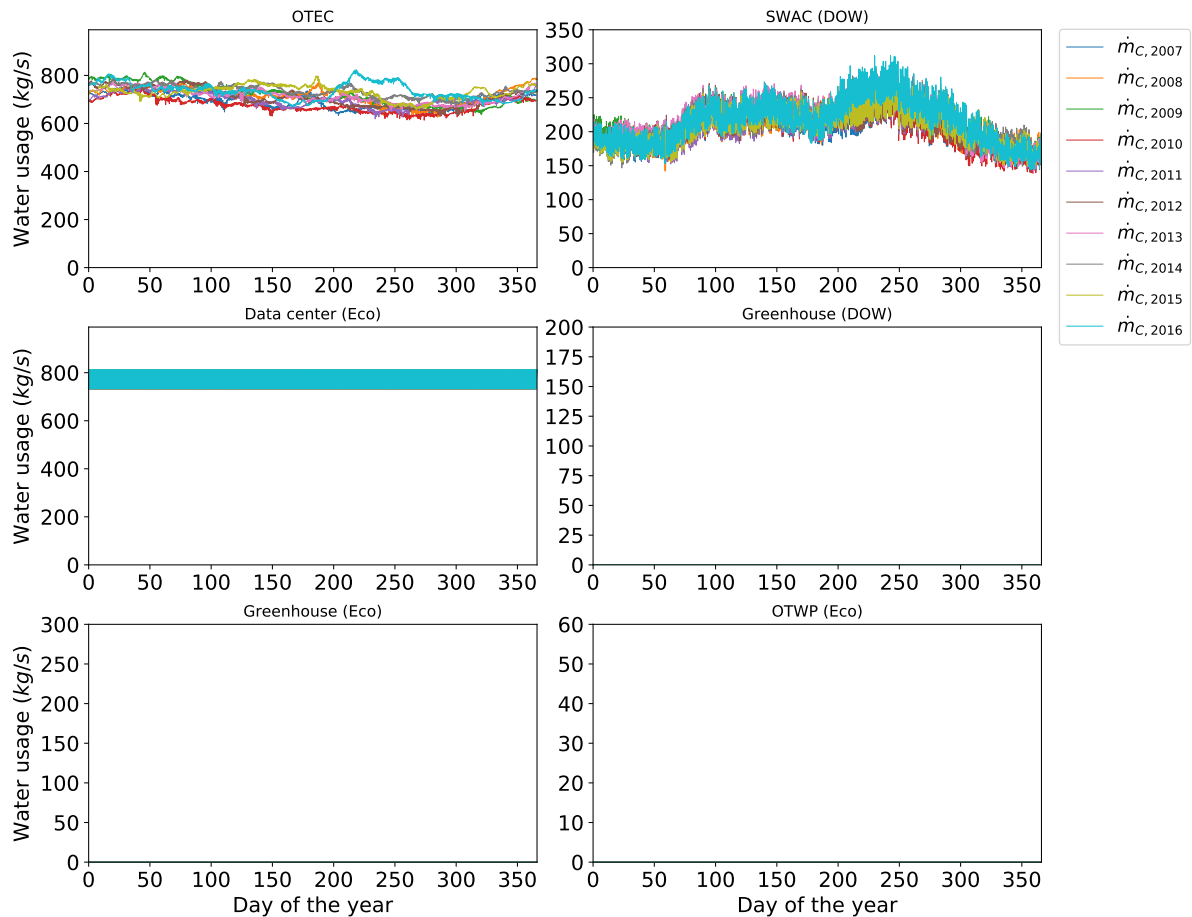


Figure D.3: Water usages of each sub-system in case of the maximum data center cooling capacity when there are no other sub-systems in the Ecopark

D.4. Maximum data center cooling demand with thermal storage

In this section the water usages per sub-system can be found in case of the maximum data center cooling capacity when only the data center uses the effluent water and with additional daily thermal storage. In the top-left corner of figure D.4 the water usage of the OTEC can be seen. In the top-right corner the water usage of the SWAC system connected to the DOW can be seen. Then in the left center the water usage of the data center connected to the effluent water can be found. The water usage of the DOW-connected greenhouse, the Ecopark-connected greenhouse and the OTWP are zero, and can be found in the left center, bottom-left corner and the bottom-right corner, respectively.

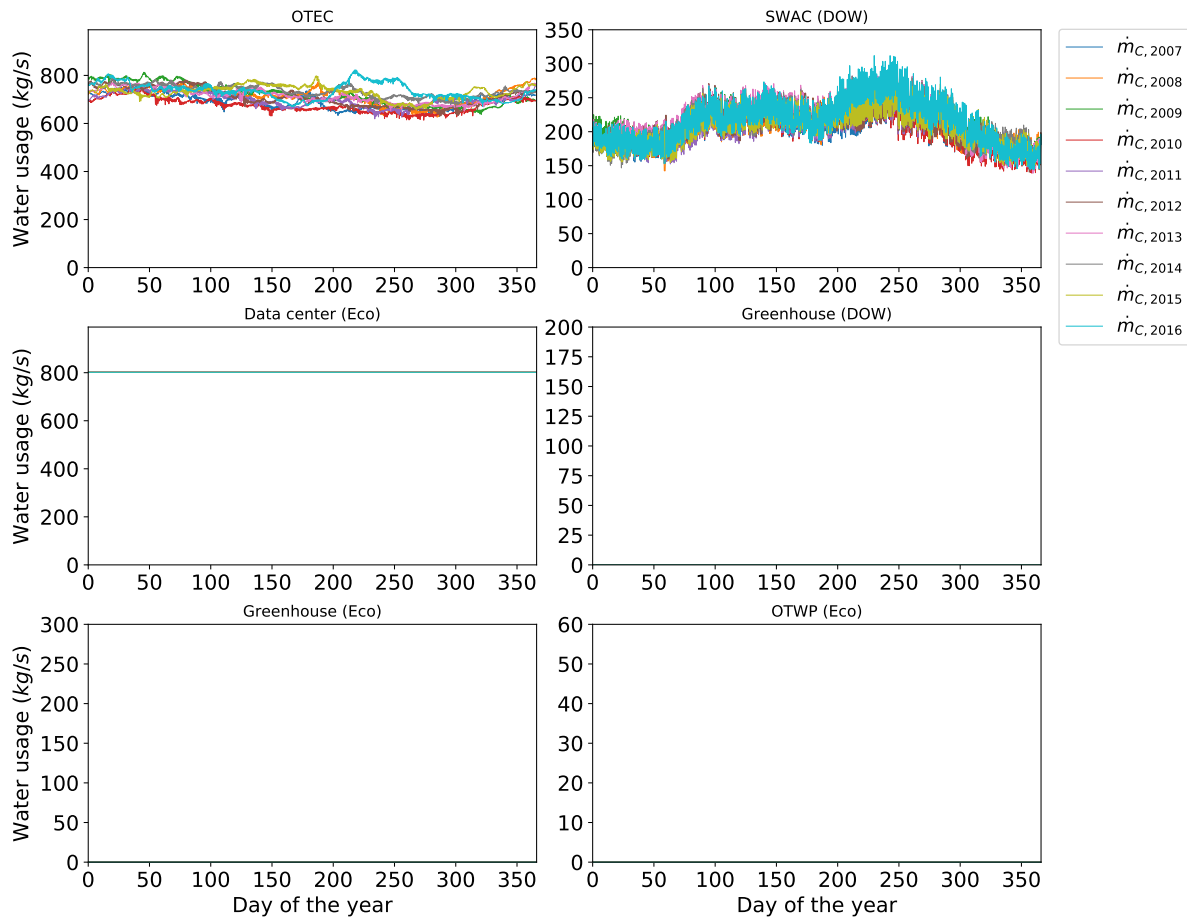


Figure D.4: Water usages of each sub-system in case of the maximum data center cooling capacity when there are no other sub-systems in the Ecopark (with daily thermal storage)

D.5. Maximum greenhouse area without thermal storage

In this section the water usages per sub-system can be found in case of the maximum greenhouse area when only the greenhouses use the effluent water in the Ecopark. In the top-left corner of figure D.5 the water usage of the OTEC can be seen. In the top-right corner the water usage of the SWAC system connected to the DOW can be seen. Then in the bottom-left corner the water usage of the greenhouses connected to the effluent water can be found. The water usage of the data center, the DOW-connected greenhouse and the OTWP are zero, and can be found in the left center, right center and the bottom-right corner, respectively.

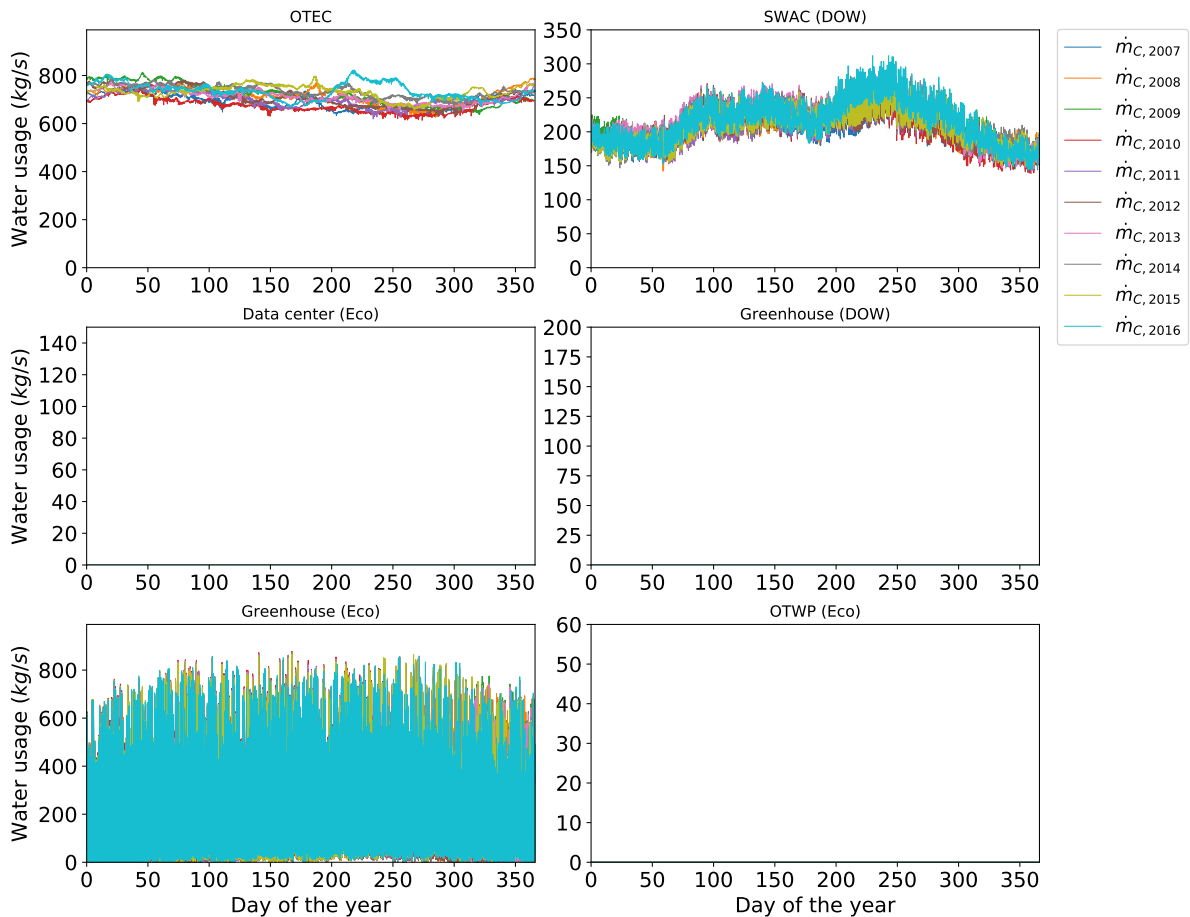


Figure D.5: Water usages of each sub-system in case of the maximum greenhouse area when there are no other sub-systems in the Ecopark

D.6. Maximum greenhouse area with thermal storage

In this section the water usages per sub-system can be found in case of the maximum greenhouse area when only the greenhouses use the effluent water and with additional daily thermal storage. In the top-left corner of figure D.6 the water usage of the OTEC can be seen. In the top-right corner the water usage of the SWAC system connected to the DOW can be seen. Then in the bottom-left corner the water usage of the greenhouses connected to the effluent water can be found. The water usage of the data center, the DOW-connected greenhouse and the OTWP are zero, and can be found in the left center, right center and the bottom-right corner, respectively.

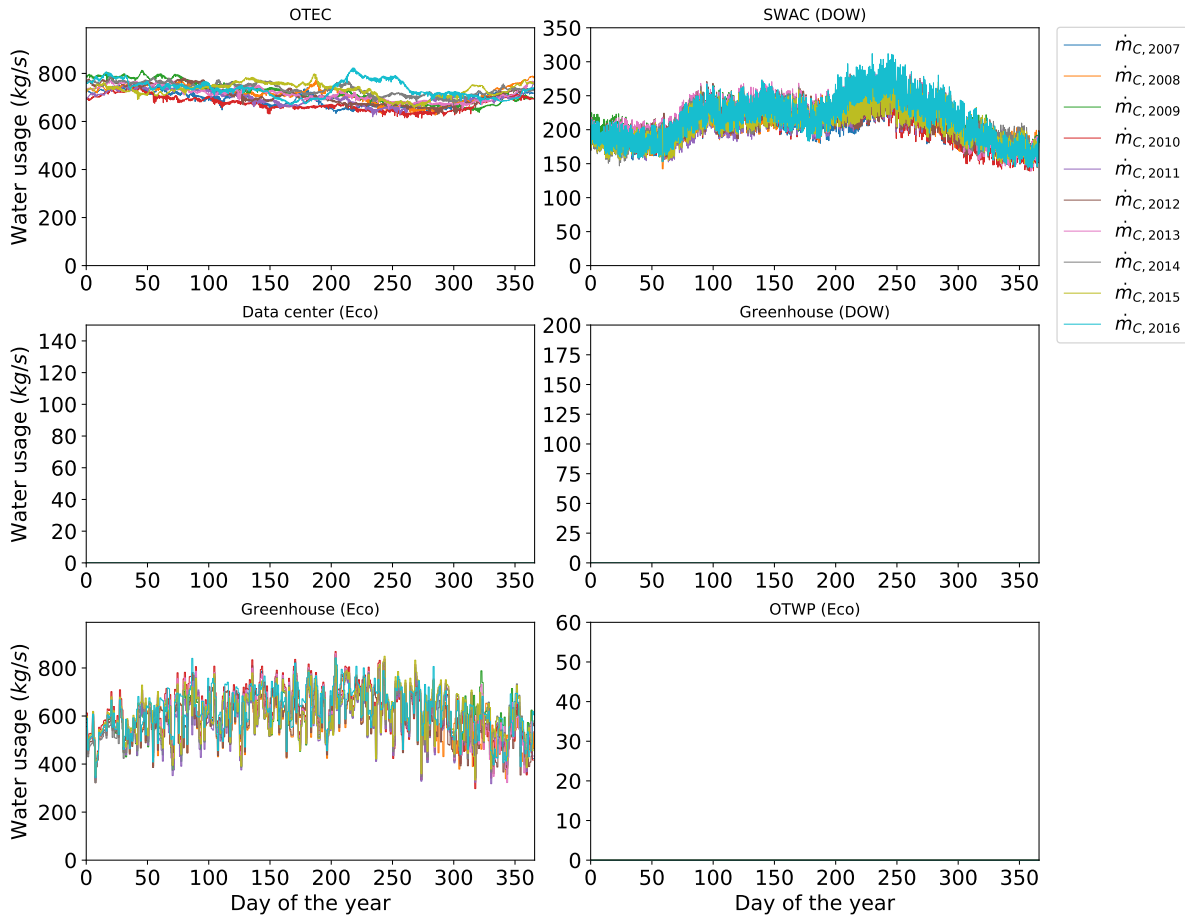


Figure D.6: Water usages of each sub-system in case of the maximum greenhouse area when there are no other sub-systems in the Ecopark (with daily thermal storage)

D.7. Maximum fresh water production without thermal storage

In this section the water usages per sub-system can be found in case of the maximum fresh water production when only the OTWP uses the effluent water. In the top-left corner of figure D.7 the water usage of the OTEC can be seen. In the top-right corner the water usage of the SWAC system connected to the DOW can be seen. Then in the bottom-right corner the water usage of the OTWP connected to the effluent water can be found. The water usage of the data center, the DOW-connected greenhouse and the Ecopark-connected greenhouse are zero, and can be found in the left center, right center and the bottom-left corner, respectively.

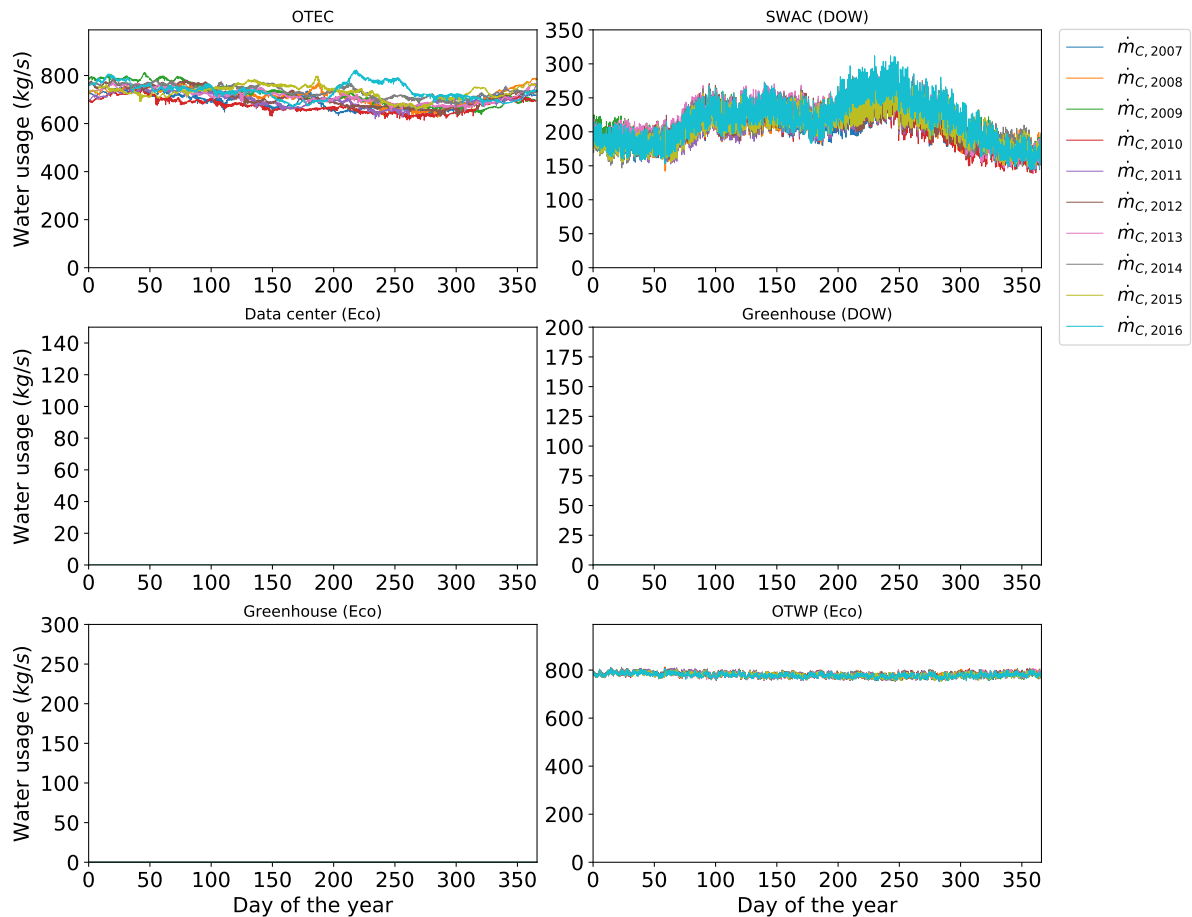


Figure D.7: Water usages of each sub-system in case of the maximum fresh water production when there are no other sub-systems in the Ecopark (With daily thermal storage)

D.8. Maximum fresh water production with thermal storage

In this section the water usages per sub-system can be found in case of the maximum fresh water production when only the OTWP uses the effluent water and with additional daily thermal storage. In the top-left corner of figure D.8 the water usage of the OTEC can be seen. In the top-right corner the water usage of the SWAC system connected to the DOW can be seen. Then in the bottom-right corner the water usage of the OTWP connected to the effluent water can be found. The water usage of the data center, the DOW-connected greenhouse and the Ecopark-connected greenhouse are zero, and can be found in the left center, right center and the bottom-left corner, respectively.

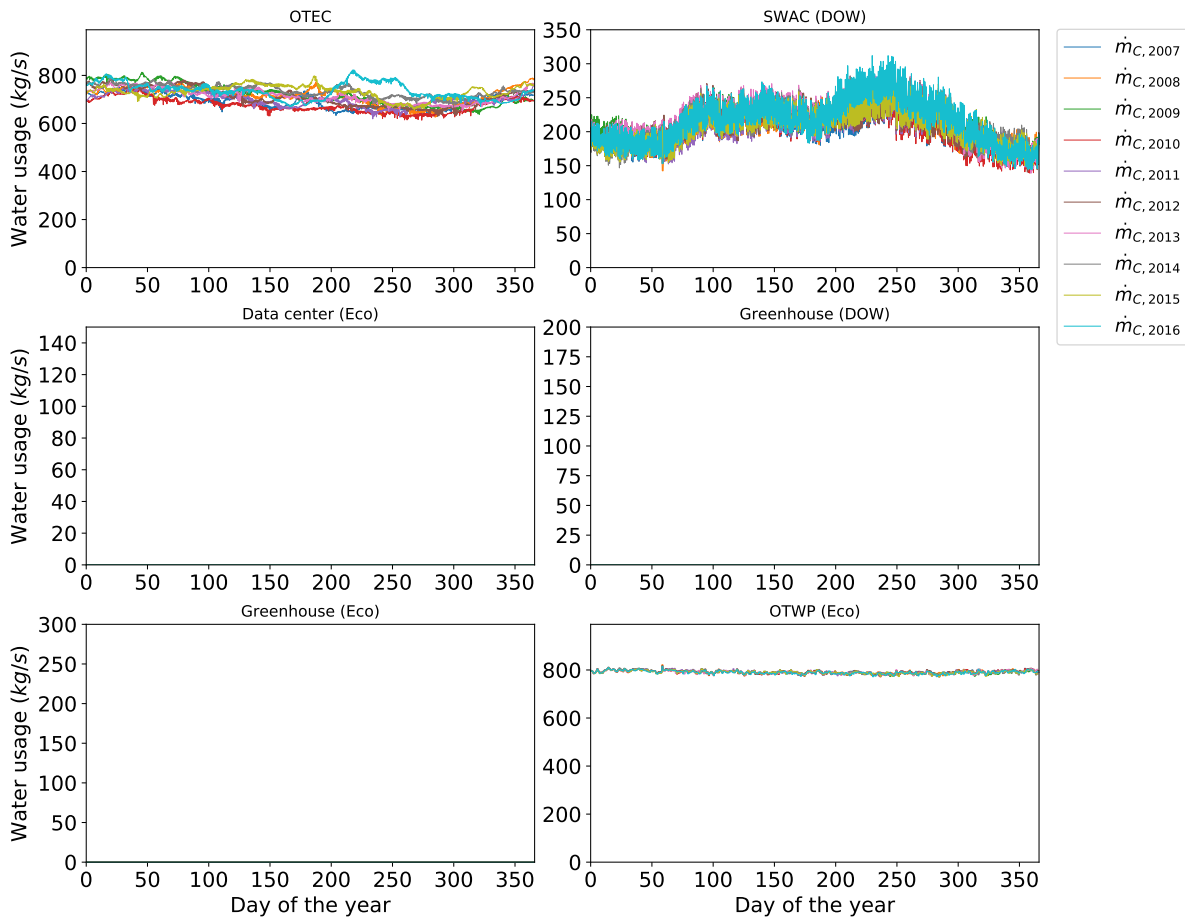
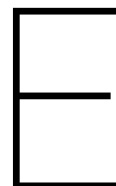


Figure D.8: Water usages of each sub-system in case of the maximum fresh water production when there are no other sub-systems in the Ecopark (with daily thermal storage)



The flaws of the Meteonorm data

In this research the climate data of Meteonorm is used for the environmental temperature and pressure, relative humidity, wind speed and solar radiation. However, the data are not measured values but calculated values based on a climate model. The drawbacks will be shown in this appendix.

E.1. Temperatures

Initially the temperature data of Meteonorm seemed very good. The temperature data for Hato Curacao International Airport for the years 2007 to 2016 can be seen in figure E.1.

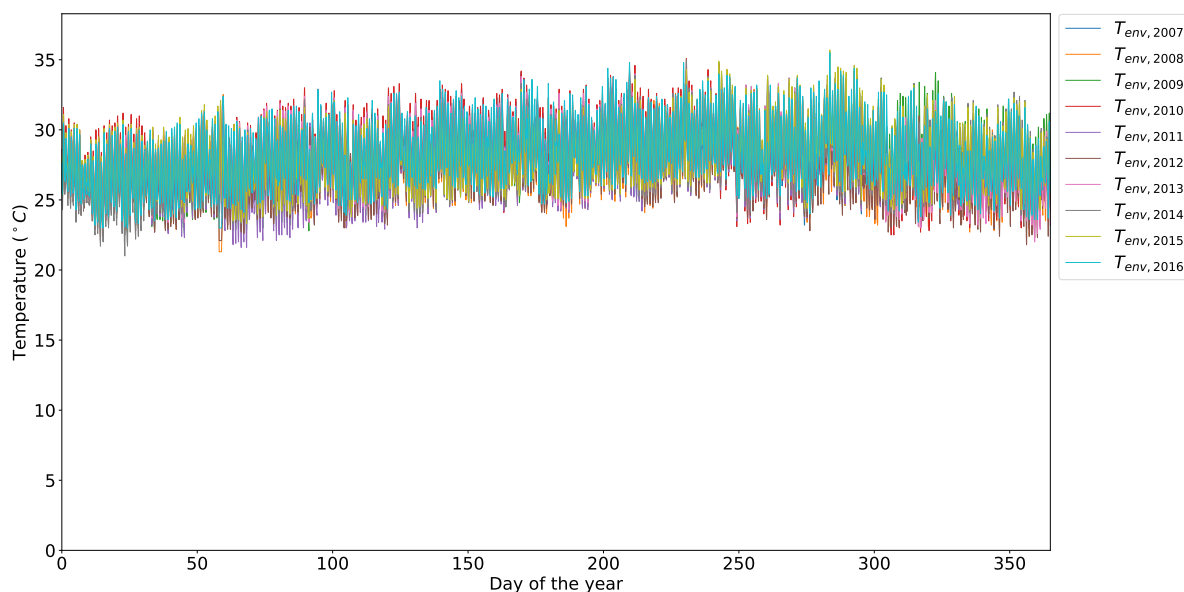


Figure E.1: Temperatures Hato Curacao International Airport generated with Meteonorm for the years 2007 to 2016

In figure E.2 data for the same years can be seen, but now zoomed into days 277 to 281. It can be seen that for some defects occur almost every year. That is no coincidence, that is a result of the use of the climate model. It is also interesting to see that the lines of three years are a little different from the other years. These years are 2008, 2012 and 2012, all three leap years. It seem like Meteonorm calculates the temperature in a different way for leap years.

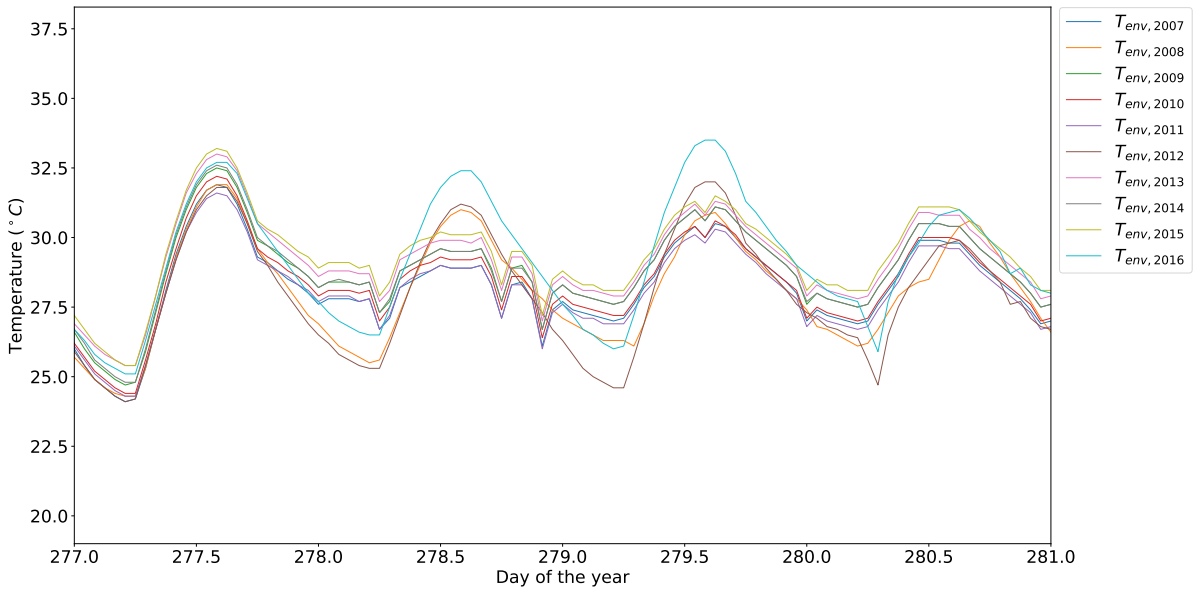


Figure E.2: Temperatures Hato Curacao International Airport generated with Meteonorm for the years 2007 to 2016 (zoomed in)

E.2. Pressure

The environmental pressure generated with the data from Meteonorm can be found in figure E.3. What could be noticed is that in the beginning of the year all the environmental pressures have the same value. Later down the year some of the values start to deviate from the rest. This can be seen in figure E.4. Only the pressures of the years 2008, 2009, 2012 and 2016 are different that the other years. But, in the end the pressure is only used to calculate the fresh water production. The relative difference between the pressure of 1010 mbar and 1000 mbar is only 1% and the difference in fresh water production is even smaller.

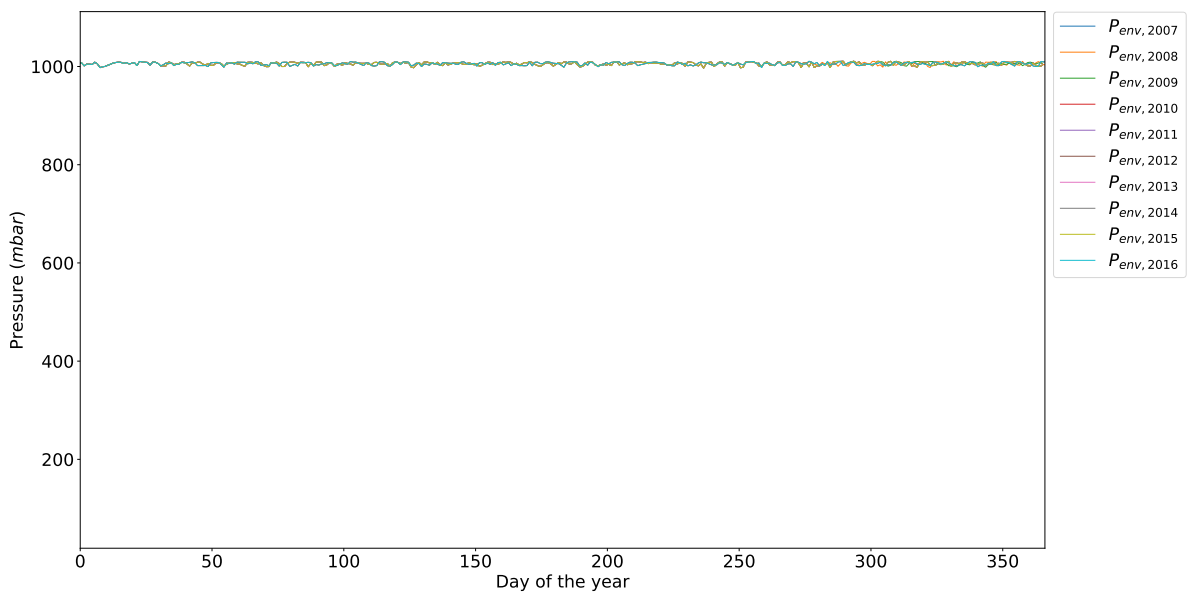


Figure E.3: Pressures Hato Curacao International Airport generated with Meteonorm for the years 2007 to 2016

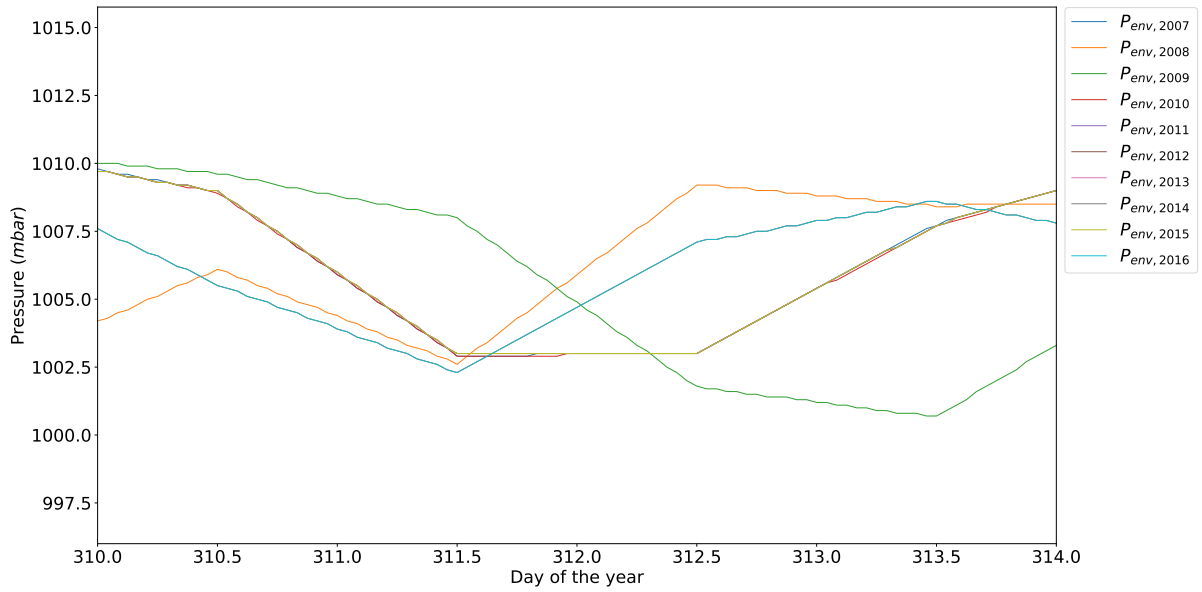


Figure E.4: Pressures Hato Curacao International Airport generated with Meteororm for the years 2007 to 2016 (zoomed in)

E.3. Relative Humidity

The relative humidity from 2007 to 2016 can be seen in figure E.5. The relative humidity seems like it is unique for every year. However, in figure E.6 the relative humidity can be seen for the days 54 to 57. Even though the values are different for each year, it is very obvious that it is not measured data. For example, looking at the time span of 55.5 to 56.0, the same patterns can be seen for each year. This can only be the result of using a climate model instead of measured data.

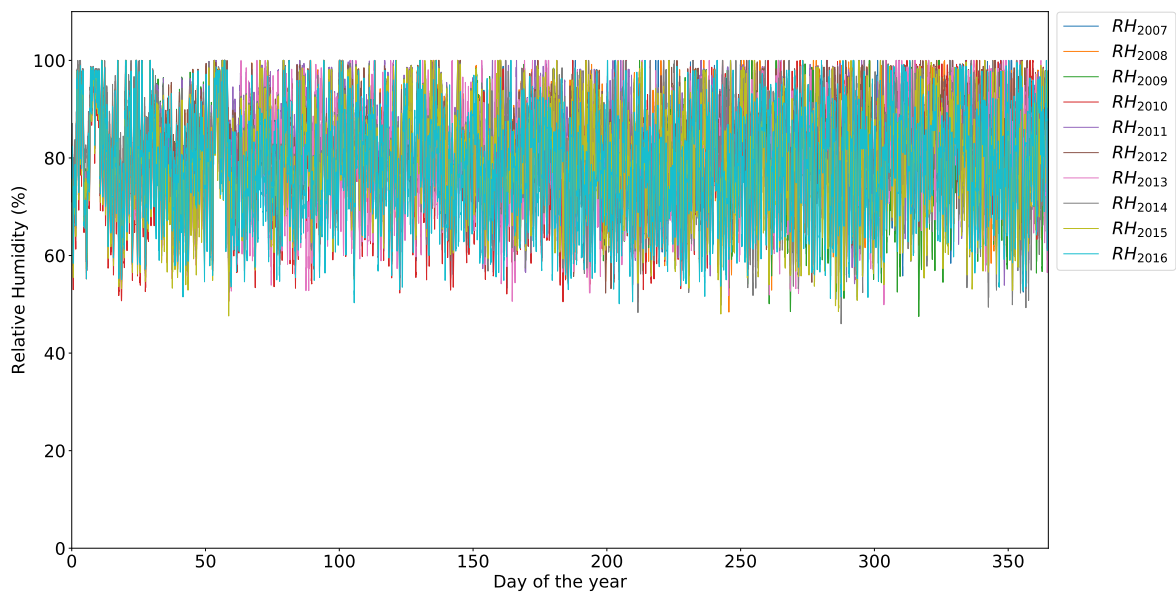


Figure E.5: Relative Humidity Hato Curacao International Airport generated with Meteororm for the years 2007 to 2016

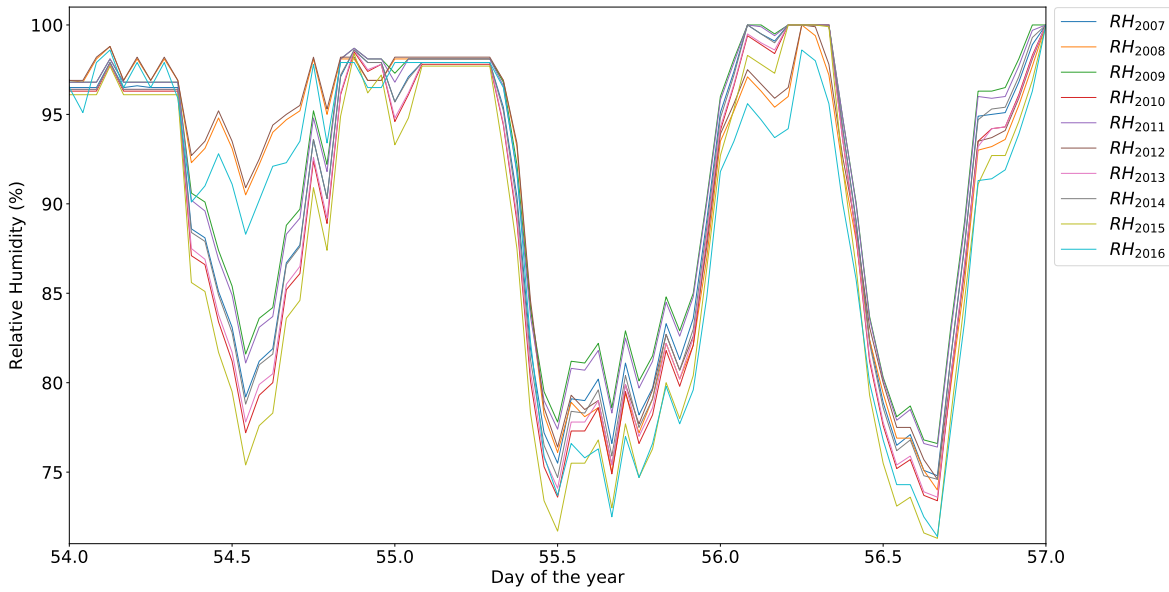


Figure E.6: Relative Humidity Hato Curacao International Airport generated with Meteororm for the years 2007 to 2016 (zoomed in)

E.4. Wind speed

In figure E.7 the wind speed on Curacao for the years 2007 to 2016 can be seen. What is noticeable is that it seems that the wind speeds for each year are almost the same. A zoomed in figure for the days 320 to 325 can be found in figure E.8. This confirms that indeed the wind speed for most years the same, or at least following the same trend. This cannot be the measured data. For example, sometimes a hurricane passes Curacao, but this cannot be noticed in figure E.7.

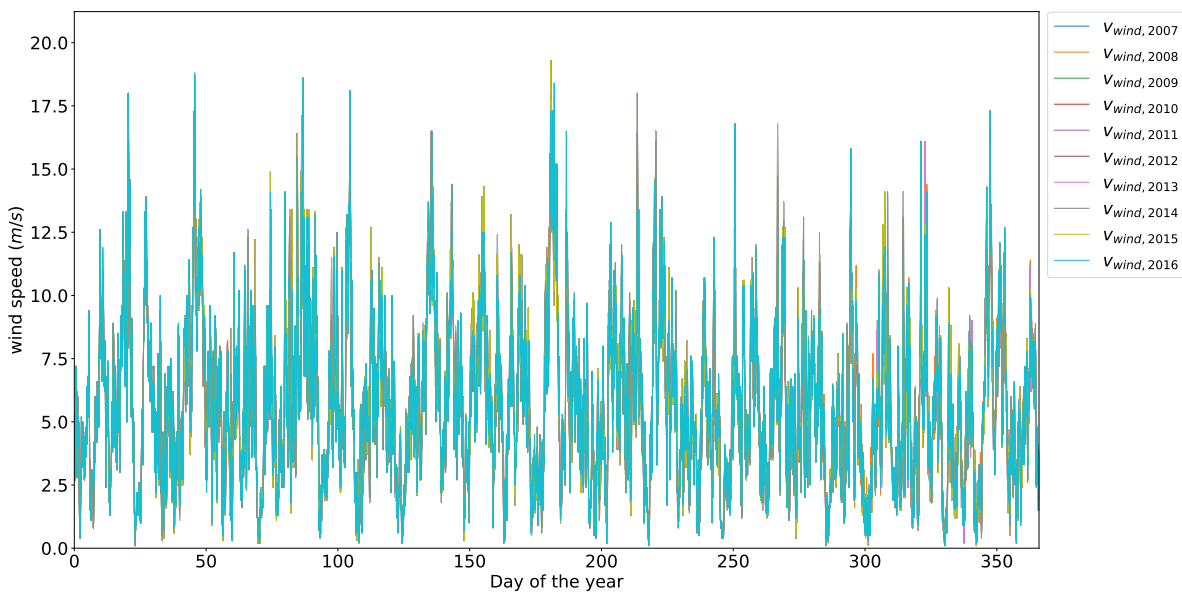


Figure E.7: Wind speed Hato Curacao International Airport generated with Meteororm for the years 2007 to 2016

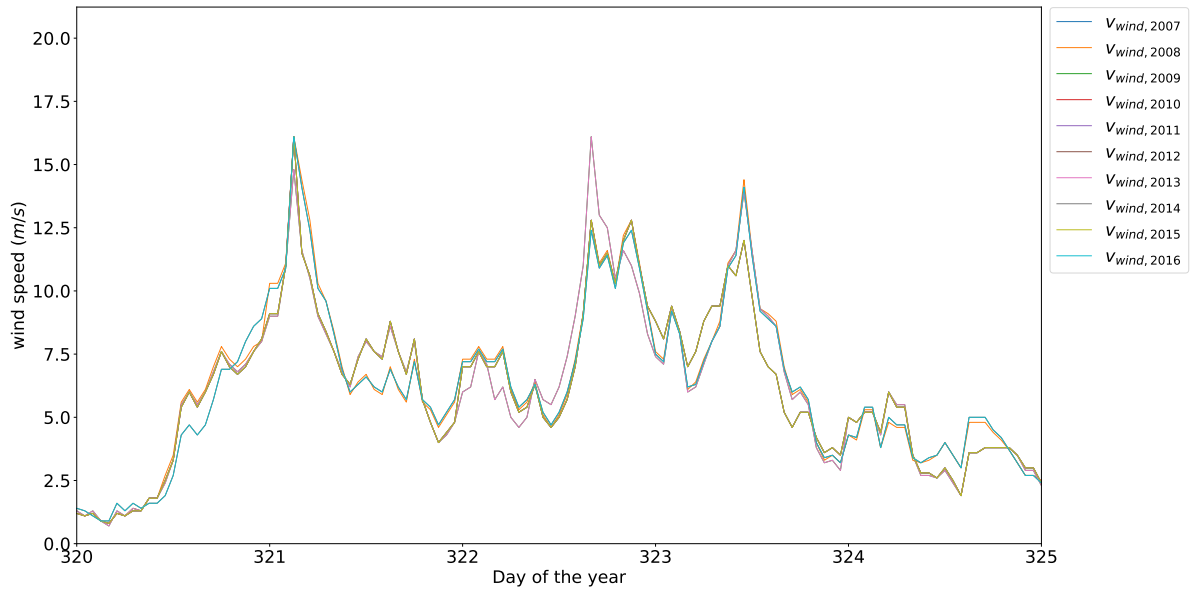


Figure E.8: Wind speed Hato Curacao International Airport generated with Meteornorm for the years 2007 to 2016 (zoomed in)

E.5. Daily global radiation

The daily global radiation for the years 2007 to 2016 can be found in figure E.9. Just like in the case of the pressure, it seems like that the daily global radiation is exactly the same during first 30 days according to Meteornorm. After that some of the years start to deviate from the others. A close up of the daily global radiation for the days 321 to 335 can be seen in figure E.10. Also in this case only the values of the years 2008, 2009, 2012 and 2016 deviate from the rest. So even though the radiation is different for some years, this is not measured data. In case of measured data each year would have different values at a specific day of the year.

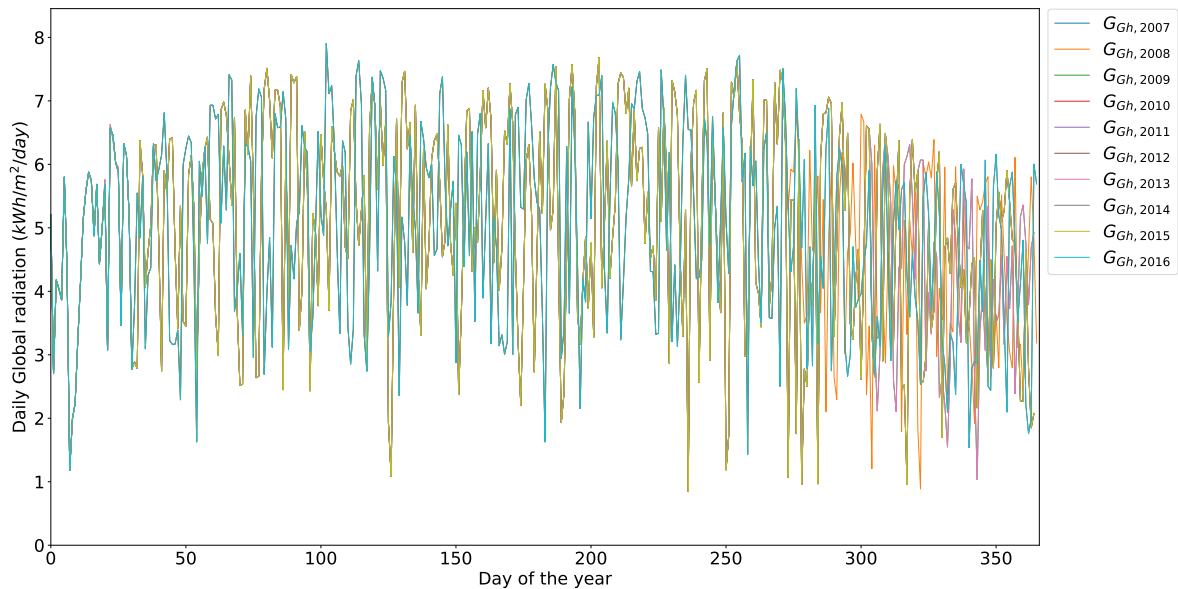


Figure E.9: Daily global radiation for Hato Curacao International Airport generated with Meteornorm for the years 2007 to 2016

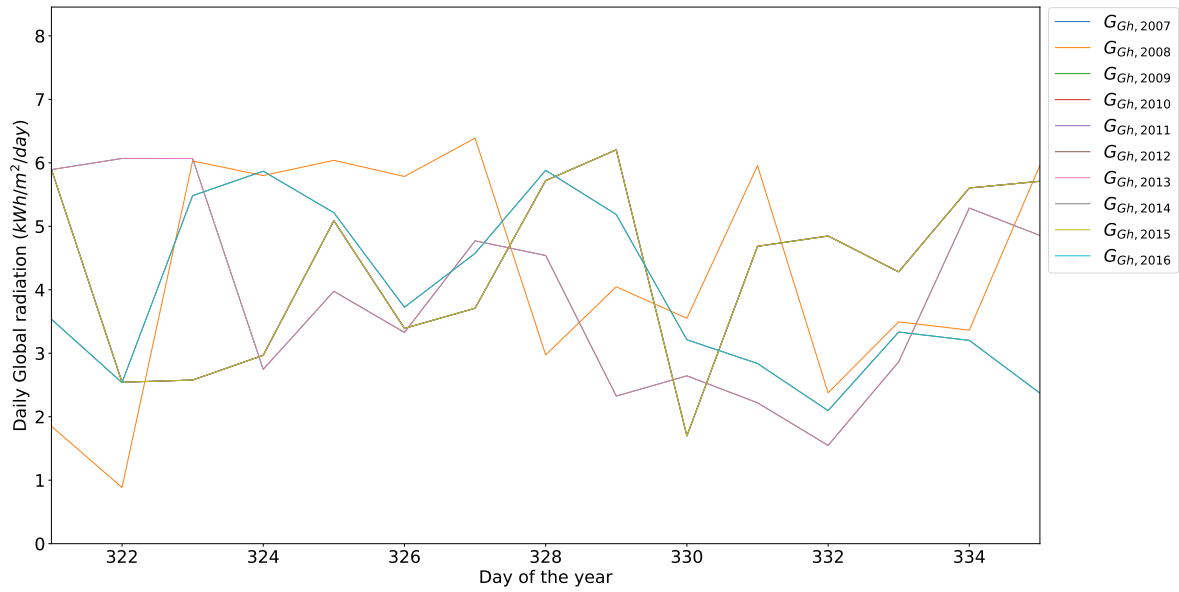


Figure E.10: Daily global radiation for Hato Curacao International Airport generated with Meteonorm for the years 2007 to 2016 (zoomed in)

E.6. Evaluation

In the end it can be concluded that the data from Meteonorm can give a good insight in the climate of a location, but it would be better when measured data is available. As shown in this appendix, it is obvious that Meteonorm uses a climate model (stochastically generated time series) to calculate the data, which can be seen in either the same patterns in the data or that the values for multiple years are exactly the same.